

Titre: Seismic water-crack interaction in gravity dams : experimental
Title: study and numerical simulations

Auteur: Farrokh Javanmardi
Author:

Date: 2003

Type: Mémoire ou thèse / Dissertation or Thesis

Référence: Javanmardi, F. (2003). Seismic water-crack interaction in gravity dams :
Citation: experimental study and numerical simulations [Thèse de doctorat, École
Polytechnique de Montréal]. PolyPublie. <https://publications.polymtl.ca/7166/>

 **Document en libre accès dans PolyPublie**
Open Access document in PolyPublie

URL de PolyPublie: <https://publications.polymtl.ca/7166/>
PolyPublie URL:

**Directeurs de
recherche:** Pierre Léger, & René Tinawi
Advisors:

Programme: Non spécifié
Program:

In compliance with the
Canadian Privacy Legislation
some supporting forms
may have been removed from
this dissertation.

While these forms may be included
in the document page count,
their removal does not represent
any loss of content from the dissertation.

UNIVERSITÉ DE MONTRÉAL

SEISMIC WATER-CRACK INTERACTION IN GRAVITY DAMS:
EXPERIMENTAL STUDY AND NUMERICAL SIMULATIONS

FARROKH JAVANMARDI
DÉPARTEMENT DES GÉNIES CIVIL, GÉOLOGIQUE ET DES MINES
ÉCOLE POLYTECHNIQUE DE MONTRÉAL

THÈSE PRÉSENTÉE EN VUE DE L'OBTENTION
DU DIPLÔME DE PHILOSOPHIAE DOCTOR (Ph.D.)
(GÉNIE CIVIL)

AOÛT 2003



National Library
of Canada

Bibliothèque nationale
du Canada

Acquisitions and
Bibliographic Services

Acquisitions et
services bibliographiques

395 Wellington Street
Ottawa ON K1A 0N4
Canada

395, rue Wellington
Ottawa ON K1A 0N4
Canada

Your file *Votre référence*

ISBN: 0-612-86444-8

Our file *Notre référence*

ISBN: 0-612-86444-8

The author has granted a non-exclusive licence allowing the National Library of Canada to reproduce, loan, distribute or sell copies of this thesis in microform, paper or electronic formats.

L'auteur a accordé une licence non exclusive permettant à la Bibliothèque nationale du Canada de reproduire, prêter, distribuer ou vendre des copies de cette thèse sous la forme de microfiche/film, de reproduction sur papier ou sur format électronique.

The author retains ownership of the copyright in this thesis. Neither the thesis nor substantial extracts from it may be printed or otherwise reproduced without the author's permission.

L'auteur conserve la propriété du droit d'auteur qui protège cette thèse. Ni la thèse ni des extraits substantiels de celle-ci ne doivent être imprimés ou autrement reproduits sans son autorisation.

Canada

UNIVERSITÉ DE MONTRÉAL
ÉCOLE POLYTECHNIQUE DE MONTRÉAL

Cette thèse intitulée:

SEISMIC WATER-CRACK INTERACTION IN GRAVITY DAMS:
EXPERIMENTAL STUDY AND NUMERICAL SIMULATIONS

présentée par: JAVANMARDI Farrokh

en vue de l'obtention du diplôme de : Philosophiae Doctor

a été dûment acceptée par le jury d'examen constitué de:

M. MASSICOTTE Bruno, Ph.D., président

M. LÉGER Pierre, Ph.D., membre et directeur de recherche

M. TINAWI René, Ph.D., membre et codirecteur de recherche

M. CORTHÉSY Robert, Ph.D., membre

M. LAU David T., Ph.D., membre

ACKNOWLEDGEMENTS

I would like to express my deep appreciation and gratitude to my supervisor, Professor Pierre Léger, for his true involvement, precious guidance and continued encouragement during all phase of this investigation. I would like to thank Professor René Tinawi for his numerous and through comments, and for his always appropriate advices.

The financial support through scholarship from Ministry of Science, Research and Technology of IRAN is acknowledged. The financial support from Hydro-Québec, Alcan, and NSERC is also gratefully acknowledged.

I would like to thanks the staff of the Structures Laboratory at the École Polytechnique Mr. Gérard Degrange, Mr. Denis Fortier, and Mr. Patrice Bélanger, for helping me during the experimental tests in laboratory. A very special thank is due Mr. Martin Leclerc who assisted me in the laboratory and helped in different ways during the course of this research. I would like to extend my thanks to everybody, particularly students who contributed in one way or another.

I wish to thank Professor Lineu Pedroso for very valuable discussions during his sabbatical at École Polytechnique.

Finally I am deeply grateful of my family, my wife and my son, for their patience and understanding. They provide me with a strong motivation to persist and successfully complete the work on my thesis.

RÉSUMÉ

Les modes d'oscillation des surfaces de contact d'une fissure, dont l'entrée est soumise à la pression de l'eau du réservoir modifieront la magnitude et la distribution spatiale de la sous-pression de l'eau dans la fissure. La sous-pression qui s'exerce le long des fissures et des joints, crée des forces externes qui favorisent la propagation de la fissure et influencent la stabilité dynamique des composantes fissurées. Les variations de la sous-pression sismique pendant les tremblements de terre demeurent une source importante d'incertitude dans la conception parasismique et l'évaluation sismique de la sécurité des barrages en béton. Les guides de sécurité des barrages indiquent que l'intensité de la sous-pression dans les fissures pendant un tremblement de terre peut varier de la pression hydrostatique du réservoir à la pression nulle. La pratique courante souligne le manque de connaissance en définissant les variations de sous-pression sismique dans les fissures existantes ou nouvelles dans les barrages en béton. L'objectif de cette étude est de développer un modèle rationnel hydromécanique d'interaction de l'eau et des fissures afin de prévoir les variations dynamiques de la sous-pression pendant les tremblements de terre.

Une étude expérimentale pour caractériser la réponse sismique transitoire des sous-pressions pour des spécimens en béton non fissuré ou avec des fissures existantes de 0.4 m a été réalisée. Des mouvements cycliques des surfaces de contact de la fissure de fréquences variant de 2 à 10 hertz ont été appliqués, pour différentes valeurs de pressions de l'eau à l'ouverture de la fissure. Les résultats d'essai avec les spécimens fissurés nous ont montré une diminution de pression de l'eau en mode d'ouverture de la fissure et augmentation en mode de fermeture. Pour la première fois on a observé le phénomène de cavitation le long des fissures en mode d'ouverture pour une fréquence d'excitation de 10 hertz.

Ensuite, un modèle dynamique d'interaction eau-fissure est formulé pour reproduire les résultats expérimentaux, et extrapoler les variations de sous-pression dans les fissures de longueurs arbitraires, qui peuvent se développer dans des barrages réels. Les gradients de pression transitoire dans une fissure d'une longueur donnée sont modélisés

en fonction du déplacement de l'ouverture de la fissure ($CMOD(t)$) et d'historique de sa pression à la frontière en contact avec le réservoir ($P_{crn}(t)$) en supposant: (i) l'écoulement unidirectionnel le long de la fissure, (ii) la condition de continuité d'un fluide incompressible d'une viscosité constante, (iii) les relations de pression-écoulement gouvernées par la conductivité hydraulique de la fissure en utilisant des variations "de la loi cubique" pour la rugosité de la fissure, (iv) les conditions de l'écoulement laminaire ou turbulent selon le nombre de Reynold, et la cavitation, (v) les surface imperméables de contacts de la fissure, et (vi) l'ouverture résiduelle de fissure pendant les mouvements cycliques (zéro ou plus grand). Basé sur le modèle proposé, un logiciel, DUP_CRACK, a été développé pour la simulation numérique des résultats expérimentaux. La pression simulée et les variations de pression mesurées expérimentalement sont en bonne concordance.

Le modèle dynamique d'interaction eau-fissure est alors mis en application dans un logiciel d'éléments finis non linéaire avec des éléments de contacts, qui représentent la fissure, pour calculer la pression dynamique de l'eau. Le logiciel développé, DUP_DAM, peut être utilisé pour l'analyse dynamique d'un barrage fissuré soumis aux tremblements de terre, considérant les effets de couplage hydromécaniques de la pression de l'eau dans la fissure et l'historique des mouvements de la surface de contact de la fissure. La réalisation des études de cas avec un barrage typique d'une hauteur de 90 m a montré qu'une petite longueur de la fissure située près de l'ouverture (L_{sat} , longueur saturée) devient saturée et la pression de l'eau a tendance à se développer seulement sur cette longueur. La longueur saturée et la valeur de la force de soulèvement varient avec le temps. Leurs valeurs minimales se produisent en mode d'ouverture de la fissure et les valeurs maximales se produisent en mode de fermeture. La magnitude de la sous-pression développée en mode de fermeture est significative et la force de soulèvement développée peut affecter le mouvement de la surface de contact de la fissure, donc l'analyse hydromécanique couplée est nécessaire pour bien représenter le mode de fermeture. En mode d'ouverture de la fissure, la force de

soulèvement développée est petite et n'affecte pas le mouvement, l'effet de couplage hydromécanique peut être négligé pour ce cas.

On a montré que le facteur critique de sécurité en glissement pour un barrage-poids, en utilisant la méthode simplifiée de gravité, se produit en mode d'ouverture de la fissure. En utilisant DUP_CRACK, une série d'analyses paramétriques a été exécutée afin de développer une procédure pour évaluer la force de soulèvement dans des barrages-poids en béton en mode d'ouverture de la fissure. Les paramètres principaux pour calculer les forces de soulèvement sont la longueur de la fissure, la pression à l'ouverture, la fréquence dominante des mouvements des surfaces de contact, amplitude de l'ouverture, et l'ouverture résiduelle en mode de fermeture. Les paramètres principaux d'entrée pourraient être (i) estimés par les analyses d'E.F. avec des éléments de contact en utilisant des logiciels commerciaux, sans modéliser les variations des pressions dynamiques de l'eau dans les fissures, ou (ii) de la formulation simplifiée (la méthode de Chopra, la dynamique de corps rigides, Westergaard pression hydrodynamique supplémentaire).

La conclusion générale est que l'écoulement et la pression de l'eau a tendance à se développer sur une petite longueur de nouvelles fissures ou de fissures existantes des barrages-poids pendant le tremblement de terre, le reste de la fissure reste insaturée et non pressurisée. Tandis que les pressions aux frontières du secteur saturé sont indépendantes des mouvements des surfaces de contact de la fissure (pression à l'ouverture de la fissure et pression nulle au secteur insaturé), la grandeur et la distribution spatiale de la pression de l'eau le long de la partie saturée de la fissure sont variables. Pour un mode de fermeture de la fissure, la pression augmente de la valeur à l'ouverture de la fissure à une valeur maximum et puis diminue à zéro à la fin de la longueur saturée. La magnitude de la pression maximale en mode de fermeture (14 MPa le long de 2 m d'une fissure a la base d'un barrage 90 m) peut être significativement plus grande que la pression statique (0.9 MPa). En mode d'ouverture, la pression de l'eau change presque linéairement de la valeur à l'ouverture à zéro sur la longueur saturée, et la force totale de soulèvement développée est négligeable. L'analyse hydromécanique

couplée est très utile pour étudier la réponse détaillée des barrages-poids en béton fissurés soumis aux tremblements de terre.

ABSTRACT

Oscillating crack wall opening and closing modes, with the crack mouth in contact with pressurized reservoir water, are going to modify the prevailing pre-seismic uplift pressure magnitude and spatial distributions in cracked concrete dams. Uplift pressures acting along cracks and joints creates external forces that favour crack propagation in the dam body and affects the dynamic stability of cracked concrete components. Seismic uplift pressure variations during earthquakes remains a major source of uncertainty in design and safety assessment of concrete dams. Review of dam safety guidelines indicates that assumptions regarding uplift pressure intensity in a crack during an earthquake may vary from full reservoir pressure to zero pressure. The state-of-the-practice illustrates the lack of knowledge in defining transient seismic uplift pressures in existing or new cracks in concrete dams. The objective of this study is thus to develop a rational seismic crack-water hydro-mechanical model to predict dynamic uplift pressure variations during earthquakes.

An experimental study to characterize the transient seismic uplift pressure response of small concrete specimens with either newly induced or existing 0.4 m long seismic cracks was first performed. Cyclic crack wall frequency motions varying from 2 to 10 Hz were applied, with different magnitudes of crack mouth water pressures. The existing crack test results show that water pressure decreases in crack opening mode and increases in closing mode. For the first time the cavitation phenomenon is observed along the cracks in opening mode with 10 Hz excitation frequency.

A dynamic water-crack interaction model is then formulated to reproduce the experimental results, and extrapolate the computed uplift pressure variations to cracks of arbitrary lengths likely to develop in actual dams. The transient pressure gradients in a crack of specified length is modelled as a function of the crack mouth opening displacement (CMOD(t)) and crack mouth pressure ($P_{cm}(t)$) time histories assuming: (i) 1D flow along the crack, (ii) continuity condition with an incompressible fluid of a constant viscosity, (iii) pressure-flow relations governed by the crack hydraulic conductivity using variations of the so called “cubic law” accounting for the crack

roughness, laminar or turbulent flow conditions according to Reynold's number, and cavitation, (iv) impervious crack walls, and (v) residual crack aperture during cyclic motions (zero or larger). Based on the proposed model a computer program, DUP_CRACK, is developed to simulate the experimental test results. The simulated pressure and the measured pressure variations are in good agreements.

The dynamic water-crack interaction model is then implemented in a nonlinear finite element program with gap-friction elements to represent the crack and compute the related dynamic water pressure. The developed computer program, DUP_DAM, can be used for dynamic analysis of cracked dam subjected to earthquake, considering the hydro-mechanical coupling effects of water pressure in the crack and the crack wall motion histories. Performing case studies with a typical 90 m high gravity dam show that a small length of crack walls close to the crack mouth (L_{sat} , saturated length) becomes saturated and water pressure develops only along this length. The saturated length and the magnitudes of developed uplift forces changes with time, their minimum magnitudes occur during the crack opening mode and their maximum magnitudes occur in crack closing mode. The developed uplift pressure in crack closing mode is large and the developed uplift force can affect the crack wall motion. In this case, the coupled hydro-mechanical analysis is necessary. In crack opening mode, the developed uplift force is small and cannot affect the crack wall motion significantly, the hydro-mechanical coupling effect may be neglected for this case.

It was shown that the critical sliding safety factor in a gravity dam, using the simplified gravity method, occurs during the crack opening mode. Using DUP_CRACK, a series of parametric analyses were performed to develop a procedure to evaluate the uplift force in concrete gravity dams in crack opening mode. The key parameters to compute uplift forces are crack length, crack mouth pressure, dominant frequency of crack wall motions, amplitude of crack mouth opening, and crack residual opening in closing mode. To estimate the magnitude of uplift forces in the opening mode, the key input parameters could be estimated either (i) from FE analyses with gap-friction elements using commercial computer programs without modelling dynamic crack

pressure variations, or (ii) from simplified formulation (Chopra's method, rigid body dynamics, Westergaard added pressure).

The general conclusion is that water flow and pressure are developing near the crack mouth along a small length of new cracks or existing cracks of concrete gravity dams during the earthquake, the rest of the crack remains unsaturated and unpressurized. While the pressures at the boundaries of the saturated area are independent of crack wall motions (pressure at crack mouth and zero pressure at the unsaturated area), the magnitude and spatial distribution of water pressure along the saturated part of crack are variable. In crack closing mode, water pressure increases from crack mouth pressure to a maximum value and then decreases to zero at the end of the saturated length. The magnitude of maximum pressure in crack closing mode (14 MPa along the first 2 m of crack in a 90 m gravity dam) can be significantly larger than the static uplift pressure (0.9 MPa). In crack opening mode, water pressure changes almost linearly from crack mouth pressure to zero along the saturated length, and the developed total uplift force is small. A simple qualitative description for transient uplift force during crack opening is an uplift force varying between zero and unchanged uplift force assumptions. The full uplift force assumption is too conservative. A rigorous novel quantitative water-crack interaction model has been developed in the thesis to quantify the uplift force in crack opening mode. The developed pressure during the crack closing mode may not propagate crack but the water-crack hydro-mechanical coupling analysis is a useful tool to investigate the detailed response of cracked concrete gravity dams subjected to earthquakes.

CONDENSÉ EN FRANÇAIS

L'évaluation de la sécurité sismique des barrages-poids en béton nouveaux et existants est un souci important dans les régions où le risque de tremblements de terre est élevé, dû à la possibilité des dommages catastrophiques que peut causer un relâchement soudain de réservoir si le barrage est endommagé sous de fortes secousses sismiques. La plupart des mécanismes sismiques de rupture de barrages-poids commencent en développant des nouvelles fissures ou en propageant les fissures existantes, qui pourraient être produites par des chargements sévères (dû aux tremblements de terre, aux inondations), des variations thermiques, les réactions alcali-agrégat, ou autres conditions environnementales. La fissuration sur la face amont du barrage, ou aux joints horizontaux de construction, permet la pénétration de l'eau, créant de la traction externe sur les surfaces de contact d'une fissure ou d'un joint. La sous pression résultante crée des forces externes qui tendent à propager les fissures et peuvent compromettre l'équilibre global des forces requises pour la stabilité structurale. Les interactions statiques et sismiques de l'eau-fissure (ou de l'eau-joint), et ses influences sur la propagation des fissures est l'un des plus importants aspects pour évaluer la stabilité d'un barrage-poids. Les valeurs appropriées de sous-pression à utiliser dans des analyses structurales, statiques et sismiques, des barrages en béton ont été le sujet de plusieurs discussions au cours du dernier siècle.

La revue des guides de sécurité des barrages, comme CDSA 1997, USACE 1995, FERC 2002, USBR 1987, et ICOLD 1986, indiquent que la recommandation concernant l'intensité de la pression de soulèvement dans une fissure pendant un séisme peut varier entre la pleine pression du réservoir et la pression nulle. Le manque de connaissance sur ce sujet et la nécessité des recherches ont été également soulignés par les chercheurs autant que par les ingénieurs praticiens. Pour une formulation appropriée de la pression transitoire de soulèvement à l'intérieur d'une fissure avec les surface de contact en mouvement, des travaux expérimentaux doivent être réalisés afin d'étudier l'influence des différents paramètres comme l'amplitude de l'ouverture de la fissure, l'ouverture et la

fréquence de fermeture, la sous-pression initiale de l'eau, la rugosité de la fissure, et sa géométrie.

Revue de la littérature

La revue de la littérature disponible indique que peu d'études sur le sujet de la sous-pression dynamique dans les barrages en béton, ont été réalisées. Il y a deux études qui ont discuté expressément de la force dynamique de soulèvement dans les barrages fissurés pendant un séisme. La première est une solution théorique présentée par Tinawi et Guizani (1994) pour formuler la pression dynamique de l'eau dans une entaille existante, et la deuxième est une formulation théorique soutenue par des données expérimentales concernant la pression dynamique évaluée pour de nouvelles fissures, par Slowick et Saouma (1994, 2000). En raison des aspects semblables de l'écoulement de l'eau dans les joints de roc et dans les fissures en béton, les résultats des recherches au sujet de l'interaction eau-joint issus de la mécanique des roches peuvent être utilisés dans cette étude. De nombreuses études expérimentales prouvent que la loi cubique bien connue pour le flux de fluide entre deux plaques parallèles peut être employée avec une modification pour l'écoulement de l'eau dans les fissures de béton et les joints de roc.

Travaux expérimentaux et résultats

L'objectif principal du programme expérimental a été défini afin de mesurer les variations de pression dynamiques de l'eau à l'intérieur des fissures en béton avec les surfaces de contact en mouvement. Deux procédures ont été développées pour mesurer la pression de l'eau dans les fissures nouvelles et existantes en utilisant le même spécimen. Cinq spécimens en béton (1.5x0.55x0.15 m) ont été utilisés pour réaliser cinq nouveaux essais de fissuration et plus de 250 essais avec une fissure existante pour étudier les influences des différents paramètres sur les variations de la pression de l'eau développée dans la fissure. La longueur moyenne de la fissure était presque 0.40 m. En utilisant un banc d'essai où les déplacements sont contrôlés, des déplacements harmoniques et des déplacements sismique ont été appliqués pour activer les surfaces de

la fissure en mouvements dynamiques. Les paramètres principaux étaient la fréquence d'excitation, la pression de l'eau à l'ouverture de la fissure, l'ouverture initiale de la fissure dans les essais avec une fissure existante et l'amplitude de l'ouverture durant les mouvements harmoniques.

Le montage pour les essais et les résultats typiques des mesures des pressions pour une nouvelle fissure et une fissure existante sont présentées aux figures 1,2 et 3.

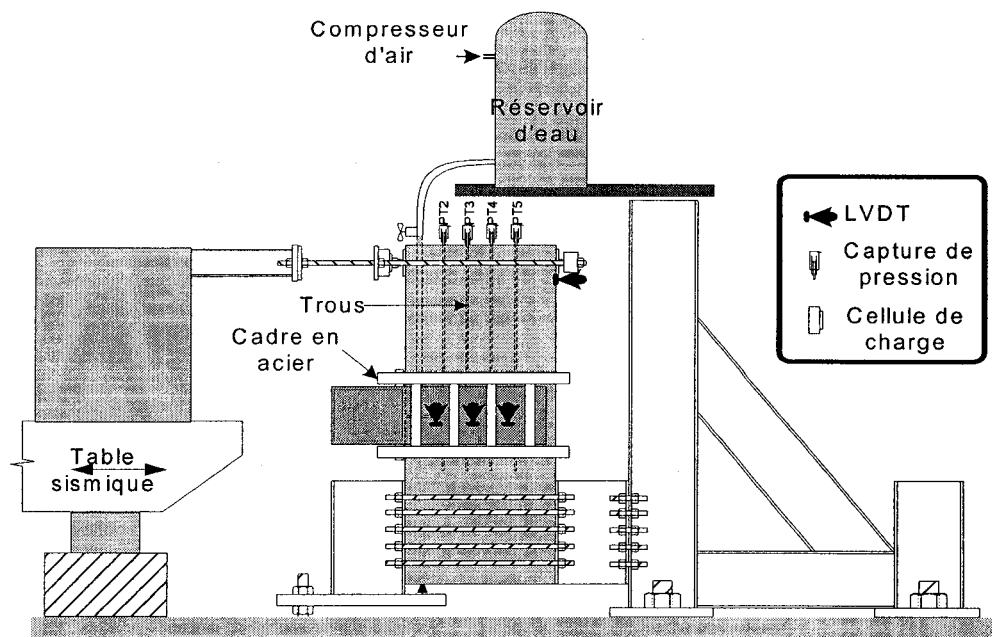


Figure 1. Banc d'essai.

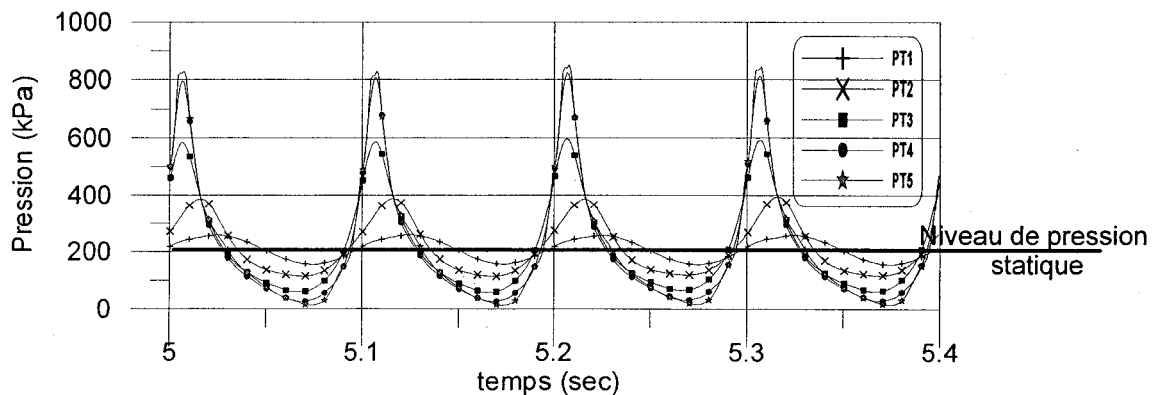


Figure 2. Résultats typique fissure existant.

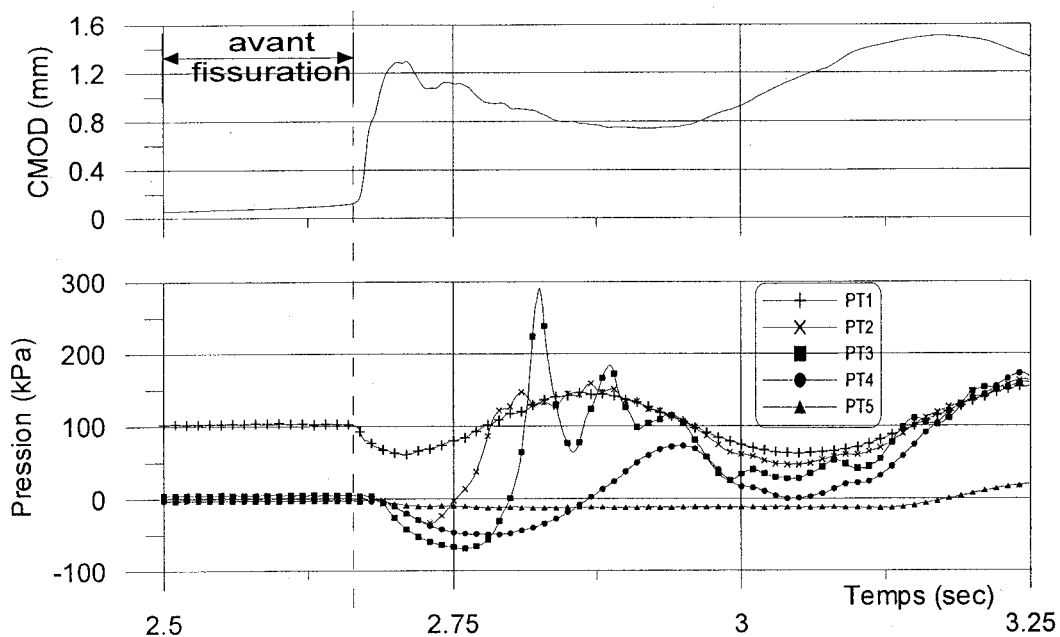


Figure 3. Résultats typiques - nouvelle fissure.

Les résultats principaux des travaux expérimentaux peuvent être résumés en les reliant à la condition initiale de fissuration (nouvelle fissure ou fissure existante). Ces résultats principaux sont :

Fissures existantes :

Dans une fissure saturée en béton avec les surfaces de contact en mouvement, la pression de l'eau n'est pas constante. Elle augmente pendant le mode de fermeture de la fissure et diminue pendant le mode d'ouverture.

- La pression statique initiale de l'eau n'a aucune influence sur la magnitude des variations de la pression dynamique développées à l'intérieur de la fissure si la cavitation ne se produit pas.
- La valeur absolue de l'amplitude de la pression dynamique augmente en s'éloignant de l'ouverture jusqu'à une valeur maximale, qui est située proche de cette ouverture de la fissure, et diminue de ce point de maximum jusqu'à la fin de la fissure.

- L'amplitude d'ouverture de la fissure et la fréquence de l'excitation peuvent être interprétées comme la vitesse des surfaces de contact en mouvement de l'ouverture et de fermeture. Alors, l'ouverture de la fissure et la vitesse de sa fermeture semblent avoir la plus importante influence sur le développement de la pression dans la fissure dont les surfaces de contact sont en mouvement.
- Le phénomène de cavitation se produit dans le cas des fréquences d'excitations de 6 Hz et de 10 Hz avec de faibles pressions statiques initiales. L'occurrence de la cavitation induit des impulsions de pression à haute fréquence dans le système.

Nouvelles fissures:

- La vitesse du front de l'eau est en fonction de l'ouverture de la fissure, de la pression statique à l'ouverture et probablement de la rugosité et de la perméabilité de la fissure. La vitesse estimée pour les conditions d'essais (COD=0.2-2millimètre et $P_{stat}=400$ kPa) est autour de 1400-2000 mm/sec.
- Des pressions négatives peuvent être développées dans le vide créé par la fissure. La pression négative, si assez basse, peut causer le phénomène de cavitation. Alors les oscillations de hautes pressions sont induites par l'explosion de la bulle de vapeur.

Le modèle théorique

Le concept de modélisation de la pression de l'eau pour une fissure dont les surfaces de contact sont en mouvement est présenté. On a prouvé que la compressibilité de l'eau peut être ignorée en écrivant l'équation de continuité. Basé sur l'équation de continuité et présumant une fissure conique avec les surfaces de contact en mouvement, une expression pour l'écoulement de l'eau le long de la fissure est dérivée. Basé sur le régime d'écoulement de l'eau à l'intérieur de la fissure, des équations d'écoulements laminaires ou turbulents sont utilisées pour évaluer le gradient de pression le long de la fissure. Les variations de la pression hydrodynamiques peuvent être évaluées par l'intégration du gradient estimé de la pression le long de la fissure selon les équations ci-dessous :

$$\text{Laminaire: } \frac{dp(x,t)}{dx} = 6\mu \left[1 + 8.8 \left(\frac{k}{2u(x,t)} \right)^{1.5} \right] \frac{L^2}{x} \frac{\dot{u}_L(t)}{u_L^3(t)}$$

$$\text{Turbulent: } \frac{dp(x,t)}{dx} = \frac{\rho g}{24 \left(\log \frac{1.9}{k/2u(x,t)} \right)^2} x L \frac{\dot{u}_L^2(t)}{u_L^3(t)}$$

$$p = p_{stat} + p_{dyn}(x,t) = P_{stat} + \int_L^{L_t} [dp(x,t)]_{turbulent} + \int_L^x [dp(x,t)]_{laminaire}$$

Où L est la longueur de la fissure, u_L et \dot{u}_L sont le déplacement et la vitesse de l'ouverture la fissure, respectivement, x est la distance à partir du bout de la fissure, ρ et μ sont la densité de masse et la viscosité dynamique de l'eau, et k est la rugosité des surfaces de contact de la fissure. Les pressions hydrodynamiques calculées à l'aide du modèle développé, sont en bon accord avec les résultats des essais, sauf pour les basses pressions où la cavitation peut se produire. Le modèle développé est ensuite modifié en considérant l'écoulement de l'eau le long de la partie saturée de la fissure en cas d'occurrence de cavitation. Basé sur le modèle proposé, un logiciel est développé et validé en simulant les résultats des essais expérimentaux avec les fissures existantes et nouvelles (dont les longueurs sont limitées à 0.4 m). Les figures 4 et 5 présentent les résultats typiques pour une nouvelle fissure et une fissure existante. En utilisant le logiciel développé, les effets de la longueur de la fissure sur la pression hydrodynamique sont étudiés en calculant la pression de l'eau dans les fissures de différentes longueurs.

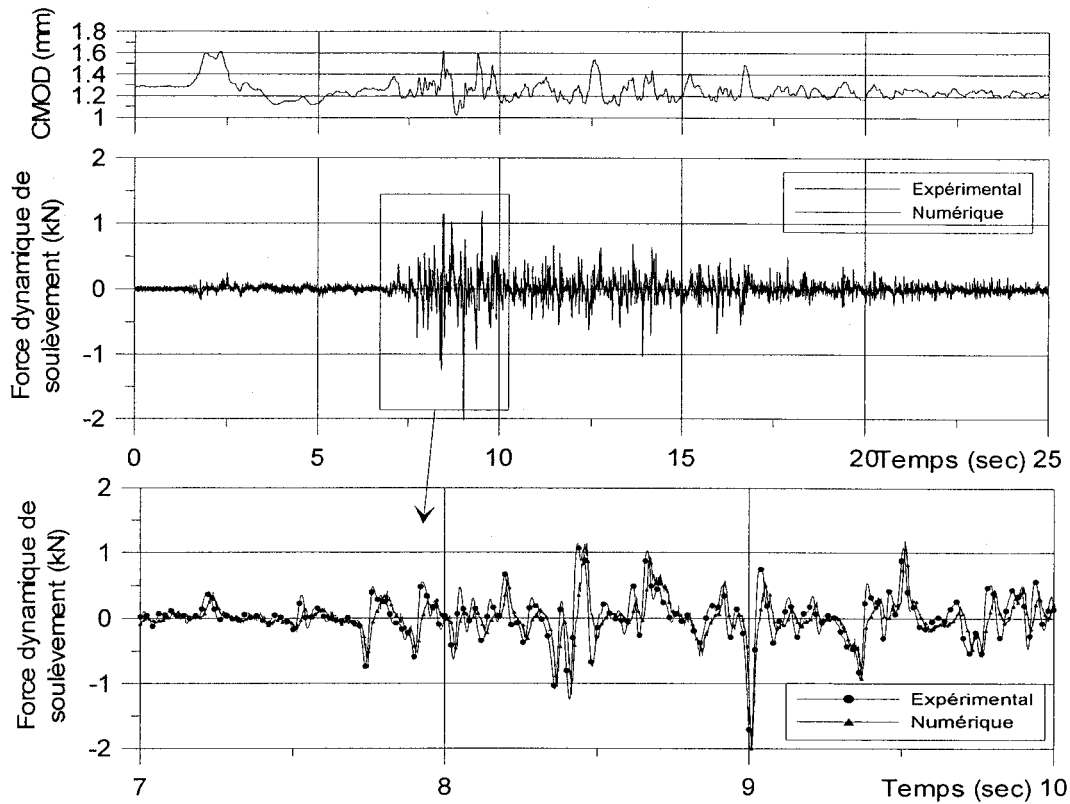


Figure 4. Essai no. PS4-81, et PS4-84 et simulations numériques correspondantes pour l'excitation sismique (Saugenay 1988 modifié).

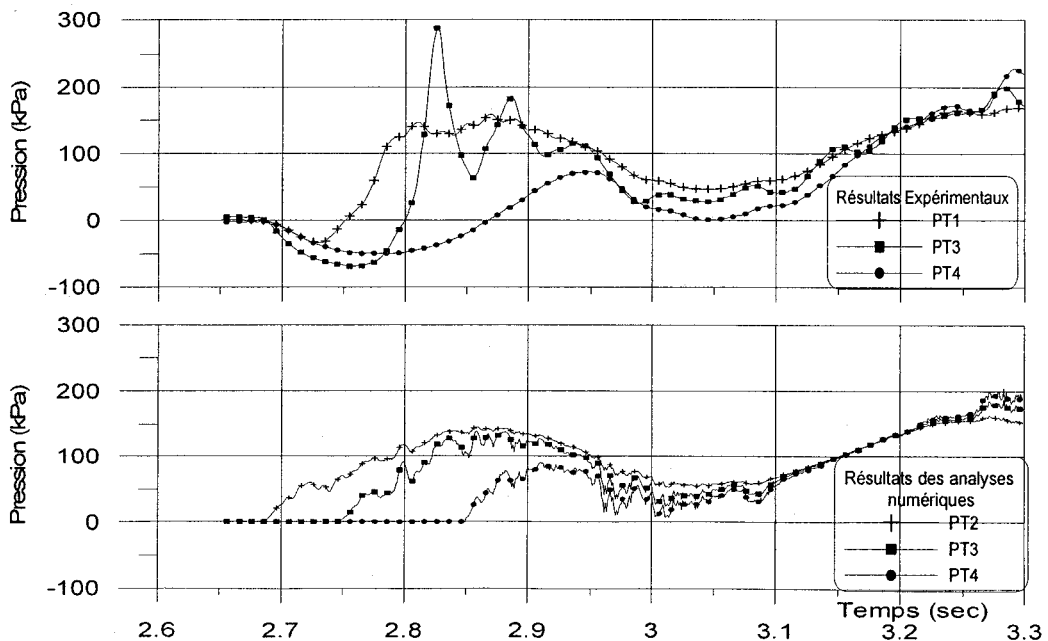


Figure 5. Résultats typiques pour une nouvelle fissure et simulations numériques.

Applications

Le modèle développé du calcul de la pression de l'eau dans les fissures avec les surfaces de contact en mouvement a été mis en application dans un logiciel d'éléments finis non linéaire en utilisant des éléments de contact pour l'analyse d'un barrage-poids fissuré où l'influence du couplage eau-fissure est incluse. La pression hydrodynamique développée est considérée en tant que force externe dans l'équation d'équilibre dynamique et la méthode modifiée de Newton-Raphson est utilisée pour les itérations d'équilibre. Le modèle développé est utilisé pour étudier les variations de pression de l'eau dans les fissures des barrages-poids en béton soumis aux tremblements de terre.

Les variations de la pression d'eau dans les fissures des barrages-poids en béton sont différentes en mode d'ouverture de la fissure par rapport au mode de fermeture. En mode d'ouverture, l'écoulement se développe dans une région près de l'ouverture de la fissure, une région saturée (L_{sat}), et le reste de la fissure est remplie de vapeur d'eau dû au phénomène de cavitation. La longueur de la région saturée change pendant le mode d'ouverture et sa grandeur est en fonction de la pression à l'ouverture (frontière) de la fissure, la magnitude de l'ouverture, la vitesse d'ouverture. La pression se développe dans cette région et sa grandeur à l'ouverture de la fissure est égale à la pression existante à ce moment et diminue vers le bout de la fissure, presque linéairement, vers zéro à la fin du secteur saturé. La longueur minimum de saturation peut être aussi petite que 0.1 m dans un barrage fissuré soumis à une forte excitation de tremblement de terre, et peut être augmentée jusqu'à 10 m dans les cas où l'excitation de la fissure est très lente. Une méthode simplifiée pour estimer la pression de l'eau en mode d'ouverture des fissures est développée. Cette méthode peut être utilisée pour une analyse sismique de stabilité des barrages en béton en utilisant les méthodes pseudo-statique et pseudo-dynamique.

Bien que la pression se développe dans une région courte près de l'ouverture de la fissure en mode d'ouverture, les mouvements cycliques des surfaces de contact de la

fissure remplissent, graduellement, l'ouverture résiduelle de la fissure à chaque mode de fermeture. La force de soulèvement augmente pendant que l'eau pénètre à l'intérieur de la fissure. La force de soulèvement augmentée insère une force de résistance contre le mouvement de fermeture de la fissure, ce qui réduit la vitesse de fermeture de la fissure, par rapport à une fissure sèche. Si la force induite de soulèvement est assez élevée par rapport à la force de fermeture de la fissure, elle peut l'empêcher de se fermer complètement, ou bien empêcher l'impact des surfaces de contact réduisant la vitesse de fermeture, ce qui causera une diminution importante de la pression de l'eau. La pression développée le long de la fissure est principalement gouvernée par l'effet de couplage mécanique-hydraulique. Il est utile d'effectuer une analyse couplée pour déterminer la réponse de barrage-poids soumis aux tremblements de terre afin de déterminer la pression le long de la fissure en mode de fermeture.

Il est montré que le facteur critique de sécurité au glissement pour un barrage-poids, en utilisant la méthode simplifiée de gravité, se produit en mode d'ouverture de la fissure. En utilisant le logiciel DUP_CRACK, une série d'analyses paramétriques a été exécutée pour développer une procédure d'évaluation de la force de soulèvement pour les barrages-poids en béton en mode d'ouverture de la fissure. Les paramètres principaux pour calculer les forces de soulèvement sont la longueur de la fissure, la pression à l'ouverture de la fissure, la fréquence dominante des mouvements des surfaces de contact, l'amplitude de l'ouverture, et l'ouverture résiduelle en mode de fermeture. Les paramètres principaux d'entrée pourraient être estimés par (i) des analyses d'éléments finis avec des éléments de contact en utilisant des logiciels commerciaux sans modéliser des variations de pressions dynamiques dans la fissure, ou (ii) par formulations simplifiées (la méthode de Chopra, la dynamique des corps rigides, la pression hydrodynamique de Westergaard).

Conclusions

La réponse dynamique d'un barrage-poids en béton soumis aux tremblements de terre est influencée par l'effet hydromécanique de couplage de la pression développée dans les fissures. Le degré de couplage change selon les propriétés structurales du barrage, l'intensité du tremblement de terre, et les caractéristiques développées de la fissure. Il est utile d'effectuer une analyse dynamique pour chaque barrages-poids en béton si on désire quantifier la réduction des forces de soulèvement lors du mode d'ouverture de la fissure. Les conclusions suivantes peuvent être tirées comme directives basées sur les résultats des résultats de cette recherche.

Des analyses prouvent que les mouvements cycliques des surfaces de contact de la fissure dans les barrages en béton pendant un tremblement de terre pousse l'eau dans la fissure pendant le mouvement de fermeture (si une ouverture résiduelle existe en mode de fermeture). Par conséquent la prétention que la nature rapide d'oscillation de l'ouverture et de fermeture la fissure ne permet pas à l'eau de réservoir de pénétrer dans la fissure (USBR 1987) peut être fortement remise en question.

La pression dynamique se développe dans une région près de l'ouverture de la fissure. La magnitude de la pression de l'eau est importante pendant le mode de fermeture de la fissure. Pour un barrage de 90 m soumis au tremblement de terre du Saguenay de 1988 avec une accélération de pointe au roc amplifiée à 0.35 g, la pression maximale pour une fissure de 2.0 m était de 14000 kPa. Cette pression est équivalente une force de soulèvement de 15000 kN et son point d'application est près de l'ouverture de la fissure (l'importance de la force statique de soulèvement est égale au 19800 kN).

Dû à la courte longueur saturée pendant le mode d'ouverture de la fissure, la force de soulèvement est non pas zéro mais relativement petite. Une constatation générale pour la pression de l'eau pendant le mode d'ouverture de fissure est que la magnitude se situe entre la sous pression nulle (USBR 1987, des zones sismiques à risque élevé de CDSA 1997) et la sous-pression constante (zone sismique à risque faible d'USACE 1995, de FERC 2002, de CDSA 1997). La magnitude de la force de soulèvement dépend

des caractéristiques de l'ouverture de la fissure et de la pression à l'ouverture de la fissure. Un nouveau modèle constitutif d'interaction eau-fissure a été développé dans cette thèse afin de quantifier la magnitude de la sous-pression sismique en mode d'ouverture d'une fissure. La supposition de la pleine sous-pression dans la fissure (ICOLD 1986) semble être très conservatrice pour le calcul de stabilité des barrages en béton fissuré pendant un tremblement de terre.

TABLE OF CONTENTS

ACKNOWLEDGEMENTS.....	iv
RÉSUMÉ.....	v
ABSTRACT.....	ix
CONDENSÉ EN FRANÇAIS.....	xii
TABLE OF CONTENTS.....	xxiii
LIST OF TABLES.....	xxviii
LIST OF FIGURES.....	xxvii
NOTATION.....	xxxv
CHAPTER 1 INTRODUCTION	1
1.1 Overview	1
1.2 Research problem.....	6
1.3 Objectives of the research	11
1.4 Original contributions of the thesis.....	12
1.5 Organisation of the thesis.....	12
CHAPTER 2 WATER PRESSURE IN CRACKS AND JOINTS OF	
CONCRETE DAMS: STATE-OF-THE-ART	14
2.1 Introduction	14
2.2 Seismic analysis of gravity dams	14
2.2.1 Discrete crack model.....	16
2.2.2 Smearred crack model	19
2.3 Uplift pressure	20
2.3.1 Pore pressure in porous media	20
2.3.2 Static uplift pressure in gravity dams.....	22
2.3.3 Dynamic uplift pressure	23
2.3.4 Static uplift pressure calculation methods	25

2.4	Water flow in cracks	27
2.4.1	Water flow in single crack	27
2.4.2	Uplift water pressure based on the water flow in crack	30
2.4.3	Numerical methods for hydro-mechanical coupled analysis in rock mechanics.....	32
2.4.4	Uplift pressure in fracture process zone.....	34
2.5	Transient seismic uplift in concrete cracks of gravity dams	36
2.5.1	Transient uplift in propagating cracks.....	37
2.5.2	Transient uplift in existing saturated cracks.....	41
2.5.3	Transient uplift due to variations in crack mouth pressure	44
2.5.4	Computer programs for seismic dam analysis	46
2.6	Compressibility of water	46
2.6.1	Cavitation	48
2.7	Conclusions.....	49
CHAPTER 3 EXPERIMENTAL PROGRAM		52
3.1	Introduction	52
3.2	Earthquake response of gravity dams and development of the experimental program.....	52
3.2.1	Selection of experimental test variables.....	54
3.2.2	Objectives of experimental program.....	54
3.3	Test set up	55
3.3.1	Geometry of specimens.....	55
3.3.2	Test set up	55
3.3.3	Instrumentation	58
3.4	Testing procedures	59
3.4.1	New crack test (specimens cracked during the test)	59
	• Supporting the specimens	59
	• Confinement of specimens.....	59

•	Filling the holes with water.....	61
•	Application of water pressure	61
•	Application of cracking displacement.....	62
3.4.2	Existing crack tests (pre-cracked specimens tests)	62
3.5	Verification of test set up	63
3.5.1	Confinement detail.....	64
3.5.2	Adding steel tank to test set up	65
3.5.3	Pressure transducer verification	68
3.6	Conclusions.....	70
CHAPTER 4 EXPERIMENTAL RESULTS AND DISCUSSIONS.....		71
4.1	Introduction.....	71
4.2	Test results as measured in the laboratory	71
4.2.1	Crack deformations	74
4.3	Existing crack tests.....	76
4.3.1	Initial static uplift pressure.....	76
4.3.2	Amplitude of crack opening during harmonic excitations.....	80
4.3.3	Frequency of harmonic excitations	80
4.3.4	Crack opening velocity during harmonic excitations.....	81
4.3.5	Minimum crack opening during harmonic excitations	83
4.3.6	Variations of pressures along crack length	83
4.3.7	Cavitation phenomenon	85
4.4	New crack tests	86
4.4.1	Steady-state response	86
4.4.2	Transient response.....	88
4.5	Conclusions.....	93
CHAPTER 5 WATER-CRACK INTERACTION MODEL		96
5.1	Introduction.....	96
5.2	Dynamic water pressure.....	97

5.3	Developed pressure based on the water flow in the crack	102
5.4	Modification for singularity	108
5.5	Modification for cavitation	109
5.6	Extension of the procedure to cracks with longer lengths	110
5.6.1	Assumptions.....	112
5.6.2	Extended computational procedure.....	114
5.6.3	Computer code developing and checking of the procedure	115
5.7	New crack vs existing crack.....	119
5.8	Crack length effects.....	122
5.8.1	Investigation of pressure variations in a 4 m existing crack	122
5.8.2	Investigation of pressure variations in a 4 m new crack	125
5.8.3	Crack length effects.....	126
5.9	Conclusions	131
CHAPTER 6 NUMERICAL SIMULATIONS AND CASE STUDIES		134
6.1	Introduction.....	134
6.2	Finite element analysis of dam considering dynamic uplift pressure	134
6.2.1	Dynamic equilibrium equation.....	135
6.2.2	Dynamic equilibrium equation for hydrodynamic coupling.....	136
6.3	Effect of coupling in developed crack water pressures.....	137
6.4	Recommendation for industrial application.....	146
6.4.1	Opening mode vs closing mode	146
6.4.2	Opening crack mode	147
6.5	Sliding safety factor of 90 m dam.....	153
6.6	Conclusions.....	153
CHAPTER 7 CONCLUSIONS.....		157
7.1	Summary of thesis.....	157
7.2	Conclusions	159
7.3	Future research and developments.....	164

7.3.1	Experimental research on transient uplift force	164
7.3.2	Theoretical formulation and numerical analysis of transient water-crack pressure.....	166
7.3.3	Seismic safety analysis of dam considering water-crack interactions	167
REFERENCES.....		168

LIST OF TABLES

Table 1.1 Concrete dams which have been subjected to significant earthquake (adapted from CEA ¹ 1990, Knight and Mason ² 1992, USCOLD ³ 1992).....	2
Table 2.1 Flow laws (Louis 1969) (Note in table: $b=e$ and $D_h=2e$).	31
Table 2.2 Samples of results from water-crack front velocity tests on concrete specimens (Saouma and Morris 1997)	40
Table 3.1 New crack tests.	63
Table 3.2 Pre-cracked tests	64
Table 4.1 Test parameters and water front velocities for new tests.	86
Table 5.1 Calculation of dV_w for PT3 based on PS4-09 test results ($P_{stat}=100$ kPa, $f=10$ Hz, $CMOD_{amp}=0.7$, $CMOD_{min}=1.0$ mm) and equations 5.1, 5.2.....	101
Table 6.1 Values of L_{satmin} in equation 6.7.....	150

LIST OF FIGURES

Figure 1.1 Sefid-Rud (Iran) buttress dam (106 m), after earthquake of magnitude 7.3 in 1990.....	3
Figure 1.2 Sefid-Rud dam,.....	4
Figure 1.3 Seismic cracking of Koyna dam (adapted from Hall 1988).	4
Figure 1.4 Hsingfengkiang dam (adapted from Chen et al., 1982).....	5
Figure 1.5 Seismic failure mechanisms of concrete gravity dams (adapted from Tinawi et al. 1998).....	6
Figure 1.6 Transient uplift pressure variations in a crack during earthquake according to different dam safety guidelines.	8
Figure 1.7 Seismic stability of typical concrete gravity dam (with drain) using different uplift pressure assumptions.	10
Figure 2.1 Seismic analysis of gravity dams.....	15
Figure 2.2 Progressive methodology for seismic analysis of dams (Tinawi et al. 1998).....	17
Figure 2.3 Pore pressure and crack pressure distributions.....	21
Figure 2.4 Parameters affecting the uplift pressures (Tinawi et al. 1998).	23
Figure 2.5 Variation of uplift pressures inside cracks during earthquakes: comparisons between new and existing cracks.....	25
Figure 2.6 Fracture geometry.....	28
Figure 2.7 An empirical relation incorporating joint roughness (JRC) and aperture which broadly satisfies the trends exhibited by available flow data (Barton 1985).	29
Figure 2.8 Flow laws (Louis 1969) (Note in figure: $b=e$; $D_h=2e$).....	31
Figure 2.9 UDEC water-crack interaction model; a is hydraulic aperture, a_0 is aperture for zero normal contact stress condition, Δa is aperture change due to mechanical stress, $K_w=\beta$, $k_j=12/\mu$	33
Figure 2.10 Experimental test set up (Bruhwiler and Saouma 1995).....	35

Figure 2.11 Normalized pressure-versus-crack opening displacement curve (Bruhwiler, Saouma 1995).....	36
Figure 2.12 Experimental set up (Slowik and Saouma 1994).....	38
Figure 2.13 Load and water pressure versus CMOD for different CMOD rates (Slowik and Saouma 2000).	39
Figure 2.14 Crack and water front versus CMOD for slow and fast loading (Slowik and Saouma 2000).	39
Figure 2.15 Water pressure in crack for cyclic loading with changing frequency and amplitude (Slowik and Saouma 1994).....	40
Figure 2.16 Geometry of assumed crack (Tinawi and Guizani 1994).....	43
Figure 2.17 Experimental setup and details of specimens (Ohmachi et al. 1998).....	45
Figure 2.18 Effect of changing shape of a fracture for a fracture with 1 cm opening at left end (open end) and different opening (from .1 to 1.9 cm) at right end (close end).	47
Figure 2.19 Bilinear equation of state for water.	48
Figure 2.20 Computed response of one dimensional fluid-structure system to harmonic ground motion (1 in.=0.025m ; 10 psi=70 kPa) (Fenves and Vargas-Loli 1988).	49
Figure 2.21 Comparisons of research studies about transient water pressure inside concrete cracks due to earthquake.	51
Figure 3.1 Dynamic pressure due to earthquake in cracks of a gravity dam.	53
Figure 3.2 Specimen geometry (dimensions in m).	56
Figure 3.3 Test set up.	57
Figure 3.4 Test set up in laboratory.	58
Figure 3.5 First glued layer of membrane with steel reservoir in front of the specimen.	60
Figure 3.6 Full confinement of specimen.	60
Figure 3.7 Pressure transducer and water tank.....	61
Figure 3.8 Harmonic displacement for new crack tests.	62

Figure 3.9 Harmonic displacement for pre-cracked tests.....	64
Figure 3.10 Test without steel reservoir in front of notch (10 Hz).	66
Figure 3.11 Test with steel reservoir in front of notch (10 Hz).	67
Figure 3.12 Pressure transducer verification tests, test set up and typical results.	69
Figure 4.1 Measured parameters (applied load and crack aperture) in an existing crack test (Test no. PS4-2, $P_{stat}=200$ kPa, $f=10$ Hz, $CMOD_{amp}=0.6$ mm, $CMOD_{min}=0.6$ mm).....	72
Figure 4.2 Measured water pressure in an existing crack test (Test no. PS4-2, $P_{stat}=200$ kPa, $f=10$ Hz, $CMOD_{amp}=0.6$ mm, $CMOD_{min}=0.6$ mm).....	73
Figure 4.3 Specimen deformation and rigid crack walls.....	75
Figure 4.4 Rigid body deformation of crack walls (Test no. PS4-2, $P_{stat}=200$ kPa, $f=10$ Hz, $CMOD_{amp}=0.6$ mm, $CMOD_{min}=0.6$ mm).....	75
Figure 4.5 Effect of static pressures on total pressure variations: (A) test no. PS4-73, $P_{stat}=200$ kPa, $f=10$ Hz, $CMOD_{amp}=0.35$ mm, $CMOD_{min}=1.0$ mm; (B) test no. PS4-74, $P_{stat}=300$ kPa, $f=10$ Hz, $CMOD_{amp}=0.35$ mm, $CMOD_{min}=1.0$ mm.	77
Figure 4.6 Dynamic pressure in PT4 for tests (A) and (B) in Fig. 4.5.....	79
Figure 4.7 Effect of $CMOD_{amp}$ on developed dynamic forces in three typical tests. (Tests no. PS4-24, PS4-25, PS4-26, $U_{stat}=12$ kN, $P_{stat}=200$ kPa, $f=6$ Hz, $CMOD_{min}=1.0$ mm).....	80
Figure 4.8 Effect of frequency content on developed dynamic forces in three typical tests. (Tests no. PS4-22, PS4-25, PS4-28, $U_{stat}=12$ kN, $P_{stat}=200$ kPa, $CMOD_{amp}=0.50$, $CMOD_{min}=1.0$ mm).....	81
Figure 4.9 Comparison of dynamic pressure variations with crack mouth opening velocity variations. (Test no. PS2-19, $P_{stat}=200$ kPa, $CMOD_{amp}=0.65$ mm, $CMOD_{min}=1.0$ mm).....	82
Figure 4.10 Effect of CMOV on developed dynamic forces. (Test no. PS6-51 to PS6-58, $U_{stat}=24$ kN, $P_{stat}=400$ kPa, $CMOD_{amp}=0.4-0.8$ mm, $CMOD_{min}=1.0$ mm).....	82

Figure 4.11 Effect of $CMOD_{min}$ on developed dynamic force in crack. (Tests no. PS4-27, PS4-37, PS4-47, $U_{stat}=12$ kN, $P_{stat}=200$ kPa, $f=10$ Hz, $CMOD_{amp}=0.4$ mm).	83
Figure 4.12 Variations of water pressures along crack length for opening and closing modes. (Test no. PS4-07, $P_{stat}=100$ kPa, $f=10$ Hz, $CMOD_{amp}=0.27$ mm, $CMOD_{min}=0.95$ mm, Test no. PS4-17, $P_{stat}=100$ kPa, $f=10$ Hz, $CMOD_{amp}=0.41$ mm $CMOD_{min}=1.55$ mm).	84
Figure 4.13 High frequency pressure oscillations after cavitation. (Test no. PS3-82, $P_{stat}=100$ kPa, $f=10$ Hz, $CMOD_{amp}=0.35$ mm, $CMOD_{min}=1.0$ mm).	86
Figure 4.14 Transient and steady-state uplift force in a new crack compared to response in an existing crack. (test no. NS1, and PS3-03, $U_{stat}=6$ kN, $P_{stat}=100$ kPa, $CMOD_{amp}=0.8$ mm, $CMOD_{min}=0.9$ mm).	87
Figure 4.15 Transient and steady-state uplift forces in a new crack compared to response in existing crack. (test no. NS5, and PS2-06, $U_{stat}=12$ kN, $P_{stat}=200$ kPa, $CMOD_{amp}=0.3$ mm, $CMOD_{min}=0.4$ mm).	87
Figure 4.16 New crack test results (NS1).	90
Figure 4.17 New crack test results (NS2).	90
Figure 4.18 New crack test results (NS3).	91
Figure 4.19 New crack test results (NS4).	91
Figure 4.20 New crack test results (NS5).	92
Figure 5.1 Piston-cylinder model for water crack-interaction.	98
Figure 5.2 Piston-cylinder model for a crack with moving walls.	98
Figure 5.3 Tapered crack geometry.	99
Figure 5.4 Results of test no PS4-17 ($U_{stat}=6$ kN, $P_{stat}=100$ kPa, $f=10$ Hz, $CMOD_{amp}=0.5$ mm, $CMOD_{min}=1.6$ mm).	105
Figure 5.5 Simulated results for test shown in Fig. 5.4.	106
Figure 5.6 Comparisons between measured and computed uplift force (test no. PS4-17).	107

Figure 5.7 Comparisons between measured and computed results for 2 Hz excitation (test no. PS5-53; $U_{stat}=24$ kN, $P_{stat}=400$ kPa, $CMOD_{amp}=0.8$ mm, $CMOD_{min}=1.15$ mm).....	107
Figure 5.8 Comparisons between measured and computed results for 6 Hz excitation (test no. PS5-56; $U_{stat}=24$ kN, $P_{stat}=400$ kPa, $CMOD_{amp}=0.8$ mm, $CMOD_{min}=1.15$ mm).....	107
Figure 5.9 Comparisons between measured and computed results for 10 Hz excitation (test no. PS4-08 $U_{stat}=6$ kN, $P_{stat}=100$ kPa, $CMOD_{amp}=0.45$ mm, $CMOD_{min}=1.0$ mm).....	108
Figure 5.10 Modification for singularity at crack tip.....	109
Figure 5.11 Modification for cavitation (test no. PS4-08 from Fig. 5.9).....	110
Figure 5.12 Numerical simulation results for dynamic pressure variations along a 4 m crack subjected to the same wall motions as test no. PS4-17 in Fig.5.4.....	111
Figure 5.13 Water flow and pressure distributions for a long crack.....	113
Figure 5.14 Test no. PS4-81 and corresponding numerical simulation results for earthquake case (El Centro 1940).....	117
Figure 5.15 Test no. PS4-81 and corresponding numerical simulation results for earthquake case (Saguenay 1988).....	118
Figure 5.16 Opening mode of: (a) an existing crack, and (b) a new crack.....	120
Figure 5.17 Simulated and measured pressures for new crack test no. NS1.....	121
Figure 5.18 Simulated and measured pressures for new crack test no. NS3.....	121
Figure 5.19 Simulated pressures for new crack test no. NS3 after modification for additional losses.....	122
Figure 5.20 CMOD variations in a 4 m crack.....	123
Figure 5.21 Pressure variations in a 4m crack with harmonic wall motion ($f=2$ Hz).....	123
Figure 5.22 Spatial pressure variations along a 4m crack in opening mode ($f=2$ Hz).....	124

Figure 5.23 Spatial pressure variations along a 4m crack in closing mode ($f=2$ Hz)	124
Figure 5.24 Pressure development along a new 4m crack due to harmonic motion ($P_{stat}=500$ kPa, $CMOD_{amp}=1.0$ mm, $CMOD_{min}=0.5$ mm, $f=2$ Hz).	127
Figure 5.25 Pressure variations along a 4 m new crack in opening and closing modes at different cycles of harmonic oscillation of crack walls (to show the pressure variations in more details, pressure curves in part (a) has been cut at the magnitude of 1000 kPa).	128
Figure 5.26 Numerical simulation results for cracks with 3 different lengths ($L=4$ m, 8 m, and 12 m; $P_{stat}=1000$ kPa, $f=2$ Hz, $CMOD_{min}=0.5$ mm , $CMOD_{amp}=1.0$ mm).	129
Figure 5.27 Pressure variations in opening mode for three different crack lengths.	130
Figure 6.1 Dam model assuming a rigid foundation and applied base accelerations. ...	138
Figure 6.2 Coupled and uncoupled responses of a 90 m dam subjected to a sinusoidal earthquake record ($\ddot{u}_g(t) = 0.35g \sin 2\pi ft$; $f=10$ Hz).	140
Figure 6.3 Coupled and uncoupled transient responses of a 90 m dam subjected to a sinusoidal earthquake record ($\ddot{u}_g(t) = 0.35g \sin 2\pi ft$; $f=10$ Hz).	141
Figure 6.4 Coupled and uncoupled steady-state responses of a 90 m dam subjected to a sinusoidal earthquake record ($\ddot{u}_g(t) = 0.35g \sin 2\pi ft$; $f=10$ Hz).	142
Figure 6.5 Coupled and uncoupled responses of a 90 m dam subjected to modified Saguenay earthquake record (PGA=0.35g).	145
Figure 6.6 Horizontal forces for opening and closing cracks.	147
Figure 6.7 Exact vs simplified pressure spatial distributions in crack opening mode.	149
Figure 6.8 Base saturation length curves for $f=2, 5, 10$ Hz	151
Figure 6.9 Procedure to compute dynamic pressure during seismic crack opening.	152
Figure 6.10 90 m dam stability considering transient uplift pressure in crack opening mode (see also Fig. 1.7 for additional information).	154

NOTATION

The following is the list of the symbols used in the text:

$\{\dot{u}\}$:	velocity vector
$\{\ddot{u}_g\}$:	ground acceleration vector
$\{\ddot{u}\}$:	relative acceleration vector
[C]	:	damping matrix
[K]	:	stiffness matrix
[M]	:	mass matrix
$\{R\}$:	restoring force vector
$\{u\}$:	displacement vector
$\{W_{pr}\}$:	load vector due to water pressure in crack
A	:	crack cross section area
CMOA	:	crack mouth opening acceleration
CMOD	:	crack mouth opening displacement
CMOD _{amp}	:	crack mouth opening displacement amplitude
CMOD _{ave}	:	average of crack mouth opening displacement
CMOD _{min}	:	minimum of crack mouth opening displacement
CMOV	:	crack mouth opening velocity
COD	:	crack opening displacement
COD _{w0}	:	critical crack opening displacement
e	:	hydraulic aperture of crack
E	:	mechanical aperture of crack
f	:	frequency of harmonic excitation
F _{hp}	:	resultant force of hydrodynamic pressure on upstream face of dam
F _I	:	dam inertia force
F _{sp}	:	resultant force of hydrostatic pressure on upstream face of dam

H	:	Reservoir height
j	:	hydraulic gradient
JRC	:	joint roughness coefficient
K	:	hydraulic conductivity of crack
k	:	roughness of crack walls
K_{pipe}	:	pipe roughness
L, L_{cr}	:	crack length
L_{cav}	:	unsaturated (cavitation) length of crack
L_{pipe}	:	pipe length
L_{sat}	:	saturated length of crack
M_L	:	magnitude of earthquake, Richter scale
P_{cav}	:	water vapour pressure
P_{crm}	:	crack mouth pressure
P_{dyn}	:	dynamic pressure in the crack
PGA	:	peak ground acceleration
P_{stat}	:	static pressure
P_v	:	water vapour pressure
Q, q	:	water flow
r	:	characteristic pore radius in equation 2.6
R	:	uplift reduction factor
R_c	:	resisting sliding force along the dam-foundation interface
Re	:	Reynold number
U	:	uplift force in a crack
$u(x,t)$:	crack opening
U_f	:	total uplift force in a crack assuming full static uplift pressure along the crack
u_L, w_1	:	crack opening displacement at $x=L$
\dot{u}_L, \dot{w}_1	:	crack opening velocity at $x=L$
V	:	volume of cylinder

v_{cr}	:	crack front velocity
V_{cr}	:	crack volume
V_e	:	volumetric strain
V_v	:	volumetric strain corresponding to $P=P_v$
v_w	:	water front velocity
V_w	:	water volume
w_0	:	constant crack opening
\ddot{w}_1	:	crack opening acceleration at $x=L$
x	:	distance along the crack from crack tip
α	:	constant exponent in Louis (1969) equation
μ	:	dynamic viscosity of water
β	:	modulus of bulk compressibility of water
η	:	crack wall porosity
ν	:	viscosity of water
ν	:	Poisson's ratio
Δ	:	Incremental variations
ξ	:	non-dimensional parameter
γ	:	specific weight of water
ρ	:	mass density of water
σ	:	effective stress in the crack
σ_τ	:	total stress in the crack
Φ	:	diameter of holes in specimens
ϕ_p	:	pipe diameter

CHAPTER 1

INTRODUCTION

1.1 Overview

According to ICOLD (1998), about 5700 large concrete dams, with heights above 15 m, exist outside China. Most of them have been in service for more than 50 years. Among them, only few concrete dams have ever experienced earthquake shocks (Table 1.1). Sefid-Rud dam in Iran suffered severe cracking while subjected to an earthquake of Richter scale magnitude $M_L=7.3$ on June 21, 1990 (Figs. 1.1, 1.2). The dam however retained the reservoir water without sudden release. Koyna dam in India subjected to a $M_L=6.5$ earthquake on December 11, 1967, and Hsingfengkiang dam in China subjected to a $M_L=6.1$ earthquake on March 1962, suffered similar distress (Figs. 1.3, 1.4). These examples have shown that concrete dams are not immune from seismic damage.

With increasing knowledge of hydrology and seismicity, the "Probable Maximum Flood" and the "Maximum Design Earthquake" magnitudes have often been increased with respect to the values selected at the design stage. These revised loading criteria, when applied to ageing concrete structures, required from many owners to re-evaluate their dams for stability under extreme conditions. The primary safety concern is with weak planes, including tensile cracking and sliding along lift joints and cracks, which, if significant enough, can result in a major catastrophe during a flood or earthquake. When cracking occurs, or is likely to occur, safety assessment should be considered as well as rehabilitation, if necessary. Recognising the importance of this problem and the high cost of construction or rehabilitation of concrete dams requires investigating, more precisely, the behaviour of dams under critical load conditions.

Table 1.1 Concrete dams which have been subjected to significant earthquake (adapted from CEA¹ 1990, Knight and Mason² 1992, USCOLD³ 1992)

Dam	Country	Type	Height (m)	Completion Date	Earthquake			
					Date	Richter magnitude	Dist. (km)	Damage
Pacoima	USA	VA	113	1929	1994	6.7	18	X
Sefid Rud	Iran	CB	106	1962	1990	7.7	v.clo.	X
Lower Crystal Springs	USA	PG	47	1906	1989	7.1	69	---
Tuai Div.	New Zealand	PG	5	---	1987	6.2	11	---
Rapel	Chile	VA	110	1890	1985	7.8	---	X
Izvorul Muntelui	Romania	PG	127	1961	1977	7.2	---	---
Poiana Usului	Romania	CB	80	1969	1977	7.2	60	---
Ambiesta	Italy	VA	59	1956	1976	6.5	22	---
Maina di Sauris	Italy	VA	136	1952	1976	6.5	43	---
Barcis	Italy	VA	50	1920	1976	6.5	48	---
Pacoima	USA	VA	113	1929	1971	6.6	6	X
Santa Anita	USA	VA	76	1927	1971	6.6	27	---
Big Tujunga	USA	VA	76	1931	1971	6.6	32	---
Granda	France	MV	88	1959	1969	---	---	---
Koyna	India	PG	103	1963	1967	6.5	3	X
Monteynard	France	VA	155	1962	1963	4.9	0	---
Kariba	Zimbabwe	VA	128	1959	1963	6.1	---	---
Kurobe	Japan	VA	186	1960	1963	5.0	10	---
Hsingfengkiang	China	CB	105	1959	1962	6.1	5	X
Blackbrook	UK	PG	30	1900	1957	---	6.4	X
Honen-Ike	Japan	MV	30	1930	1946	---	---	X
Marathon	Greece	PG	43	1930	1938	5	---	---
Hoover	USA	VA	220	1936	1936	5	8	---
Lower Crystal Springs	USA	PG	47	1906	1906	8.3	0.4	---
Ponteba	Algeria	PG	---	1954	---	6.8	---	X
Monteynard	France	VA	155	1963	---	---	---	---
Bicas	Romania	PG	---	1977	---	7.3	---	---
Poiana Usului	Romania	CB	---	1977	---	7.3	---	---
Vidraru	Romania	VA	---	1977	---	7.3	---	---

PG = Gravity dam; VA = Arch dam; MV = Multiple-arch dam; CB = Buttress dam

¹ Lesson from the effects of earthquakes on dams, Water Power and Dam Construction, March 1992, pp. 44-46.

² Safety assessment of existing dams for earthquake conditions, Vol. c.4

³ Observed performance of dams during earthquake

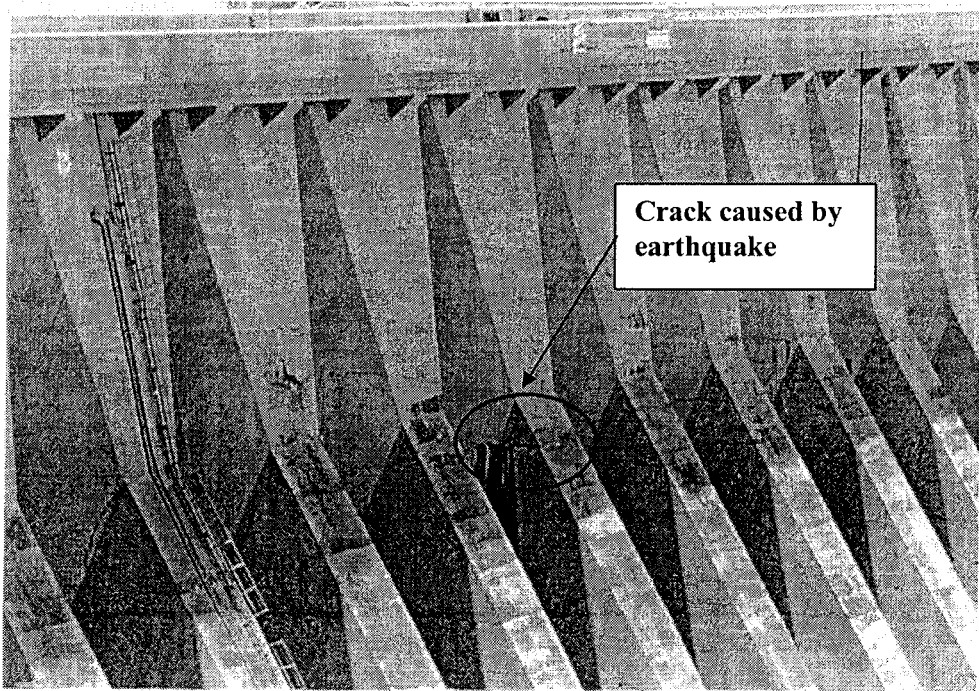
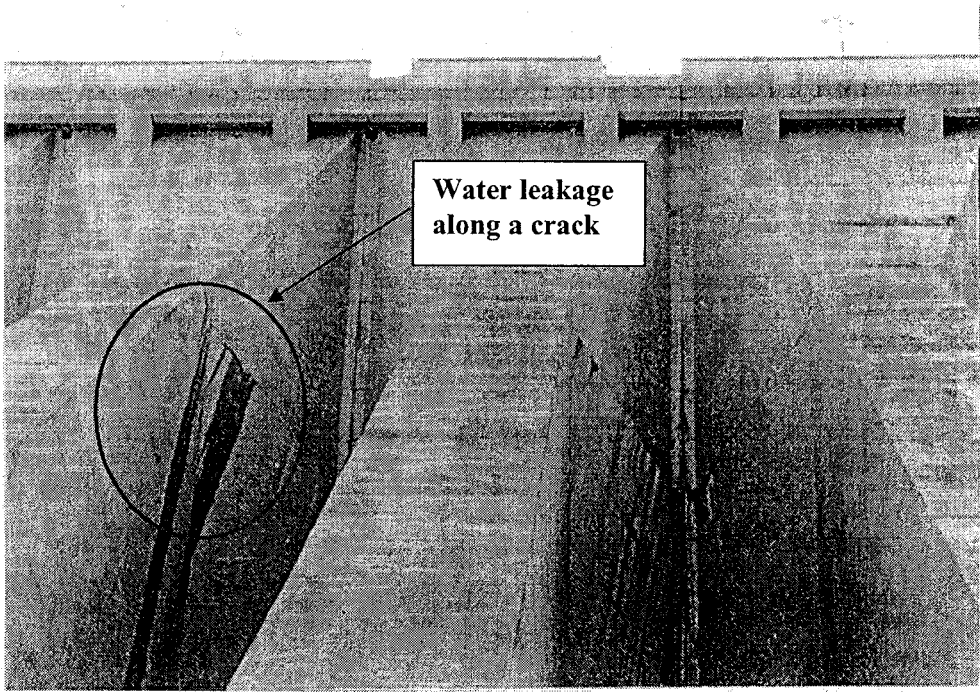


Figure 1.1 Sefid-Rud (Iran) buttress dam (106 m), after earthquake of magnitude 7.3 in 1990.

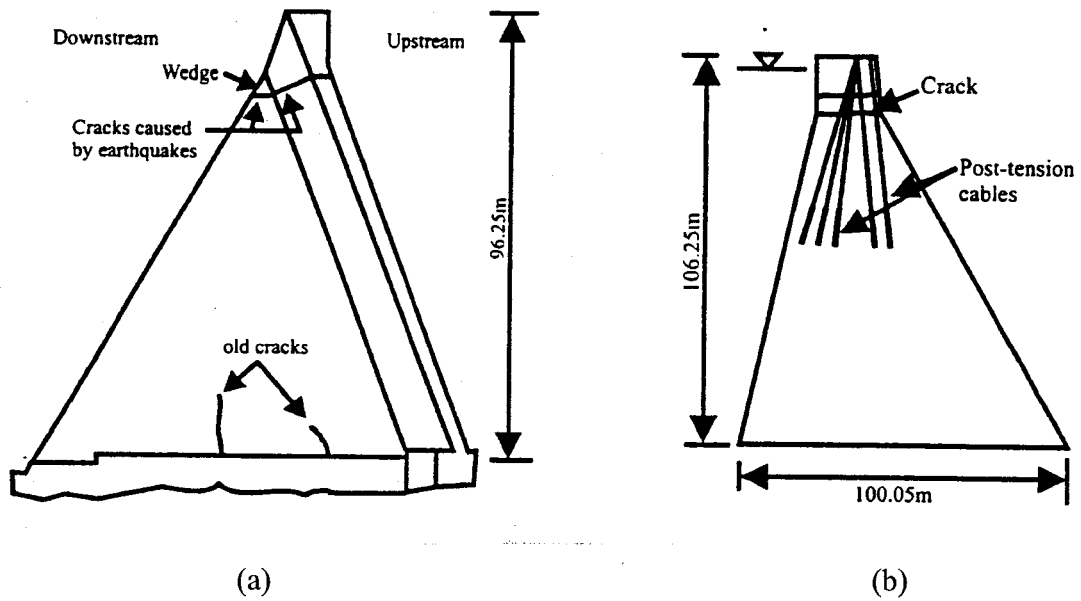


Figure 1.2 Sefid-Rud dam,

(a) Crack map of the left hand side of buttress no. 15 (adapted from Indermaur et al., 1992); (b) Post-tension cables (adapted from Arcangeli and Ciabbarri, 1994).

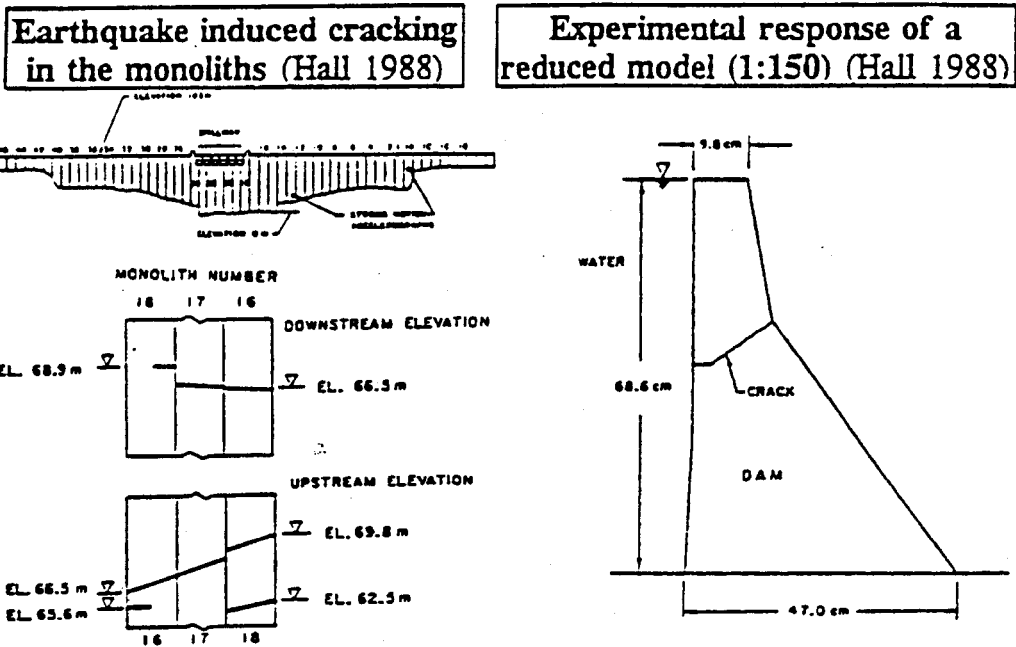


Figure 1.3 Seismic cracking of Koyna dam (adapted from Hall 1988).

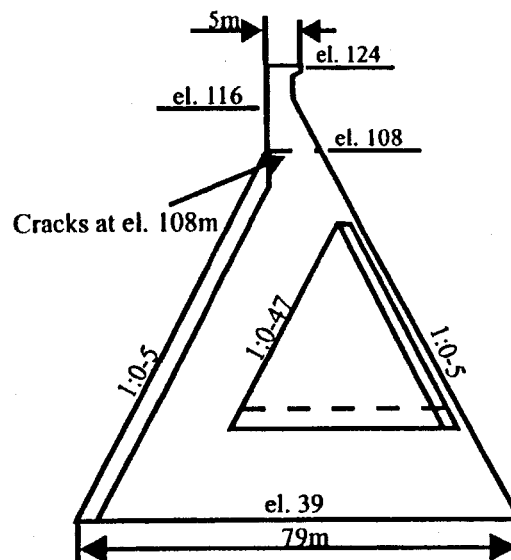
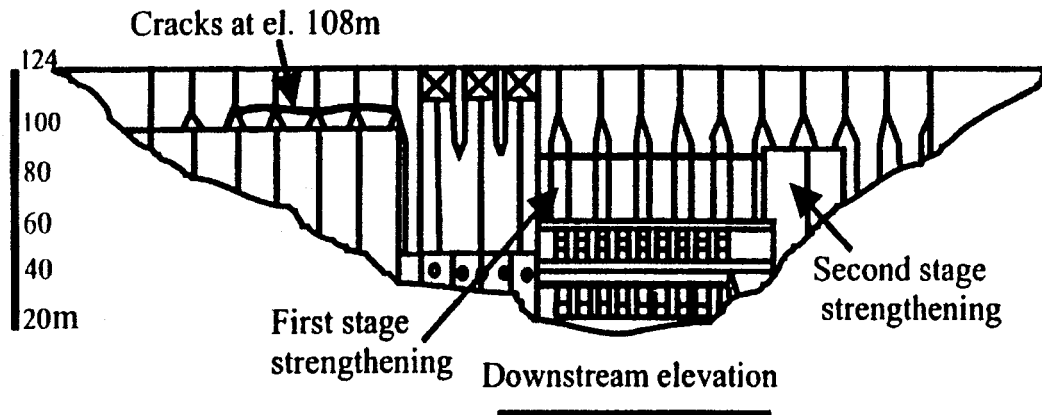


Figure 1.4 Hsingfengkiang dam (adapted from Chen et al., 1982).

Figure 1.5 shows seismic failure mechanisms of a gravity dam due to earthquake. Most failure conditions initiate by developing new cracks or propagating previously existing cracks, which might have been produced by severe load applications (past earthquakes, floods), thermal variations, alkali-aggregate reaction, or other environmental conditions. Cracking at the upstream face, or weak horizontal joints, allows water penetration, creating external traction on the walls of a crack or an opened

joint. The resulting uplift pressure creates external forces that tend to propagate cracks and may jeopardise the global force equilibrium needed for structural stability. The static and seismic interactions of water-crack (or water-joint), and its effects on crack propagation is one of the most important aspects to evaluate the stability of an existing gravity dam. However, the appropriate uplift pressure magnitudes to use in static and seismic structural analyses of concrete dams have been the subject of a lot of debate over the last century.

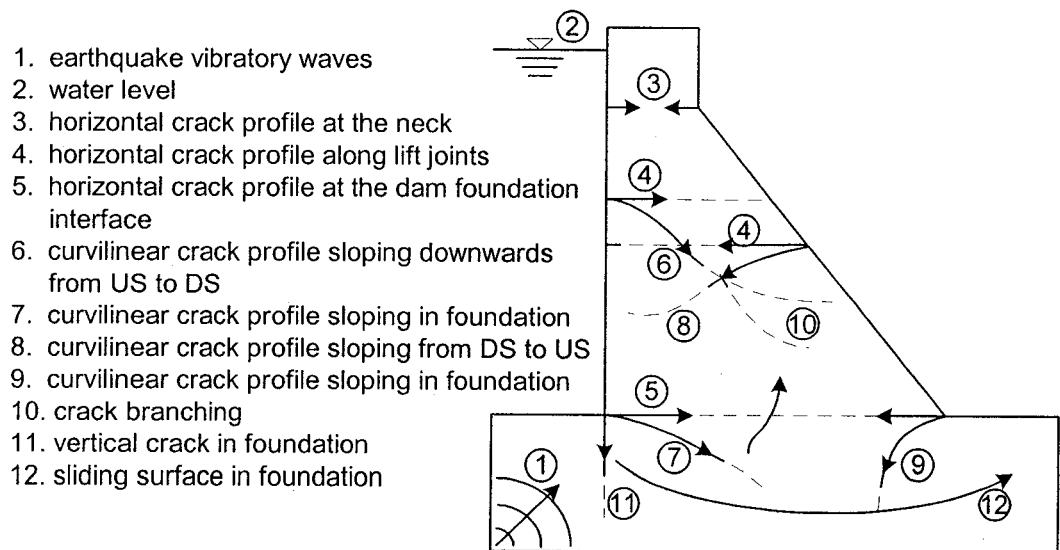


Figure 1.5 Seismic failure mechanisms of concrete gravity dams (adapted from Tinawi et al. 1998).

1.2 Research problem

There are different degrees of complexity for static or dynamic analysis of structure-reservoir-foundation system considering their interactions. One can proceed by simplified methods based on rigid body and beam theory or proceed with more sophisticated numerical simulations. During recent decades, new and efficient numerical methods based on finite element technology were developed to predict the behaviour of dams with as much realism as possible. Using linear or nonlinear fracture mechanic concepts, one can analyse the response of cracked dams for static or dynamic loads. The

possibility for developing uplift pressure in the cracks, using either simplified or advanced methods, should be considered due to its importance in stability of cracked section. A rigorous determination of uplift pressure in cracks of concrete dams during earthquake requires a water-crack interaction analysis. But there is not any universally recognised and validated model to analyse the interaction of water inside the moving walls of cracks in a concrete gravity dam during an earthquake.

Dam safety guidelines such as CDSA 1997, USACE 1995, FERC 2002, USBR 1987, and ICOLD 1986 define equivalent hydrostatic pressure models to represent the water uplift pressure inside a seismic crack. But there are great differences in equivalent hydrostatic pressure values specified in dam safety guidelines. According to these guidelines, uplift pressure intensity in a crack during an earthquake may vary from full reservoir hydrostatic pressure to zero pressure (Fig. 1.6):

- Full uplift pressure in cracks initiated during the earthquake: according to ICOLD 1986 “assuming that pore pressure equal to the reservoir head is instantly attained in cracks is probably safe and adequate” (Fig. 1.6-d).
- Unchanged uplift pressure in existing cracks and joints during the earthquake: according to USACE 1995 and FERC 2002 uplift pressure in cracks and joints should be assumed to be unaffected by earthquake (Fig. 1.6-c).
- Zero uplift pressure during earthquake: according to USBR 1987 “when a crack develops during an earthquake event, uplift pressure within the crack is assumed to be zero. This assumption is based on studies that show the opening of a crack during an earthquake relieves internal water pressure, and rapidly cycling nature of opening and closing the crack does not allow reservoir water, and the associated pressure, to penetrate” (Fig. 1.6-b).
- Zero or unchanged uplift pressure according to seismicity conditions: according to CDSA 1997, in areas of low seismicity, the uplift pressure prior to the seismic event is normally assumed to be maintained during the earthquake even if cracking occurs

(Fig. 1.6 c). In areas of high seismicity, uplift pressure on the cracked surface is assumed to be zero during the earthquake when the seismic forces are tending to open the crack (Fig. 1.6 b).

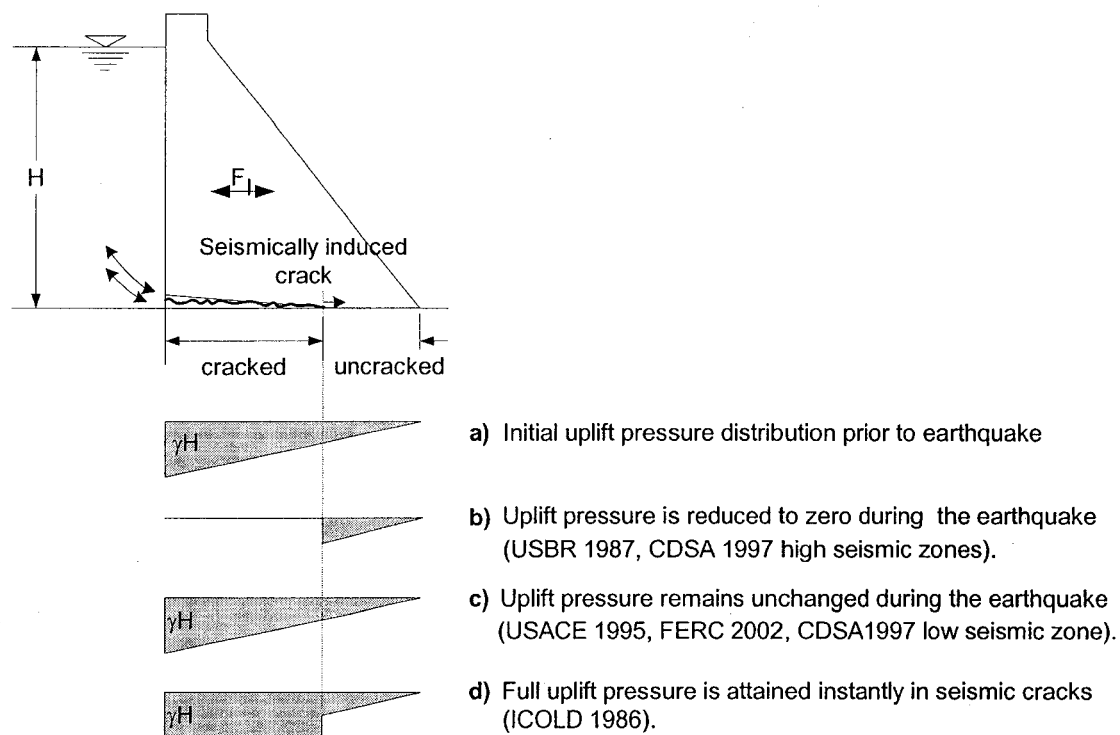


Figure 1.6 Transient uplift pressure variations in a crack during an earthquake according to different dam safety guidelines.

To show the importance of the problem and how different uplift pressure assumptions may change the results for seismic stability assessment of gravity dams, a typical 90 m high gravity dam was analysed assuming a rigid foundation (Chopra 1988). Figure 1.7 shows the geometry of dam and the other assumptions used to analyse the dam. The pseudo-dynamic method is used to compute the sliding safety factor (SSF) of dam subjected to modified Saguenay earthquake record with peak ground acceleration equal to 0.35g. The SSF is equal to the ratio of the available shear strength to the net driving shear force. This seismic analysis has been done using the computer program CADAM (Leclerc et al. 2002). The earthquake record and its spectrum are also shown in

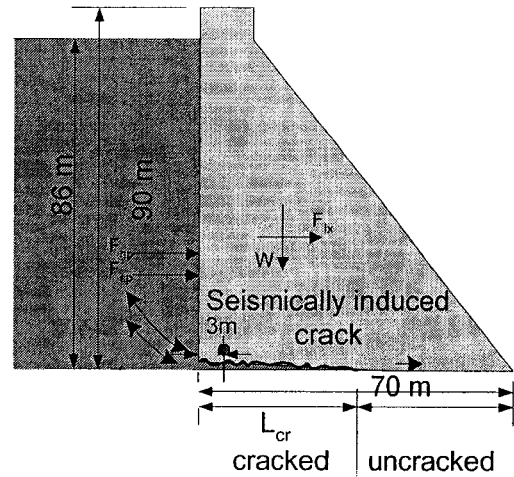
Fig. 1.7. The natural period of vibration of dam section considering the added mass of reservoir is 0.27 sec. The spectral acceleration of dam using the earthquake spectrum, for $T=0.27$ sec is equal to 0.5g. Three different assumptions (zero, unchanged, and the full uplift pressures inside the base crack) were used to calculate the crack length and the Sliding Safety Factor (SSF). The results of these analyses, shown in Fig. 1.7, indicate that the magnitudes of uplift pressure has significant effects on seismic sliding stability analysis of gravity dams, which may change a sliding safety factor from an acceptable value ($SSF \geq 1$) to an unstable condition ($SSF < 1$).

Although the importance of uplift pressure in cracks of concrete gravity dams has been recognised, its effect during earthquakes remains a major source of uncertainty in design and safety assessment of concrete gravity dams. The lack of knowledge in this area and the necessity for further studies have also been recognised by researchers (NRC 1990) as well as practising engineers (Yeh 1999). During recent years, few experimental tests and theoretical formulations have been developed to study transient uplift pressures inside cracked concrete specimens during earthquakes and their effects on the response of concrete gravity dams (Slowik and Saouma 2000, Tinawi and Guizani 1994, Ohmachi et al. 1998). Chapter 2 presents a detailed literature review of theoretical and experimental studies about seismic-water crack interaction. To define appropriate formulations and to verify them, more experimental data are needed. The main purpose of this study is to perform laboratory experiments to measure water pressure variations in seismically induced or existing cracks in small concrete specimens due to cyclic opening and closing of cracks walls considering different excitation frequencies and boundary conditions. Based on the experimental results, a constitutive model for water-crack interaction is developed. The use of the water-crack interaction model to perform seismic stability analysis of gravity dams using either simplified method based on rigid body equilibrium and beam theory or finite element analysis is presented. A case study concerning a 90 m high gravity dam is discussed.

Sliding Safety Factor (SSF)

$$SSF = \frac{(W - U) \tan \phi + cA}{F_{Ix} + F_{sp} + F_{hp}}$$

- W= Dam weight
- U= Uplift force
- ϕ = Sliding friction angle
- c= Cohesion
- A= Contact area
- U= Uplift force
- F_{Ix} = Horizontal inertia force
- F_{sp} = Hydrostatic force
- F_{hp} = Hydrodynamic force

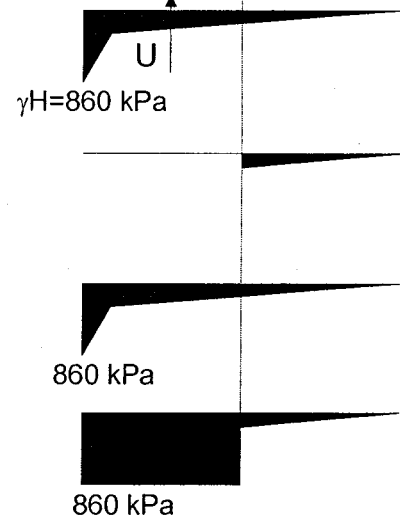


a) Preseismic static analysis

Initial uplift pressure distribution prior to earthquake
 $L_{cr}=0$ m, $SSF=1.48$, $U=19800$ kN ($\phi=45^\circ$; $C=0$)

b) Pseudo-dynamic seismic analysis

- i) Uplift pressure is reduced to zero during the earthquake
 $L_{cr}=41$ m, $SSF=1.22$, $U=3418$ kN
- ii) Uplift pressure remains unchanged during the earthquake
 $L_{cr}=70$ m, $SSF=0.94$, $U=19800$ kN
- iii) Full uplift pressure is attained instantly in seismic cracks
 $L_{cr}=70$ m, $SSF=0.25$, $U=59050$ kN



c) Modified 1988 Saguenay EQ. Record and Spectrum

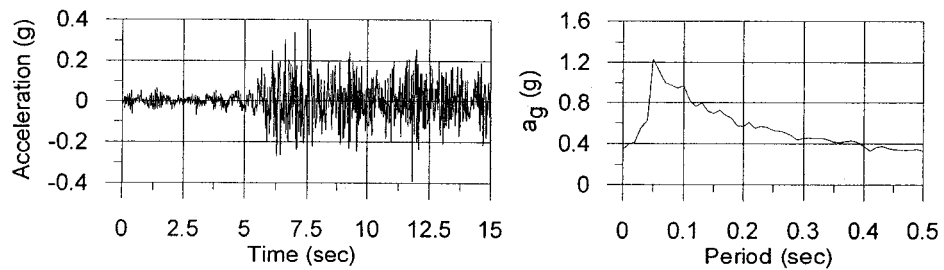


Figure 1.7 Seismic stability of typical concrete gravity dam (with drain) using different uplift pressure assumptions.

1.3 Objectives of the research

The following objectives are considered in this thesis:

- (i) To determine the state-of-the-practice and the state-of-the-research on the dynamic crack-water interaction problem.
- (ii) To develop an experimental procedure to seal and pressurise water inside small cracked concrete specimens and to measure transient crack uplift pressure while subjecting them to cyclic motions.
- (iii) To measure experimentally the uplift pressure in cracks of small cantilever concrete beams (1.5 m x 0.55 m x 0.15 m) subjected to harmonic or earthquake loads.
- (iv) To study the effect of frequency contents (2 Hz to 10 Hz) and amplitudes of crack wall cyclic motions on transient uplift pressure in pre-existing cracks induced in small cantilever concrete beams.
- (v) To study the effect of hydraulic boundary condition at the crack mouth on transient uplift pressure in pre-existing cracks induced in small cantilever concrete beams.
- (vi) To compare water pressure variation between existing cracks and newly formed propagating cracks in small cantilever concrete beams.
- (vii) To develop a theoretical model for seismic water-crack interaction and simulation of the experimental tests results using the model.
- (viii) To implement the developed model in a finite element based computer program for dynamic analysis of cracking in concrete gravity dam subjected to earthquake, including complete hydro-mechanical coupling.
- (ix) To conduct a case study and parametric analyses on a typical gravity dam to assess the incidence of water-crack interaction on seismic safety.
- (x) To formulate recommendations to consider seismic water crack interaction for industrial applications.

1.4 Original contributions of the thesis

To the best of the author's knowledge, the following items could be considered as original contributions of this thesis:

- A comprehensive literature review of water-crack interaction research and development work.
- An experimental testing procedure for measuring water pressure inside the cracks of a concrete dam model specimen.
- New experimental data on transient uplift pressure during earthquakes.
- A new theoretical water-crack interaction model.
- A computer program for dynamic analysis of concrete gravity dams including complete water-crack coupling effects.
- A new simplified procedure to evaluate uplift pressure during earthquake to be used within the context of the gravity method.
- A case study analysis of seismic response of a concrete gravity dam with water-crack interaction.

1.5 Organisation of the thesis

This thesis is organised in seven chapters. Following the Introduction, Chapter 2 presents a state-of-the-art relevant to the objectives of the thesis. The basic concepts in earthquake safety evaluation of dams including the methods of analysis are described. A literature review of experimental and theoretical studies about steady-state and transient water pressures in concrete cracks are presented. Concepts of water compressibility and cavitation are presented. A brief discussion and conclusions about previous work and research needs related to seismic water-crack interaction end this chapter.

The experimental program is presented in Chapter 3. First, the objectives of the experimental program are specified, and the specimens developed for the experimental tests are described. Section 3.4 presents the test set up, instrumentation, and test

procedures for new crack and existing crack cases. The preliminary tests to verify the different procedures and instrumentation to be used in the experimental program are covered in section 3.6.

Experimental tests results are presented in Chapter 4. The effects of frequency of crack wall motions, amplitude of crack openings, initial crack openings, and static water pressure on measured pressures along the existing cracks are presented. Results related to the evolution of uplift pressure in new seismically induced propagating crack are also discussed.

Chapter 5 presents theoretical aspects of the proposed water-crack interaction model. The computed results are presented and compared to the test results for verification of the proposed model. A computer program is developed, DUP_CRCRACK, and used to simulate water pressure variations in cracks of arbitrary lengths, to investigate the pressure variation in longer cracks.

Chapter 6 presents the procedure to implement the developed model in a finite element based computer program for complete hydro-mechanical coupling analysis of concrete gravity dams. The case of a 90 m dam subjected to earthquake ground motions is analysed to investigate the effects of coupling in developed pressure and dam response. And finally a procedure is developed to evaluate seismic water pressure in opening mode of crack that can be used in pseudo-static and pseudo-dynamic analysis of gravity dams.

The conclusions of this research program and recommendations for further studies are presented in Chapter 7.

CHAPTER 2

WATER PRESSURE IN CRACKS AND JOINTS OF CONCRETE DAMS: STATE-OF-THE-ART

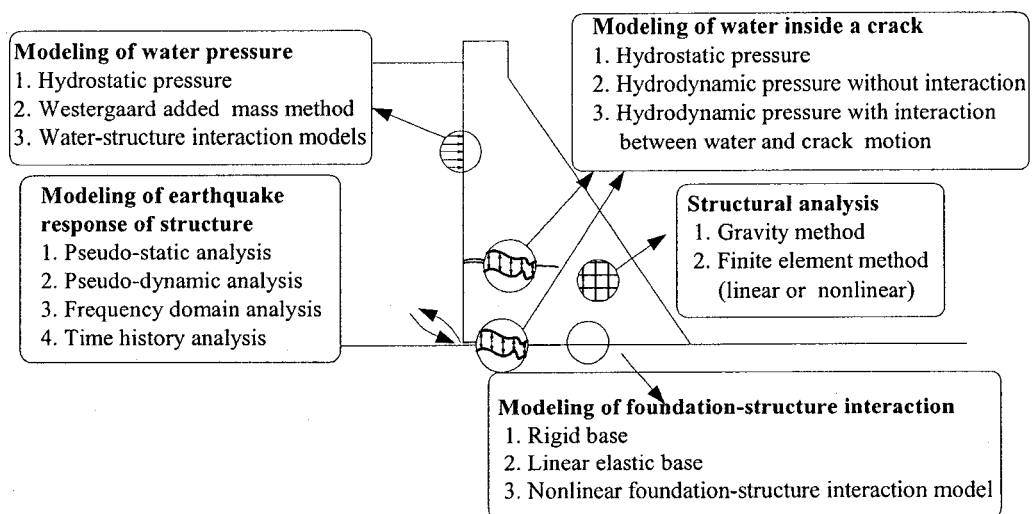
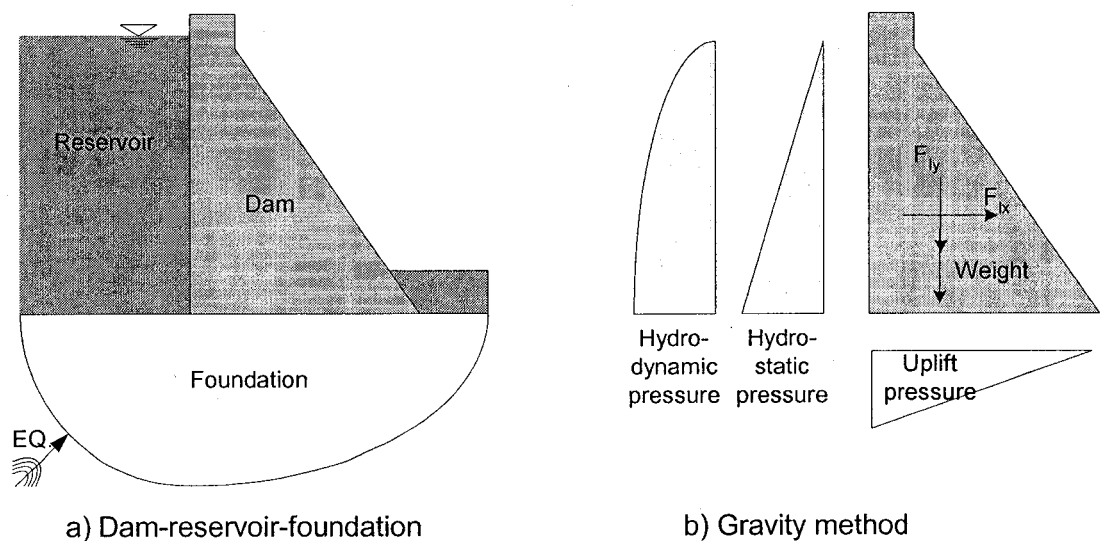
2.1 Introduction

This chapter presents a review of the concepts and literature relevant to the main theme of the research. General analysis methods for earthquake safety assessment of concrete gravity dams are presented in section two. Uplift pressure magnitude and distributions defined according to different dam safety guidelines for static and dynamic analyses are presented in section three. A review of past theoretical, numerical, and experimental investigations related to the water flow through rock joints and concrete cracks is presented in section four. In section five a review of literature related to seismic water-crack interaction in dams is presented. A review of the effect of compressibility of water and the cavitation phenomenon that may occur in a crack with moving walls are discussed in section six. A synthesis of the past theoretical and experimental research works related to seismic water pressures inside concrete cracks present in concrete gravity dams concludes this chapter.

2.2 Seismic analysis of gravity dams

The gravity method and finite element analysis are two methods that dam designers generally use for structural analysis of dams (Fig. 2.1). The most common method for the analysis of gravity dams has been the gravity method. The main assumptions in this method are that the dam behaviour is two dimensional, and normal stresses are assumed to be distributed linearly on horizontal planes. Stresses in dam body and dam foundation, and factors of safety for sliding and overturning can be computed by elementary strength of material and beam theory. Pseudo-static and pseudo-dynamic analyses of dam against earthquake are possible by this method. All the applied forces including the hydrostatic

and hydrodynamic pressures, uplift pressure, earthquake load, and dam weight should be defined prior to an analysis by the gravity method. While the hydrostatic and hydrodynamic pressures and earthquake loads defined in dam safety guidelines are conceptually similar, there is not a universally accepted value for uplift pressure in cracks of concrete dams during earthquake.



c) Different aspects of structural modeling of dam-reservoir-foundation system

Figure 2.1 Seismic analysis of gravity dams.

In the finite element method, stresses in the elements are determined from the strain field derived from computed nodal displacements. Due to the rapid development of computer software and hardware as well as computational methods in structural analysis in recent years, sophisticated finite element analyses are now possible for rigorous analysis of dams. Both linear and nonlinear analyses with reservoir-dam-foundation interaction possibilities can be utilized in finite element analyses of concrete gravity dams (Fig 2.1). Pseudo-static, pseudo-dynamic, and dynamic analyses can be used for seismic analysis of dams by the finite element method. Depending on the available input data and the required output results, the finite element method with different levels of complexity may be used for seismic safety evaluation of gravity dams. Figure 2.2 shows five analysis levels that are defined by increasing complexity of modeling procedures and representations of seismic input motions. Uplift pressures in concrete cracks can be defined directly like in the gravity method or should be evaluated by a proper water-crack interaction model in more detailed finite element analysis where crack walls displacements and velocities are computed. Cracking of concrete could be described or predicted by various constitutive models based on strength of materials, fracture mechanics, damage mechanics, etc. Two approaches have generally been used for finite element modelling of cracks in concrete structures: the discrete model and the smeared crack model. Both models have been used over the decades because of the advantages and the inconveniences that they bring to the numerical implementation of the constitutive models in finite element crack propagation analysis of concrete structures.

2.2.1 Discrete crack model

The discrete crack model, in a finite element program, introduces displacement discontinuity along the crack by altering the mesh to accommodate propagating cracks. Therefore different nodes must be used on each side of the crack at common points. To predict the crack propagation, it is possible to evaluate the nodal forces at the tip of the

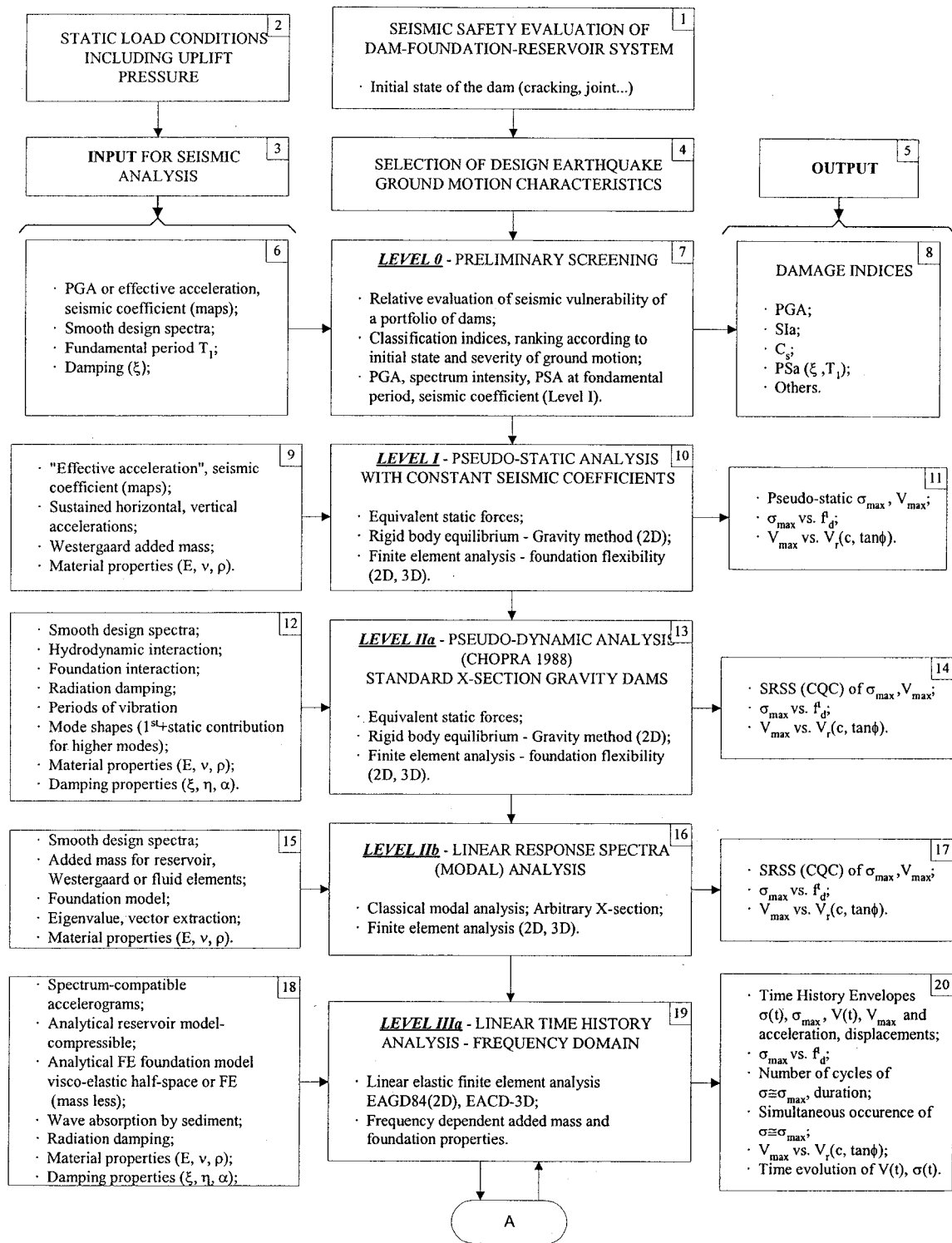
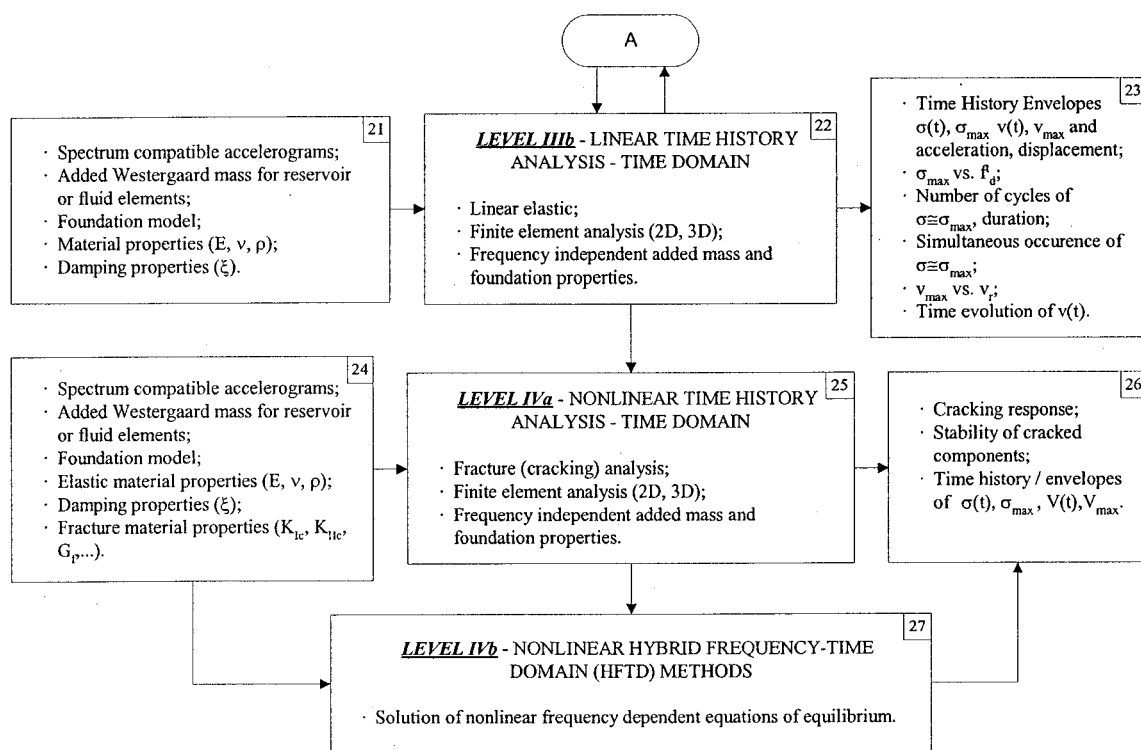


Figure 2.2 Progressive methodology for seismic analysis of dams (Tinawi et al. 1998).



NOTE: σ = Stresses;

f_d = Concrete dynamic tensile strength;

E = Elastic modulus (static / dynamic);

ν = Poisson's ratio;

ρ = Mass density;

η = Hysteretic damping;

α = Wave absorption by bottom sediment;

K_{Ic} = Fracture toughness mode I;

K_{IIc} = Fracture toughness mode II;

G_f = Fracture energy (strain softening law);

ξ = Viscous damping (equivalent);

V = Driving shear force on failure plane ($\int \tau_{xy}$);

V_r = Resisting shear force on failure plane

$$SSF = \frac{(W - U - EQV + P) \tan \phi + cA}{EQH + H_d + H_s}$$

SSF = Sliding safety factor (V/V_r)

PGA = Peak ground acceleration;

PSa = Pseudo-spectral acceleration.

U = Uplift pressures;

W = Static weight;

EQH = Horizontal inertia forces;

EQV = Vertical inertia forces;

P = Post-tension force;

$\tan \phi$ = Sliding friction coefficient;

c = Cohesion;

H_d = Hydrodynamic interaction force;

H_s = Hydrostatic reservoir force;

SlA = Acceleration spectrum intensity;

C_s = Seismic coefficient;

T_1 = Fundamental period.

Fig. 2.2 Progressive methodology for seismic analysis of dams (Cont.)

crack by using suitable criteria based for example on linear or nonlinear fracture mechanics. The discrete crack model is a realistic representation of a physical discontinuity and water penetration and uplift pressure can be easily modelled as external loads along the crack face in a finite element mesh. The specific advantages of

discrete crack models are the ability to estimate the crack-opening-displacement (COD) profile, and the ability to model the sliding friction mechanisms such as the aggregate interlock in a rough crack. A special case of discrete crack modelling is the application of interface elements to represent the a priori weak joints in the system, such as the dam-foundation interface and construction joints where a Mohr-Coulomb sliding friction constitutive model in the crack tangential direction is used in conjunction with a tensile cracking model in the normal crack direction. The main disadvantages of this method are the high computational cost for practical application in seismic response analysis, difficulty to extend from 2D to 3D models, and the effect of non objectivity of finite element meshes and crack length increments as well as high frequency impact shockwave phenomenon for rapid crack closure.

2.2.2 Smearred crack model

In a finite element analysis it is often much more convenient to change the element properties than to change the topology of the finite element mesh. This concept is the basic procedure used in the smeared crack method that assumes the crack zone corresponds to a material degradation in the finite element domain. The mechanical properties of the finite element, monitored at Gauss integration points, are modified along the path of the crack according to the selected constitutive relationships, to represent the loss of strength and stiffness. The main advantage of this model is its simplicity and cost effectiveness. In particular, the model is very effective in complex structural analyses, such as the seismic response study of concrete gravity dams, when the location and orientation of cracks may not be known a priori. Moreover, the smeared crack finite element model can efficiently represents pre-existing diffused crack pattern in a structure. The most serious disadvantage of classical smeared crack models based on strength of materials is that results may depend significantly on the choice of the element size by the analyst. However, it has been recognised that fracture energy conserving constitutive models, based on the nonlinear fracture mechanics theory, for example, are able to produce mesh independent results compatible with experimental

finding as opposed to the results using classical strength of material criterion (principal stresses vs tensile strength) that vary as the mesh is refined. Smearred crack models do not yield directly the evolution of a crack opening and closing displacement response. Moreover, uplift pressures in cracks elements are difficult to introduce.

2.3 Uplift pressure

The physical concept of uplift pressure and its definition for static and dynamic conditions according to dam safety guidelines are presented in this section. A brief review of the theoretical and numerical methods to determine uplift pressures in dam foundation and along the dam-reservoir interface is also presented.

2.3.1 Pore pressure in porous media

Concrete is not entirely impermeable, water pressure might develop within its porous media. Figure 2.3 shows a section of a concrete block with water pressure P applied on its left side. Due to pressure gradient, slow seepage of water through concrete is building up. This flow is a transient flow as it starts but after a while it becomes a steady flow. The time required to build up a steady flow depends on the permeability of concrete, the magnitude of water pressure, and the thickness of the concrete section. In steady seepage condition, the pressure of water at the inlet surface of the block is gradually reduced by friction within the pores until it reaches the value of the pressure at the outlet surface (for a uniform porosity along the section it is linear). The developed pressure inside the porous media, known as pore pressure, is a self equilibrating internal pressure that reduces the compressive stresses and increase tensile stresses in concrete (Fig 2.3).

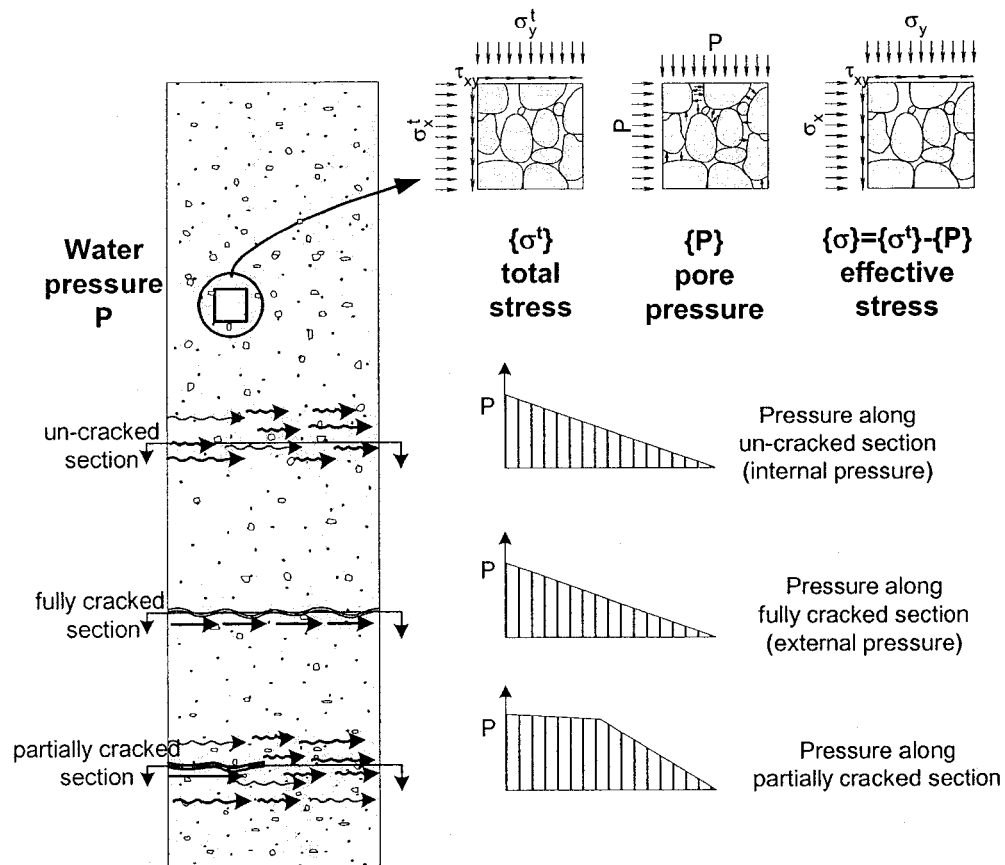


Figure 2.3 Pore pressure and crack pressure distributions.

Concrete permeability changes with cracking; it has been shown that for cracks in concrete with aperture larger than 0.03 mm, the permeability is larger than un-cracked concrete (Reinhardt et al. 1998). Water flow and the developed pressure inside a full length crack (that starts from one face and crosses the block to other face) with constant aperture, is the same as for un-cracked section except that permeability of the cracked section is greater and the steady state flow develops faster than for un-cracked section. The other difference between pore pressure and water pressure in crack is that the second is considered as an external pressure. For a crack that starts from the left side in contact with the water and stop inside the concrete block, the water pressure distribution after developing a steady state flow condition is shown in Fig 2.3. The slope of the linear pressure variation in each part depends on the relative permeability of the crack and

concrete. Permeability of the crack mainly depends on its aperture and for large crack aperture, due to its larger permeability relative to un-cracked section, the slope of the uplift pressure in cracked part is almost zero.

2.3.2 Static uplift pressure in gravity dams

A portion of the normal compressive loads applied to mass concrete in any section of a dam or its interface with the foundation is carried by pore pressure (internal) or water pressure in cracks (external) which is generally called uplift pressure. Water percolation inside the dam body and the dam foundation starts as soon as water pressure developed due to filling of the dam reservoir. The water flow through the dam body and cracks is a transient flow and it takes time for the steady-state to develop. Water pressure in a steady-state flow condition is greater than water pressure in initial transient flow condition; therefore water pressure is computed for the steady-state case in dam analysis.

Concrete has very low permeability and computations have been shown that it may take many hundred years for water to saturate the voids and move from the upstream face to the downstream face of a typical dam (Bazant, 1975). Therefore, the pore pressure in a section through the body of the dam should be small. USACE 1995 assumes that pore pressures varies from 50% of headwater at the upstream face, to 50% of tailwater or zero, as appropriate, at downstream face. However, for practical purpose, the areas of interest that affect the stability of the dam body are generally the construction joints. Uplift pressure in construction joints depends on the quality of the joints and whether cracking is present. Most guidelines (USACE 1995, CDSA 1997, FERC 2002) assume static uplift variations from 100% headwater to 100% tailwater in construction joints. The condition at the dam-foundation interface is similar to construction joint and when no drainage system is present, all current dam safety guidelines consider that on a horizontal section at the base of the dam there is a linear variation of hydrostatic uplift pressure from the 100% headwater to 100% tailwater.

Grout curtain and drain system are used in dam engineering to reduce the effective uplift pressure from the above mentioned values. In general, static uplift pressures at the dam foundation interface is a function of foundation permeability, grout curtain dimensions and effectiveness of drains. Figure 2-4 shows the most important factors that may affect the quasi static uplift pressure along the dam body or its foundation.

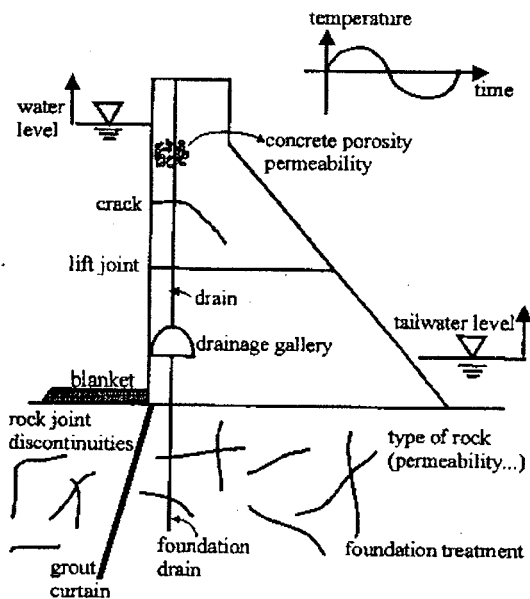


Figure 2.4 Parameters affecting the uplift pressures (Tinawi et al. 1998).

2.3.3 Dynamic uplift pressure

During an earthquake, when a dam vibrates, internal stresses as well as pore pressures change in dam body. For seismic loading conditions, when the dam moves downstream, compressive stresses are developed in the downstream portion of the dam and pore pressure increases due to reduction of pore volume in concrete. While the pore pressure decrease in the upstream portion of the dam where tensile stresses are developed. Increased pore pressures in upstream and decreased pore pressures in downstream, will occur for the upstream motion of the dam. Higher pore pressure is

usually accompanied by a larger increase in total pressure and it may not significantly affect the stability during seismic loading conditions (NRC 1990).

The condition for cracked section in a dam is somehow similar. If the movement of the dam due to the earthquake is such that the existing cracks close, the water pressure will be increased due to crack closure, but for the crack opening case, the water pressure will be reduced. According to experimental evidences (Slowik and Saouma 1994) during cyclic opening and closing of existing cracks, uplift pressure inside the crack is varying and its average magnitude may be less than initial hydrostatic uplift pressure for opening mode of crack, and higher than initial hydrostatic uplift pressure for closing mode (Fig 2.5). While for new developing cracks during earthquakes, water uplift pressure may develop inside the propagating crack and its magnitude depends on the relative velocity of water front and crack front (Fig 2.5). For water velocities (V_w) smaller than the crack front velocity (V_{cr}), only a part of cracked concrete will be filled and pressurised with water. However, when the water velocity is equal or greater than the crack velocity, full uplift pressure will be developed in the whole cracked length.

Although the importance of uplift pressure in cracks of concrete gravity dams has been recognised, its effect during earthquakes remains a major source of uncertainty in design and safety assessment of concrete gravity dams. Existing dam safety guidelines define an equivalent hydrostatic pressure model to represent the water pressure inside a seismic crack. As presented in Chapter 1, seismic crack pressures range from the instantaneous attainment of full hydrostatic pressure in a new seismically induced crack (ICOLD 1986) to no pressure at all presuming that uplift pressure is decreased by crack opening and that water has no time in a seismic pulse to penetrate in the crack (USBR 1987). Meanwhile, there is no recommended transient model, in dam safety guidelines, for transient uplift pressure to be used in finite element analyses where crack wall motions are computed explicitly.

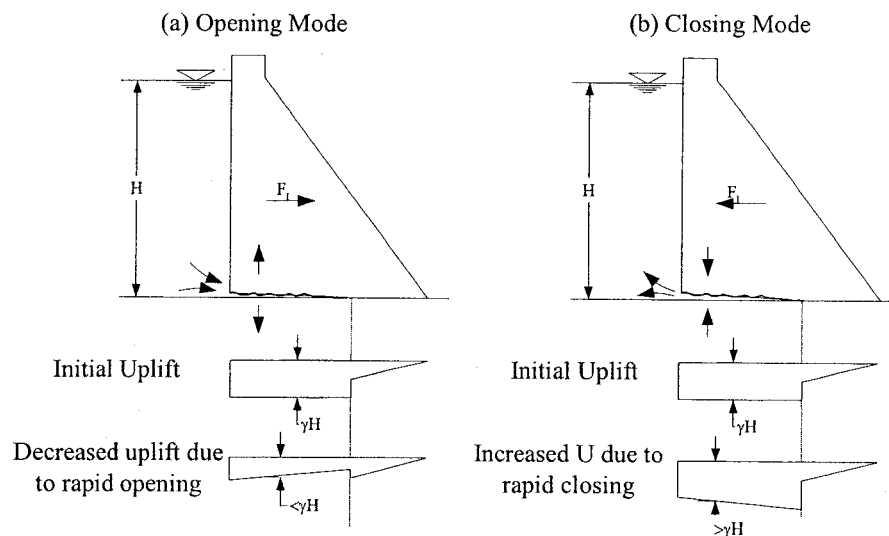
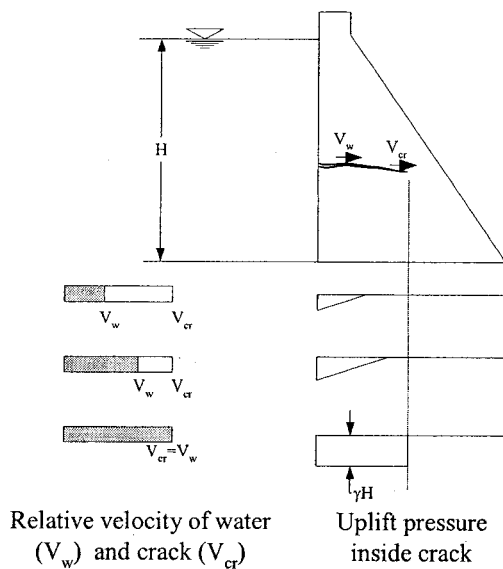
(1) Existing cracks:**(2) New cracks:**

Figure 2.5 Variation of uplift pressures inside cracks during earthquakes: comparisons between new and existing cracks.

2.3.4 Static uplift pressure calculation methods

There are two different methods, the continuum and discrete modelling approaches, to study uplift pressures in dam-foundation interface. In the continuum approach, the

foundation mass is assumed as an equivalent continuum regardless of the type of foundation material (rock or soil). In a fractured rock foundation condition, an equivalent permeability is defined. Theoretical seepage analysis assuming constant permeability of foundation has been used to determine uplift pressure magnitude and distribution in dam-foundation interface by dam designer pioneers (Casagrande 1961). The governing differential equation, the Laplace equation, is solved to determine uplift pressure in the foundation and along the dam-foundation interface. Computer software like SEEP2D and ANSYS, based on the finite element method, are capable to consider complicated conditions of real dam-foundation system.

The discontinuum or discrete approach, on the other hand, considers major rock fractures separately. Two methods have been used with this approach:

- The distinct element method (DEM) that assume the rock mass as an assembly of discrete blocks, rigid or deformable, separated by various discontinuities. Fluid flow is considered as flow through the network of joints while blocks are considered impermeable.
- The finite element method (FEM) in which rock blocks are discretized by means of standard continuum finite element, and discontinuities by means of joint elements. This method is the same as the discrete crack method in structural analysis as discussed in section 2.2.1 the fluid flow is modeled in a similar fashion in the DEM.

The applicability of continuum mechanics approach to determine uplift pressures along dam foundation interface depends on the relative dimensions of dam and foundation discontinuities and it is applicable when the dam base length is of a larger order of magnitude than the space between fractures in foundation. The observations reported by EPRI (1992) indicate that this procedure is not appropriate for the jointed rock conditions. This procedure is still applicable in rock mechanics when the scales of fractures are considerably smaller than the dimension of dam. It seems that the discrete approach is more accurate than continuum approach in static uplift pressure determination if the information to model explicitly the fractures is available. Moreover,

due to the explicit definition of joint (cracks) in discrete methods, it is possible to consider water-crack interaction due to opening or closing of cracks. Since the flow of water through a single crack is the base of the hydro-mechanical interaction calculations in the discrete approach, theoretical aspects and literature review of fluid flow through single crack (with more emphasise on topics related to objectives of this research) is presented in the next sections.

2.4 Water flow in cracks

2.4.1 Water flow in single crack

A crack in concrete could be simply characterised by its aperture. Since the crack walls are rough surfaces their mechanical aperture (E) is defined as the average point-to-point distance (perpendicular to a selected crack plane) between two crack walls (Fig 2.6 a). Studying water flow inside cracks requires more detailed definitions for the crack geometry. A definition of the most important geometric parameters was presented by Hakami 1995, as shown in Fig 2.6 b. These parameters are:

Mechanical aperture (E): average distance between two rough crack walls,

Roughness (k): surface height distribution or the shape of the surfaces,

Contact area: the area in contact along the crack,

Matedness: how well matched the surface are,

Spatial correlation: rate of aperture changes from one point to another point,

Tortuosity: the forced bending of the stream lines due to variations in joint aperture,

Channelling: differences in flow velocity along certain paths.

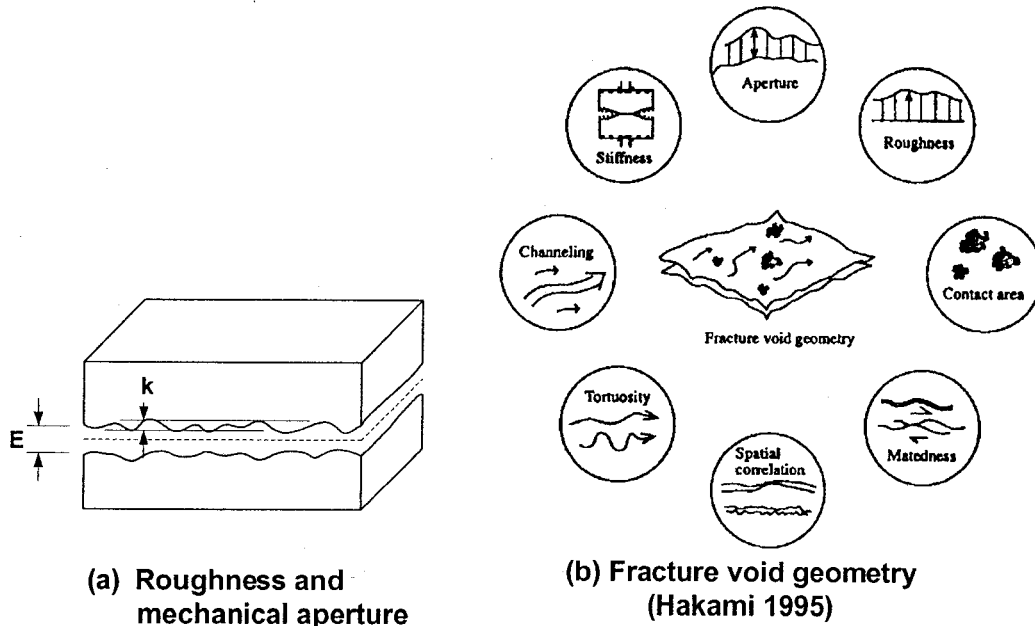


Figure 2.6 Fracture geometry.

To formulate water flow through rock joints and concrete cracks it is common to consider that cracks or joints are composed of two parallel smooth plates with aperture e . It is also assumed that the flow is steady, laminar and water is incompressible. Under these conditions water flow per unit width of crack, q , can be defined by the following equation which is known as the cubic law.

$$q = -\frac{e^3}{12\mu} j \quad (2.1)$$

where e is the normal distance between two plates, μ is the dynamic viscosity of the water, and j is the dimensionless hydraulic gradient. The average velocity, v , of water through the plates can be found by dividing both sides of equation 2.1 by e .

$$v = -\frac{e^2}{12\mu} j \quad (2.2)$$

Using the mechanical aperture of the crack instead of e in Equation 2.1 or 2.2 gives greater values for flow or velocity comparing with real ones which is due the simplified modelling of a real rough crack by two smooth parallel plates. The parameters that

control crack geometry (as mentioned above) may reduce the water flow through a real crack compared to flow through smooth parallel plates. Two different approaches have been utilized to consider the effects of crack geometry in equation 2.1 and 2.2.

In a first approach, the joint roughness coefficient (JRC) which is a coefficient related to the crack geometry, is used to modify equation 2.1. On the basis of experimental data, Barton (1985) proposed the following relation between e (which is called the hydraulic aperture) and E , the mechanical aperture:

$$e = \frac{E^2}{JRC^{2.5}} \quad (2.3)$$

The curves in Fig. (2-7) show the relation, according to this equation, between the hydraulic aperture (e) and ratio of mechanical to hydraulic aperture for different values of JRC.

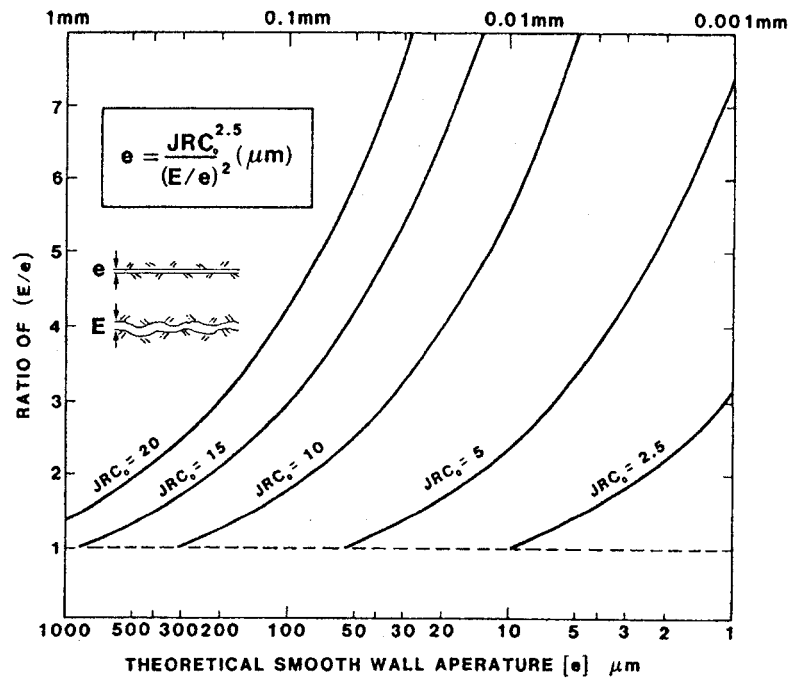


Figure 2.7 An empirical relation incorporating joint roughness (JRC) and aperture which broadly satisfies the trends exhibited by available flow data (Barton 1985).

Louis (1969) conducted an extensive study on flow through joints. He considered the effects of joint roughness and flow condition (turbulent or laminar) in his study. A new parameter referred to as 'relative roughness' k/E , is defined to consider the crack roughness. Where k is the absolute roughness or average asperity height of crack walls, and E is mechanical aperture of crack (Fig 2.6 a). According to Louis (1969) test results, laminar-turbulent flow transition depends on the Reynold's number $Re=2Ev/\nu$ where ν is the kinematic viscosity of water. Figure 2-8 shows different flow conditions in cracks as a function of Reynold's number and relative roughness of crack walls as reported by Louis (1969). The velocity of water flow in a crack, is defined in a general form as follows:

$$v = -Kj^\alpha \quad (2.4)$$

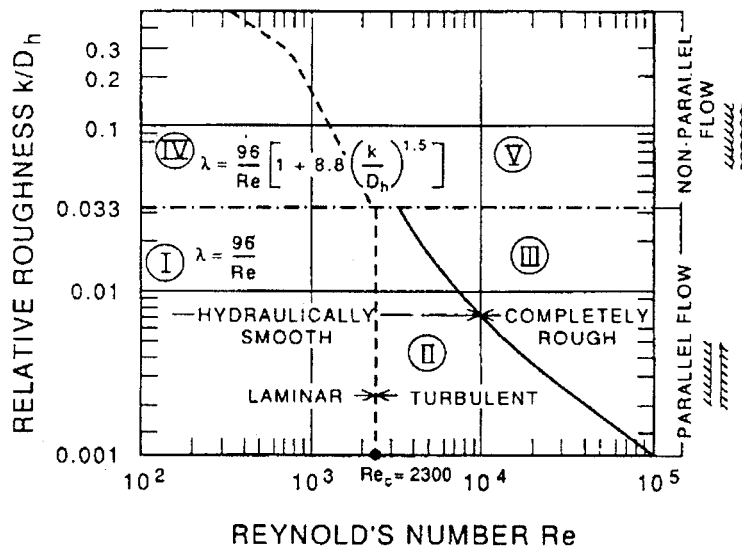
where K is hydraulic conductivity of the crack, j is gradient of total pressure, and α is a constant exponent which depends of hydraulic zones according to Fig 2.8. Table 2-1 shows reported values of K and α by Louis (1969).

2.4.2 Uplift water pressure based on the water flow in crack

Goodman et al. (1983) used this concept, for the first time, to study uplift pressure in a crack at the base of a concrete gravity dam. An analytical solution for water flow through a horizontal crack, with finite length in the upstream downstream direction but infinite along the dam longitudinal axis, drained by a series of vertical drains was proposed. The solution is used to derive uplift pressure distribution in a horizontal crack of a gravity dam in direct connection with the reservoir. Their procedure was extended by Amadei et al. (1989, 1991) that allowed the crack to be of finite dimensions. The crack was modelled as a confined rectangular aquifer with constant aperture and constant surface roughness. They also developed a finite element program, called CRFLOOD, to overcome these limitations. This program is capable of handling cracks of complex and more realistic geometry. The coupling effects of water pressure and the crack deformation is not considered in these analyses.

Table 2.1 Flow laws (Louis 1969) (Note in table: b=e and D_h=2e).

Hydraulic zone*	Hydraulic Conductivity, K	Exponent, α	Flow condition
I	$\frac{g \cdot b^2}{12\nu}$	1.0	Laminar
II	$\frac{1}{b} \left[\frac{g}{0.079} \left(\frac{2}{\nu} \right)^{0.25} \cdot b^3 \right]^{\frac{4}{7}}$	4/7	Turbulent
III	$4 \sqrt{g} \log \left[\frac{3.7}{k/D_h} \right] \sqrt{b}$	0.5	Turbulent
IV	$\frac{g b^2}{12\nu [1 + 8.8(k/D_h)^{1.5}]}$	1.0	Laminar
V	$4 \sqrt{g} \log \left[\frac{1.9}{k/D_h} \right] \sqrt{b}$	0.5	Turbulent



- LIMIT LAMINAR - TURBULENT FLOW
- - - - - LIMIT PARALLEL - NON PARALLEL FLOW
- LIMIT HYDRAULICALLY SMOOTH - COMPLETELY ROUGH FLOW REGIMES
- λ FRICTION COEFFICIENT ASSOCIATED WITH LOSSES OF ENERGY IN THE CRACK

Figure 2.8 Flow laws (Louis 1969) (Note in figure: b=e; D_h=2e).

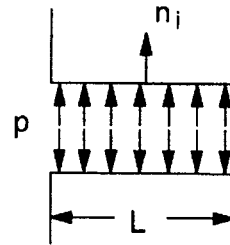
2.4.3 Numerical methods for hydro-mechanical coupled analysis in rock mechanics

The water flow and the rock deformations are fully coupled. Changes in fluid pressure and in fluid volume induce joint deformations; simultaneously, joint deformations alter fluid flow rates and fluid pressure. Mathematical methods and computer programs for hydro-mechanical process have been developed in the past decades, using the continuum or discrete approaches. An international co-operative research project has been established under name DECOVALEX for theoretical and experimental studies of coupled thermal, hydrological and mechanical process in hard rock (Jing et al. 1995). Different mathematical models and computer codes as THAMES, MOTIF, CASTEM 2000, ROCMAS, HYDREF, and UDEC were used to study the rock mass response to storage of radioactive waste and spent fuel. The thermal and mechanical results compare rather well, while hydraulic results show pronounced differences which can be partly attributed to the nonlinear dependences on the fracture hydraulic conductivity in terms of the aperture. UDEC and HDRREF are developed based on the discrete approach and may be used to determine uplift pressure along the discrete cracks in gravity dams.

UDEC (Universal Distinct Element Code) is a commercially available program, that was developed by Dr. Cundall and co-workers in the 1970's mainly for the analysis of jointed rocks in rock mechanics. To the best of the author knowledge UDEC is the only commercially available program that can simulate a fully coupled mechanical-hydraulic analysis for an intersecting joint system. In the distinct element method, a rock mass is presented as an assembly of discrete blocks and joints (or cracks) are viewed as interface between blocks. Through a series of calculations that trace the movement of blocks, the contact forces and displacements at the interface are calculated. Water flow between joints is assumed to be steady laminar flow and cubic law is used to calculate water flow along the joints. A fully coupled mechanical-hydraulic analysis is possible by considering the interaction between block movements and joint fluid flow. The effects considered in UDEC to model fluid-structure interactions are summarised in Fig. 2.9.

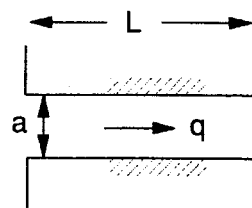
The following effects are modelled in *UDEEC*-

1. Pressure effect



$$F_i = p n_i L$$

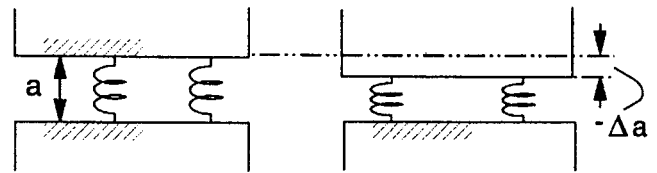
2. Flow



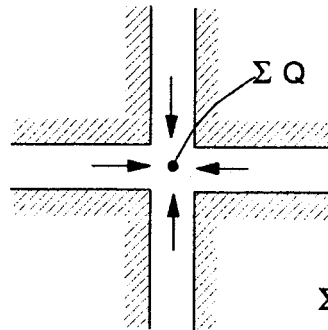
$$q = -k_j a^3 \frac{\Delta p}{L}$$

3. Mechanical effect on aperture

$$a = a_0 + \Delta a$$



4. Pressure generation



$$\Delta p = \frac{K_w}{V} \{ \Sigma Q \Delta t - \Delta V \}$$

ΣQ = flow into node

ΔV = mechanical volume change

Figure 2.9 *UDEEC* water-crack interaction model; a is hydraulic aperture, a_0 is aperture for zero normal contact stress condition, Δa is aperture change due to mechanical stress, $K_w = \beta$, $k_j = 12/\mu$.

This program is applicable for static and dynamic analysis of dams considering water-crack interaction. It can be used for modelling steady uplift pressure and drain flow (for example at Bluestone Dam by Deschamps et. al (1999)). Its applicability for transient seismic water-crack interaction of gravity dams has never been verified experimentally and an attempt to simulate the experimental results of this study by UDEC was not successful.

2.4.4 Uplift pressure in fracture process zone

Water may affect new crack development in concrete due to changing of fracture properties of concrete. This effect and developed water pressure in cracked part of a dam section change the dam cracking response to applied loads. A comprehensive research program on the applicability of fracture mechanics to concrete dams, has been conducted at the University of Colorado (Saouma and Morris 1997). This work involved a number of studies dealing with cracks in concrete dams, specifically cracks modelling and effects related to crack modelling. Bruhwiler and Saouma (1991-1995) conducted an experimental program using wedge splitting tests to study quasi-static water fracture interaction in concrete. The objective of the investigation was to determine the effect of water on fracture properties of concrete and the variation of water pressure along the crack and the fracture process zone (FPZ, region of micro-cracking ahead of the stress-free crack) during crack formation and growth. This was achieved by pressurising the notch, while the wedge opens it. They used 5 pressure transducers to measure water pressure along the propagated crack. The experimental set up is shown in Fig. 2.10.

According to their observations, increasing water pressure inside a concrete crack shortens the fracture process zone size and reduces fracture properties, fracture energy G_f and fracture toughness K_{IC} . They also concluded that full water pressure is built up along the stress-free crack and a substantial portion of the FPZ. However it is not extended along the total fracture process zone, the part close to the tip of the FPZ is not pressurized. Hydrostatic pressure along the fracture process zone is characterised by a

gradual transition from full headwater pressure to zero, and depends on the applied hydrostatic pressure and crack opening displacements.

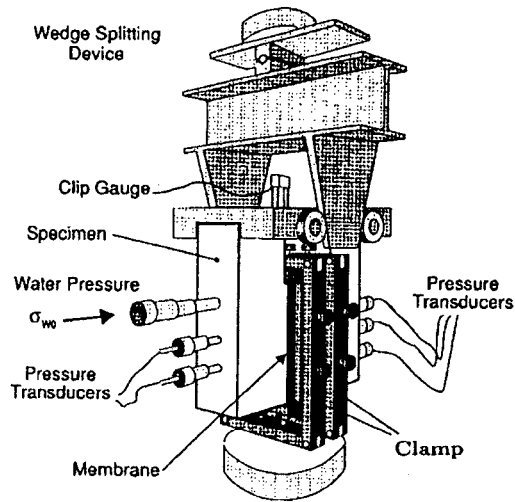


Figure 2.10 Experimental test set up (Bruhwiler and Saouma 1995).

They derived a non-dimensional equation for water pressure in terms of the COD (Crack Opening Displacement) for fracture process zone as follows:

$$\frac{\sigma_w}{\sigma_{w0}} = 2 \frac{COD}{COD_{w0}} - \left(\frac{COD}{COD_{w0}} \right)^2 \quad (2.5)$$

where σ_w is the water pressure in the fracture process zone with crack opening equal to COD, and σ_{w0} is the water pressure in the notch. COD_{w0} is defined as the critical opening displacement below which the water pressure σ_w becomes smaller than σ_{w0} . Figure 2-11 shows variation of water pressure according to equation 2.5 along the fracture process zone close to crack tip. Since they did not measure crack opening displacement, they used the finite element method to evaluate crack opening displacements along the cracked section. Based on the calculated COD and measure water pressure they determined numerical values for the critical opening displacements

COD_{w0} . Calculated values of COD_{w0} range from 0.02 to 0.098 mm for static water pressure 0.9 MPa to 0.1 MPa correspondingly.

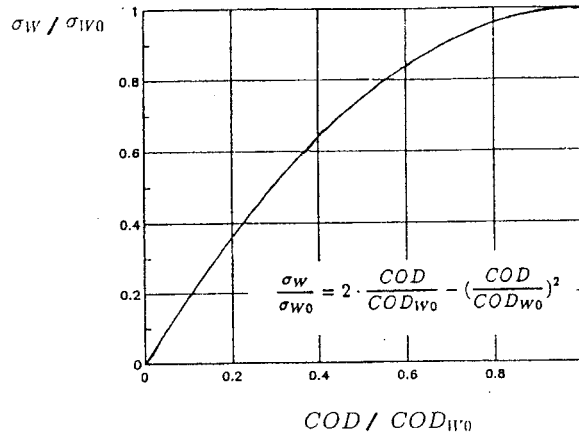


Figure 2.11 Normalized pressure-versus-crack opening displacement curve (Bruhwiler, Saouma 1995).

2.5 Transient seismic uplift in concrete cracks of gravity dams

There is no doubt that uplift pressure changes in cracks in concrete gravity dams during earthquake. The pressure evolution in cracks of concrete gravity dam during an earthquake is a complicated problem due to several coupled phenomena that occur in the system. Depending on the considered phenomena, theoretical researches and experimental tests to investigate water pressure variations inside the cracks of concrete gravity dams during earthquake can be classified in two categories. In first category, the opening and closing of crack is considered as main source of water pressure variations inside the crack, water pressure in crack mouth is considered constant during the earthquake. In the second category, water pressure variation in crack mouth is assumed to be responsible for water pressure variation inside the crack so in this case crack walls are assumed to be un-moveable during earthquake.

2.5.1 Transient uplift in propagating cracks

The experimental tests that can be classified in first group have been done by Slowik and Saouma (1994, 2000). They mainly studied water pressure variation in fracture process zone of a new developing crack. They adjusted the loading device of Bruhwiler and Saouma (1991) to be able to dynamically open or close a crack. Their loading device is shown in Fig 2.12. In addition they have used parallel wires across the specimen to detect the water front, electrically, through the closing of an electric circuit by the saline water. Wedge-splitting tests with two different CMOD (Crack Mouth Opening Displacement) rates were conducted to compare the velocity of water pressure build up in the fracture process zone. Figure 2.13 shows the experimental results for load and water pressure versus CMOD curves for slow ($2 \mu\text{m/s}$) and fast ($200 \mu\text{m/s}$) crack opening. It was observed that the crack opening rate could have important consequence on the internal water pressure distribution. Using a nonlinear fracture model they simulated the crack front numerically, since they could not measure its evolution experimentally, they reported the location of water and crack front in terms of the CMOD for typical tests as shown in Fig 2.14. There is almost no difference in concrete crack front curves for slow and fast loading case, however, a substantial difference can be found in water crack fronts. For rapid crack opening, distance gap between water front and crack front (vertical distance between two curves in Fig 2.14) is greater than the corresponding value for slow crack opening. Table 2.2 shows sample results for measured water front velocities and calculated crack front velocities by same researchers. They have concluded that, the larger crack front velocity relative to water front velocity, quantitatively reinforce the assumption of 'no water pressure inside a propagating crack during the earthquake'. As mentioned by Saouma and Morris (1997), although crack front velocity is greater than water front velocity for fast loading case but they are of the same order of magnitude. Thus the assumption for zero uplift pressure in concrete cracks during earthquake may dangerously underestimate uplift pressure value, and more experimental studies are necessary.

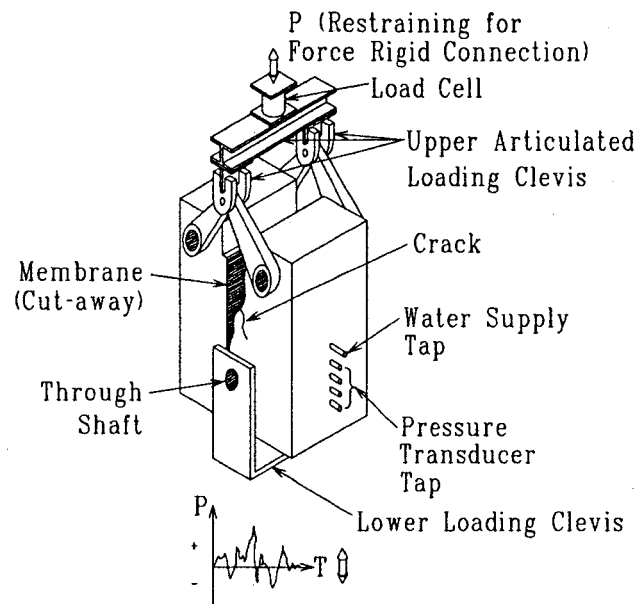


Figure 2.12 Experimental set up (Slowik and Saouma 1994).

They conducted another test to measure the water pressure in a saturated existing crack (a pre-cracked specimen) during a sudden crack closure. The results indicate that during sudden closure water is trapped in the crack resulting in a temporary over-pressurisation. In this particular case, the water pressure was about three times the initial one. The trapped water acts as a wedge resisting complete crack closure, additional stresses are induced, causing failure at the lower end of the specimen (known as wedge effect). They noted that the initial pressure in the notch increased as well but not as much as the one measured in the fracture process zone. They have also reported an experimental test with cyclic loading (crack opening and closing) in Fig 2.15, but they have not done any systematic study about this aspect.

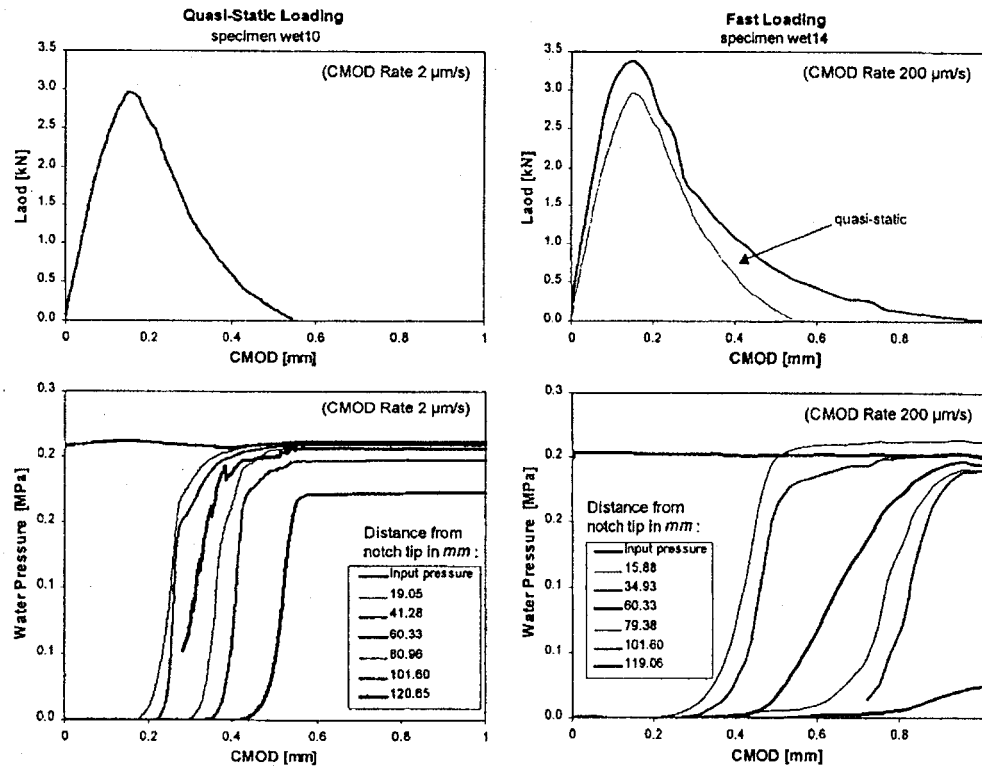


Figure 2.13 Load and water pressure versus CMOD for different CMOD rates (Slowik and Saouma 2000).

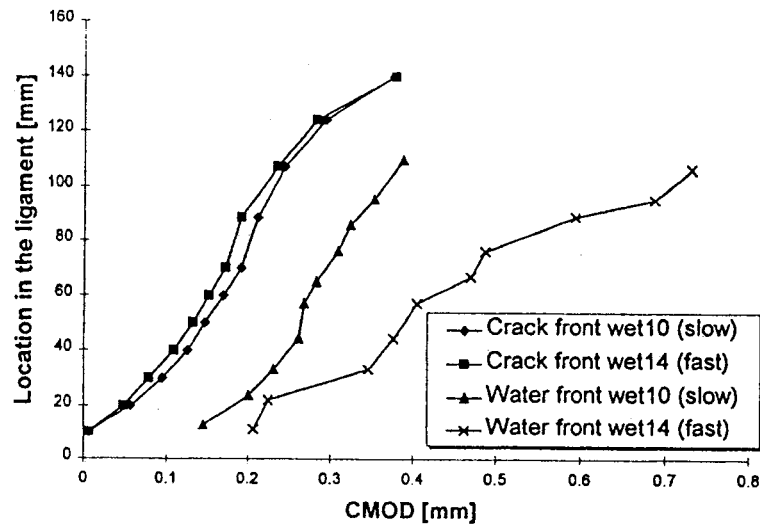


Figure 2.14 Crack and water front versus CMOD for slow and fast loading (Slowik and Saouma 2000).

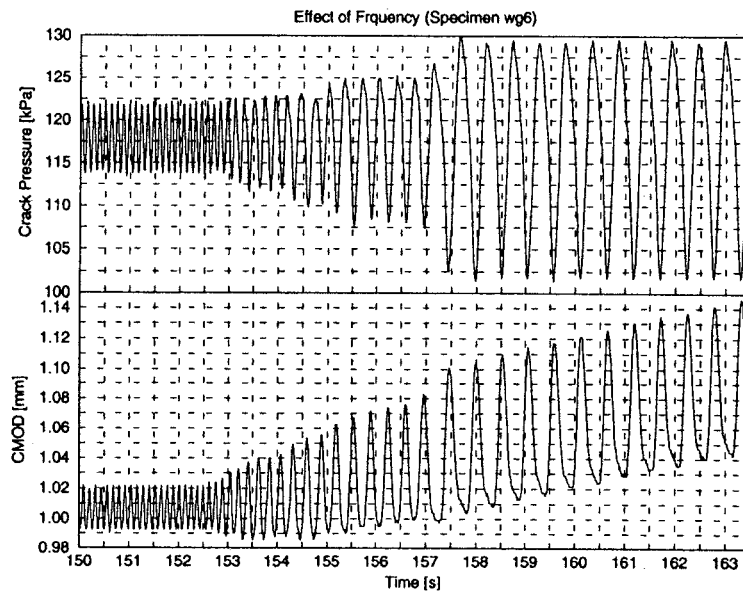


Figure 2.15 Water pressure in crack for cyclic loading with changing frequency and amplitude (Slowik and Saouma 1994).

Table 2.2 Samples of results from water-crack front velocity tests on concrete specimens (Saouma and Morris 1997)

Specimen	Wet10	Wet14	Wet32	Wet35
Input water pressure (MPa)	0.21	0.21	0.63	0.63
Loading rates ($\mu\text{m}/\text{sec}$)	2	200	2	200
Water front velocity from Water front detectors (mm/sec)	0.693	28.13	-	45.39
Water front velocity from Pressure transducers (mm/sec)	0.637	48.08	0.347	45.90
Crack front velocity (mm/sec)	0.608	61.13	0.403	56.70

Finally, they developed a theoretical model to compute water pressure along the propagating crack. They assumed incompressible laminar flow in the crack, and used Darcy's law (equation 2.4 with $\alpha=1$) in their formulation. Using continuity equation of

water and the process of filling of cavities, formed during crack formation, with water they derived a differential equation for developed pressure along the crack as follows:

$$\frac{dp}{dt} = C_1 \frac{d^2 p}{dx^2} + C_2 \frac{dp}{dx} + C \quad (2.6)$$

$$\text{with } C_1 = f(p, \dot{w}, (Kd)) = \frac{(Kd)p^2}{(w + 2r\eta)(p_0 - R\dot{w})}$$

$$C_2 = f(p, \dot{w}, (Kd)) = \frac{\frac{d(Kd)}{dx} p^2}{(w + 2r\eta)(p_0 - R\dot{w})}$$

$$C_3 = f(p, \dot{w}) = \frac{-(p - p_0 + R\dot{w})\dot{w}p}{(w + 2r\eta)(p_0 - R\dot{w})}$$

where p is the water pressure, w is the crack opening displacement, r is the characteristic pore radius, η is the porosity, p_0 is the static water pressure, and R is a material constant that account for resistance against the air exchange between the crack and the surrounding material. A new term was defined Kd , called crack conductivity, where K is permeability and d is the width of assumed stream of water inside the crack which is assumed to be smaller than crack opening. Experimental results were used through backward analyses to determine crack conductivity as a function of crack opening. This model can be used in a numerical analysis to predict the water pressure along a propagating crack (only for the opening mode of crack). It is not applicable for the closing mode of the crack. While opening and closing of a crack occurs in a dam subjected to earthquake base motion, this model cannot be readily used for earthquake analysis of concrete dams. Meanwhile, definition of some physical parameters like R , and r in model, which are unfamiliar for dam engineers, makes it complicated for practical applications.

2.5.2 Transient uplift in existing saturated cracks

A purely theoretical investigation of water crack interaction, that can be classified in first group, has been done by Tinawi and Guizani (1994). They developed an

analytical formulation based on the finite control volume approach for the evaluation of seismic hydrodynamic pressure inside pre-existing cracks. A horizontal crack with a constant initial aperture and a constant length was considered (Fig 2.16). Moreover, they assumed that water is incompressible and water flow inside crack is laminar to simplify their governing equations. Using fluid mechanic basic equations they derived an expression for pressure variations inside the crack which is made up of three terms as follows:

$$p = -\frac{\rho L^2 (1-\xi^3)}{6w_0} \dot{w}_1 - \frac{3\rho L^2 (1-\xi^4)}{10w_0^2} \dot{w}_1^2 - \frac{2\rho L \nu (1-\xi^3)}{w_0^3} \dot{w}_1 \quad (2.7)$$

where: L is the length of crack

w_0 is the initial CMOD (crack mouth opening displacement)

\dot{w}_1 is the CMOV (crack mouth opening velocity)

\ddot{w}_1 is the CMOA (crack mouth opening acceleration)

ρ is water density

ν is the kinematic viscosity of water

ξ is a non-dimensional parameter defined by $\xi=1-x/L$

The first term is proportional to the relative acceleration of crack lips, the second term is proportional to the square velocity, and the third term is proportional to the velocity and viscosity of the water. By a parametric study, they showed that the first term is dominant for cracks with aperture exceeding 2 mm, while the third term becomes significant for cracks less than 1 mm in aperture, and second term is negligible.

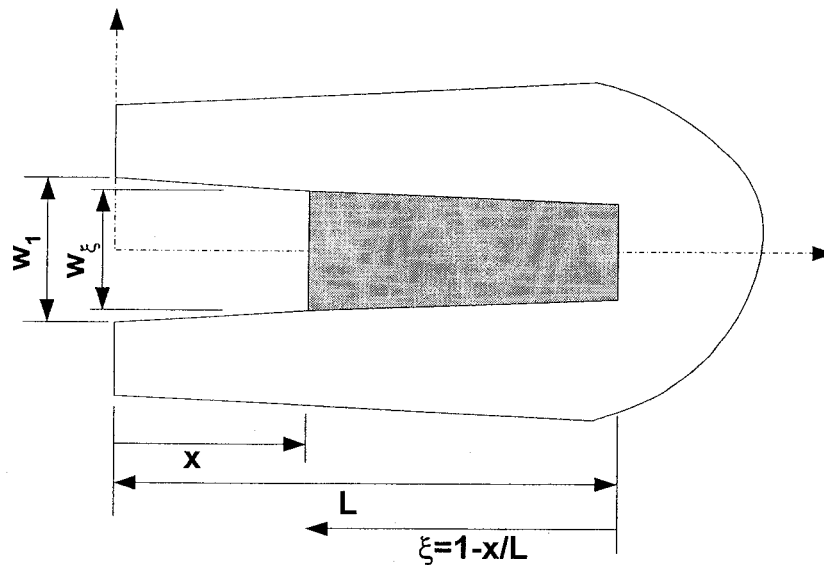


Figure 2.16 Geometry of assumed crack (Tinawi and Guizani 1994).

By introducing dynamic pressure as external forces acting on the nodes of a finite element mesh, an equivalent added mass matrix and damping matrix were defined (only the first and third term of equation 2.7 were used). These matrices must be added to the global structural mass and damping matrices at the associated degree of freedom. This implementation has the major advantage that a linear analysis including water interaction inside a crack can be carried out. They used ANSYS to analyse a cracked dam (the crack length was 2m), 55 m high with an initial crack opening of 2 mm at the base or near the crest, subjected to two different ground motion acceleration records. For high frequency ground motions, the seismic hydrodynamic pressure inside the crack, at the base of the dam, appeared to be 50 per cent higher than the corresponding hydrostatic pressure. This procedure is the first theoretical procedure that could calculate pressure variation in a crack due to crack wall movement but it has two main shortcomings. The first is that it is applicable only for small opening or closing of crack (relative to its initial aperture) and the second is that the effect of cavitation development is not considered in their formulation.

2.5.3 Transient uplift due to variations in crack mouth pressure

The only experimental work in the second category of transient water-crack interaction model has been done by Ohmachi et al. (1998). They conducted a series of shake table experiments to investigate the hydrodynamic pressure inside narrow cavities like cracks in concrete gravity dams. A rectangular water container with three rectangular acrylic boxes with 300 mm-long horizontal notches with different widths (1.5 mm, 5 mm, and 10 mm) was used. Sinusoidal base motion with different excitation amplitudes and frequencies were applied at the base of the water container by a shaking table. The specimens and experimental set up is shown in Fig. 2.17. In the experiment, hydrodynamic pressure sensors, installed on both sides of notch surfaces, were used to measure hydrodynamic pressure at several points along the cavities. According to their findings from the experiments, the hydrodynamic pressures inside cavities increase linearly as the distance from the mouth of the cavity increases. They also noticed that the pressure changes not only with the acceleration of input motion but also with the frequency and the cavity opening. Neglecting the pressure variation with frequency and cavity opening they accepted linear variation for hydrodynamic uplift pressure, P , along the cavity according to following equation:

$$P = P_w + \rho a_x x \quad (2.8)$$

where P_w is the hydrodynamic pressure at the crack mouth, ρ is the water density, a_x is horizontal acceleration, and x is the distance from notch mouth.

They also used a smeared crack model to analyse the nonlinear tensile behaviour of concrete (Zhang and Ohmachi 1998). An improved solution method of dynamic equation was presented and applied to a case study of Koyna Dam. Hydrodynamic pressure is evaluated by equation 2.8 and applied at the location of damaged elements, then effective uplift forces in each node is computed. Since the calculated force is a function of unknown acceleration in each node, a Newmark β -method is used for iterative solution of dynamic equilibrium equation. The effect of hydrodynamic pressure inside cracks on the cracking in the dam body was investigated and the computation showed that hydrodynamic pressure inside cracks tended to increase the length of crack.

There are two major assumptions that have been considered in equation 2.8 and using this equation to formulate hydrodynamic water pressure in the cracks of concrete gravity dams subjected to earthquake may not be accurate. The first assumption is that the crack walls motions have not been considered, while crack walls in a gravity dam move during the earthquake and the significant pressure change due to crack wall motions have been shown theoretically and experimentally as discussed before. It is also assumed that the crack in a concrete gravity dam is fully saturated during crack development and motion, while the saturation of crack has not been proven yet.

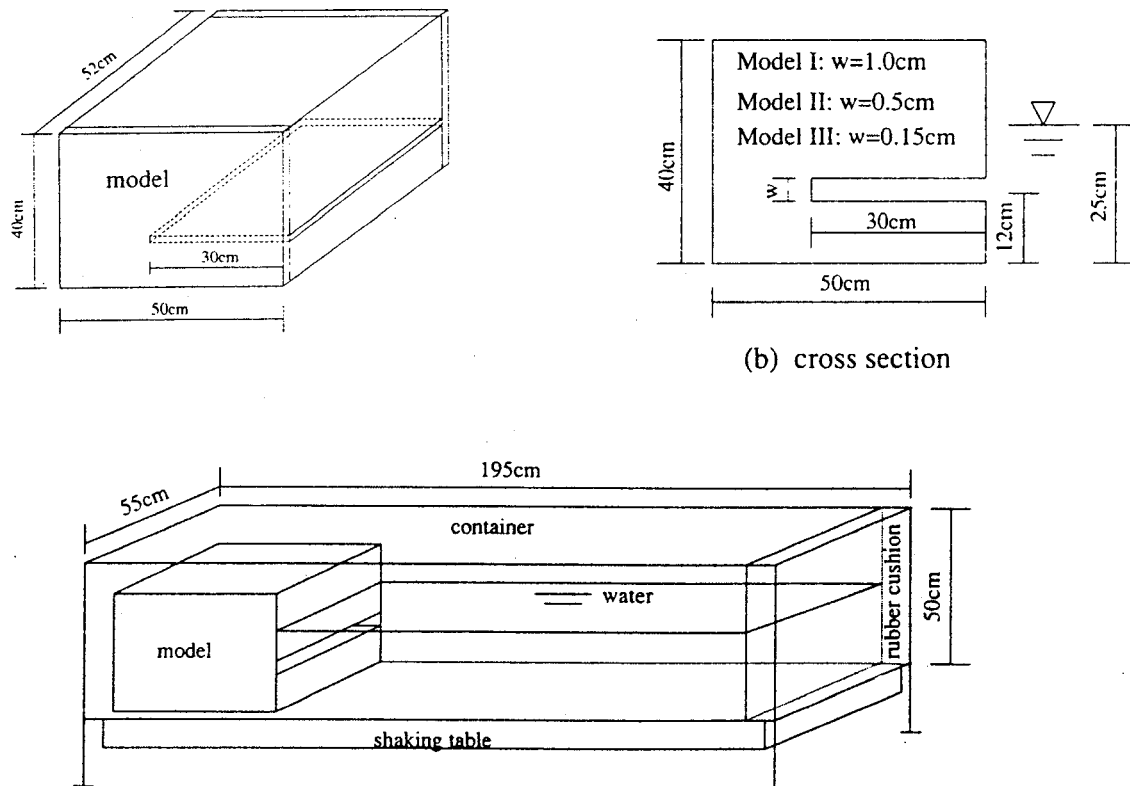


Figure 2.17 Experimental setup and details of specimens (Ohmachi et al. 1998).

2.5.4 Computer programs for seismic dam analysis

In some general purpose or specially developed computer programs for analysis of dam, hydrodynamic effects of water in concrete cracks have been considered. In SCADA 1996 (Smearred Crack Arch Dam Analysis) that was developed by Hall 1997 for nonlinear seismic analysis of arch dams, a simple option to include water pressure in cracks during earthquake has been presented. The calculated hydrodynamic pressure at crack mouth (at the upstream face of dam) due to dam-reservoir interaction is distributed linearly across the dam thickness without any modifications for the pressure variations due to crack motions.

2.6 Compressibility of water

Water like other liquids is compressible to some degree. The pressure and density changes in liquids are related to the bulk compressibility modulus β , as:

$$\beta = \frac{dp}{(d\rho/\rho)} \quad (2.9)$$

where $d\rho$ is the change in water density due to change in water pressure dp . β is a function of temperature and initial pressure of liquid; for water at atmospheric pressure and 25 °C, it is around $\beta=2$ GPa.

When a fluid moves steadily at the speed much less than the speed of sound, its density remain constant and an incompressible flow is adequate. However in unsteady, low speed flow of liquids (or gases) flow, the propagation of pressure disturbances can produce a flow field significantly different from that predicted by an incompressible analysis even when the changes in density are quite small. It is common to refer to these pressure disturbances as waves, and due to similarity between pressure waves in fluids (or solids) and sound waves in gases they are called acoustic waves.

In geophysics, the dependency of velocity and attenuation of acoustic waves on pore geometry and fluid properties serve as a diagnostic of material structure. The

compressibility of the pore fluid is an important factor affecting the internal flow under wave excitation of material. The most relevant study to main purpose of this project has been done by Doverkin et al. (1990, 1992). They formulated a 2-D problem of oscillatory flow of a viscous compressible fluid in an arbitrarily shaped fracture due to normal harmonic oscillation of fracture walls. Considering small amplitude of oscillation (relative to fracture aperture) the solution of the problem is reduced to an ordinary second-order differential equation that can be solved numerically. They also considered permeability of fracture walls and developed solution for this case, with the same simplification assumptions. Figure 2.18 shows the effect of crack shape on resonance frequency of fracture due to harmonic oscillation of fracture walls. According to their computations these are relatively high frequencies compared to the dominant frequencies of strong motions during earthquakes (normally between 1 to 10 Hz). Since their solution is valid for harmonic oscillations with small amplitude their answer is not applicable for crack wall motions due to earthquake where crack wall motions may be greater than initial crack aperture.

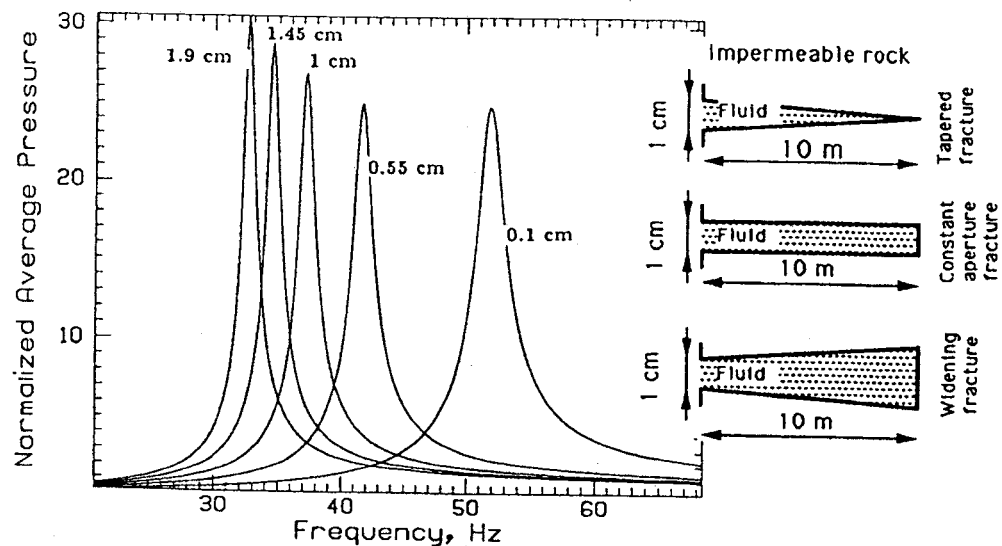


Figure 2.18 Effect of changing shape of a fracture for a fracture with 1 cm opening at left end (open end) and different opening (from .1 to 1.9 cm) at right end (close end).

2.6.1 Cavitation

Cavitation may occur whenever the total pressure falls below the vapour pressure of water P_v . When this occurs, the water flashes to vapour locally and forms a vapour cavity. Water compressibility changes after cavitation and equation 2.9 is not applicable for this case. For mathematical formulation of cavitation in fluid structure interaction studies, a bilinear variation as shown in Fig 2.19 is considered (El-Aidi 1988). Numerical analysis of dam reservoir interaction for earthquake loading shows the possibility of cavitation occurrence in reservoir and dam interface. It has also been shown that closure of a region of cavitation results in a sharp spike of compression pressure followed by high frequency oscillations (Fig. 2.20). However, cavitation appears to have a small effect on the earthquake response of gravity dams (Fenves and Vargas-Loli 1988). Cavitation phenomena may occur during earthquake in a crack for crack opening case when water pressure drops to the vapour pressure of water. This phenomenon was never considered by researchers in water crack interaction studies, but possibility of its occurrences reported by Tinawi and Guizani (1994) when they were studying seismic response of a dam considering water-crack interaction.

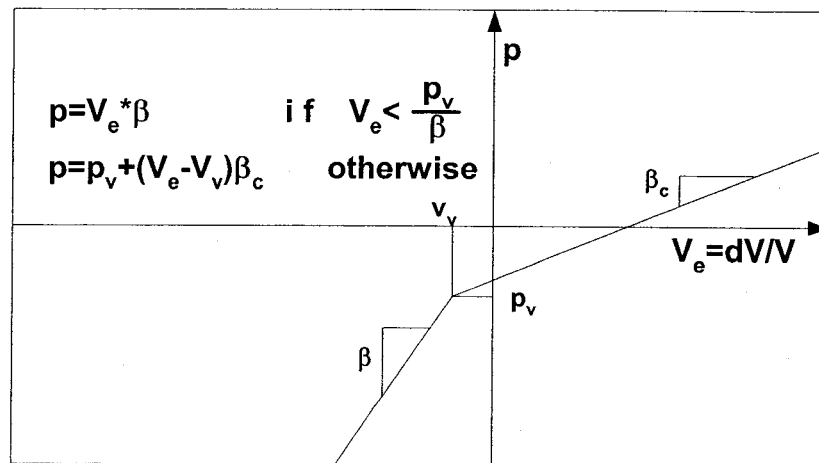


Figure 2.19 Bilinear equation of state for water.

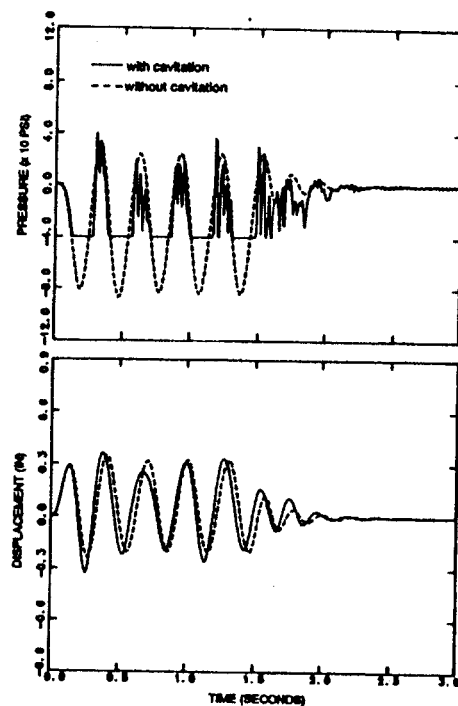


Figure 2.20 Computed response of one dimensional fluid-structure system to harmonic ground motion (1 in.=0.025m ; 10 psi=70 kPa) Fennes and Vargas-Loli 1988.

2.7 Conclusions

The pressure evolution in cracks of concrete gravity dam during an earthquake is a complicated problem due to several coupled phenomena that occur in the system. The physical mechanisms that cause pressure changes during earthquakes can be classified as follows:

- Flow of water inside the new propagating crack.

Only one experimental test has been done so far that shows that relative velocities of water front and crack front in a propagating crack have important effects in developed water pressure inside the crack.

- Flow of water inside the saturated existing crack.

Water flow through cracks and joints with unmoveable walls has been investigated experimentally and theoretically. Although there are few theoretical solutions for water

pressure inside the concrete cracks with moving walls, but due to simplification assumptions made in these solutions, their validity are questionable.

- Compression and decompression of water due to opening and closing of crack.

The compressibility of water is considered some researches and computer programs like UDEC, while in most researches it is assumed incompressible. The importance of compressibility in the magnitude of developed water pressure has never been investigated.

- Water pressure variation along the crack due to hydrodynamic pressure variation at crack mouth.

Variation of water pressure at the crack mouth changes the water pressure variation along the crack.

- Cavitation

It has been shown numerically that cavitation may occur in cracks, but it is never considered in existing seismic water-crack interaction formulations.

Figure 2.21 shows a summary of theoretical or experimental studies that have been done so far by researchers. The considered physical phenomena and the type of researches are summarized in this figure.

A numerical solution of the problem considering all the phenomena is very complicated and there is not any appropriate solution. Although some of these phenomena have been considered experimentally or theoretically by researchers the findings so far are not adequate for a complete seismic water-crack analysis of concrete dams. More experimental and numerical studies are thus needed in this field as presented in the following chapters of this thesis.

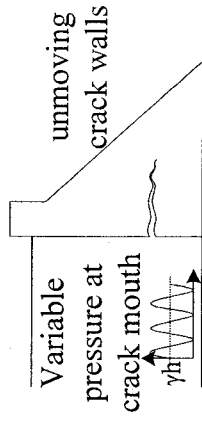
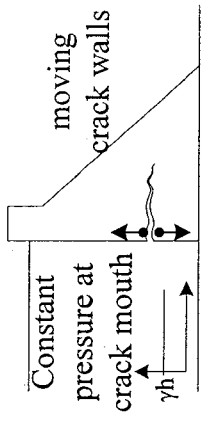
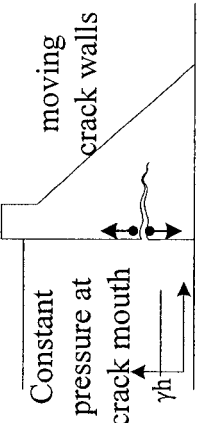
Objective	Phenomena studied	Type of research and researcher
 <p>Diagram showing unmovable crack walls. The crack mouth is labeled with γh. A wavy line indicates variable pressure at the crack mouth.</p>	Variation of pressure in crack due to hydrodynamic pressure in reservoir	Experimental by Ohmachi et al. 1998
 <p>Diagram showing moving crack walls. The crack mouth is labeled with γh. A horizontal arrow indicates constant pressure at the crack mouth.</p>	Pressure variations due to water intrusion and extrusion in a crack with moving walls	Theoretical by Tinawi and Guizani 1994
 <p>Diagram showing moving crack walls. The crack mouth is labeled with γh. A horizontal arrow indicates constant pressure at the crack mouth.</p>	Pressure variation due to rapid opening or closing of crack	Experimental by Slowik and Saouma 1994-2000

Figure 2.21 Comparisons of research studies about transient water pressure inside concrete cracks due to earthquake.

CHAPTER 3 EXPERIMENTAL PROGRAM

3.1 Introduction

To study the dynamic water pressure variations in a new or an existing crack of concrete gravity dam two testing procedures are defined. The development of the experimental program and the selection of experimental testing variables as well as the objectives of the experimental program are presented in section two of this chapter. Geometry of specimens, test set up, and instrumentation are explained in section three. Section four presents two types of testing procedures including new crack tests and existing crack tests. Preliminary tests to develop the appropriate technology to apply, control, and measure seismic water pressures in cracks without leakage are presented in section five. Conclusions related to the testing procedures end this chapter.

3.2 Earthquake response of gravity dams and development of the experimental program

Based on the literature review and the phenomenological aspects, presented in Chapter 2, there are three basic parameters that have major impact on magnitude of water pressure in a cracked concrete with moving walls. These are the uplift pressure at crack mouth, the relative motion of the crack walls, and the crack geometrical, mechanical and hydraulic characteristics. Figure 3.1 shows these parameters in a concrete gravity dam for two cracks developed in different locations; in dam body, and along the dam-foundation interface. The magnitude of uplift pressure at the crack mouth (static pressures plus dynamic pressure due to dam reservoir interaction) changes with the crack elevation. For example, the static (initial) uplift pressure is greater for a crack at the base of dam compare to a crack at the top of dam. The relative motions of crack walls, should be determined by an interaction analysis of the dam-reservoir-foundation

system. For an existing crack, the time history of crack wall motions, including dominant frequency and magnitude of opening or closing, is a function of the applied earthquake ground motions. The application of typical East North American earthquake records (ENA) with predominant frequency content of 10 Hz will result in different crack wall motions in a dam compared to results of application of typical Western North America earthquake records (WNA) with predominant frequency content around 2 Hz to the same dam. The exact geometric, stiffness and hydraulic parameters of a crack should be determined by investigation of the crack at the site. But it is possible to make reasonable assumptions about their magnitudes.

Due to practical limitations in modeling of concrete dam with all the components (earthquake records, reservoir, foundation) a cantilever concrete beam is used to model a dam with a cracked section (Fig. 3.1). The water pressure can be applied at the crack mouth by confining the specimen all around, and the crack wall motions are possible by the application of dynamic loads on a cantilever beam.

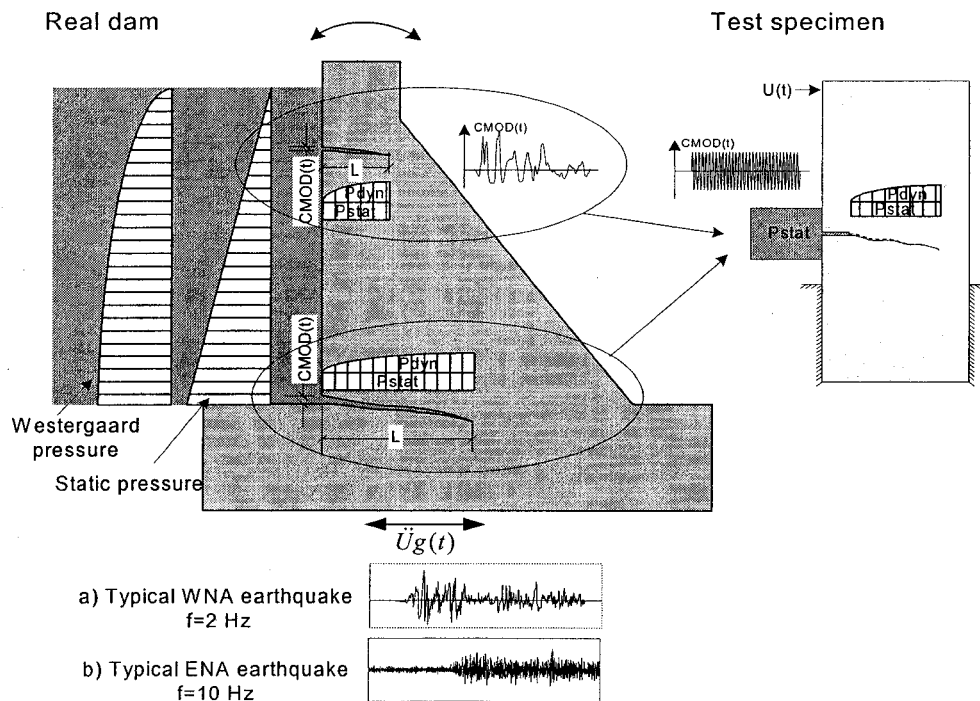


Figure 3.1 Dynamic pressure due to earthquake in cracks of a gravity dam.

3.2.1 Selection of experimental test variables

Therefore, the objective is defined to have a crack in a specimen that can open or close with pressurised water in the crack. Considering the experimental limitations, the order of magnitude of the main variables in the test should be close to the magnitude of similar variables in real dams.

- **Initial uplift pressure:** The magnitude of initial water pressure should range from few meters of water to more than 100 m of water which is the typical range of water pressure behind a real dam. The range of 10 kPa to 500 kPa (1m to 50 m of water) is used because of practical limitations to confine greater water pressure around the specimens.
- **Crack geometry:** Among different geometric parameters only the roughness of crack, that has major effect in water flow inside the crack, is considered in this study which is mainly a function of concrete components size. The concrete crack walls are assumed impervious.
- **Crack length:** Due to practical limitation the maximum width of specimen is chosen 0.5 m and the maximum crack length cannot be greater than 0.4 m.
- **Crack walls motions:** Harmonic excitation is used to simulate crack wall motions in the testing program. Three different excitation frequencies including 2 Hz, 6Hz, and 10 Hz are used, where 2 Hz is the dominant frequency for WNA and 10 Hz is the dominant frequency for ENA. Performing a series of linear elastic analysis of concrete gravity dams, with cracks in different elevations and with different lengths, subjected to typical earthquake records (1940 Elcentro record, 1988 Saguanay records, and sinusoidal excitation at 2 Hz and 10Hz) show that crack mouth opening is ranging from very small values close to zero up to 5 or 6 mm. Due to limitation in crack length it is not possible to open cracks greater than 2.5 mm.

3.2.2 Objectives of experimental program

The main objectives of the experimental tests are as follows:

1. To measure water pressure variations inside concrete cracks due to harmonic opening and closing of crack walls.
2. To determine the effects of the following parameters on water pressure variations inside cracks:
 - frequency of crack walls opening-closing (2 Hz, 6 Hz, and 10 Hz)
 - crack mouth opening displacements amplitude
 - minimum (residual) crack mouth opening displacement
 - initial water pressure
3. To compare water pressure variation in new crack, induced by the applied harmonic load, and an existing crack due to harmonic opening and closing of cracked walls.

3.3 Test set up

Based on the objectives of the experimental program, the available facilities in the structure laboratory, and literature review of previous experimental work, the testing specimens have been designed. The objective is to have a crack in the specimen that can open or close by applying dynamic displacement with pressurised water in the crack.

3.3.1 Geometry of specimens

Figure 3.2 shows the geometry of a typical specimen. It is a small cantilever beam loaded at the top by a rigid link fixed to the shake table to apply static or harmonic loads (displacements). A crack initiates at a certain elevation, due to an existing small notch, by applying displacements at the top of specimen. Five holes are created in the specimen during casting such that they intercept the estimated crack trajectory.

3.3.2 Test set up

The complete test set up is shown in Fig. 3.3. The specimen is fixed to a very stiff steel supporting structure and is attached to the shake table by a rigid link to apply static, harmonic, or seismic displacements. A small notch in the specimen induces a crack at

the desired elevation when a concentrated load is applied at top. To measure the water pressure inside the crack, a similar set up as the one used by Slowik and Saouma (1994) was adopted. A thin waterproof membrane is glued to the concrete surface around the notch and the cracked path. Water inside the tank, pressurised by an air compressor, enters into the notch (and crack) through the pipe at a constant pressure. A steel frame and rubber membrane applies a constant pressure on the concrete surface to confine the water pressure inside the notch and crack. Water pressure along the crack is measured by pressure transducers installed at the end of prefabricated holes in the specimen.

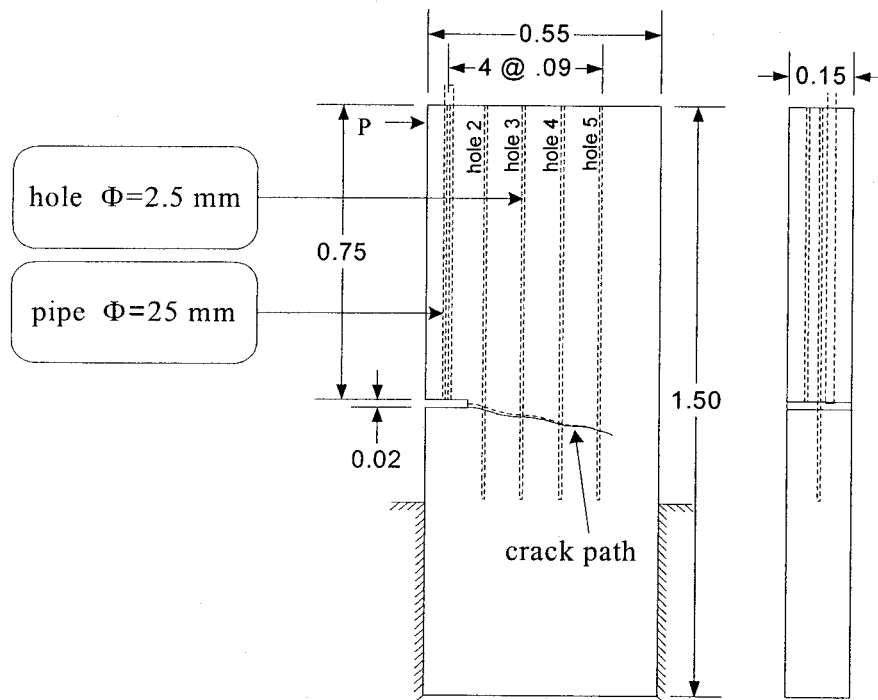


Figure 3.2 Specimen geometry (dimensions in m).

Four specimens were built to perform some preliminary tests. During these tests, the procedure for water confinement was developed and the ability to measure water pressure through the existing holes were examined. During preliminary tests, that are discussed in section 3.5, the option of adding a small water reservoir in front of the notch was considered for the test set up. This reservoir provides the opportunity to do tests with different hydraulic boundary conditions at the crack mouth.

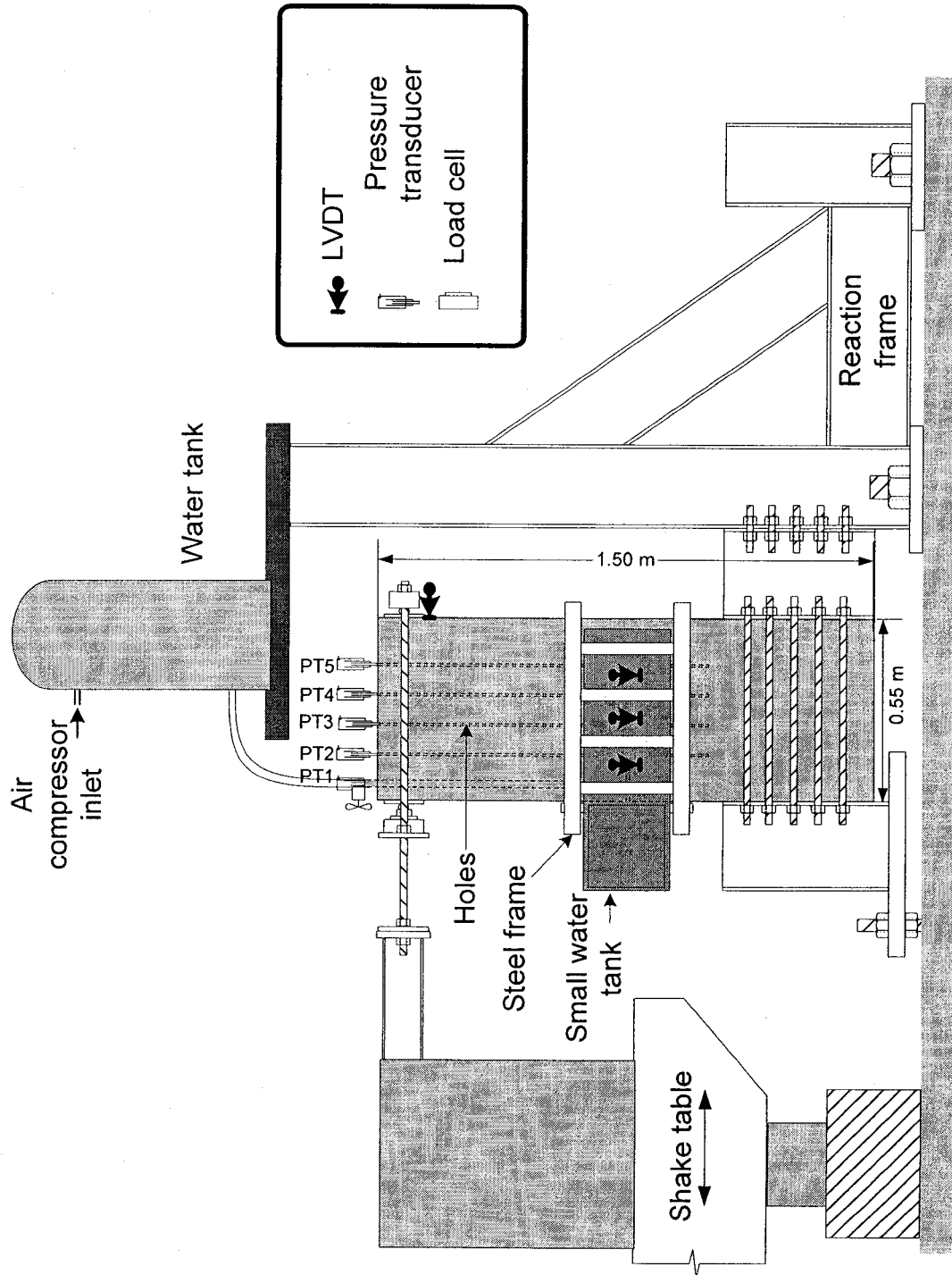


Figure 3.3 Test set up.

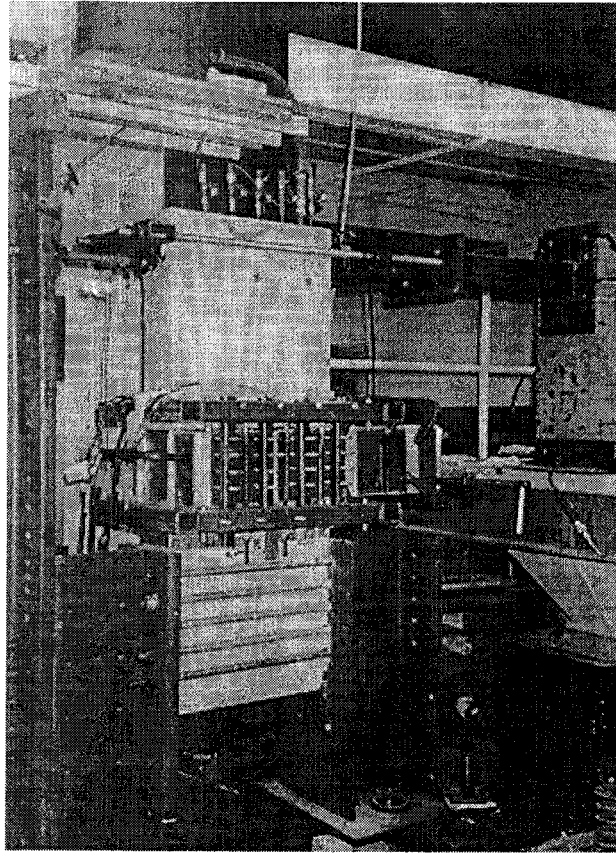


Figure 3.4 Test set up in laboratory.

3.3.3 Instrumentation

Figure 3.3 illustrates the instrumentation, two linear variable differential transformers (LVDT) are installed just at the end of the notch, on both sides of the specimen, to measure the crack mouth opening displacement (CMOD). Four other LVDTs, installed along the proposed crack trajectory on both sides of the specimen, measure the crack opening displacement along its length. A load cell installed on the rigid link, that transfers the load from the shake table to the specimen, measures the applied load. Five pressure transducers measure the water pressure inside the system. One of these pressure transducers measures the input pressure in the notch through a hole that is connected to the notch, and the others measure the uplift water pressure inside the crack at equal distances.

3.4 Testing procedures

According to the objectives of the experimental program, two different test procedures have been defined. These include specimens that are cracked during the test (to model new cracks), and for pre-cracked specimens (to model existing cracks).

3.4.1 New crack test (specimens cracked during the test)

In this case, variations of uplift pressure in the new developing crack due to harmonic loads are studied. The procedures for these tests are as follows:

- **Supporting the specimens**

In a first step, the specimen is attached to the steel supporting frame by 6 high strength steel bars on each side of the specimen to provide a virtually fixed support. Since the relative displacement of crack walls are measured by LVDTs during the tests, small deformations of the specimen due to support deformations or rotations do not affect the results.

- **Confinement of specimens**

A thin flexible membrane was glued to the surface of concrete all around the notch and proposed cracking area. The membrane is cut around the notch to provide access into the notch. The steel frame of the reservoir is put in front of the specimen (Fig. 3.5) and another membrane is glued on each side of the steel frame and the specimen. Another membrane (pure gum with 0.012 m thickness) and steel plate is used on each side of the specimen to apply a pressure on the glued membranes to confine the water pressure in notch crack and reservoir. A closed steel frame with adjustable bolts is used to apply the confining pressure on the steel plates (Fig. 3.6). Despite of normal confinement pressure all around the cracked area of specimen, relative motion of cracked parts of specimens is possible due to the high in plane flexibility of the membranes as well as possibility for lateral motions of membranes, steel plates and the steel frame with respect to each others. Since relative motions of the crack's walls are measured during the test, the small resistance against the relative motions of the cracked

parts do not affect the test results.

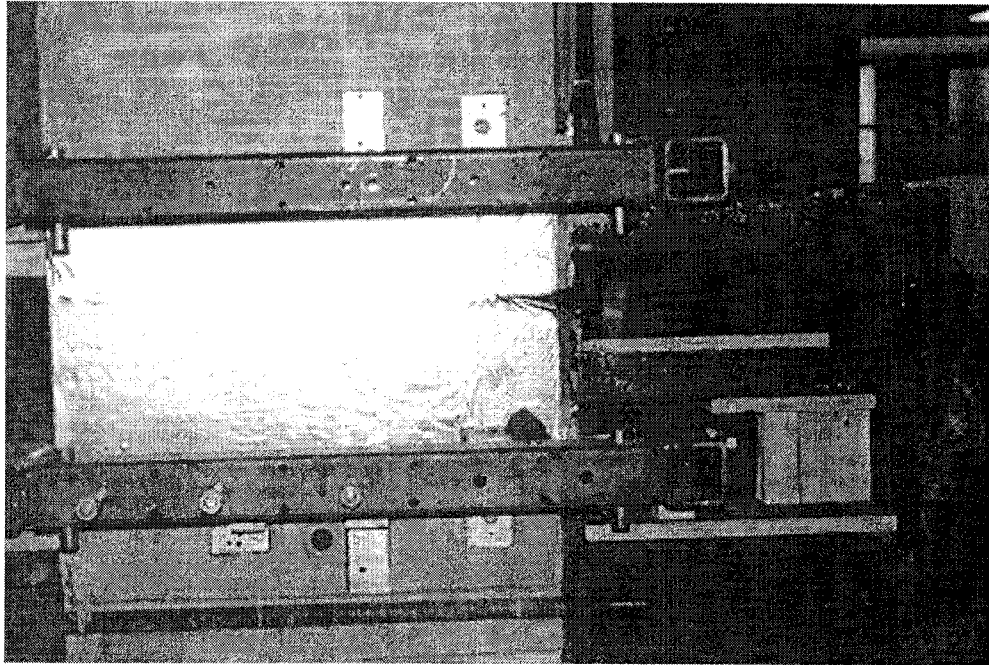


Figure 3.5 First glued layer of membrane with steel reservoir in front of the specimen.

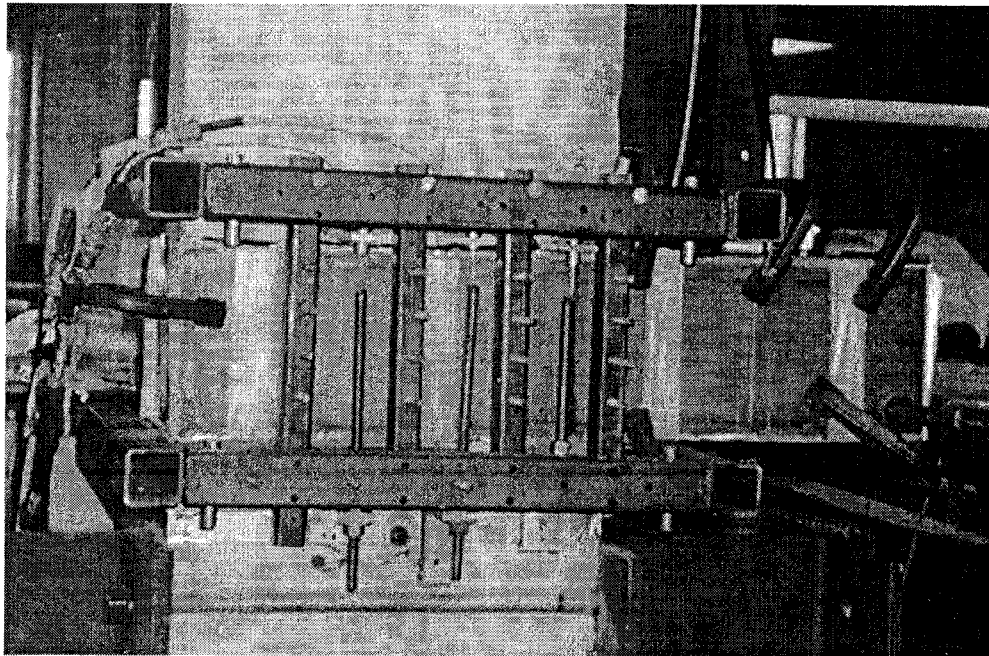


Figure 3.6 Full confinement of specimen.

- **Filling the holes with water**

Using very thin plastic tubes holes number 2, 3, 4, 5 (Fig. 3.2) are filled with water. To fill the holes, plastic tubes are first inserted all along the length of the holes and water filling is started from the dead end of the holes to make sure no trapped air remains in the holes. After the water filling operation the plastic tubes are removed from the holes. Since the absorption of water by dry concrete may affect the results of pressure measurements during the tests, holes are filled one day before doing tests. The pressure transducers are fixed to short copper pipes that have been installed inside the holes during the concrete pouring (Fig. 3.7).

- **Application of water pressure**

Finally the small tank in front of specimen and the notch are filled with water by opening the input pipe valve which connects the big water tank to the notch. A valve installed in the steel reservoir is used to purge all the remaining air from the system. Water pressure in the notch and tank measured by the first pressure transducer is adjusted by application of the air pressure at the top of the big tank. Different pressures ranging from 0.1 MPa to 0.5 MPa were used in this study.

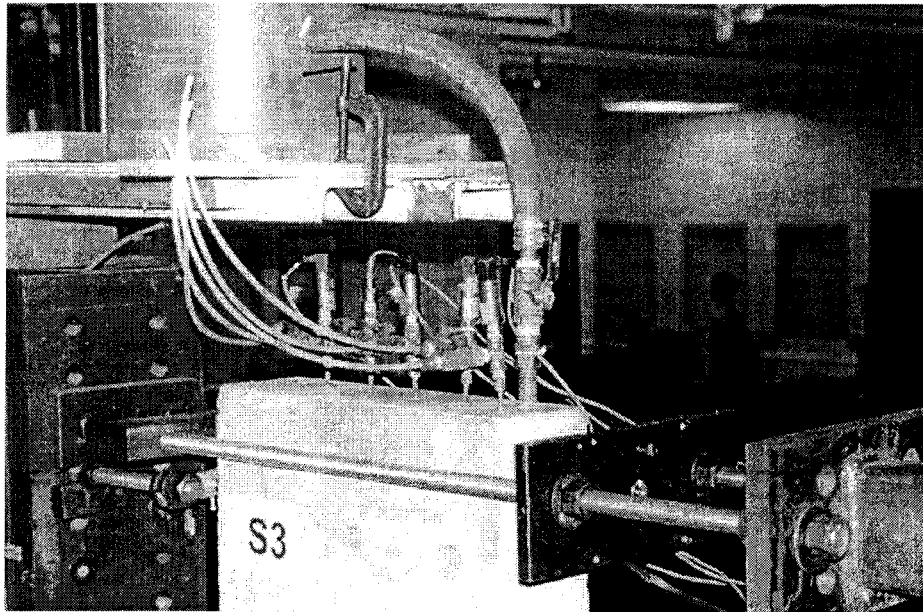


Figure 3.7 Pressure transducer and water tank.

- **Application of cracking displacement**

The general shape of sinusoidal displacement that is applied at the top of the specimen by the shake table is shown in Fig. 3.8. The applied displacement starts from zero and increases sinusoidally to its maximum value d_{max} and then decreases to its minimum value d_{min} which is greater than zero. After that, the applied displacement has a normal sinusoidal variation with minimum and maximum equal to d_{min} and d_{max} . The expected CMOD curve is also shown in Fig. 3.8, choosing d_{min} greater than zero prevents cracked specimens from complete closure which may crack the specimen completely and produce mechanical impact damage and related shock wave propagation phenomenon. The harmonic displacement is applied for 20 sec to get a steady-state response.

Five uncracked tests have been performed using five specimens. Summary of test variables for these five specimens including frequencies, initial static pressures, and applied displacements are shown in Table 3.1.

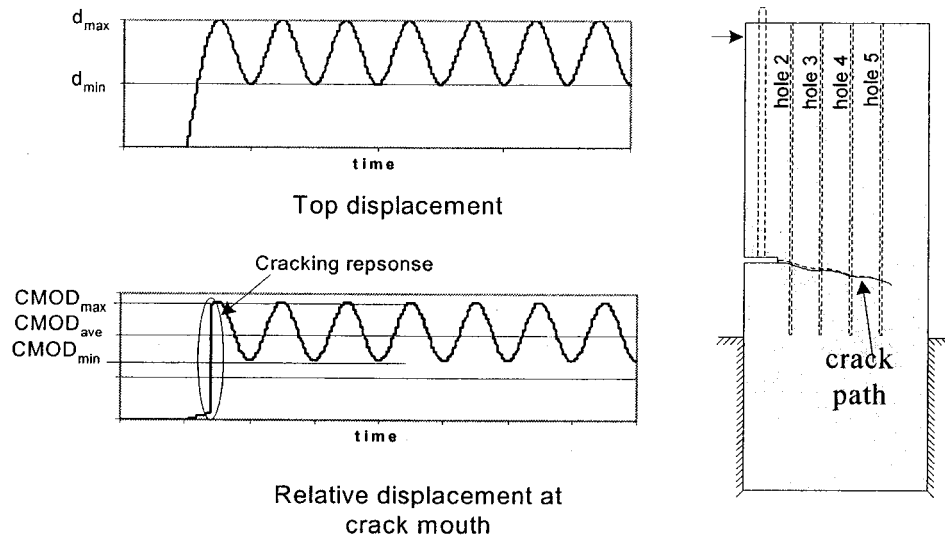


Figure 3.8 Harmonic displacement for new crack tests.

3.4.2 Existing crack tests (pre-cracked specimens tests)

In this case, the variation of uplift pressure in a pre-existing crack is studied. After finishing a new crack test, pressurized water fills the crack, and the static water pressure

along the crack, measured by the pressure transducers, are equal. A cracked specimen resulting from the new crack test can be used for the existing crack tests without any additional adjustments. The existing crack tests can be started by adjusting the applied static water pressure to the desired pressures and applying harmonic displacements at the top of the specimens. Applied displacements in these cases are sinusoidal displacements as shown in Fig. 3.9. The crack mouth opening displacements are set to the desired initial values ($CMOD_{min}$) by adjusting the shake table initial position before starting the tests. Using this procedure, it becomes possible to perform a number of existing crack tests, with different harmonic motions, initial crack mouth opening displacement, static water pressure, as well as boundary conditions, with the same specimen. Six specimens were used to perform tests in different conditions. A summary of variables for these tests including frequencies, initial static pressures, and applied displacements amplitude are shown in Table 3.2.

Table 3.1 New crack tests.

Test number	Frequency Hz	Initial pressure kPa
NS1	2	100
NS2	2	100
NS3	2	400
NS4	10	100
NS5	10	200

3.5 Verification of test set up

There were two practical points in the proposed test set up that were checked before starting the main tests. The first one was the confinement details of specimens, and the second one was related to the capability of the pressure transducer to measure the correct dynamic water pressure.

Table 3.2 Pre-cracked tests

Specimen No.	Initial pressure (kPa)	CMOD d^*	Frequency (Hz)	Boundary condition	Number of tests
PS1	100,200,400	0.5d,0.75d,d	2,6,10	With reservoir	20
PS2	100,200,400	0.5d,0.75d,d	2,6,10	With reservoir	22
PS3	10,100,200	0.5d,0.75d,d	2,6,10	With reservoir	63
PS4	100,200,400	0.5d,0.75d,d	2,6,10	With reservoir	54
PS5	200,400,500	0.5d,0.75d,d	2,6,10	With reservoir	81

* d is a predefined amplitude that changes from test to test.

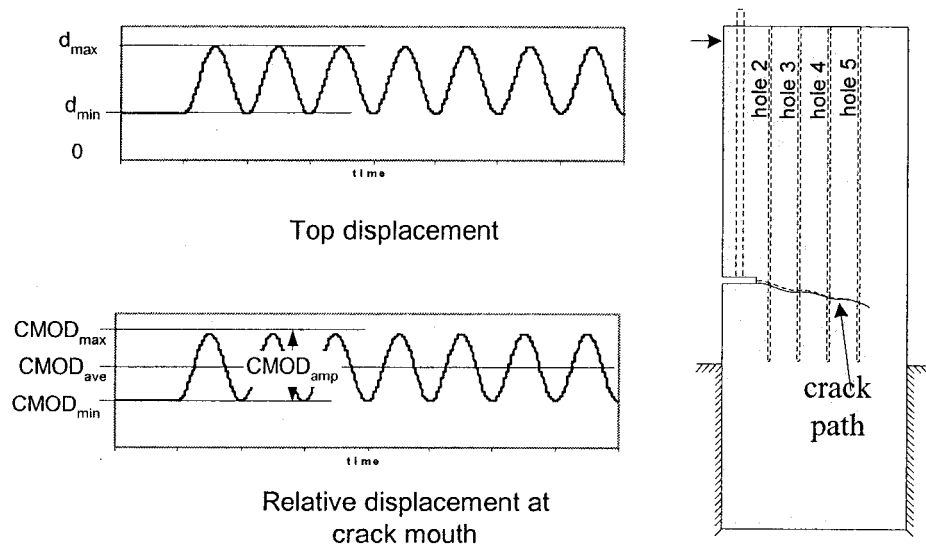


Figure 3.9 Harmonic displacement for pre-cracked tests.

3.5.1 Confinement detail

The pre-cracked specimen procedure was implemented to verify the confinement of water in cracked specimens and to find suitable membranes for this purpose. After several tests with different type of material, a pure gum membrane and a steel frame to support the membrane was adopted. Static water pressure equal to 0.50MPa could then be applied with virtually no leakage.

3.5.2 Adding steel tank to test set up

The first suggested test set up for pre-cracked and new crack tests did not include the steel reservoir in front of the specimen. The results of preliminary tests with this set up showed that, contrary to our objective to provide nearly constant water pressure in the notch, water pressure in the notch changed significantly during the application of dynamic loads. Differences of notch pressure from initial static pressure were greater for 10 Hz excitations relative to 2 Hz excitations. That means that the discharge of water through the pipe, connecting the notch to the water tank, is not as fast as the crack opening or closing. However water can flow in or out of a crack through the reservoir of a dam. The compression or decompression and flow of trapped water inside the system (crack and notch) causes significant pressure variations in the notch and crack. To adjust the system, the pipe must be made shorter and bigger such that water can flow through it as fast as water flow through the crack and notch. Another way to adjust the system is to provide a water reservoir in front of the notch to increase the total volume of water in the system. A small steel tank (150 mm x 200 mm x 300 mm) was added in front of the notch to increase the total volume of water in the system. Figure 3.2 shows the adjusted final set up. Similar tests have been done to compare the results of tests with and without steel tank to determine the effect of the added water reservoir on the notch pressure variation. Figures 3.10 and 3.11 show test results for two typical tests. Since the frequency and amplitude of applied CMOD are similar, the differences in measured water pressures are related to the presence of the steel tank. Comparisons of water pressure variations in the notch and along the crack for these two tests show that the added reservoir has a significant effect on water pressure variations in the notch as well as the water pressure variations along the crack.

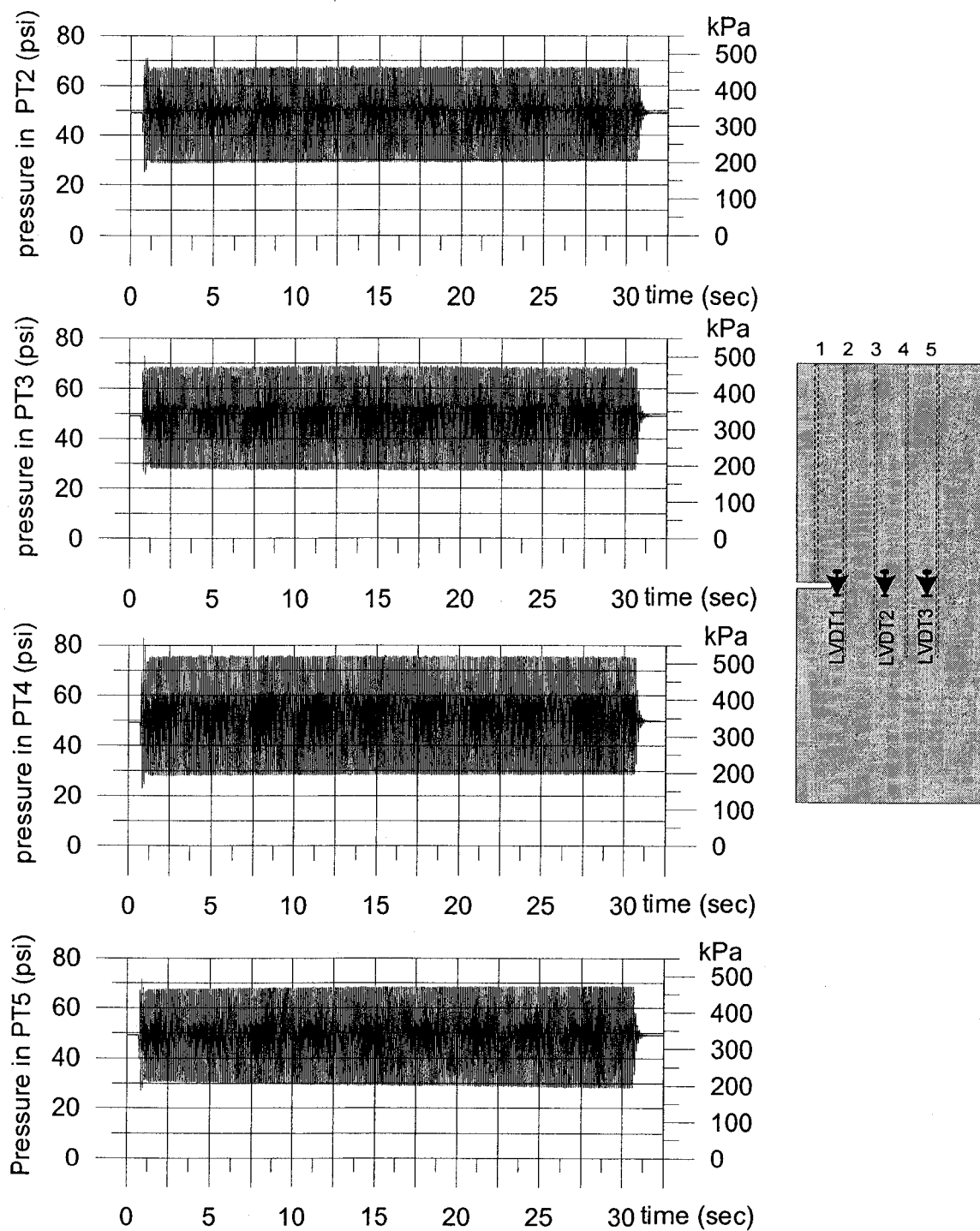


Figure 3.10 Test without steel reservoir in front of notch (10 Hz).

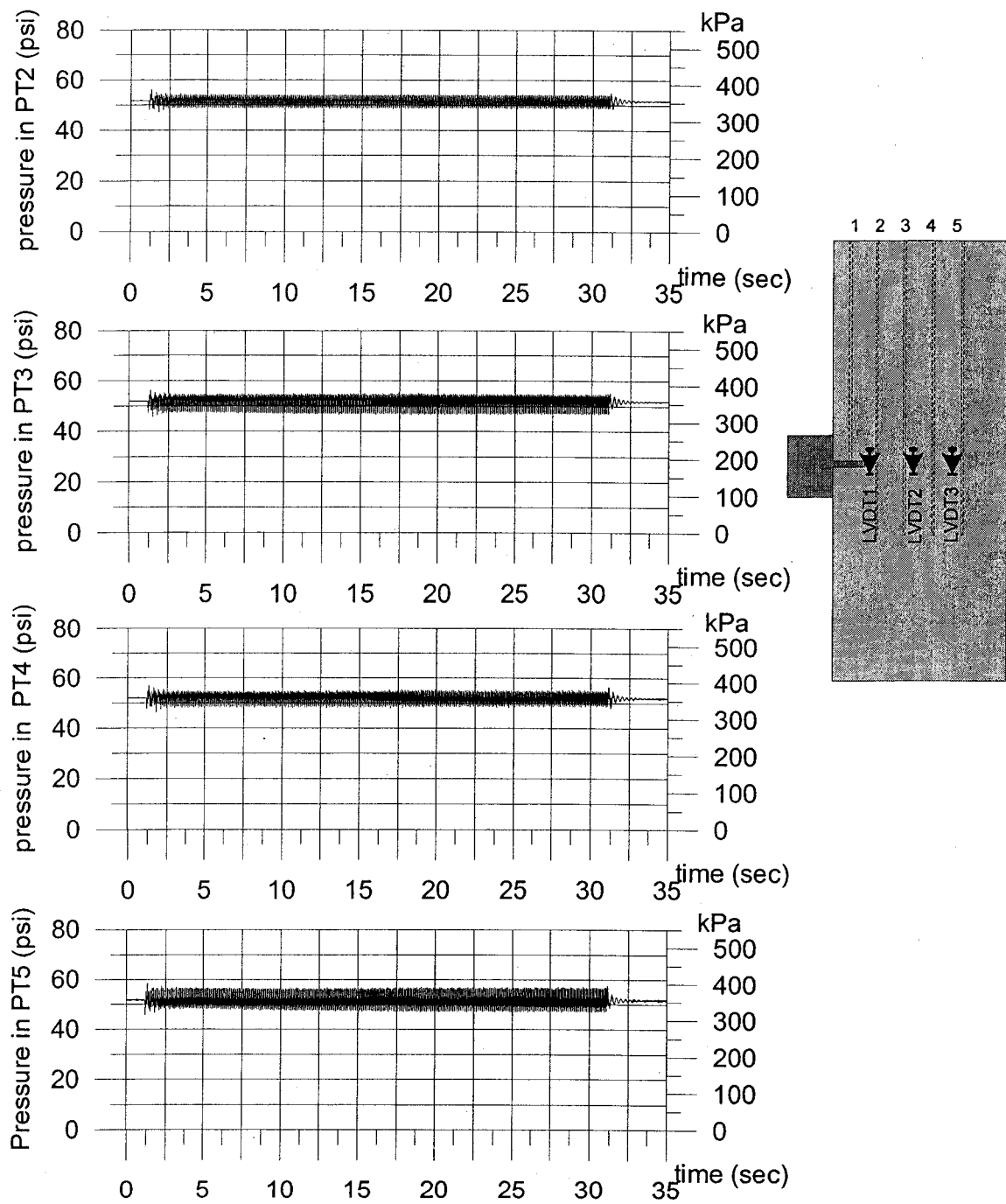


Figure 3.11 Test with steel reservoir in front of notch (10 Hz).

3.5.3 Pressure transducer verification

The purpose of the tests is to measure water pressure inside the crack, however, the installed pressure transducers measure the water pressure at the end of 5 vertical holes (2.5 mm in diameter and 750 mm in length). Differences (magnitude and time delay) that may exist between the actual water pressure in the crack and the measured water pressure at the top of the holes should be studied. These holes, filled with water, were used to connect the crack to pressure transducers at the top of the specimen. The water pressure variations inside the crack due to its closing or opening pressurize the water inside the holes, and these pressures are measured by pressure transducers. The pressure in the holes propagates as a wave through the tube of water inside the hole. It has been shown that the acoustic wave equation can be used to formulate the pressure wave propagation for this case. Another problem that may arise from the existence of holes along the crack is the interaction of reflected and transmitted wave from different holes along the crack or the water tank. The phenomena of wave transmission and reflection along the crack, the holes, and the tank may change the pressure that exists in a real crack without holes. Applying wave propagation theory it is shown, that the measured pressure at the end of a hole is virtually equal to the pressure at the other end of a hole at the crack elevation and the existence of holes does not alter significantly the pressure inside the crack compared to a crack without holes.

The possible differences between the measured pressures at the ends of specimen's holes were also verified experimentally. We also wanted to assess if the existing pressure transducers in our laboratory are capable to measure dynamic pressure variations. To examine these two problems, a preliminary verification test was designed. A simple cylinder-piston system was used to apply harmonic pressure on water and two pressure transducers were used to measure the water pressure variations along a pipe. One pressure transducer was installed close to the cylinder and the other installed at the end of the pipe. The distance between the two pressure transducers was equal to the length of the hole in the beam type specimens to simulate similar conditions as in the actual test. The results of the test showed that the pressure transducers could measure the

dynamic water pressure variations, and the differences related to magnitude and time delay between two pressure transducers due to different locations can be ignored. Test set up and a typical result of this experiment is shown in Fig. 3.12.

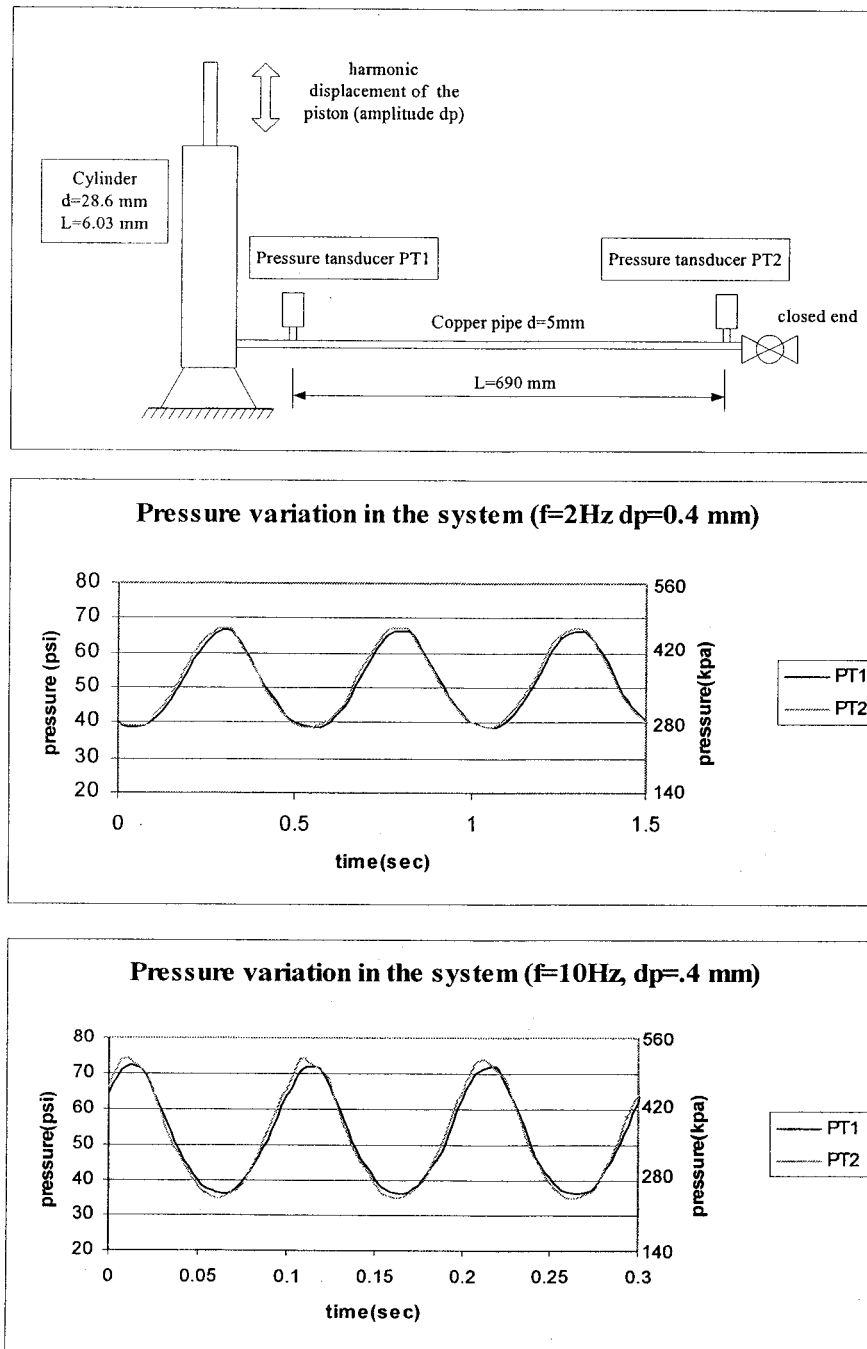


Figure 3.12 Pressure transducer verification tests, test set up and typical results.

3.6 Conclusions

The experimental program has been described in this chapter. The procedure for experimental tests in this study is to provide a nearly constant (static) water pressure in front of a cracked concrete specimen subjected to harmonic motions of crack's walls. Therefore, the experimental results may represent water pressure variations due to coupling effects of all the phenomena described in Chapter 2, excluding the water pressure variations in crack due to hydrodynamic pressure variations at crack mouth (Westergaard effect).

The development of the technology to apply and measure water pressure in cracks, required some adjustments to the initial test set up for the type of membrane and confining frame. Significant pressure changes in the notch were observed during the preliminary tests and a small steel reservoir was therefore added to overcome this problem. Test procedures are used to measure water pressure inside the new cracks and existing cracks of concrete specimens. Five new crack tests and more than 240 existing crack tests have been done. The results of these tests are presented in the next Chapter.

CHAPTER 4 EXPERIMENTAL RESULTS AND DISCUSSIONS

4.1 Introduction

The important observations and findings of the experimental program are discussed in this chapter. The measured parameters in a typical test are first explained and a simple model for crack wall motions is developed based on these results. Existing crack test results are investigated and the effects of variations in selected parameters on the test results are discussed in section three. The results of new crack tests and the discussion about these results are presented in section four. Summary of the main findings of the experimental program concludes the chapter.

4.2 Test results as measured in the laboratory

Twelve measuring devices are installed on each specimen, as discussed in chapter three, and the harmonic excitation is applied for 20 seconds. The data acquisition system was set up such that measured quantities were recorded every 0.001 second (1000 Hz) and considering the 25 seconds of data acquisition, a large volume of data is recorded for each test. Figure 4.1 and 4.2 show typical test results as measured in the laboratory for an existing crack test. Data acquisition starts before specimen excitation and ends after the excitation stops. The constant part at the beginning and at the end of each graph shows the static value of the measured quantity before and after test. The constant load at the beginning and at the end of the first graph in Fig. 4.1, which is the measured load by a load cell, represents the magnitude of the pretension load applied on the steel bars to keep them in contact with the specimen during cyclic excitations. The applied load variations on the top of the specimen can be computed by subtracting this value from measured values during the test.

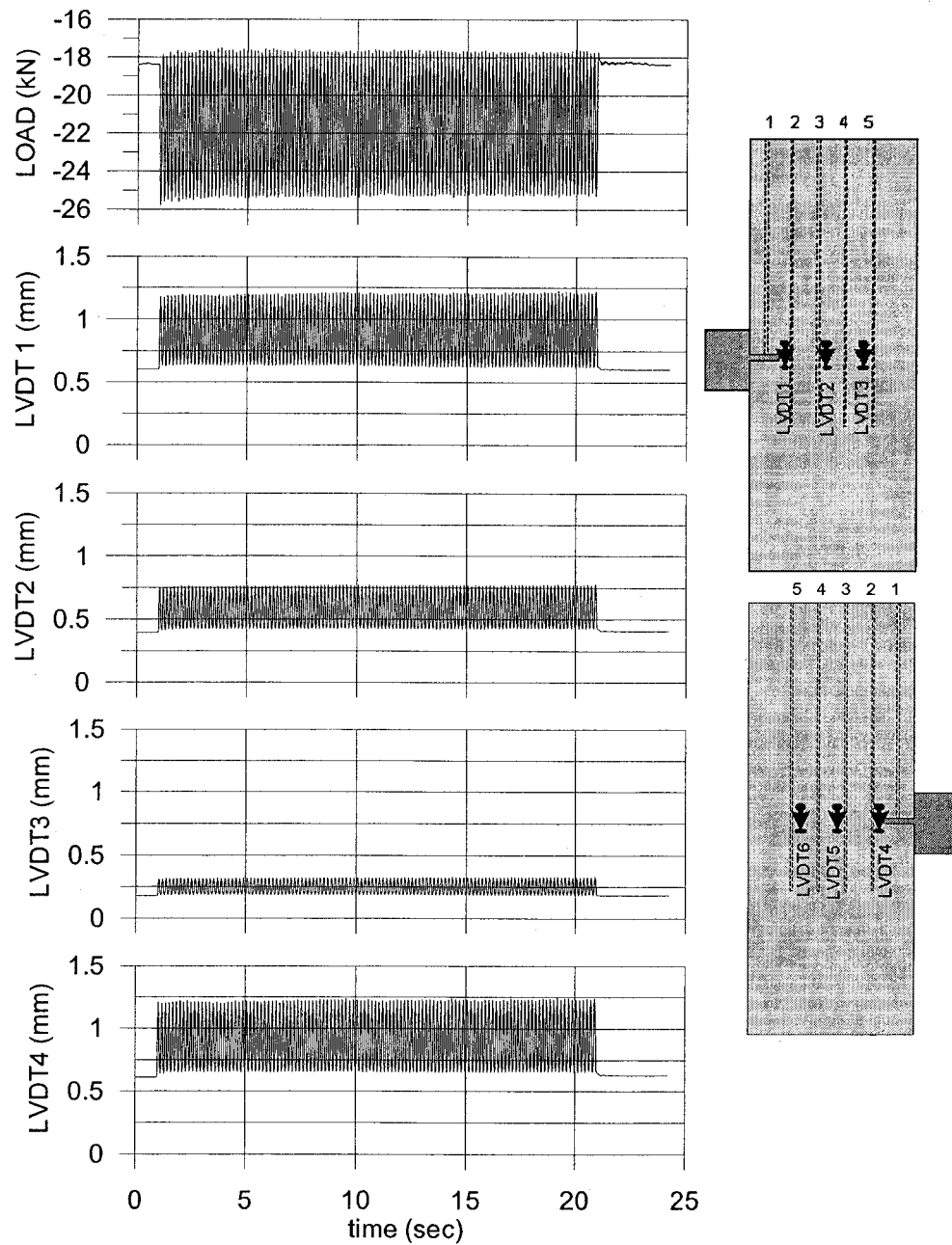


Figure 4.1 Measured parameters (applied load and crack aperture) in an existing crack test (Test no. PS4-2, $P_{stat}=200$ kPa, $f=10$ Hz, $CMOD_{amp}=0.6$ mm, $CMOD_{min}=0.6$ mm).

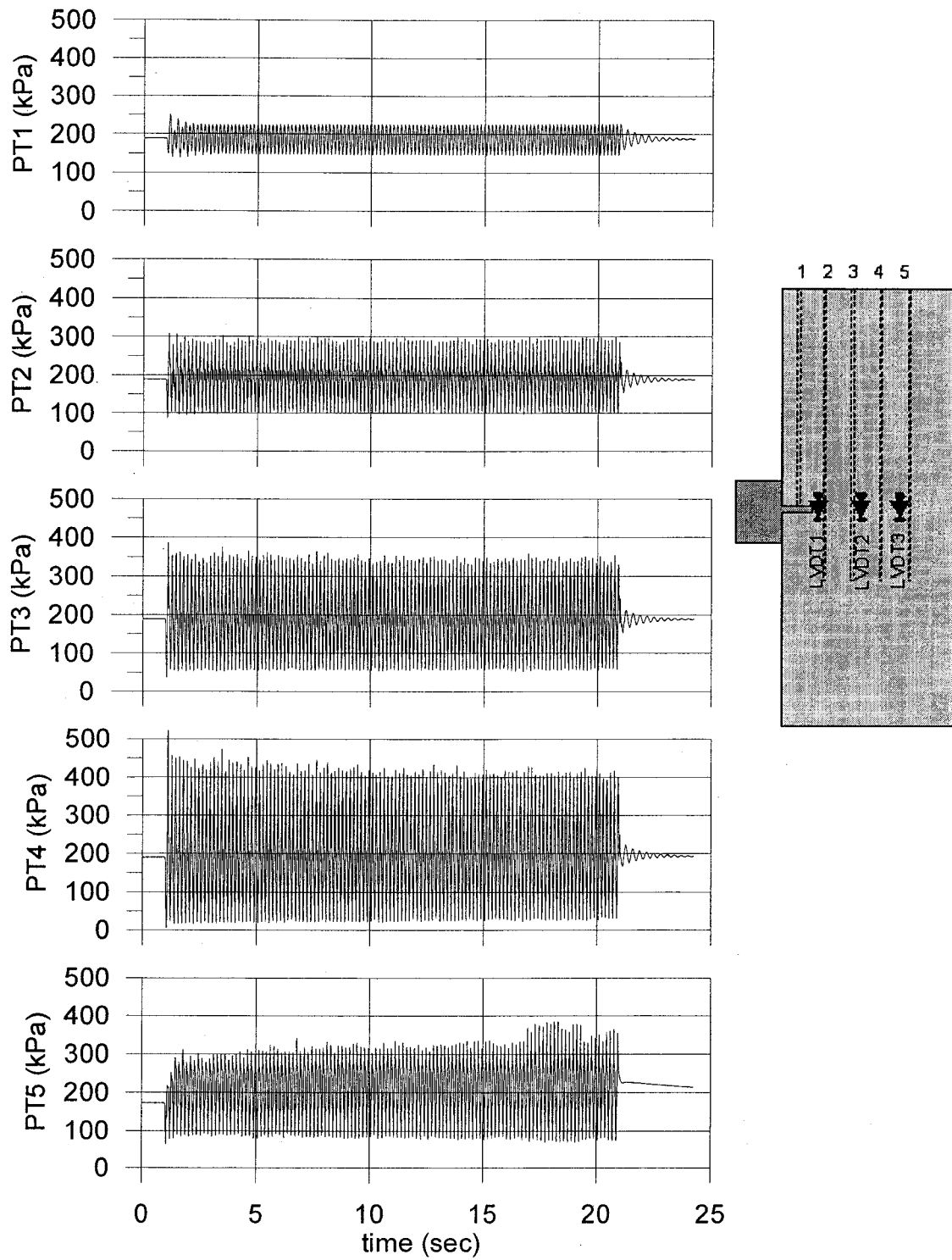


Figure 4.2 Measured water pressure in an existing crack test (Test no. PS4-2, $P_{stat}=200$ kPa, $f=10$ Hz, $CMOD_{amp}=0.6$ mm, $CMOD_{min}=0.6$ mm).

4.2.1 Crack deformations

The measured crack openings at three different locations along the crack, on one face of the crack, are shown in three subsequent graphs in Fig. 4.1 (LVDT1, LVDT2, and LVDT3). Crack opening displacements are also measured at the same locations on the other side of the specimen and the last graph in Fig 4.1 shows only one opening measurement which is at the crack mouth (LVDT4). Comparing the magnitude of LVDT1 and LVDT4, it is concluded that the crack opening displacements are not exactly equal on both sides of specimens. In other word, the specimens have small out of plane deformations. In the theoretical formulation the average magnitude of the crack opening in both sides would be used. The crack walls do not deform significantly during opening and closing due to large in plane stiffness of the cracked specimens. The steel reinforcement at the end of the specimens stops single crack propagation by developing a uniform strain in the region close to the steel location. In this region, the single crack is replaced by a system of very fine cracks, distributed uniformly over the region. This part, and the remaining section of un-cracked specimen, perform like a reinforced concrete beam. The detailed deformation of a typical cracked specimen is shown in Fig. 4.3. To simplify the theoretical formulation of the problem, it is assumed that there is only one single crack with rigid impervious walls, and these walls rotate rigidly around a virtual crack tip (Fig. 4.3.c). Using this model, only the crack length and CMOD variations are needed to represent crack wall motions.

The measured crack opening displacements (COD) along the crack for a typical test are plotted in Fig. 4.4 at three different instant of time. The linear trend of each graph is also plotted. Assuming that the horizontal axis in this figure represents a lower stationary crack wall, each line may be interpreted as the position of the upper crack wall at the corresponding time. The linear relations between crack openings in each instant of time confirm the rigid body motion of crack walls. Continuing the line trends of these graphs, one can find the virtual crack tip based on the measured crack aperture and the rigid crack wall assumption. Using the test results, the average crack length by this method is determined to be around $L=400$ mm. The range of measured crack lengths

which are between 370 mm and 400, mm confirms the proposed simplified rigid body model of the cracked components.

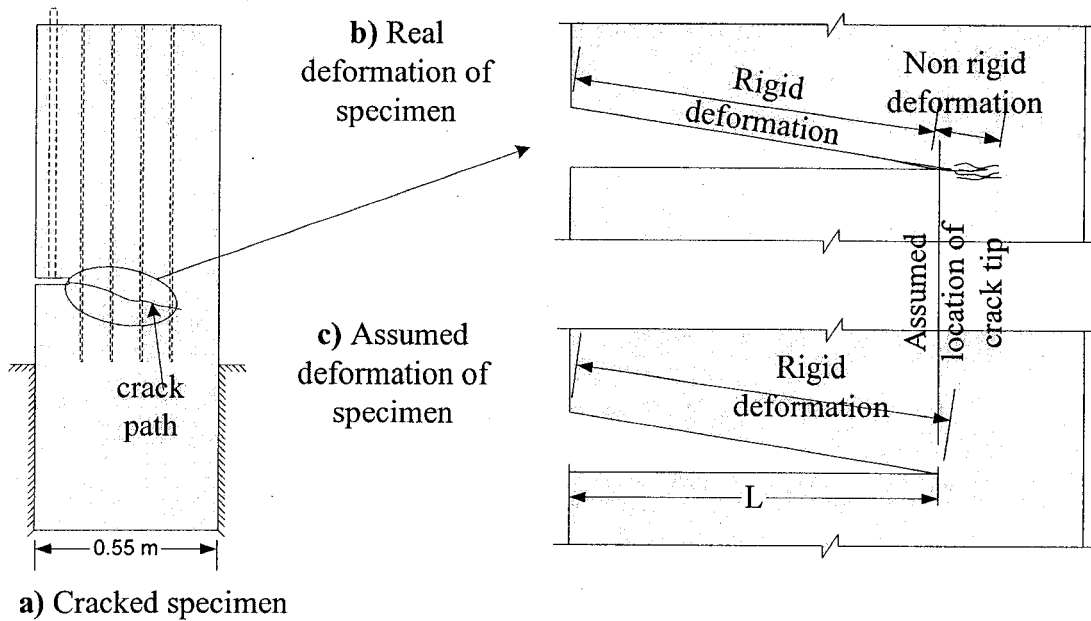


Figure 4.3 Specimen deformation and rigid crack walls.

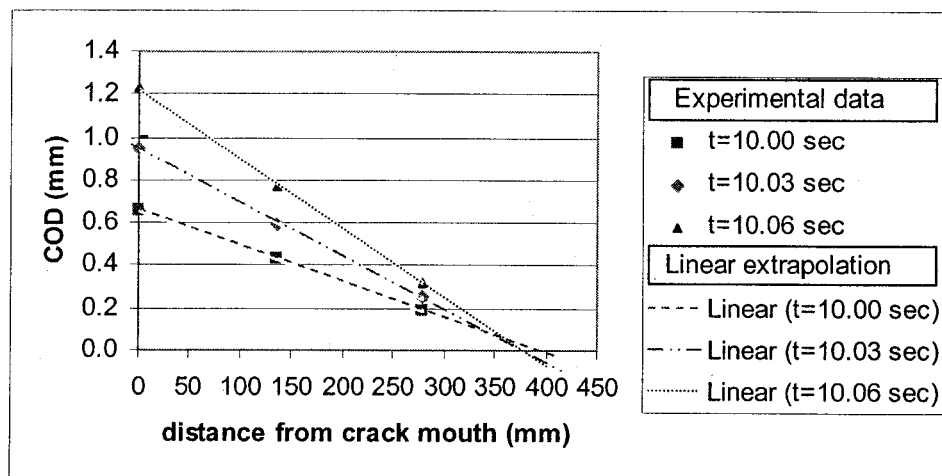


Figure 4.4 Rigid body deformation of crack walls (Test no. PS4-2, $P_{stat}=200$ kPa, $f=10$ Hz, $CMOD_{amp}=0.6$ mm, $CMOD_{min}=0.6$ mm).

4.3 Existing crack tests

To study the effects of variations of selected parameters on the pressure variations in cracks with moving walls, existing crack tests have been repeated by changing one parameter and keeping other parameters constant. It is then possible to study the effects of each parameter on the dynamic water pressure variations individually. These parameters are the initial static pressure P_{stat} , the frequency of harmonic excitation f , the amplitude of crack mouth opening displacement $CMOD_{amp}$, and the minimum crack mouth opening displacement $CMOD_{min}$.

4.3.1 Initial static uplift pressure

Figure 4.5 shows the measured uplift pressures for two different tests ((A) and (B)) that have been done with similar parameters (f , $CMOD_{amp}$, $CMOD_{min}$), except for the applied initial static pressure in the notch. The applied static pressure for test (A) is 200 kPa, and for test (B) 300 kPa. Comparing the measured pressures for the two tests, it can be concluded that the measured pressures have similar shapes (spatial distribution) but the pressures in test (B) are 100 kPa greater than the corresponding pressure in the first test. It is clear that these differences come from the different initial static pressures. We can compute the dynamic pressure, which is defined as the pressure change in the crack relative to the initial static pressure, by subtracting the measured pressure from the initial static pressure (because of small variations in applied static pressure during the tests, the dynamic pressure is computed by subtracting the measured pressure along the crack from the measured pressure in the notch). The dynamic pressure variation is computed for pressure transducer PT4 in these two tests, and the results are shown in Fig. 4.6, the equal dynamic pressure variations for the two tests are clear. The important conclusion is that water pressure variations along a crack with moving walls are independent of the initial crack pressure (in absence of cavitation where crack remains fully saturated during crack wall motion). Therefore for two similar cracks, one at the mid-height of a

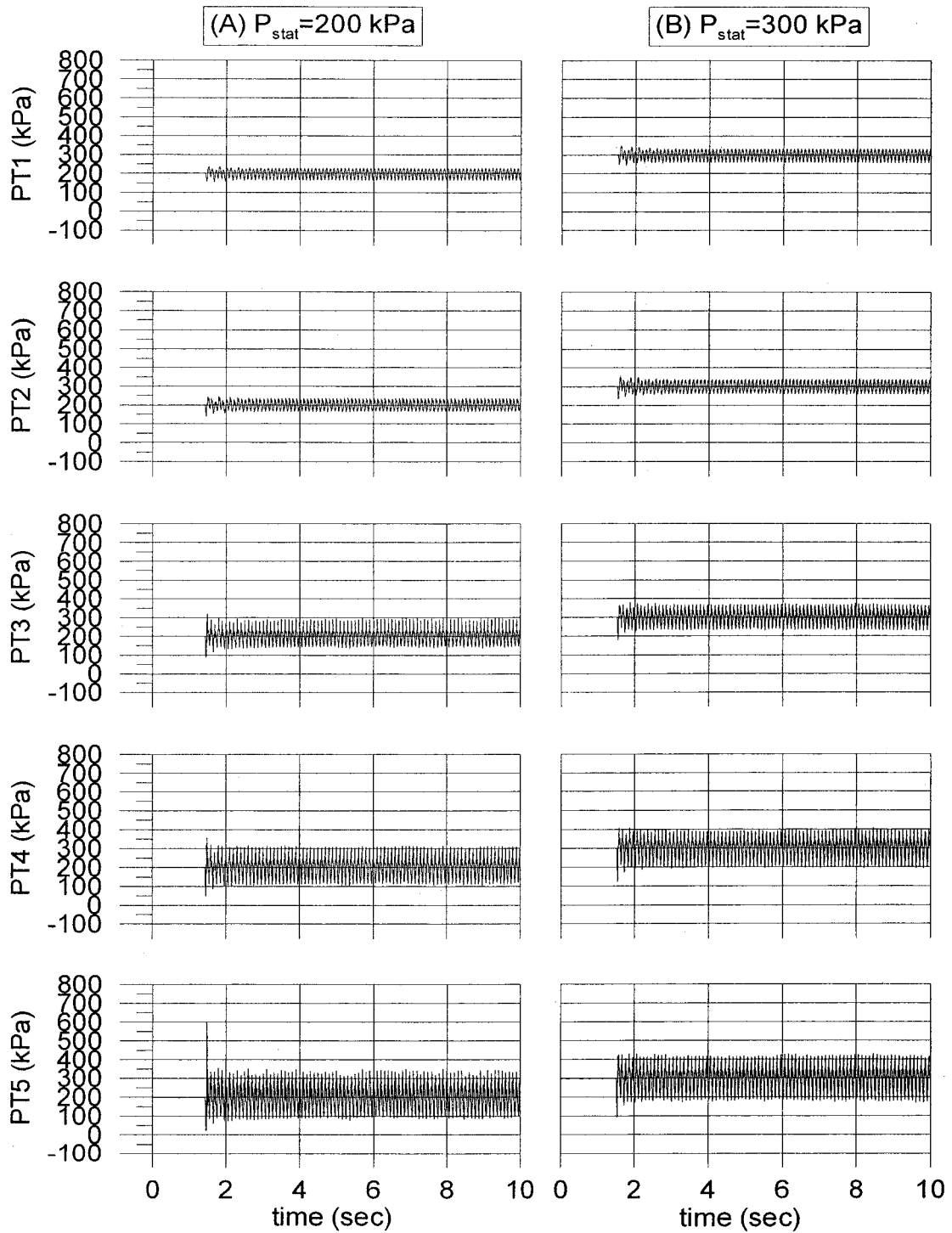


Figure 4.5 Effect of static pressures on total pressure variations: (A) test no. PS4-73, $P_{\text{stat}}=200 \text{ kPa}$, $f=10 \text{ Hz}$, $\text{CMOD}_{\text{amp}}=0.35 \text{ mm}$, $\text{CMOD}_{\text{min}}=1.0 \text{ mm}$; (B) test no. PS4-74, $P_{\text{stat}}=300 \text{ kPa}$, $f=10 \text{ Hz}$, $\text{CMOD}_{\text{amp}}=0.35 \text{ mm}$, $\text{CMOD}_{\text{min}}=1.0 \text{ mm}$.

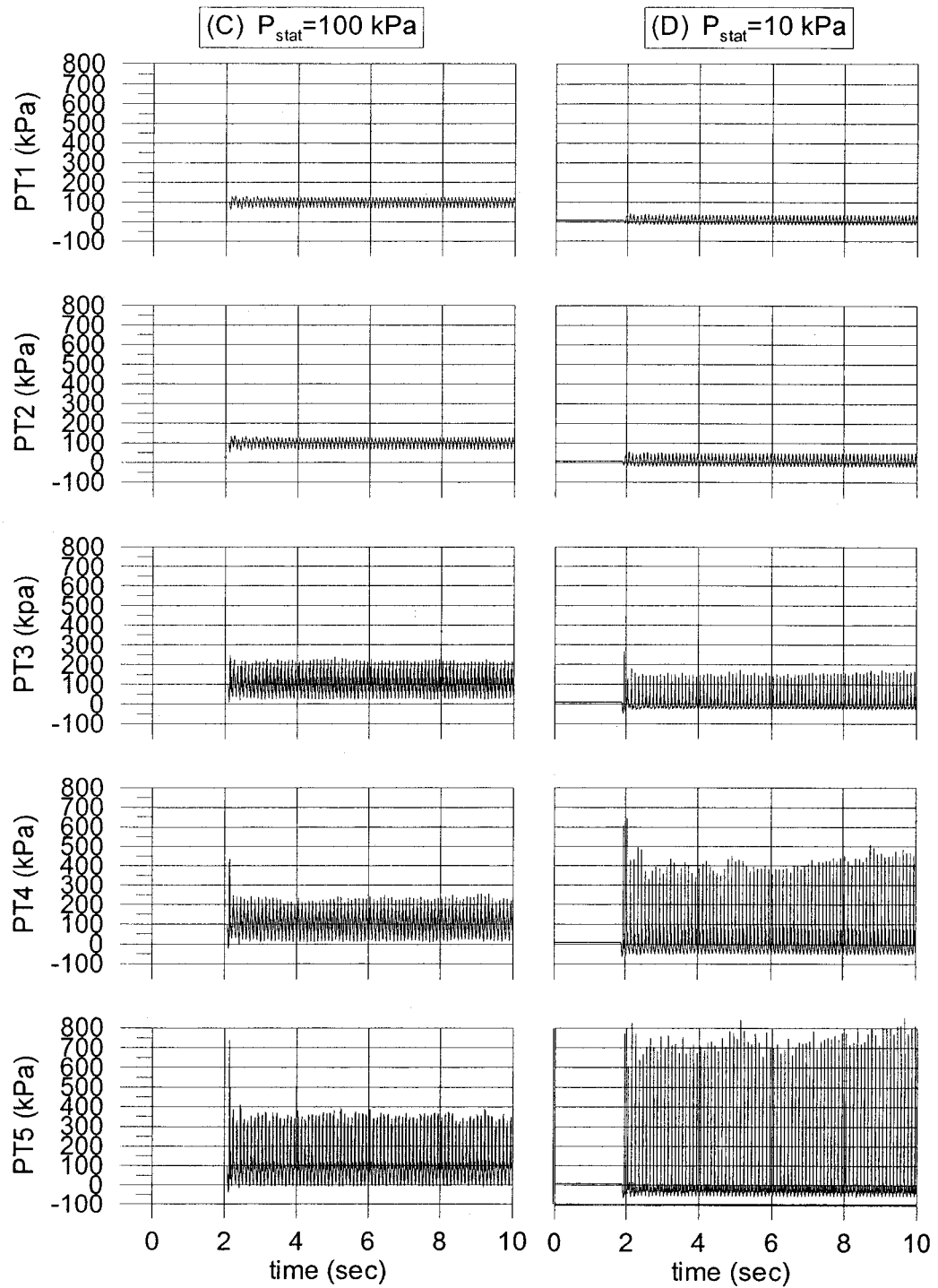


Figure 4.5 continued, Effect of static pressures on total pressure variations: (C) test no. PS4-71, $P_{stat}=100$ kPa, $f=10$ Hz, $CMOD_{amp}=0.35$ mm, $CMOD_{min}=1.0$ mm; (D) test no. PS4-72, $P_{stat}=10$ kPa, $f=10$ Hz, $CMOD_{amp}=0.35$ mm, $CMOD_{min}=1.0$ mm.

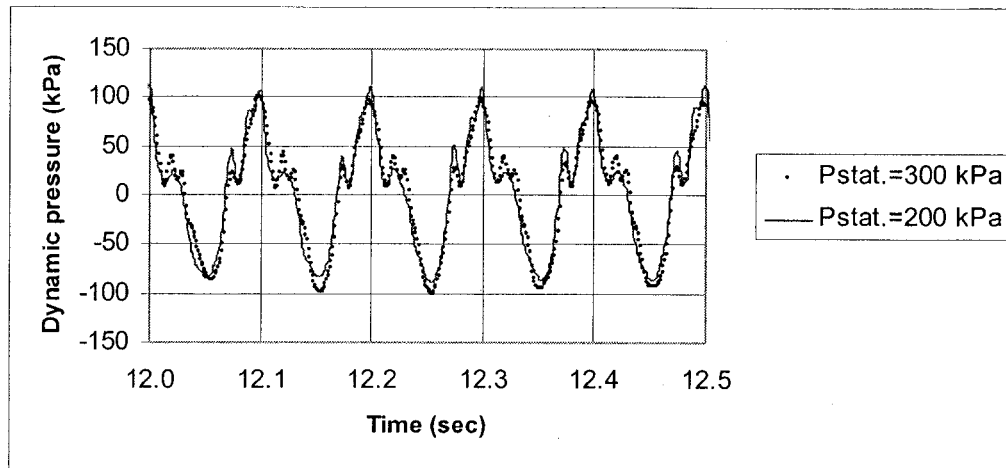


Figure 4.6 Dynamic pressure in PT4 for tests (A) and (B) in Fig. 4.5.

dam and the other at the bottom of the dam, with different hydrostatic pressure in the crack, the developed dynamic pressures will be the same if the crack wall motions and the other characteristics of the cracks are similar.

Other tests, similar to these two tests, showed that this conclusion is correct as long as the minimum measured pressure is not negative (promoting cavitation). Two other tests similar to tests (A) and (B) (Fig. 4.5) are performed with different static pressures in the notch, and the measured pressures are shown in Fig. 4.5 ((C) and (D)). The static pressure in test (C) is 100 kPa and the same pressure variations, with a step equal to 100 kPa, is expected compared to pressure variation in test (A). But the results shows that the maximum pressures in PT4 and PT5 for this test are greater than corresponding values in tests (A) and (B) (where $P_{stat}=200$ or 300 kPa). For the test (D), where the applied static pressure is $P_{stat}=10$ kPa, the maximum measured pressures by PT3, PT4, and PT5 are greater than similar values in other tests. Investigation of measured pressures by these pressure transducers reveals that minimum pressures in tests (C) and (D) are negative due to cavitation. It is believed the collapse of air bubbles following the cavitation phenomenon is responsible for high (“impact” type) pressures in these cases. This phenomenon will be discussed later in this chapter. The final conclusion is that the

developed dynamic pressure variations are independent of the magnitude of initial hydrostatic pressure as long as a cavitation phenomenon does not occur in the crack.

4.3.2 Amplitude of crack opening during harmonic excitations

To investigate the effects of $CMOD_{amp}$ on pressure variations in the crack, the results of similar tests with the same parameters but different $CMOD_{amp}$ are compared. To simplify the comparisons, the effective dynamic uplift forces on crack walls are used. These forces are computed by multiplying the dynamic pressure in each pressure transducer by its tributary area and adding the results for all pressure transducers. Figure 4.7 shows the maximum and minimum dynamic uplift forces for three tests with different $CMOD_{amp}$. The vertical distance between maximum and minimum forces presents the amplitude of developed dynamic uplift force in each test. From Fig. 4.7 it can be concluded that an increase in $CMOD_{amp}$ causes the amplitude of dynamic forces to increase, and vice-versa.

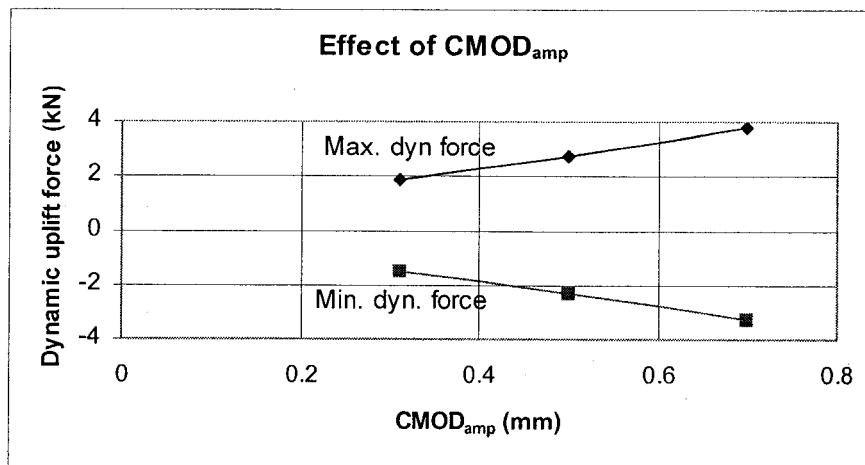


Figure 4.7 Effect of $CMOD_{amp}$ on developed dynamic forces in three typical tests. (Tests no. PS4-24, PS4-25, PS4-26, $U_{stat}=12$ kN, $P_{stat}=200$ kPa, $f=6$ Hz, $CMOD_{min}=1.0$ mm)

4.3.3 Frequency of harmonic excitations

Figure 4.8 shows the maximum and minimum dynamic uplift forces in the crack for three tests with different excitation frequencies including 2, 6, and 10 Hz while other

parameters are the same. Repeating similar tests show that there is a linear relation between the frequency and maximum or minimum developed dynamic forces in the crack. It is concluded that for two tests with the same parameters but different excitation frequencies, higher pressure variations are expected for the test with higher frequencies.

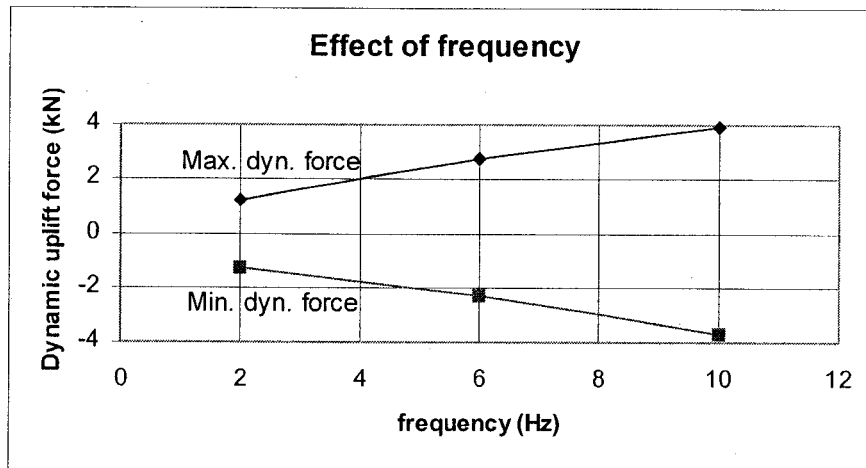


Figure 4.8 Effect of frequency content on developed dynamic forces in three typical tests. (Tests no. PS4-22, PS4-25, PS4-28, $U_{stat}=12$ kN, $P_{stat}=200$ kPa, $CMOD_{amp}=0.50$, $CMOD_{min}=1.0$ mm)

4.3.4 Crack opening velocity during harmonic excitations

Investigation of results shows that the maximum dynamic pressure occurs when the closing velocity of crack walls is maximum, and the maximum opening velocity cause minimum dynamic pressure along the crack. This concept is shown for a typical test in Fig. 4.9. This figure shows the developed dynamic pressure in four pressure transducers and the measured CMOD. The CMOV is computed by numerical differentiation of measured CMOD for this case and shown on the same graph with CMOD using different vertical scale (right axis in Fig. 4.9). Since the applied excitation in experimental tests is harmonic, the product of frequency and amplitude of crack wall motion is proportional to the crack wall velocity. The two selected parameters, frequency of excitation and crack mouth opening displacement amplitude, can be replaced by one parameter which is the crack mouth opening velocity. In Fig. 4.10 maximum and minimum dynamic uplift forces versus $CMOV_{max}$ are plotted for three typical tests with different $CMOD_{amp}$ and different excitation frequencies. From this

figure it is clear that an increase in CMOV causes the amplitude of developed pressure to increase.

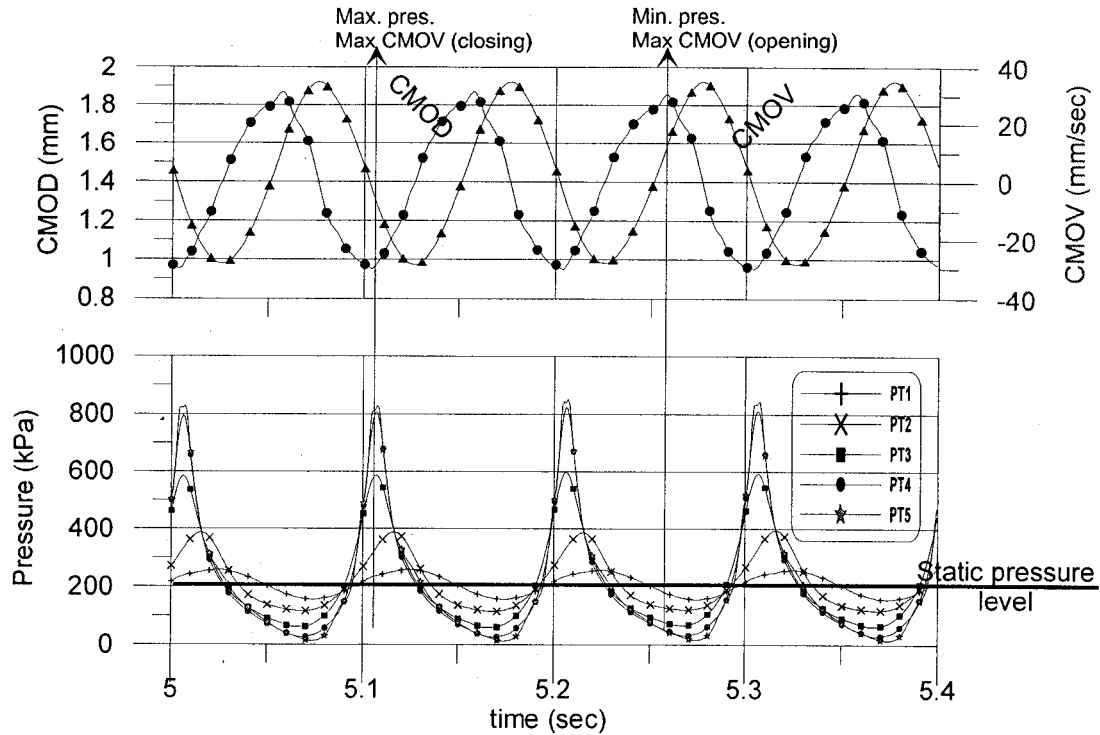


Figure 4.9 Comparison of dynamic pressure variations with crack mouth opening velocity variations. (Test no. PS2-19, $P_{stat}=200$ kPa, $CMOD_{amp}=0.65$ mm, $CMOD_{min}=1.0$ mm).

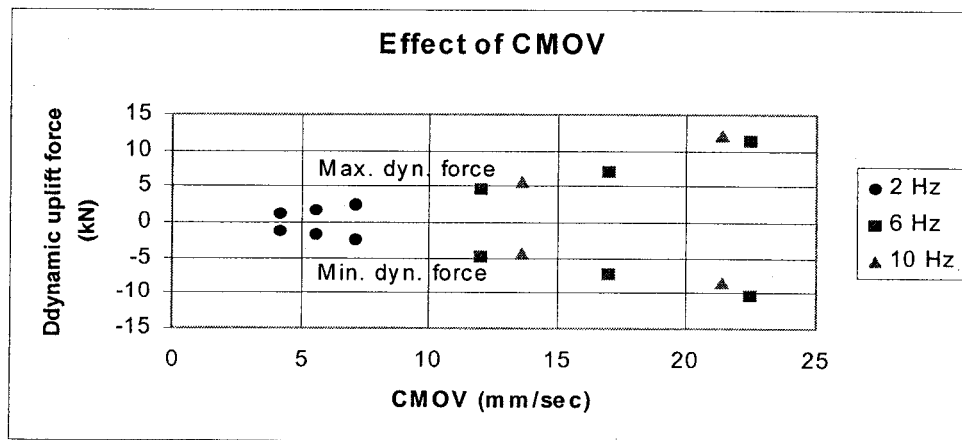


Figure 4.10 Effect of CMOV on developed dynamic forces. (Test no. PS6-51 to PS6-58, $U_{stat}=24$ kN, $P_{stat}=400$ kPa, $CMOD_{amp}=0.4-0.8$ mm, $CMOD_{min}=1.0$ mm).

4.3.5 Minimum crack opening during harmonic excitations

The variations of maximum and minimum uplift dynamic forces with minimum crack mouth opening displacements are shown in Fig.4.11. With increasing the average crack opening displacement the amplitude of pressure decreases. This means that during an earthquake, the cracks with small openings may be more critical than the cracks with greater openings.

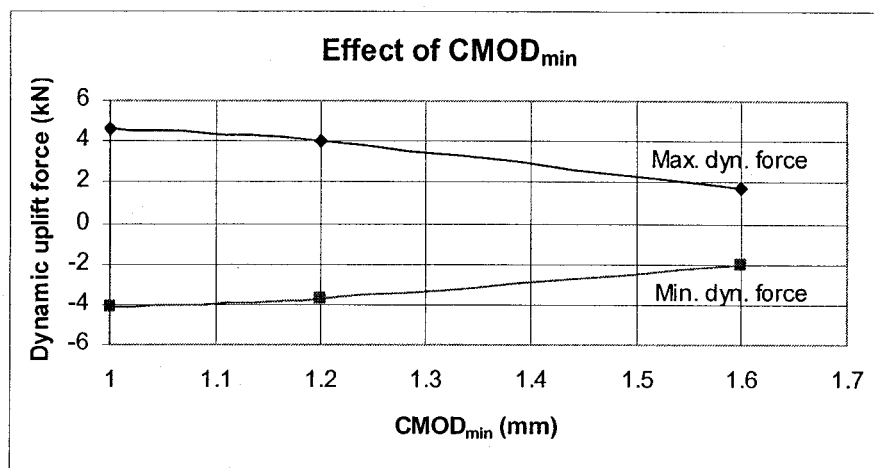


Figure 4.11 Effect of CMOD_{min} on developed dynamic force in crack. (Tests no. PS4-27, PS4-37, PS4-47, U_{stat}=12 kN, P_{stat}=200 kPa, f=10 Hz, CMOD_{amp}=0.4 mm).

4.3.6 Variations of pressures along crack length

In most cases, the dynamic water pressure along the crack increases from crack mouth toward its tip in closing mode of crack (in opening mode the absolute value of dynamic water pressure has the same variations if cavitation does not occur). In some special cases, it was observed that pressure in the last pressure transducer (PT5) is smaller than the measured pressure in the fourth pressure transducer (Fig. 4.2). A plot of developed dynamic pressures along the crack length, in an arbitrary instant of time during closing and opening modes, for two different tests is shown in Fig. 4.12. The different water pressure profiles along the crack in these two tests can be interpreted if we compare the crack opening for these cases. This phenomenon is somehow similar to

the case reported by Bruhwiler and Saouma (1995), that there is not a constant hydrostatic water pressure along an existing crack except in the region close to crack tip (fracture process zone) where the water pressure diminishes. They assumed a parabolic variation for the hydrostatic pressure reduction along the fracture process zone (Fig. 2.10). A decrease in dynamic pressure measured by PT5 has been observed in few existing crack tests performed directly after a new crack test where the CMOD is small. The crack aperture for these tests, where pressure reductions in the last hole is observed, is very small. In these cases, it is believed that the fracture process zone starts somewhere between the last and forth hole in the specimen. The developed hydrostatic water pressure in PT5, which is smaller than the pressure developed in the notch or other PTs (see the initial static pressure in PT5 with the similar pressure in other pressure transducers in Fig. 4.2), confirms this point. Since the initial hydrostatic pressure in the last hole is smaller than the hydrostatic pressure in the fourth hole, the dynamic pressure may also have the same variations.

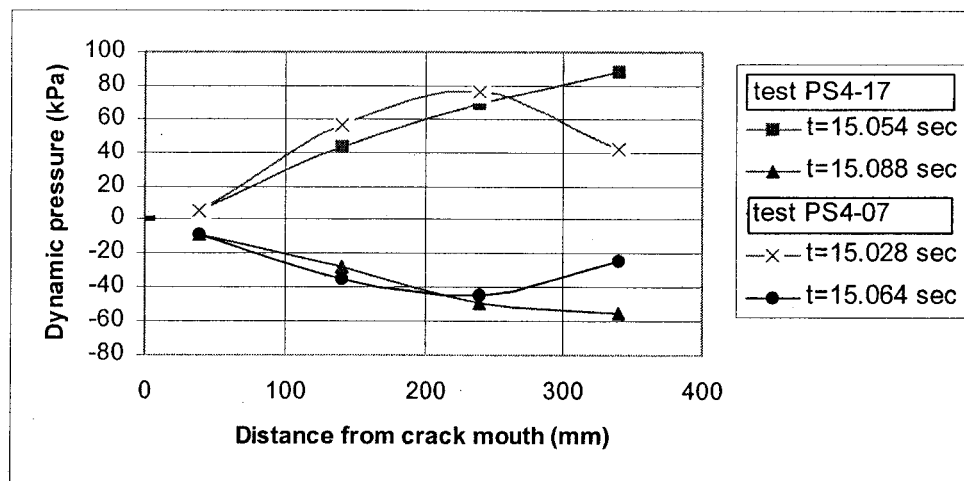


Figure 4.12 Variations of water pressures along crack length for opening and closing modes. (Test no. PS4-07, $P_{stat}=100$ kPa, $f=10$ Hz, $CMOD_{amp}=0.27$ mm $CMOD_{min}=0.95$ mm, Test no. PS4-17, $P_{stat}=100$ kPa, $f=10$ Hz, $CMOD_{amp}=0.41$ mm $CMOD_{min}=1.55$ mm).

4.3.7 Cavitation phenomenon

The cavitation phenomenon occurs whenever the local water pressure falls below the water vapour pressure and vapour filled cavities are formed. When the pressure increases, these vapour pockets collapse rapidly and generate high localized pressure peaks which are normally accompanied by noise. The cavitation phenomenon is observed in some tests with 6 and 10 Hz excitation frequency but there is no cavitation in 2 Hz tests. It should be noted that the occurrence of cavitation in 6 and 10 Hz tests is not considered as a general conclusion. The initial static pressure, opening velocity of crack walls, crack aperture (and crack length as we will see later in chapter 5) are the parameters that affect minimum pressure in the crack and occurrence of cavitation in cracks. For example a cavitation phenomenon is possible in a 2 Hz crack test, if we increase the $CMOD_{amp}$ such that the $CMOV$ becomes equal to $CMOV$ of a 6 or 10 Hz tests where cavitation occurs.

Figure 4.13 shows the time history of measured pressures for a typical test where cavitation occurred. Because the pressure transducers are not accurate for negative pressure measurements, the measured negative pressures in most cases are greater than the water vapour pressure. However these negative pressures are not detrimental to the global stability of a cracked component (a cut-off value at zero pressure is appropriate for stability evaluation). Moreover, the high pressure oscillations and the noise during the tests confirmed the occurrence of the cavitation phenomenon in these tests.

Since the mechanism of developed high pressures after cavitation is different, the results of tests with cavitation may not be compared with the other tests without cavitation. All the tests results that were used in previous sections, to investigate the effects of parameter variations on developed pressures, were tests without cavitation. It should also be noted that dynamic water pressure variations for the tests without cavitation are almost symmetric. The absolute values of maximum and minimum dynamic pressure are almost equal for most of the tests.

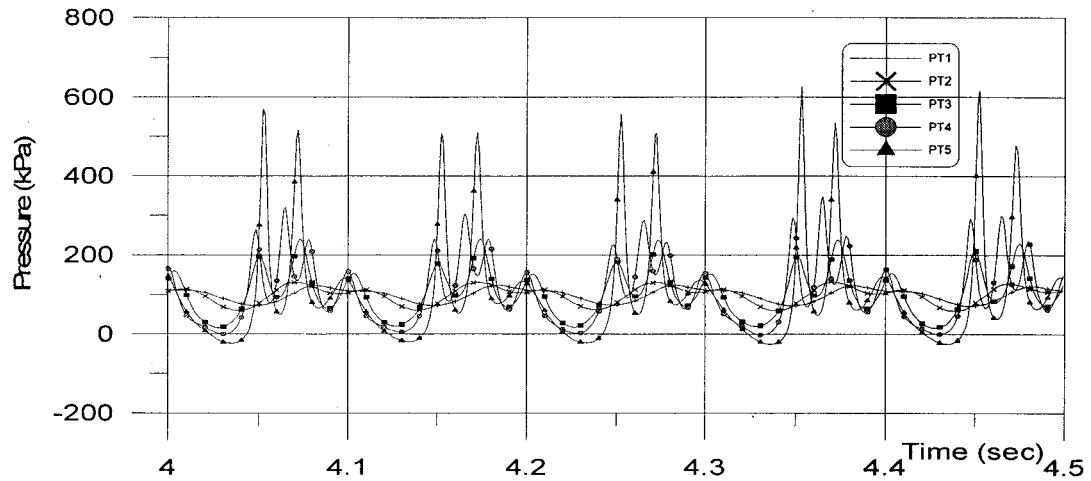


Figure 4.13 High frequency pressure oscillations after cavitation. (Test no. PS3-82, $P_{stat}=100$ kPa, $f=10$ Hz, $CMOD_{amp}=0.35$ mm, $CMOD_{min}=1.0$ mm).

4.4 New crack tests

Five new crack tests have been performed. Table 4.1 shows the testing parameters related to these tests. The transient dynamic pressure variations just after cracking of a specimen followed by the steady-state pressure variations are observed in all tests.

Table 4.1 Test parameters and water front velocities for new tests.

Specimen No.	P_{stat} (kPa)	f (Hz)	$CMOD_{amp}$ mm	$CMOD_{min}$ mm	Water front velocity (mm/sec)
NS1	100	2	0.8	0.9	1400
NS2	100	2	0.8	0.6	1400
NS3	400	2	0.5	1.0	2000
NS4	100	10	0.8	0.9	1400
NS5	200	10	0.3	0.4	-

4.4.1 Steady-state response

Steady-state pressure variations do not start immediately after cracking of a specimen, and it takes a few cycles of excitation to reach the steady-state response. Figures 4.14 and 4.15 compare the steady-state pressure responses in a new crack test

with an existing crack test with similar parameters. The developed steady-state response in a new crack test is generally similar to an existing crack test with similar conditions. The required times to obtain the steady-state response are different in these figures. According to Fig. 4.14, it takes 1.5 sec to develop steady-state response in test NS1 and this time is 8 sec according to Fig. 4.15 for test NS5. This time is a function of excitation frequency, crack aperture, and applied static water pressure at crack mouth.

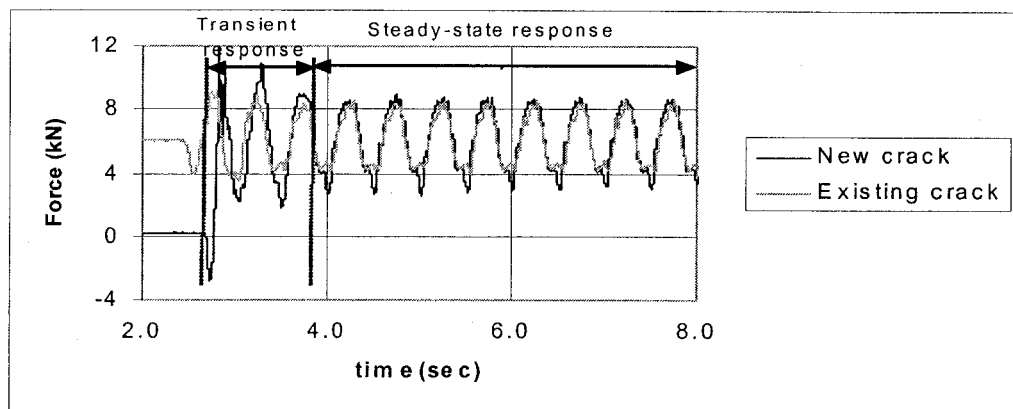


Figure 4.14 Transient and steady-state uplift force in a new crack compared to response in an existing crack. (test no. NS1, and PS3-03, $U_{stat}=6$ kN, $P_{stat}=100$ kPa, $CMOD_{amp}=0.8$ mm, $CMOD_{min}=0.9$ mm).

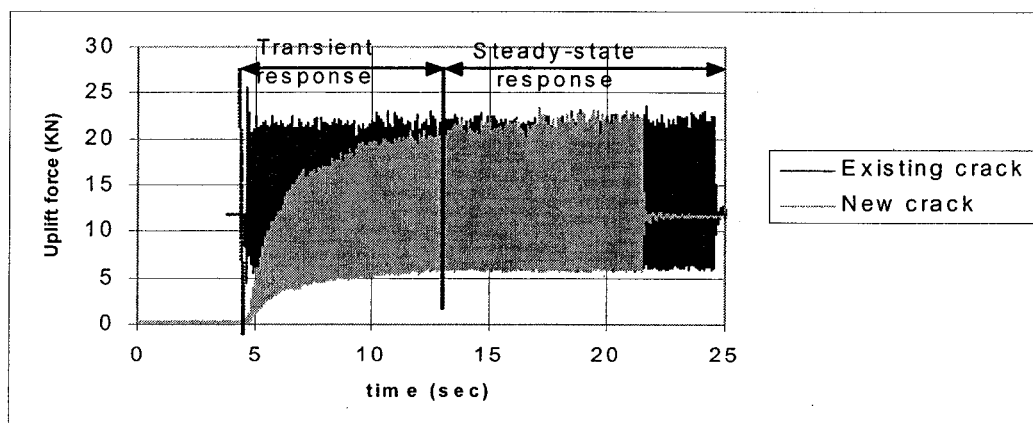


Figure 4.15 Transient and steady-state uplift forces in a new crack compared to response in existing crack. (test no. NS5, and PS2-06, $U_{stat}=12$ kN, $P_{stat}=200$ kPa, $CMOD_{amp}=0.3$ mm, $CMOD_{min}=0.4$ mm).

The general conclusion is that there are not any differences in developed pressures between an existing crack and a new crack, if water could fill the new crack. The same model can be used to formulate the steady-state response of an existing crack and a new crack filled with water. So it is appropriate to study the cracking phase during new crack tests, and the water penetration in the crack during the transient response period.

4.4.2 Transient response

Development of water pressure in the propagating crack and during the first few cycles of harmonic motion is investigated. The test results for the five new crack tests are shown in the Fig. 4.16 through Fig. 4.20. The first graph in each figure shows the measured CMOD and the second graph shows the measured pressure variations in five pressure transducers. In the first and second tests, one hole was blocked by concrete so no pressure was measured by corresponding pressure transducer. Comparing these figures, the following conclusions are made:

- **Water front velocity**

In the first four new crack tests, Figs. 4.16 to 4.19, the crack propagates instantaneously as soon as the test begins. After cracking, cyclic opening or closing modes develop without any significant further crack propagation. As soon as a crack develops and propagates, a pressure drop is recorded in notch pressure by PT1. Cracking of a specimen increases the volume of the notch instantaneously and the water pressure decreases at the notch and crack mouth due to decompression of the existing water in the notch and water reservoir. It was explained in Chapter 3 that the addition of the steel tank reduces the water pressure variations significantly in the notch but there is still small pressure variation in the notch. The pressures in the other pressure transducers reduce to a negative pressure. After a while the pressure in the second pressure transducer increases gradually to become zero and by a further increase in pressure, it becomes close to the applied static pressure in the notch. The other pressure transducers, from left to right, record similar pressure variations with some time delays. The moment

when negative pressure starts at each pressure transducer can be interpreted as the crossing of that hole by the crack front. The pressure differences between the crack mouth and the crack front cause water flow from the crack mouth to the crack tip. The pressure increases gradually from left to right as water fills the void while penetrating in the crack. The instant of time when the pressure becomes zero can be interpreted as crossing of a hole by the water front. Therefore the time period corresponding to negative pressure in each pressure transducer is an indicator of the delay between the crack front and the water front as they pass the hole. While it takes almost 0.17 second for the negative pressure in the fourth hole to become zero, in NS1, NS2, and NS4 tests, this time period is around 0.12 second for test NS3. This phenomenon shows that the water front velocity is smaller than crack front velocity as reported by Slowik and Saouma (1994). The test data are not so accurate to determine the crack front velocity but a range for water front velocity can be estimated. Assuming that crack develops instantaneously, the average water front velocity (from crack mouth to fourth hole) can be computed by dividing the distance between fourth hole and crack mouth (0.24 m) by the time required that water front reach this hole (0.12 second for NS3 and 0.17 second for other tests). The range of water front velocity according to the results is between 1400 mm/sec and 2000 mm/sec (Table 4.1). It should be emphasized that different parameters may affect the water front velocity in crack like static pressure at crack mouth, crack front velocity, crack aperture, and crack wall roughness and permeability. The computed water velocity is for crack aperture around 0.6 mm and static pressure ranging from 100 kPa to 400 kPa. However, an important point is that although the pressure could be zero (or negative) near the crack tip, some uplift pressure could build up in the crack portion near reservoir for high and low frequency excitations. The USBR (1987) and CDSA (1997 for high seismic zone) assumptions of zero uplift pressure in an opening (new) crack can thus be seriously questioned.

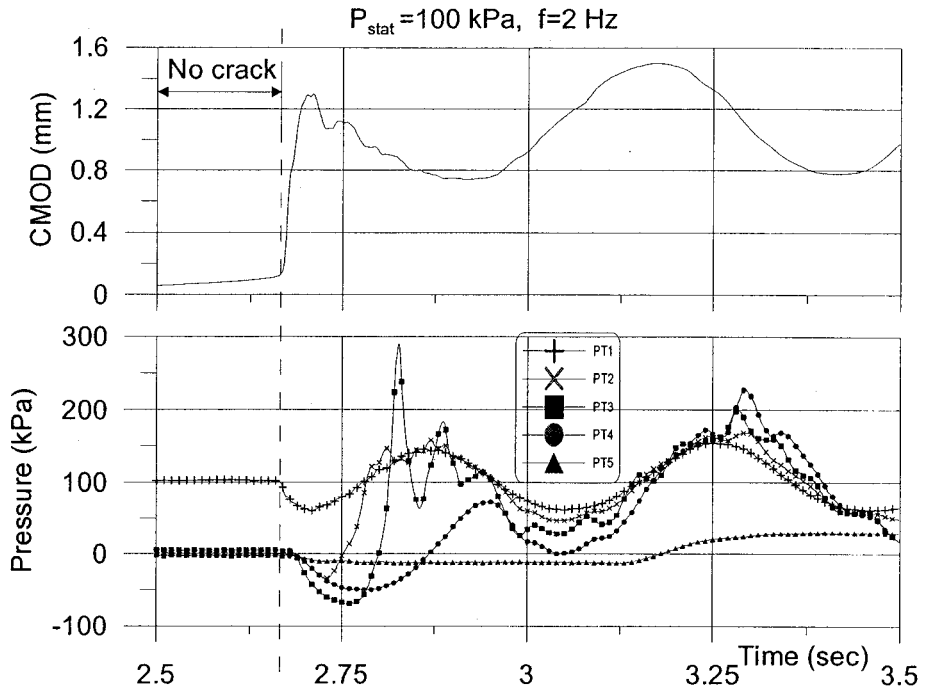


Figure 4.16 New crack test results (NS1).

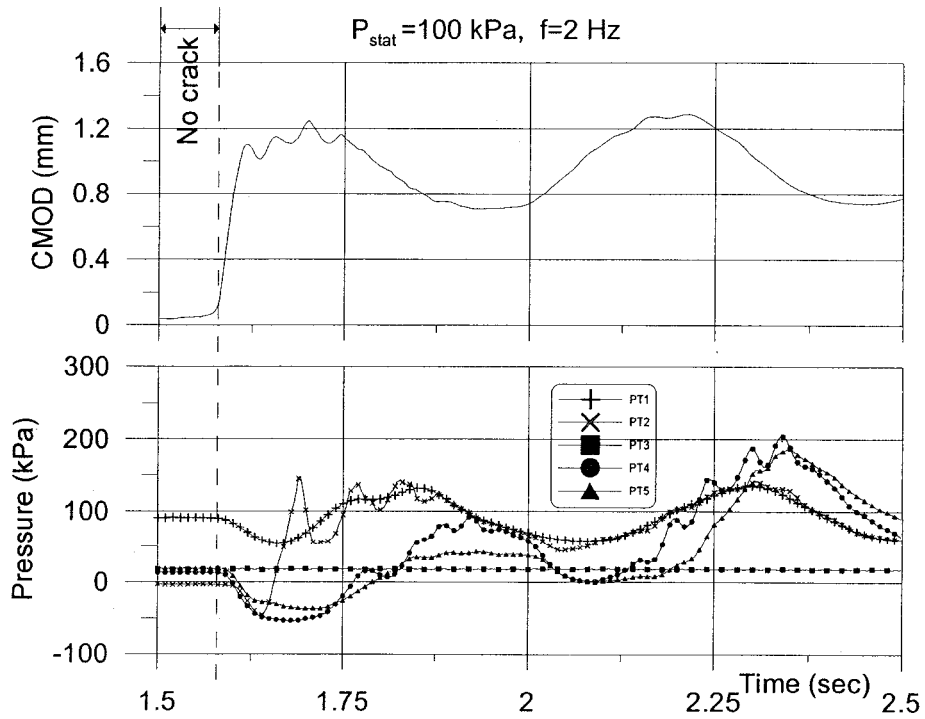


Figure 4.17 New crack test results (NS2).

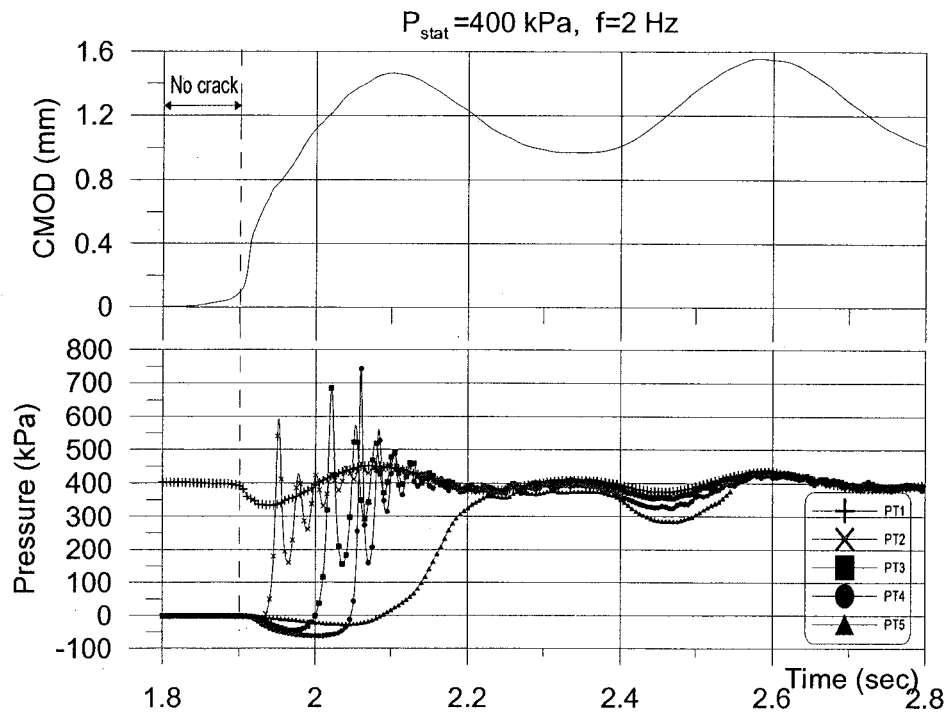


Figure 4.18 New crack test results (NS3).

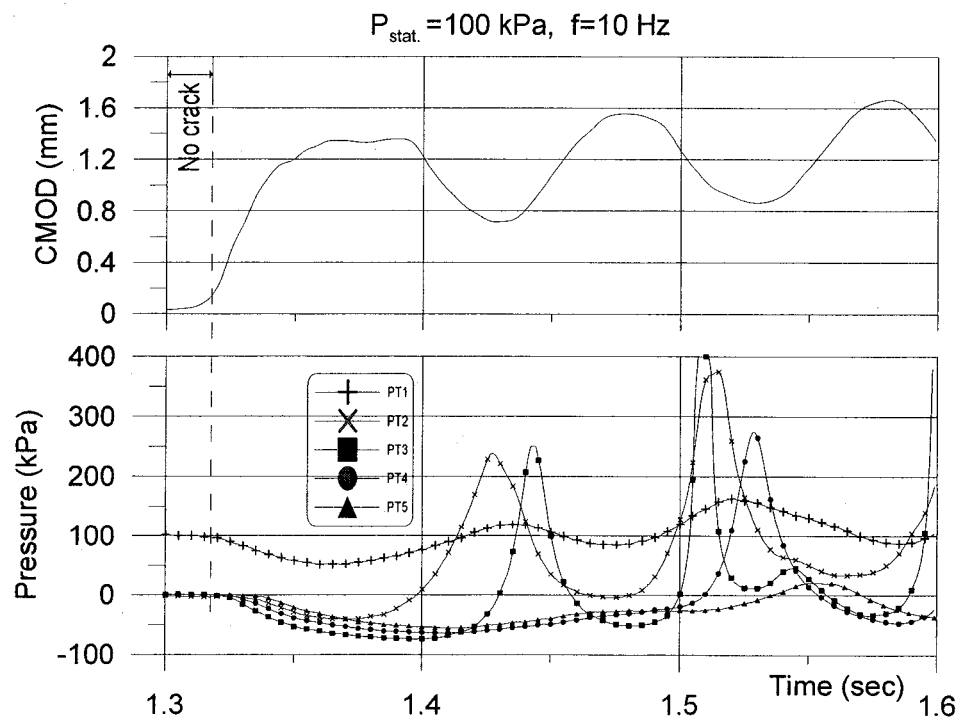


Figure 4.19 New crack test results (NS4).

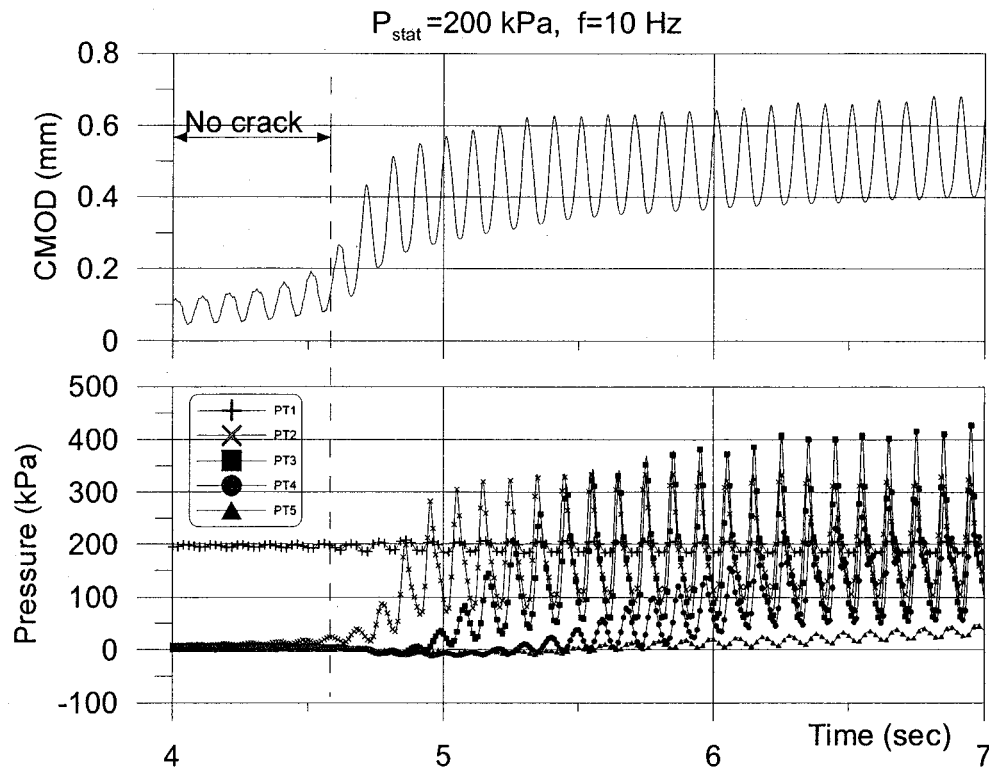


Figure 4.20 New crack test results (NS5).

A very special case is observed in test NS5 (Fig.4.20). Here the applied harmonic displacement is small. The crack development and propagation does not occur instantaneously. The crack propagates further during its opening in each subsequent excitation cycle for few cycles after cracking. Furthermore, in this case, the crack aperture is smaller relative to other tests. Two points can be made from this test. The crack propagation velocity, like the water front velocity, is not a constant velocity and it depends on the rate and magnitude of applied load (strain or energy) and the material properties of concrete. Because of the small magnitude of crack aperture as well as gradual propagation of the crack in this test, no negative pressure has been observed. Comparing the developed pressure in the last hole PT5, with the similar pressures in other tests (NS1 to NS4) confirms the slow development of water pressure in the crack with a small aperture.

The general conclusion is that development of water pressure in new cracks during earthquake is possible but its magnitude and time variation changes depending on the different parameters. The most important parameters are the crack opening velocity, crack aperture, crack length, the static pressure at crack mouth, and probably the roughness and permeability of the crack. According to the results of these tests for the part of a crack with an aperture greater than 0.4 mm, water pressure develops instantaneously in the crack, but for smaller crack aperture it takes few cycles for the pressure to develop in the crack. More detailed experimental studies with longer crack using a test set up that can record more accurately water and crack front velocities and related crack aperture would be useful.

- **Cavitation**

Negative pressures are observed in the first four tests (NS1-NS4). High frequency pressure variations also occurred in three or four pressure transducers just after the negative pressure which confirms the cavitation phenomenon in cracks. There is no sign for cavitation occurrence in the fifth test (NS5) where the crack develops gradually compared to other tests. It seems that the key parameter that controls the occurrence of cavitation is the velocity of crack propagation. The results of these tests are not sufficient to propose a theoretical criterion for cavitation in propagating cracks as more tests are needed.

4.5 Conclusions

The main findings of the experimental tests may be summarized for two cases related either to new cracks or existing cracks. These main findings are:

Existing cracks:

- In a saturated concrete crack with moving walls, water pressure is not constant. It increases during the crack closing mode, and decreases during the crack opening mode.

- The initial static water pressure does not have any effect on the magnitude of the developed dynamic pressure variations inside the crack if cavitation is not occurring.
- The absolute value of developed dynamic pressure amplitude increases from the crack mouth toward its tip but decreases after reaching a maximum value close to the crack tip.
- The frequency of excitation, amplitude of crack aperture, and the average crack aperture are the most important factors that affect the magnitude of the developed seismic water pressures in nearly impervious concrete crack with moving walls.
- The crack aperture amplitude and frequency of excitation can be interpreted as the velocity of crack walls in harmonic opening and closing motions. So the crack opening and closing velocity appeared to have the most important effect on pressure development in crack with moving walls.
- The cavitation phenomenon occurs in the case of 6 Hz and 10 Hz exciting frequencies with small initial static pressures. The occurrence of cavitation causes high frequency pressure responses in the system.
- The length of crack in experimental tests is very small (0.40 m) to extend the results for longer cracks in real dams. However it can be concluded at this point that the water pressure increases for closing mode, and decreases for opening mode. Consideration of constant pressure (zero, unchanged, or full uplift pressure) during dynamic analysis of dams is not accurate.
- The minimum pressure along the crack corresponds to occurrence of cavitation along the crack. In this case, water pressure at crack mouth is the full uplift pressure and decreases gradually until zero in the cavitation area. The hypothesis to consider zero uplift pressure all along the crack during earthquake (USBR 1987 and CDSA 1997 for high seismic zone) is questionable.

New cracks:

- Development of water pressure in a new crack is a function of relative velocity of concrete crack front and water front.

- Water front velocity is a function of aperture of crack, static pressure at crack mouth and probably the roughness and permeability of crack estimated water front velocity for the experimental test conditions (COD=0.2-2 mm and $P_{stat}=400$ kPa) is around 1400-2000 mm/sec.
- Negative pressure may be developed in the created void by the crack. Negative pressure if low enough, may cause a cavitation phenomenon in the crack. Then high pressure oscillations could occur with the collapse of the vapour bubble.
- Water could flow into the new developed crack in a concrete gravity dam subjected to earthquake. The water front velocity is considerable (it is 1400-2000 mm/sec for COD=0.2-2 mm and $P_{stat}=100-400$ kPa. It should be greater for the case of a crack in a dam with greater opening and higher hydrostatic pressure) to fill some part of the developed cracks during the earthquake and to build transient water pressure along this part of crack.

CHAPTER 5 WATER-CRACK INTERACTION MODEL

5.1 Introduction

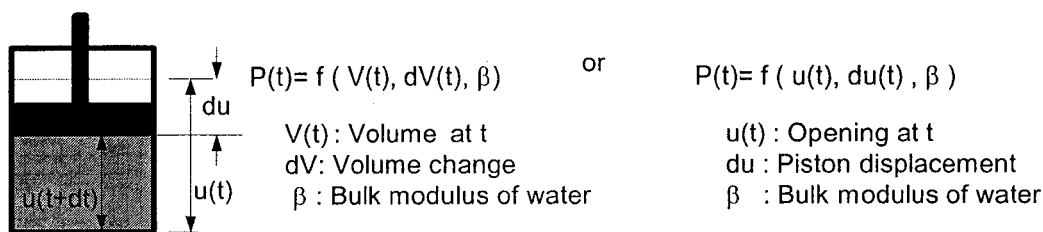
The theoretical formulation of water crack interaction is a complicated problem due to different phenomena that occur during the crack wall motions. By ignoring some phenomena that have small contributions to the developed pressure, it is possible to simplify the problem. The concept of water pressure development for a crack with moving walls is presented. It is shown that the water compressibility can be ignored in writing the continuity equation. Based on continuity equation and assuming a tapered crack with moving walls an expression for water flow along the crack is derived. The water pressure variations inside the crack with moving walls are formulated directly from water flow inside the crack in section 5.3. Based on the water flow regime inside the crack, laminar or turbulent flow equations are used to evaluate the pressure gradient along the crack. The dynamic water pressure variations are computed by integration of the estimated pressure gradient along the crack. The computed water pressures, based on the developed model, are in good agreement with the test results except for low pressure where the cavitation may occur. The developed procedure is modified to consider the cavitation phenomenon in the model, by simply limiting the computed negative pressures at cavitation pressure magnitude. This method is modified and extended by considering the water flow along the saturated part of the crack. The proposed model and the simplification assumptions are presented in section 5.6. Based on the proposed model, a computer program is developed and validated by simulating the existing and new crack test results (where crack length limited to 0.4 m). Using the developed computer program, effects of the crack length on the developed dynamic water pressure is investigated by computing the water pressure in cracks with different lengths.

5.2 Dynamic water pressure

A saturated crack with moving walls in a concrete dam is similar to a piston-cylinder system filled with water as shown in Fig 5.1a. Closing the crack is equivalent to the downward motion of the piston which increases water pressure inside the cylinder. The main difference between these two systems is the possibility of extrusion (intrusion) of water from the crack which is not possible for trapped water in the cylinder. The condition for the two systems will be more similar if a pipe is added to connect the cylinder to a reservoir (Fig 5.1b). By pressing the piston in the new system, a portion of water is compressed and a portion of water leaves the cylinder to reach the reservoir through the pipe. The water flow rate through the pipe affects the developed pressure in the cylinder. The developed pressure in the cylinder increases as the flow rate decreases in the pipe and vice versa. All the parameters that affect the magnitude of water flow in the pipe may change the developed pressure in the cylinder. The pressure variations in the cylinder for this case should be a function of the volume of the cylinder V (or u the cylinder motion), rate of closing of piston du/dt , pipe diameter ϕ_{pipe} , pipe length L_{pipe} , pipe roughness K_{pipe} , kinematic viscosity of water ν , and bulk modulus of water β .

Using the piston-cylinder concept, a real crack can be simplified as a series of pistons and cylinders that are connected to a reservoir by a series of pipes (or parallel plates) with different diameters (apertures) as shown in Fig. 5.2. It should also be noted that initial volumes of cylinders in this model decrease from left to right due to the reduced aperture in a tapered crack. Due to downward motions of the pistons, the pressure will be increased, the magnitude of pressure increase in the cylinders close to the end of the crack is greater than the magnitude of the pressure increase in the cylinders close to left end (notch). The pressure gradient along the pipe causes water flow from crack tip to crack mouth. Water flow in the crack will be developed in opposite direction when crack walls open.

a) piston-cylinder



b) piston-cylinder with opening

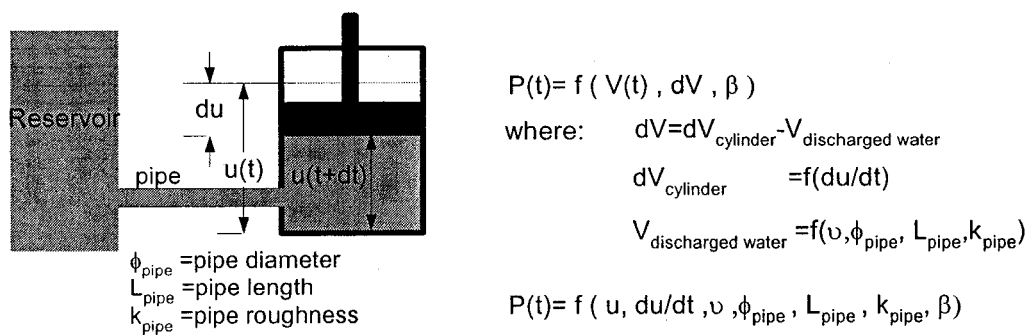


Figure 5.1 Piston-cylinder model for water crack-interaction.

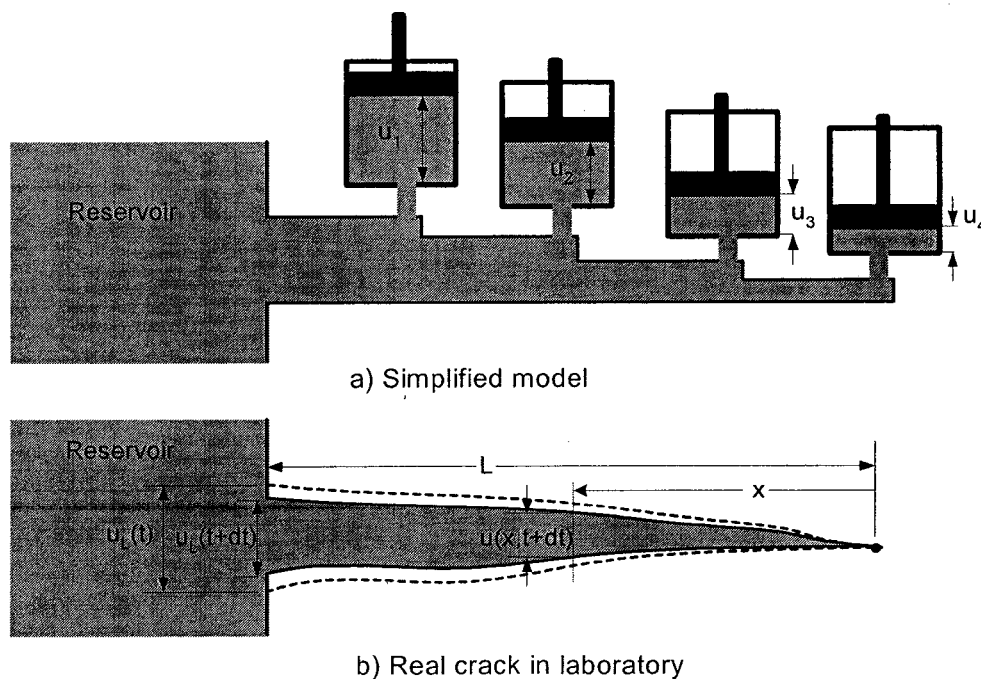


Figure 5.2 Piston-cylinder model for a crack with moving walls.

We can formulate water pressure variations in a crack with moving walls using the same concepts presented for the piston-cylinder system. For simplicity, we assume a tapered crack with rigid and impervious walls. Figure 5.3 shows the geometry of the assumed crack and the parameters defined for this purpose. We define the CMOD at time t as $u(t)$, then $u(t+dt)$ is the CMOD at time $t+dt$. Considering part of a crack with length x , the parameter dV_{cr} in Fig. 5.3 (grey area) represents the reduced crack volume due to its closing walls. If we consider the water discharge from the crack equal to $Q(t)$, the volume of water that leaves the cracked area is $Q(t)*dt$. The volume dV_{cr} is greater than $Q(t)*dt$. The difference between these two volumes, represented by $dV_w = dV_{cr} - Q(t)*dt$, is the volume of trapped water in crack that cannot leave the cracked area instantaneously. Since the volume of existing water in the crack at time $t+dt$, ($V_{cr}(t) - Q(t)*dt$) is greater than the volume of the crack ($V_{cr}(t+dt)$) at time $t+dt$, water should be compressed to fit in crack. Therefore the final volume of compressed water will be equal to ($V_{cr}(t+dt)$) and its pressure should be increased appropriately due to its compression. As a result of water compression water density will be increased.

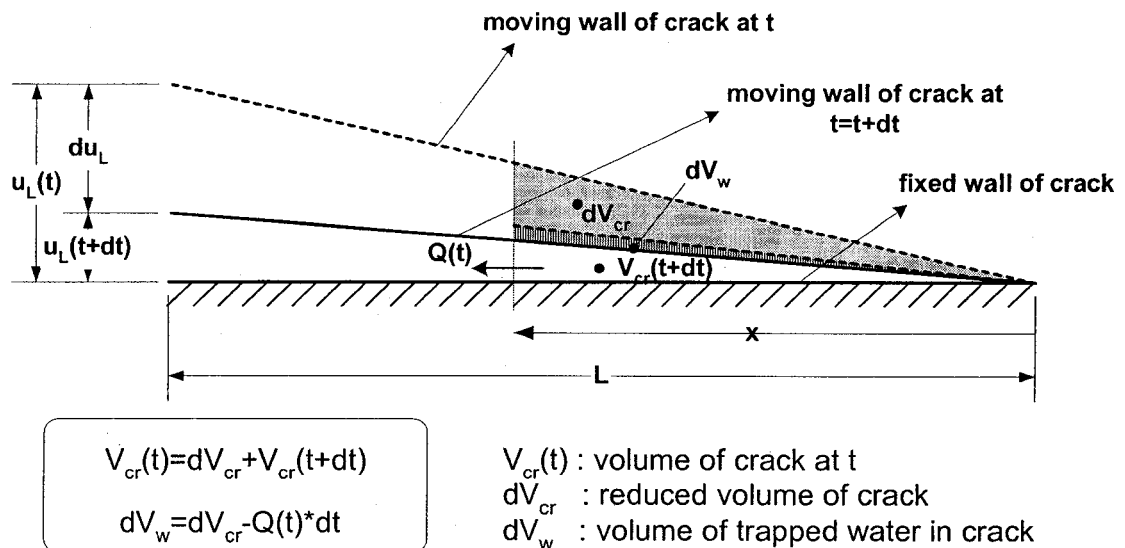


Figure 5.3 Tapered crack geometry.

Knowing the values of dV_w , $V_{cr}(t+dt)$ and the bulk modulus of water β we can calculate, theoretically, the pressure variation dp between t and $t+dt$ for crack closing or opening by substituting the appropriate terms in equation (2.9) :

$$dp = \beta \frac{dV_w}{V_{cr}(t+dt)} \quad (5.1)$$

Since the length of crack is known and its CMOD is measured during the test, we can estimate the volumes of crack ($V_{cr}(t)$, $V_{cr}(t+dt)$, and dV_{cr}) at any time. The volume of compressed water dV_w can be computed using the following equation:

$$dV_w = dV_{cr} - Q \cdot dt \quad (5.2)$$

However, water discharge was not measured during the experiments so we cannot obtain directly the magnitude of dV_w using experimental measurements. Actually the magnitude of dV_w is too small relative to the V_{cr} and it is too difficult to measure it experimentally. To show the order of magnitude of dV_w relative to V_{cr} we can still use equation 5.1 and the measured pressures and crack geometry in a typical test to compute the values of dV_w in typical experimental tests. Table 5.1 shows the calculated values of dV_w for a typical test results.

In table 5.1, $u(t)$ and pressures are measured quantities during the test, and V_{cr} , dV_{cr} , du/dt , and dp are computed based on test results and assumed crack geometry. The parameter dV_w is computed using equation (5.1), by rearranging its term and using the test results. Table 5.1 shows that dV_w is very small relative to V_{cr} or dV_{cr} , and we can assume that the volume of water discharged from the crack ($Q(t) \cdot dt$) is equal to the reduced volume of the crack due to closing walls, dV_{cr} :

$$dV_w \ll V_{cr} \Rightarrow Q_{(t)} * dt = dV_{cr} \quad (5.3)$$

In other word, the change in water volume (or change in water density) due to closing of the crack is small, such that we can neglect it and water flow in the crack can be estimated directly using the mass continuity equation (5.3) and the measured crack geometry. The change of the crack volume due to closing, dV_{cr} , can be expressed in terms of parameters defined for the assumed crack geometry as:

$$dV_{cr} = \frac{1}{2}x du_x = \frac{1}{2} \frac{x^2}{L} du_L \quad (5.4)$$

Water flow inside the crack, as a function of space and time, should be represented as $Q(x,t)$ and can be computed by substituting equation (5.4) in equation (5.3).

$$Q(x,t) = \frac{dV_{cr(x,t)}}{dt} = \frac{1}{2} \frac{x^2}{L} \dot{u}_L \quad (5.5)$$

Actually the equation (5.3) or (5.5) is the continuity equation of water flow in the crack, which was derived neglecting small variation in water density (incompressible flow). Using equation 5.5, the transient water flow along the crack can be computed using only the crack wall motion history and crack geometry, without determination of water pressure along the crack. The developed flow along the crack shows the existence of pressure gradient along the crack that can be evaluated using the known water flow along the crack. The details of the procedure to compute the transient pressure variations along the crack are presented in the next section.

Table 5.1 Calculation of dV_w for PT3 based on PS4-09 test results ($P_{stat}=100$ kPa, $f=10$ Hz, $CMOD_{amp}=0.7$, $CMOD_{min}=1.0$ mm) and equations 5.1, 5.2.

time sec	Test results		Calculations						
	pressure kPa	$u(t)$ mm	dp kPa	du/dt mm/sec	V_{cr} mm ³	dV_{cr} mm ³	dV_w mm ³	dV_w/V_{cr}	dV_w/dV_{cr}
20.014	563.9	0.5415			5888.8				
20.015	522.7	0.5324	-41.2	-9.10	5789.8	99.0	-0.1135	-1.96E-05	-1.15E-03
20.016	446.7	0.5237	-76.0	-8.74	5694.7	95.1	-0.2061	-3.62E-05	-2.17E-03
20.017	364.8	0.5149	-81.9	-8.74	5599.7	95.1	-0.2185	-3.90E-05	-2.30E-03
20.018	292.7	0.5063	-72.1	-8.58	5506.4	93.3	-0.1891	-3.43E-05	-2.03E-03
20.019	233.8	0.4982	-58.9	-8.14	5417.9	88.5	-0.1520	-2.81E-05	-1.72E-03
20.020	188.9	0.4903	-44.9	-7.85	5332.5	85.4	-0.1140	-2.14E-05	-1.33E-03
20.021	155.9	0.4827	-33.0	-7.61	5249.7	82.8	-0.0825	-1.57E-05	-9.96E-04
20.022	131.1	0.4754	-24.8	-7.29	5170.4	79.3	-0.0611	-1.18E-05	-7.70E-04
20.023	112.0	0.4682	-19.0	-7.25	5091.6	78.8	-0.0462	-9.07E-06	-5.86E-04
20.024	98.1	0.4613	-14.0	-6.89	5016.7	74.9	-0.0333	-6.65E-06	-4.45E-04
20.025	87.0	0.4548	-11.0	-6.53	4945.7	71.0	-0.0260	-5.25E-06	-3.66E-04
20.026	78.6	0.4483	-8.4	-6.48	4875.2	70.5	-0.0196	-4.02E-06	-2.78E-04

5.3 Developed pressure based on the water flow in the crack

It was shown, in section 5.2 that due to compression of water in cracks with moving walls pressure gradient develops along the crack length. The developed pressure gradient causes water flow in the crack. It was shown also that the magnitude of bulk modulus of water is high such that water flow can be computed using the continuity equation along the crack neglecting small variations in water density. Knowing water flow along the crack, it is possible to compute the pressure gradient along the crack using a suitable flow equation. The dynamic pressure variations along the crack can be computed by integrating the pressure gradient along the crack. The integration should begin from crack mouth, where the pressure has a known value, and should end at the point of interest. The general form of flow equation in cracks as proposed by the Louis (1969) (equation 2.4) is given as:

$$Q = -KAj^\alpha \quad (5.6)$$

where K is the hydraulic conductivity of the crack, A is crack cross section area, j is the total pressure gradient, and α is a constant exponent which depends on hydraulic zones according to Fig. 2-8 and Table 2-1. Assuming laminar flow in a rough crack, the value of α and the expression for K can be determined from Table 2.2. By substituting values of K and α in equation (5.6) and rearranging the terms, the pressure loss expression for laminar flow in a rough crack is:

$$\frac{dp(x,t)}{dx} = \frac{12\mu[1 + 8.8(k/2u(x,t))^{1.5}]Q(x,t)}{u^3(x,t)} \quad (5.7)$$

where μ is the water viscosity, and u is the mechanical crack aperture. The total pressure at each point can be computed by adding the quasi-static pressure at the mouth of crack P_{stat} , and the sum of pressure gradient from crack mouth to the point of interest:

$$p(x,t) = P_{stat} + \int_L^x dp(x,t) = P_{stat} + \int_L^x \frac{12\mu[1 + 8.8(k/2u(x,t))^{1.5}]Q(x,t)}{u^3(x,t)} dx \quad (5.8)$$

For the tapered crack geometry as in Fig. 5.3, equations 5.7 and 5.8 are simplified as follows:

$$\frac{dp(x,t)}{dx} = 6\mu \left[1 + 8.8(k/2u(x,t))^{1.5} \right] \frac{L^2}{x} \frac{\dot{u}_L(t)}{u_L^3(t)} \quad (5.9)$$

$$p(x,t) = p_{stat.} + 6\mu \left[1 + 8.8(k/2u(x,t))^{1.5} \right] L^2 \ln \frac{x}{L} \frac{\dot{u}_L(t)}{u_L^3(t)} \quad (5.10)$$

It should be noted that in computing equation (5.10) it was assumed that the relative crack wall roughness is not a function of x . According to Louis (1969), relative roughness magnitude varies between 0 and 0.5. For concrete cracks the recommended value is 0.5 because of the small crack aperture relative to the size of the sand and aggregate in the concrete. The existence of a logarithmic term in equation 5.10 make it singular at point $x=0$. A physical interpretation and a modification method for this singularity is discussed in section 5.4.

It is interesting to compare the equation 5.1 with the equation 2.7 (derived by Tinawi and Guizani 1994). They showed by a parametric analysis that the last term in equation 2.7 is dominant for cracks less than 2 mm in aperture. The derived equation to compute the dynamic pressure variation, the second term in equation (5.10), is similar to the third term of equation 2.7, these equations contain two distinct parts that are somehow similar. The first part ($\frac{\dot{u}_L(t)}{u_L^3(t)}$ in equation 5.10, $\frac{\dot{w}_1(t)}{w_0^3}$ in equation 2.7) is a function of time that represents time variation of dynamic pressure that are basically similar and the difference comes from the small crack wall motion assumption made by Tinawi and Guizani. The second part ($\ln \frac{x}{L}$ in equation 5.10, $1 - \xi^3$ in equation 2.7) is a function of distance x that represents spatial variation of pressure along the crack length. The differences come from different crack geometry assumed in two cases. Therefore, these two equations are basically the same. The case of turbulent flow condition along the crack can be considered easily in the formulation proposed herein as well as laminar flow.

The test results show the possibility of occurrence of turbulent flow inside the crack for the cases of high frequency excitations. Using the turbulent flow equation from Table 2.1 and the tapered geometry of crack, equations (5.9) and (5.10) can be modified for the turbulent flow case. Reynold's number should be computed, using the estimated water velocity at each point along the crack, and the corresponding equation should be utilized to compute the pressure gradient. The following methodology can be applied to compute pressure variations along the crack for a general case.

(1) Calculate water flow based on the crack mouth motion, and crack geometry:

Known: $V_{cr}, dV_{cr}, u_L(t)$

$$\text{Calculate: } Q(x,t) \quad Q(x,t) = \frac{dV_{cr}(x,t)}{dt} = \frac{1}{2} \frac{x^2}{L} \dot{u}_L \quad (5.11)$$

(2) Calculate water flow velocity and Reynold's number:

Known: $Q(x,t), u_L(t)$

$$\text{Calculate: } v(x,t), \text{Re}(x,t) \quad v = \frac{Q(x,t)}{u(x,t)} = \frac{1}{2} x \frac{\dot{u}_L}{u_L} \quad (5.12)$$

$$\text{Re} = \frac{2u(x,t)v}{\nu} = \frac{x^2}{\nu L} \dot{u}_L \quad (5.13)$$

(3) Calculate pressure head gradient along the crack at time t:

Known: $Q(x,t), \text{Re}(x,t)$

Calculate: $dp(x,t)/dx$

$$\text{Laminar: } \frac{dp(x,t)}{dx} = 6\mu \left[1 + 8.8(k/2u(x,t))^{1.5} \right] \frac{L^2}{x} \frac{\dot{u}_L(t)}{u_L^3(t)} \quad (5.14)$$

$$\text{Turbulent: } \frac{dp(x,t)}{dx} = \frac{\rho g}{24 \left(\log \frac{1.9}{k/2u(x,t)} \right)^2} xL \frac{\dot{u}_L^2(t)}{u_L^3(t)} \quad (5.15)$$

(4) Calculate dynamic pressure variations along the crack for time t:

Known: $dp(x,t)/dx$
 Calculate: $p_{dyn}(x,t)$

$$p_{dyn}(x,t) = \int_L^x dp(x,t)$$

$$p_{dyn}(x,t) = \int_L^{L_t} [dp(x,t)]_{turbulent} + \int_{L_t}^x [dp(x,t)]_{laminar} \quad (5.16)$$

It is the point where transition from laminar flow to turbulent flow occurs. Reynold's number increases from the crack tip (at the crack tip it is zero) to the crack mouth, and the water flow in the region close to the crack tip is laminar. Depending on the crack length and the crack mouth velocity, the laminar condition may dominate the flow all along the crack and the pressure will be computed based on the laminar flow equation. The measured history of crack wall motions in experimental tests are used to simulate the test results (measured pressure) using the proposed procedure. The computed pressure variations are generally in good agreement with the measured pressure variations during the tests. Figure 5.4 shows the measured dynamic pressure variations by four pressure transducers in a typical test, and Fig. 5.5 shows the computed dynamic pressures by the proposed method. To compare the results in a single graph, the dynamic uplift force variations in the existing crack are computed (by integrating the water pressure along the crack). Using the measured and computed pressure variations in Fig. 5.4 and Fig. 5.5, the computed and measured dynamic uplift forces are shown in Fig. 5.6.

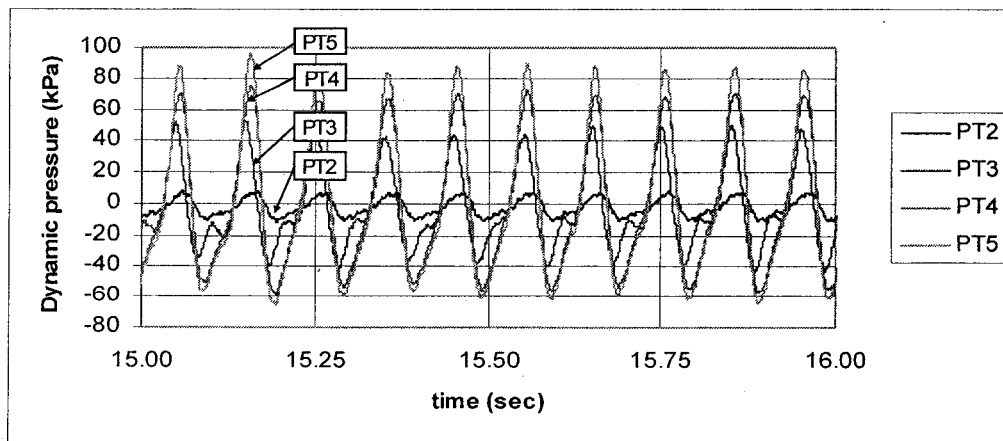


Figure 5.4 Results of test no PS4-17 ($U_{stat}=6$ kN, $P_{stat}=100$ kPa, $f=10$ Hz, $CMOD_{amp}=0.5$ mm, $CMOD_{min}=1.6$ mm).

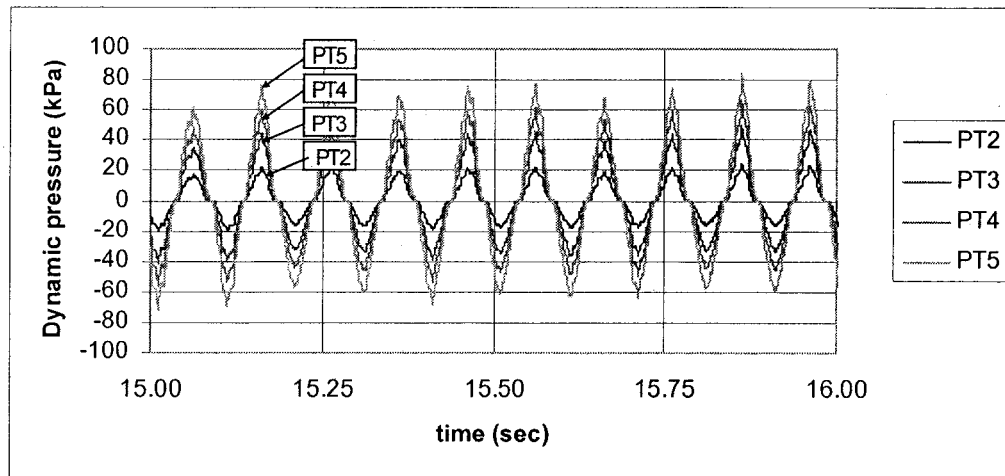


Figure 5.5 Simulated results for test shown in Fig. 5.4.

The comparisons between the computed and the measured uplift dynamic forces for three other tests including 2 Hz, 6 Hz, and 10 Hz excitations are shown in Figs. 5.7, 5.8, and 5.9. The simulated uplift force variations in Fig. 5.8 and Fig. 5.7 are acceptably close to the measured uplift force variations, but there are great differences between the simulated and measured forces in Fig. 5.9 for the negative values. This case corresponds to the occurrences of cavitation along the crack. When cavitation occurs the proposed procedure does not work any more because the flow in the crack is a very complicated phenomenon due to mixture of water and vapour which would rigorously require a two phase flow analysis in the crack. The overall proposed methodology is still valid but some modifications are necessary. These are modifications to consider cavitation, and modifications for the singularity point at the crack tip in the pressure function for laminar flow case.

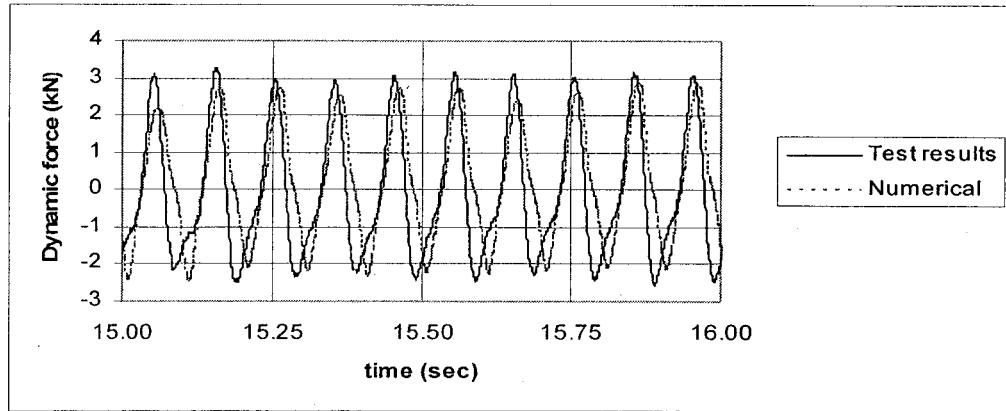


Figure 5.6 Comparisons between measured and computed uplift force (test no. PS4-17).

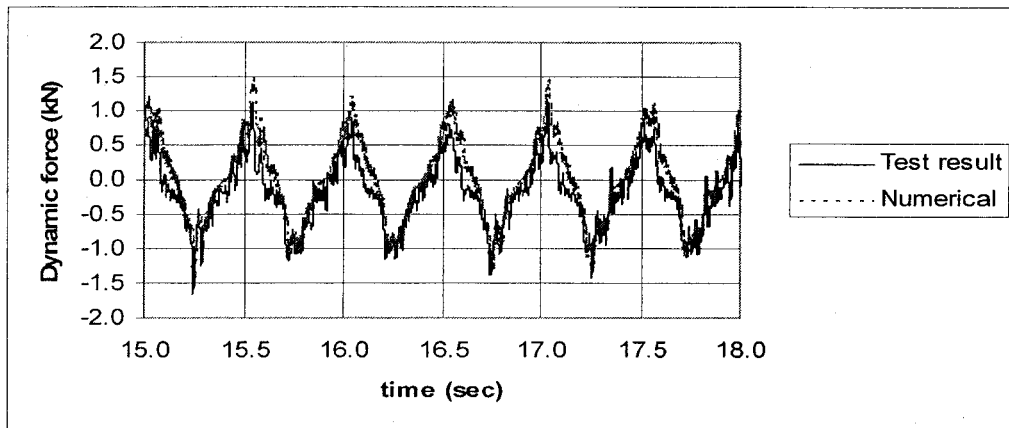


Figure 5.7 Comparisons between measured and computed results for 2 Hz excitation (test no. PS5-53; $U_{stat}=24$ kN, $P_{stat}=400$ kPa, $CMOD_{amp}=0.8$ mm, $CMOD_{min}=1.15$ mm).

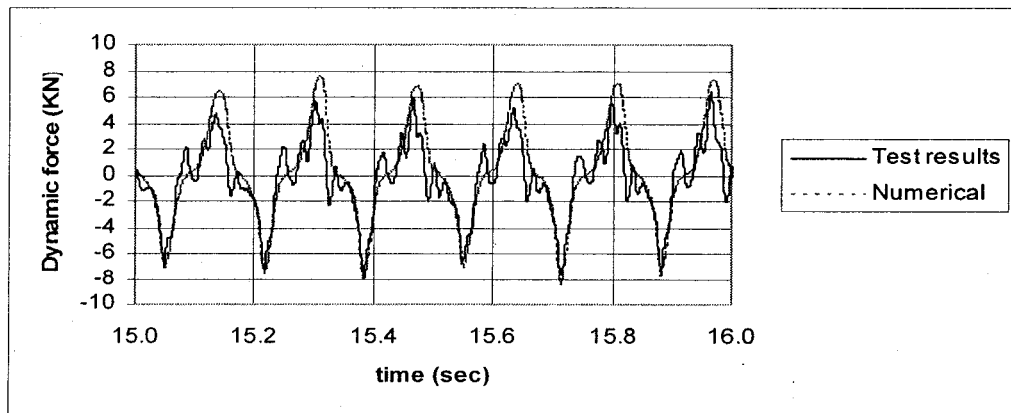


Figure 5.8 Comparisons between measured and computed results for 6 Hz excitation (test no. PS5-56; $U_{stat}=24$ kN, $P_{stat}=400$ kPa, $CMOD_{amp}=0.8$ mm, $CMOD_{min}=1.15$ mm).

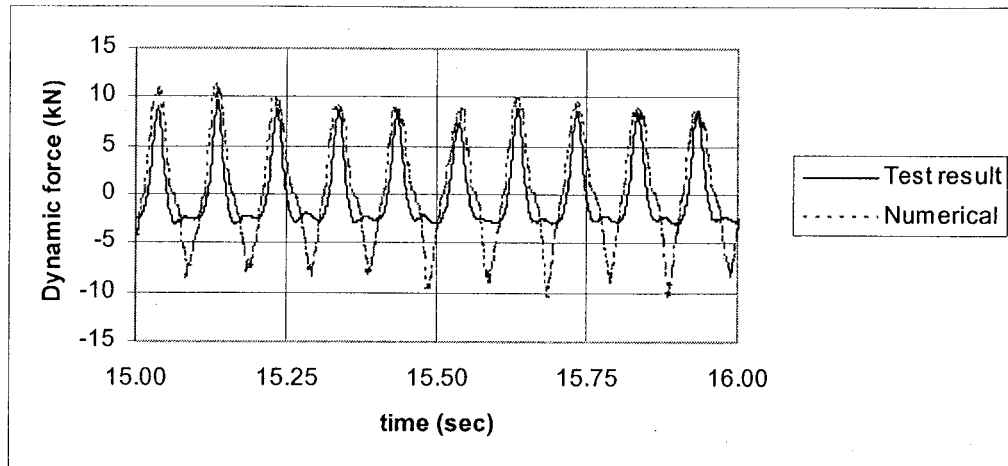


Figure 5.9 Comparisons between measured and computed results for 10 Hz excitation (test no. PS4-08 $U_{\text{stat}}=6$ kN, $P_{\text{stat}}=100$ kPa, $\text{CMOD}_{\text{amp}}=0.45$ mm, $\text{CMOD}_{\text{min}}=1.0$ mm).

5.4 Modification for singularity

The dynamic pressure function for the laminar case, equation 5.10, is a singular function when $x=0$; this concept is shown in Fig. 5.10 for a hypothetical crack with 1 m length and $\text{CMOD}_{\text{min}}=1.0$ mm. It is clear from this figure that the pressure value increases rapidly in a region close to the crack tip. But the length of this region is very small relative to the total length of the crack such that it does not affect the resultant of the effective dynamic uplift force in the crack. However, it may have local effect promoting further crack propagation. We can use the formula proposed by Bruhwiler and Saouma (1991-1995), presented in section 2.4.1, to modify equation 5.10 in the region close to the crack tip. According to their research, the uplift pressure in the Fracture Process Zone (FPZ) of the crack is not the full uplift pressure for static condition. They defined a critical crack opening displacement (COD_{w0}) below which the water pressure in FPZ becomes smaller than the water pressure in opened crack. The reported values of COD_{w0} ranges from 0.02 to 0.098 mm for static water pressure 900 kPa to 100 kPa, respectively. They assumed a parabolic variation from full static uplift pressure at this section to zero at the tip of the FPZ. In our work, we can use a more simple variation for water pressure close to the crack tip during the earthquake. The

value of COD_{w0} is initially defined to be equal to 0.1 mm and it will remain as a user specified constant model input parameter. So the dynamic pressure is computed, using equation (5.16) up to the point where $COD=0.1$ mm, and it is assumed that this pressure remains constant in the region between this point to the crack tip. It should also be noted that using this modification does not affect computed pressures in section 5.3 (Figs. 5.4 to 5.9), because the minimum crack aperture at the last pressure transducer (PT5) location is greater than 0.1 mm in these tests. The computed pressure profiles along a typical crack ($L=1$ m) using the developed model, before and after modifications, are shown in Fig. 5.10. It is clear from this graph that this modification affects only the results for a very small region close to the crack tip and do not alter significantly the uplift pressure force resultant.

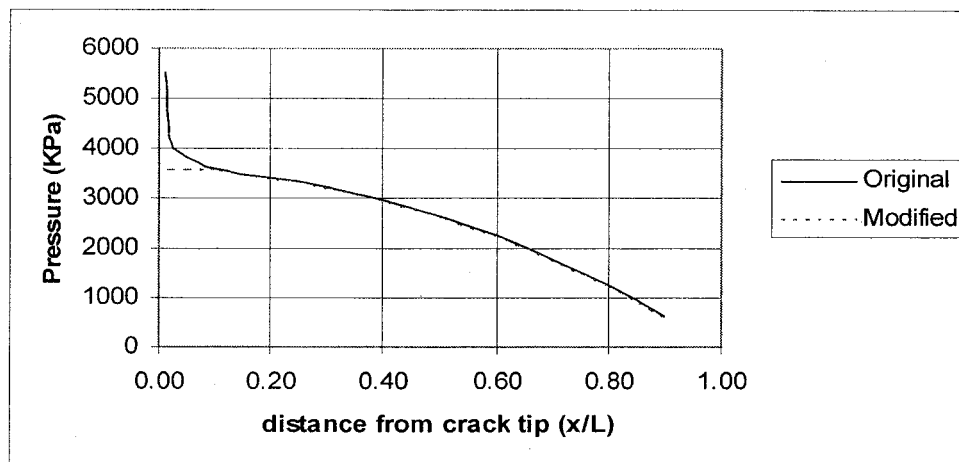


Figure 5.10 Modification for singularity at crack tip.

5.5 Modification for cavitation

The only significant difference between the measured and computed pressure is observed when the negative dynamic pressure is lower than the initial quasi-static pressure in the crack. Theoretically, when the water pressure becomes equal to the vapour pressure of water, cavitation occurs and the pressure remains nearly constant due

to evaporation of water. The developed model should be modified for this condition. Since the computed positive pressures are adequately represented, it seems that the negative pressure may be modified simply by cutting the pressure curve at the cavitation pressure magnitude. In other word, the dynamic pressure is computed at desired points by equation 5.16, and the values smaller than the water vapour pressure are assumed to be equal to water vapour pressure. This procedure is applied to the test results in Fig. 5.9 and the results are shown in Fig 5.11.

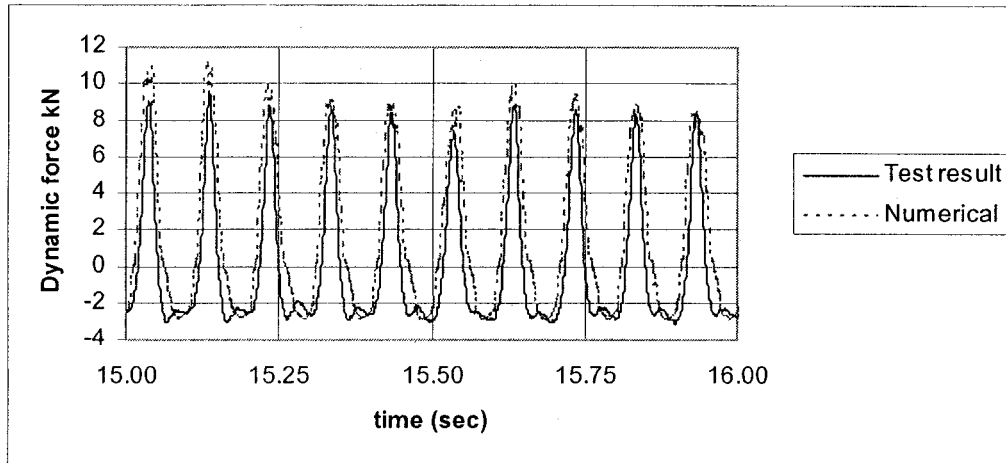


Figure 5.11 Modification for cavitation (test no. PS4-08 from Fig. 5.9).

5.6 Extension of the procedure to cracks with longer lengths

The proposed method is verified using the experimental test results where the crack length is about 0.4 m. According to equation 5.10, for laminar water flow in the crack, dynamic pressures are proportional to the square of crack length (L^2). For a typical crack, with a length equal to 4 m, the expected dynamic pressure should be 100 times greater than dynamic pressure measured in a test. In longer cracks, the water flow in most part of the crack is turbulent and the magnitude of water pressure should be larger than the predicted value by laminar flow equation.

The CMOD and CMOV histories of test no. PS4-17 ($P_{\text{stat}}=100$ kPa, $f=10$ Hz, $\text{CMOD}_{\text{amp}}=0.5$ mm, $\text{CMOD}_{\text{min}}=1.6$ mm) are applied to a 4 m crack and the simulated results at the four different points along the crack are shown in Fig. 5.12. The distances of the selected points from the crack mouth are 0.35 m, 1.35 m, 2.4 m, and 3.5 m that are proportionally similar to the locations of pressure transducers in the test (0.035m, 0.135 m, 0.240 m, 0.350 m). Comparisons of these graphs show while the maximum dynamic pressure is almost 80 kPa in the test (Fig 5.7), the estimated pressure in a 4 m crack is about 70000 kPa (for turbulent flow the dynamic pressure is proportional to L^3).

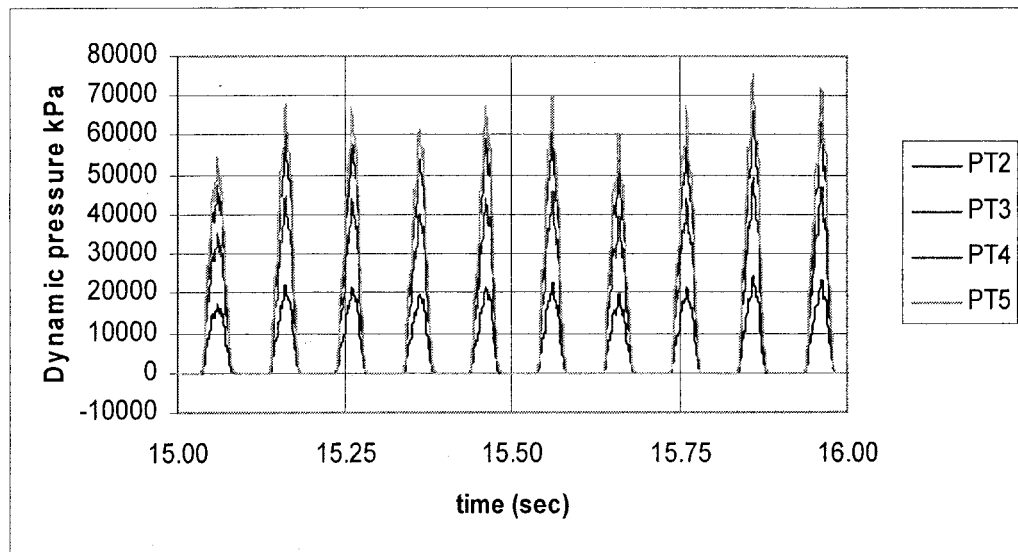


Figure 5.12 Numerical simulation results for dynamic pressure variations along a 4 m crack subjected to the same wall motions as test no. PS4-17 in Fig.5.4.

Assuming that such positive pressure can be developed during the crack closing mode, the assumed pressure variations along the crack is shown in Fig. 5.13-a. The computed negative pressure could not be developed due to negative pressure limitation (vapor pressure), and the cavitation phenomenon occurs in a part of the crack where the computed total pressure is lower than vapor pressure of water. It is assumed that pressure remains constant at the value of the vapor pressure magnitude (Fig. 5.13-b). In short cracks, (like cracks in experimental tests) the cavitation region is filled rapidly at the end of the opening mode (or starting of the closing mode), so the crack can be

considered saturated during the closing mode. That is why a simple modification for computed negative pressure, limiting pressure at the cavitation pressure magnitude, and using saturated crack assumption for closing mode works fine and the computed results are in good agreement with the test results as shown in section 5.3 and 5.5. In a longer crack, water could not fill entirely the opening crack, and the developed voids during cavitation could remain in some parts of the crack (close to the crack tip). The existing crack can not be considered fully saturated in closing mode, due to the existence of voids along the crack. In this condition, the developed procedure for the water flow along the crack and the estimated water pressure, in closing mode, is not valid any more. The developed model should be modified considering existence of a saturated part (L_{sat}) and an unsaturated part (L_{cav}) in computing water flow during the closing mode along the crack (Fig 5.13).

5.6.1 Assumptions

The main assumptions to modify and extend the model for long cracks are:

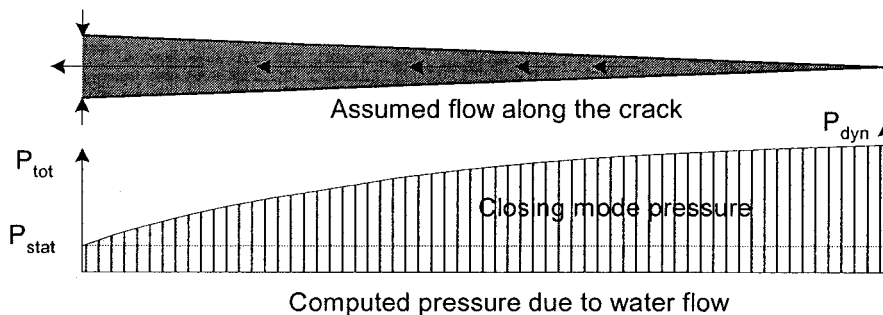
- If cavitation occurs, two regions will exist along the crack length, a saturated region close to the crack mouth filled with water, and an unsaturated region close to the crack tip where cavitation occurs.
- Unsaturated (cavitation) region is filled with a mixture of water and void (water vapour).

Opening of a crack increases the void volume in the cavitation region, and closing of crack decreases the void volume.

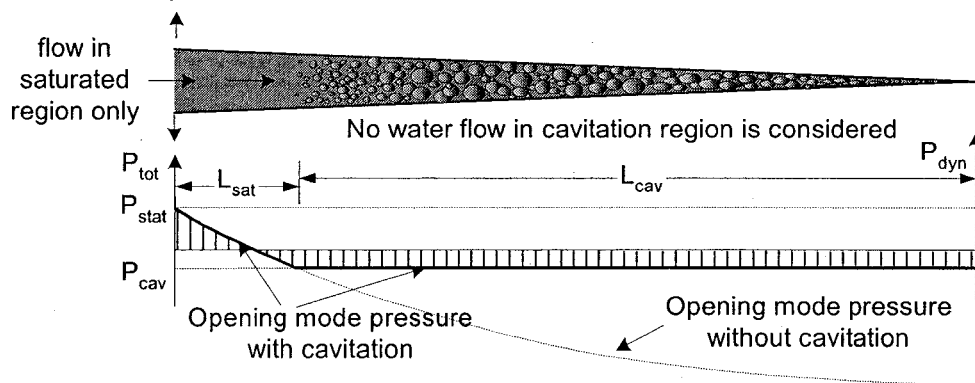
- Constant pressure exists in unsaturated region.

In the unsaturated region the pressure remains constant and equal to zero.

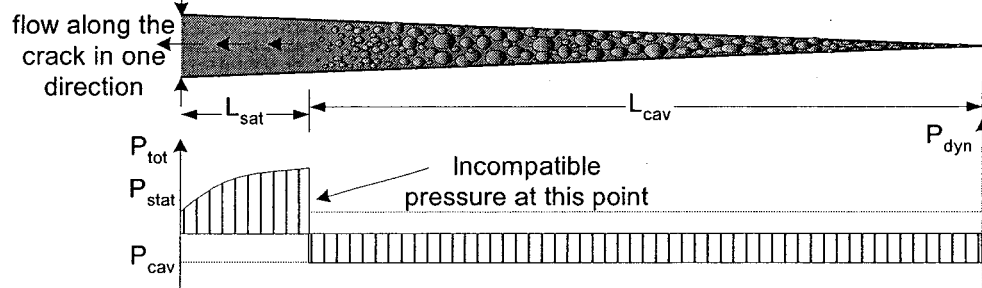
(a) Closing mode (saturated crack)



(b) Opening mode



(c) Closing mode (unsaturated crack)



(d) Closing mode (unsaturated crack)

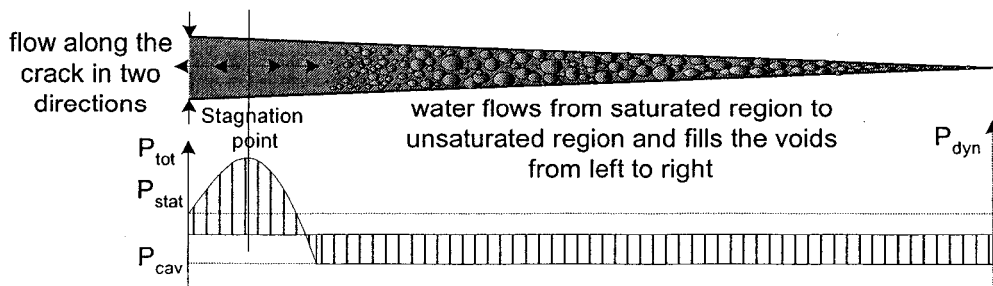


Figure 5.13 Water flow and pressure distributions for a long crack.

- Water could flow in saturated region, and from saturated region to unsaturated region but water flow is not possible in unsaturated region.

Due to existing pressure gradient water flow occurs in saturated part but there is no water flow between two points in the unsaturated region due to constant pressure along this region. Water may enter the unsaturated region from the saturated region to fill the voids (Fig 5.13-b,d).

- The cavitation region is eliminated from left to right (crack mouth to crack tip). Closing of crack or water flow from the saturated region to unsaturated region makes voids disappearing from left to right in the unsaturated region. Disappearing of void at a point is interpreted as the elimination of cavitation, and the water saturation of the crack at that point (Fig. 5.13-d).
- The same concepts, as used in a fully saturated crack, are still applicable for pressure computations in the saturated region.

5.6.2 Extended computational procedure

Water flow is computed using the history of crack wall motions and the continuity condition considering the possibilities for cavitation along the crack. The water flow is different for the crack opening mode as compared to its closing mode. The opening mode and closing mode are therefore considered separately.

(a) Opening mode:

Water flow along the crack, starting from the crack mouth, is computed by the continuity equation. Pressure variations along the crack are computed by Equation (5.16). From the point where the computed pressure becomes equal to the vapour pressure toward the crack tip, (unsaturated region), it is assumed that water pressure remains constant (equal to zero). The increased volume of crack in the unsaturated region is not filled with water so it remains as a void that is filled with water vapour. No flow is assumed in the unsaturated area and the water content in this area remains constant. This behaviour is maintained until the crack begins to close.

(b) Closing mode:

The procedure to compute dynamic uplift pressure for the closing mode of a crack, if there is not any cavitation (full crack saturation), is the same as before. If the closing mode starts with cavitation already present in a part of the crack, and water in the rest of crack, the water flow pattern will be completely different. In this case, despite the saturated crack closing mode, assuming water flow from left to right (from crack tip to crack mouth) leads to a contradiction. If we assume that water flows only in one direction as in the saturated closing case, the computed pressure at the point where cavitation starts will not be compatible with existing pressure which is the cavitation pressure (Fig. 5.13-c). In this region, water does not flow only in one direction and it should flow in two opposite directions to satisfy pressure compatibility. So there should be a stagnation point, with zero flow, where water flow starts in two opposite directions, one from the stagnation point toward the cavitation region, and the other from the stagnation point toward the crack mouth. The pressure at the stagnation point has the maximum magnitude. The pressure in the front flow toward the crack tip is the cavitation pressure, and the pressure in the crack mouth is the quasi-static pressure (Fig. 5.13-d). Water flow toward the crack tip fills the voids and eliminates cavitation from left to right, as soon as all the voids are filled with water, the cavitation phenomenon ends, and a fully saturated flow starts. For long cracks, the closing mode may end without filling all the voids in the cavitation region, and the opening mode starts with an existing cavitation region along the crack.

5.6.3 Computer code developing and checking of the procedure

Based on the proposed procedure, a computer program called DUP_CRACK is developed to compute water flow and water pressure along a crack with moving walls. In the computer program, the crack wall displacement histories are used to compute the crack volume change and water flow as explained in section 5.6.2. The DUP-CRACK algorithm to compute water flow and dynamic pressures along the crack is discretizing the crack in small elements. Therefore, the results of a finite element analysis of a crack

motion can be used directly by the program to evaluate the uplift pressure along the crack.

The DUP-CRACK is used to compute the pressure variation along the crack for the tests presented in sections 5.3 and 5.5. The computed results are identical with the computed results obtained in section 5.3 and 5.5 (as in Figs. 5.6 to 5.9), showing that for short cracks, there is no difference between the results of the simple cut off method used in section 5.5 to consider cavitation, and the results of the more precise method presented here. Because for short crack length, the crack fills with water at the end of the opening mode, the crack is likely to act as a saturated crack in closing mode.

To show the accuracy of procedure and DUP-CRACK, two earthquake displacement records (El Centro 1940 with a predominant frequency of ground shaking near 2 Hz and Saguenay 1988 with a predominant frequency of ground shaking near 10 Hz) are applied to the specimen to compute dynamic uplift pressure and make comparisons with the experimental data when the same earthquake records were applied to a specimen. The measured dynamic uplift forces and the numerical simulations results as well as the applied CMOD histories are shown in Fig. 5.14 and Fig. 5.15. For real earthquake records the experimentally measured dynamic uplift force and the corresponding computed values using the measured CMOD(t) as an input data are nearly identical for both earthquake records.

The validity of model is also checked by using the new crack test results during the opening mode of the propagating crack and the developed transient pressure along the crack in the next section.

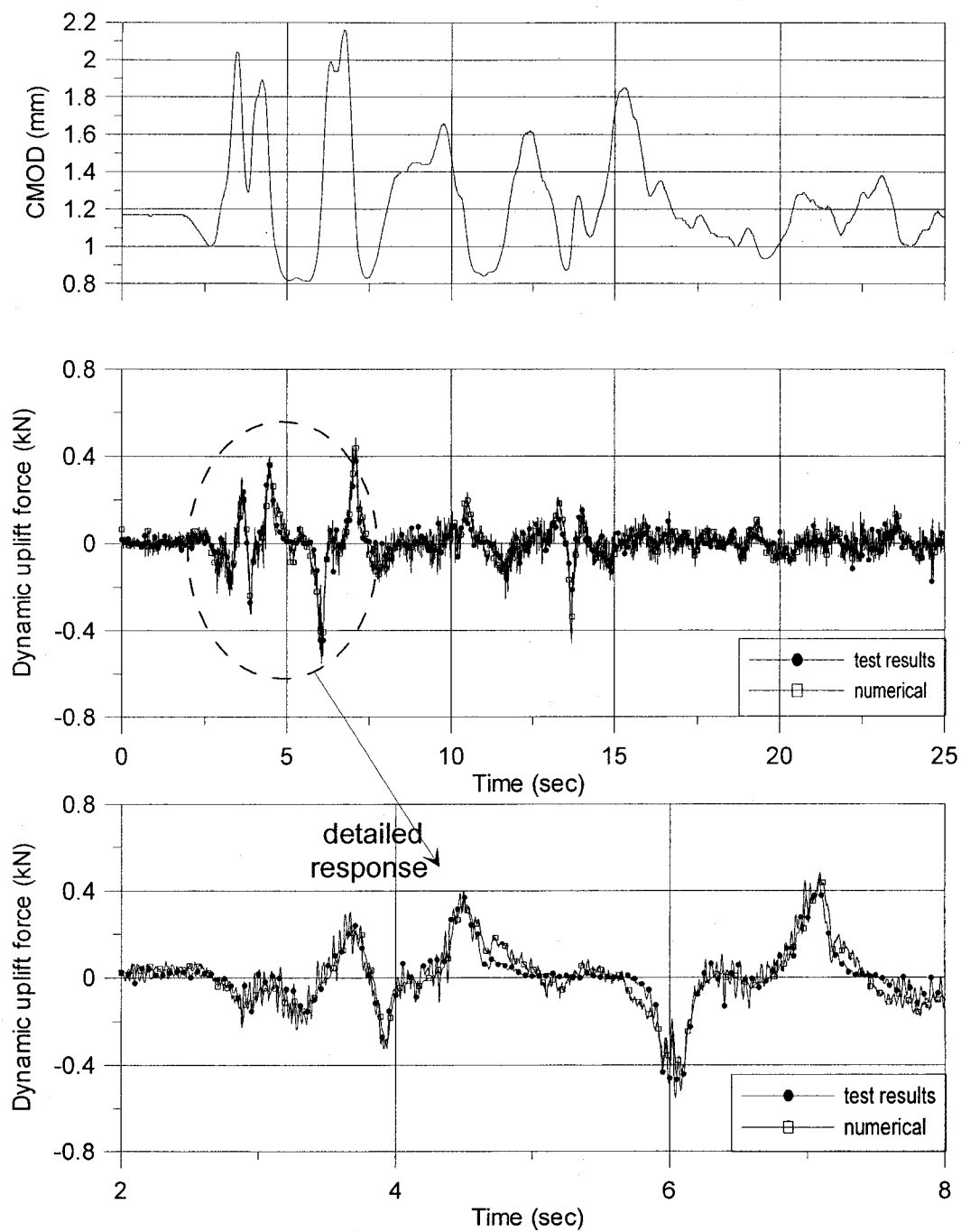


Figure 5.14 Test no. PS4-81 and corresponding numerical simulation results for earthquake case (El Centro 1940).

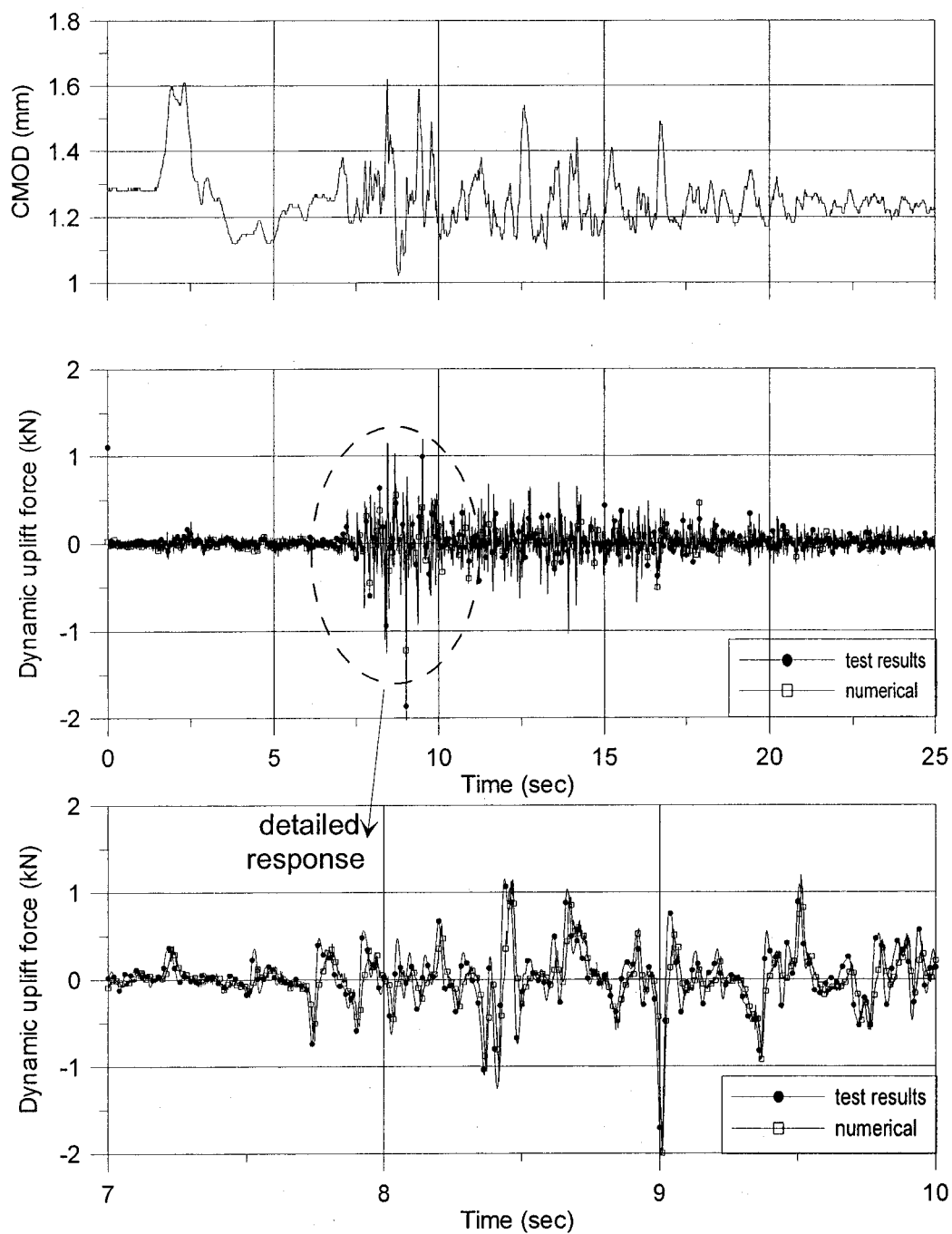


Figure 5.15 Test no. PS4-81 and corresponding numerical simulation results for earthquake case (Saguenay 1988).

5.7 New crack vs existing crack

The uplift pressure development mechanism in a new developing and propagating crack is similar to the opening mode of an existing crack. The water flow develops in a newly developing crack or opening mode of an existing crack due to the existing pressure head at the crack mouth. If we ignore the transient propagation of a new crack and assume it possesses a constant initial length, it is possible to analyse a new crack with the developed procedure assuming that it starts opening with no initial (residual) opening. Figure 5.16 shows this concept for a new crack and an existing crack.

Water flow develops in a part of the crack (the saturated region, L_{sat}) for both cases, the remaining area in the existing crack is filled with water and void but in a new crack, there is not any water in the remaining part of the crack. For the closing mode, the conditions are the same for the two types of cracks. The main difference between a new crack and an existing crack is the initial (or residual) opening of the existing crack (filled with water). If we assume that crack wall motions are the same at a certain time interval for the two types of cracks, L_{sat} for the existing crack will be longer than L_{sat} for the new crack due to larger crack opening and smaller flow head loss along the crack.

The DUP_CRACK computer program is used to simulate the new crack test results to verify the validity of crack-water interaction model for this case. The simulated and the measured water pressures along the crack for the test no. NS1 and NS3 are shown in the Fig 5.17 and Fig. 5.18. It is assumed that the cavitation pressure is equal to zero so the differences between negative measured pressures and estimated zero pressure just after cracking comes from this assumption. Comparisons of the computed and the measured pressures along the crack shows that the computed pressures are reasonably close to the measured pressures in these two cases (in these comparisons the measured pressures that oscillate due to collapsing of vapour pocket are replaced by a smoothed curve as shown in Fig. 5.17 and Fig. 5.18). There is a time delay between the measured pressures and the simulated ones. In other word, the water penetration velocity in the test condition is smaller than the predicted velocity by the model. Two phenomena that have not been considered in the proposed model may cause these differences. The cavitation

phenomenon and collapse of vapour pockets increase, locally, the flow head loss in this area (minor loss). The second phenomenon is the absorption of water by dry crack walls that can reduce the water front velocity in a new crack test compared to the simulated results. To account for these phenomena additional head loss should be considered in the flow law which can be done by introducing some minor loss coefficients (similar to experimental minor loss coefficients are used in pipe flow analysis for section change or bent) or introducing a new head loss coefficient to cubic law. For example if we apply a coefficient equal to 2 to equations 4.15 and 5.15 the computed results will be closer to the measured results as shown in Fig. 5.19. More new crack tests are required to determine experimentally a more precise method to modify the proposed model for these effects. Since the observed differences are not very significant and the results from the proposed model may overestimate the developed pressure, the proposed model without modification will be used to compute the dynamic pressure for the new crack case.

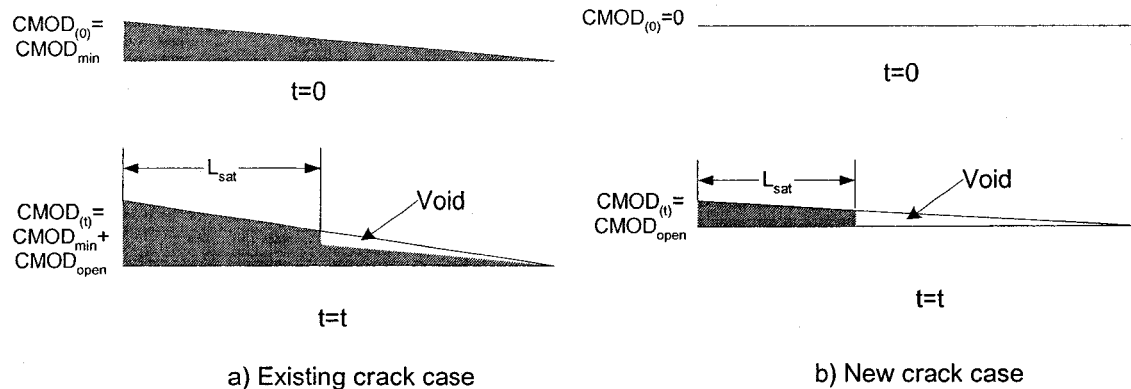


Figure 5.16 Opening mode of: (a) an existing crack, and (b) a new crack.

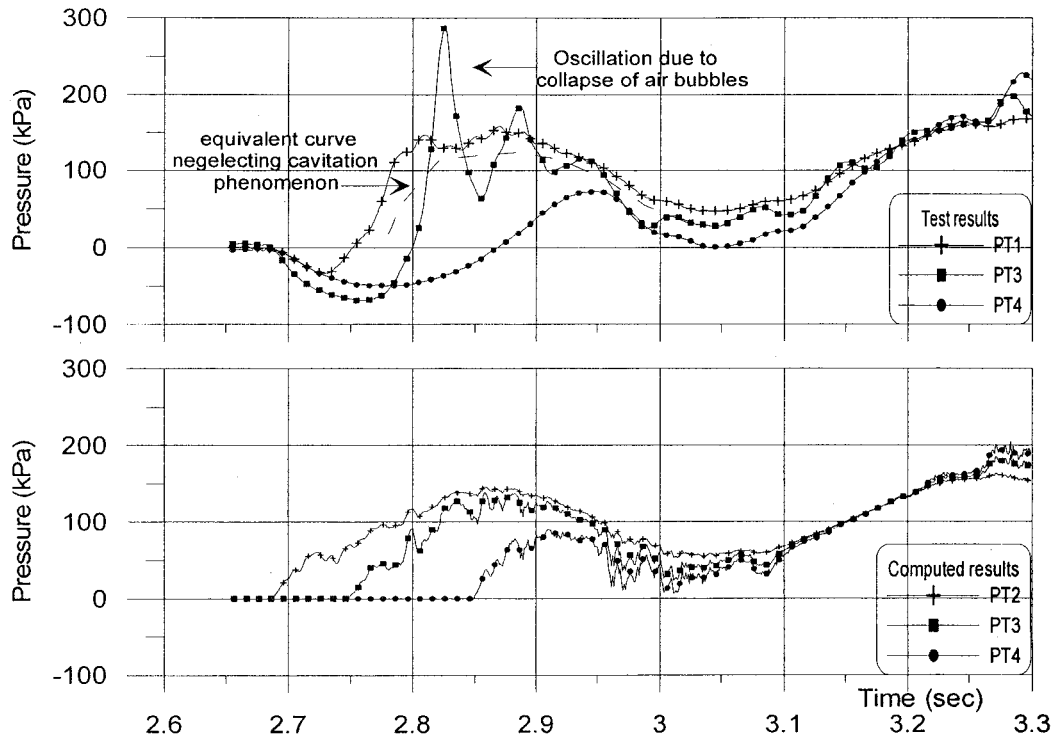


Figure 5.17 Simulated and measured pressures for new crack test no. NS1.

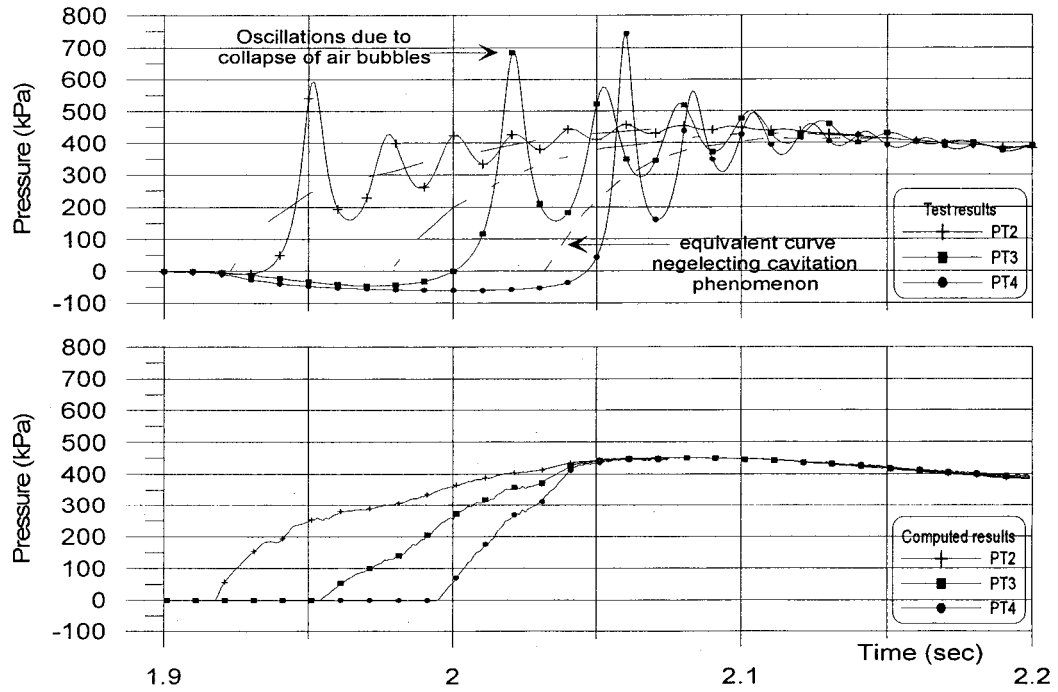


Figure 5.18 Simulated and measured pressures for new crack test no. NS3.

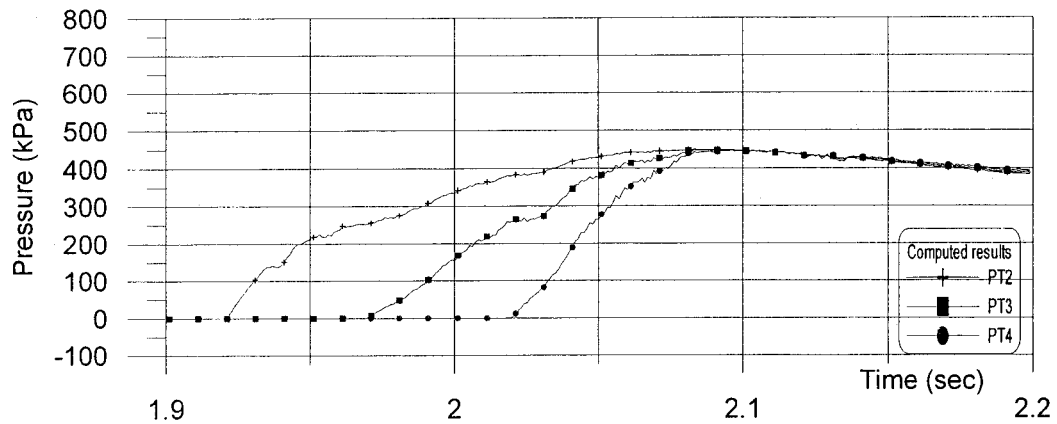


Figure 5.19 Simulated pressures for new crack test no. NS3 after modification for additional losses.

5.8 Crack length effects

All the simulated and experimental test results that have been presented so far, are related to the cracks with 0.40 m length. Using the developed computer program, it is possible to compute pressure variation for longer cracks. In this section, the developed pressures in a 4 m existing crack, and a 4 m new crack are computed and compared. The differences between development pressure in three cracks with different lengths 4 m, 8 m, and 12 m are also compared.

5.8.1 Investigation of pressure variations in a 4 m existing crack

An existing 4 m crack, with initial crack mouth opening equal to 0.5 mm is considered. It is assumed that crack walls motion is a harmonic motion with a maximum opening of 1.5 mm ($CMOD_{amp}=1.0$ mm) and the frequency of oscillation is 2 Hz. The crack mouth pressure is assumed equal to 500 kPa that remain constant during crack wall motions. DUP_CRACK is used to compute the water pressure variations along the crack. The assumed crack wall motion and the computed uplift pressure along the crack for one cycle of motion are shown in Figs. 5.20 and 5.21 (since the same pressure variations is repeated in next cycles, only the response of one cycle is shown here). The spatial variations of the pressure along the crack during opening and closing mode of

crack are shown in Figs. 5.22 and 5.23. Figure 5.22 shows that the assumed static full uplift pressure along the existing crack decreases as soon as the opening of crack is initiated ($t=0.001$ sec). Due to further opening (increasing opening velocity) the cavitation phenomenon occurs along the crack ($t=0.01, 0.02$ sec), and saturated length of crack decreases. The minimum saturation length correspond to $t=0.07$ sec ($L_{sat}=0.40$ m) and with further opening the saturation length increases till the end of opening mode at $t=0.25$ sec.

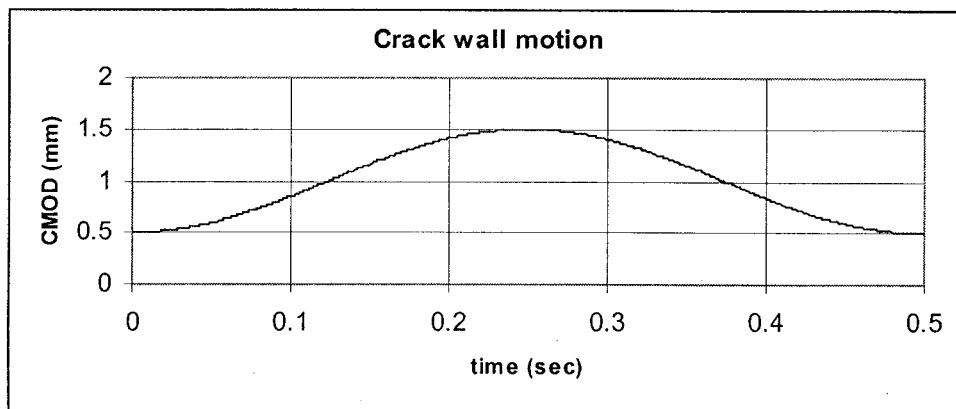


Figure 5.20 CMOD variations in a 4 m crack.

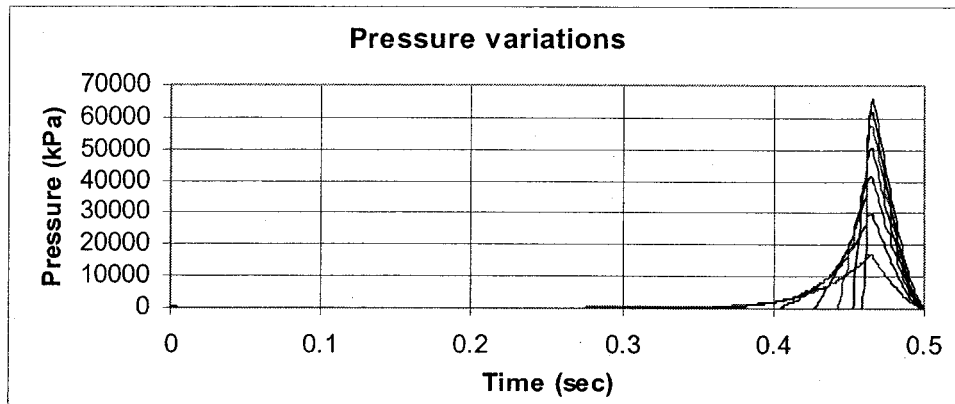


Figure 5.21 Pressure variations in a 4m crack with harmonic wall motion ($f=2$ Hz).

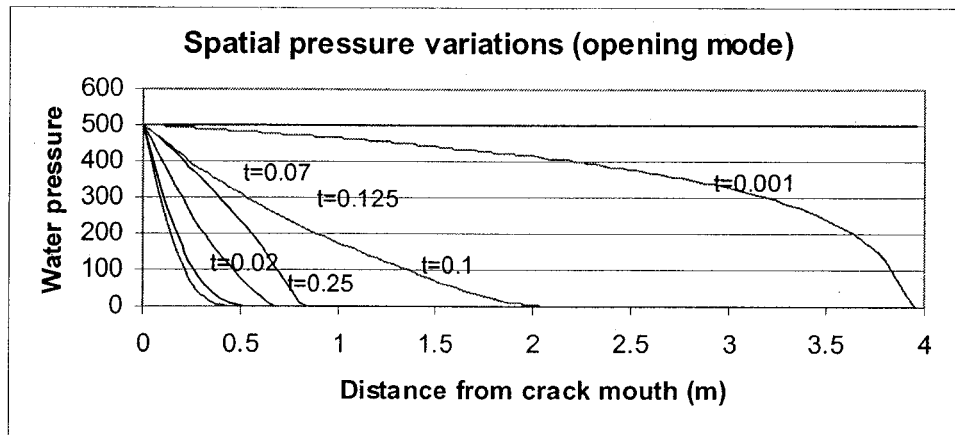


Figure 5.22 Spatial pressure variations along a 4m crack in opening mode ($f=2$ Hz).

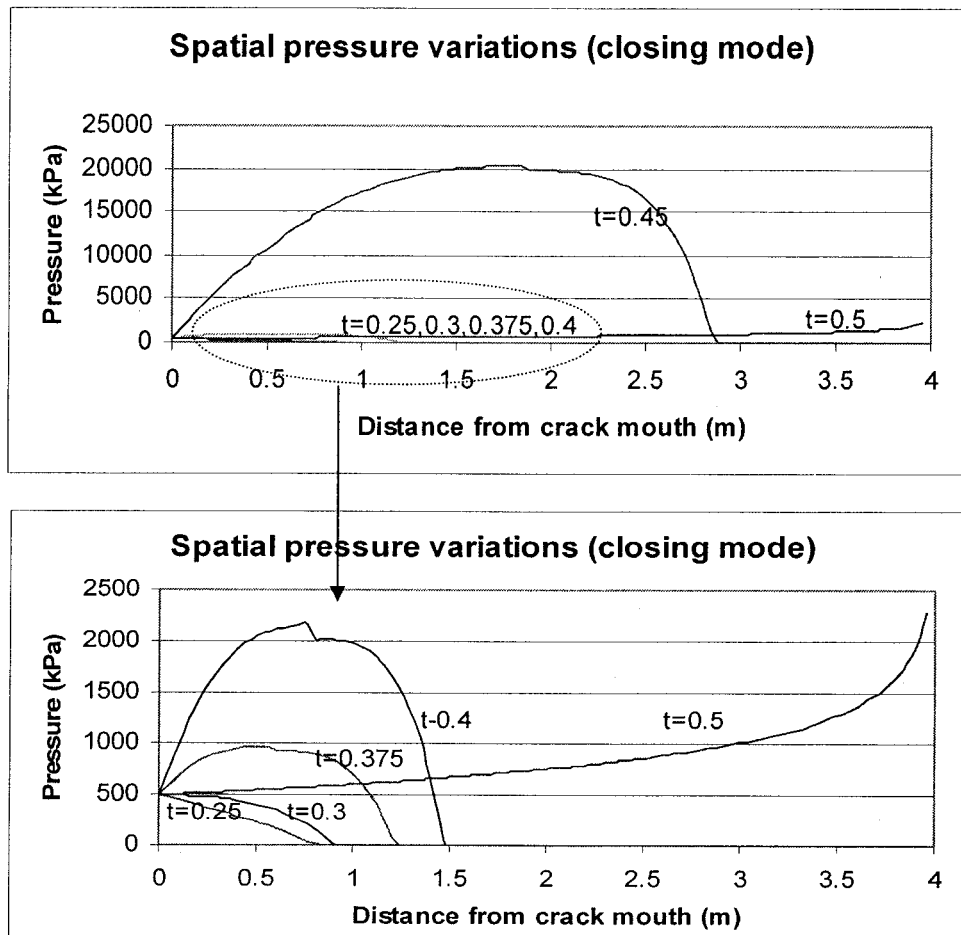


Figure 5.23 Spatial pressure variations along a 4m crack in closing mode ($f=2$ Hz)

As crack closing phase starts, the increase in saturated length continues and the magnitude of the developed pressures in the saturated part of the crack increases. The full saturation case starts at $t=0.48$ sec and after that, the water pressure variation is like a fully saturated crack (modification for singularity at crack tip has not been considered in this case).

5.8.2 Investigation of pressure variations in a 4 m new crack

To compare the developed pressure in a new crack and existing crack, a new crack with 4 m length is considered. It is assumed that crack starts opening (cracking) with no initial opening but after cracking a residual opening will exist during the closing mode, and the crack does not close completely again. The residual opening is assumed equal to $CMOD_{min}=0.5$ mm, and DUP_CRAK is used to analyse the 4 m crack that starts opening with $CMOD=0.0$ and oscillates the same way as an existing crack in section 5.8.1. Unlike the existing crack, the computed pressures are not repeated in the subsequent cycles and after some cycles that steady-state water pressure is developed (this concept was also shown, experimentally, in Chapter 4). Figure 5.24 shows the developed uplift forces in the crack as well as pressures in four different points along the crack. The uplift force variations graph shows that steady-state pressure variation is started after 11th cycle of harmonic motion. The pressure development at $x_c=0.4$ m is started in the first cycle of crack closing, while the pressure at $x_c=1.2$ m, $x_c=2.6$ m, and $x_c=3.6$ m are started in second, fourth, and 8th cycles, respectively. The progressive development of water pressure along the crack shows the crack front location and its propagation at each closing cycle. The complete saturation of crack in the 11th cycle makes a new crack similar to an existing crack, that becomes fully saturated during the closing mode, and after that, water pressure variations in the new crack are similar to that of the existing crack (Fig. 5.21). The progressive penetration of water in the crack shows that crack cyclic motion is similar to a mechanical pump that sucks the water in opening mode and enforces it (actually only a part of sucked water) to flow into the crack to fill the residual opening of the crack. The assumption made by USBR (1987)

that “ the rapidly cycling nature of opening and closing mode the crack do not allow reservoir water, and the associated pressure to penetrate” is not adequate. It should be mentioned that this conclusion is based on the assumption that a new crack cannot be closed completely and a residual opening will be exist during the crack closing period.

Another interesting observation is related to the water pressure in opening mode of new crack. Figure 5.25 shows the developed water pressure in five different time period. Comparing the pressure in different opening modes (Fig 5.25-a), it can be concluded that pressure variation along the crack for opening mode in different cycles are similar. In other word, steady-state water pressure (in opening mode) is developed in second cycle of crack opening, while full steady-state (including closing mode) occur after 11th cycle. As the crack closing phase starts, the water pressures are still similar (in different cycles) along the crack, but the magnitude of pressure starts to increase rapidly as the saturation length increases due to closing of crack.

5.8.3 Crack length effects

Three new cracks with different lengths 4 m, 8 m, and 12 m are considered. The crack mouth motions for all cracks are assumed to be the same ($P_{stat}=1000$ kPa, $f=2$ Hz, $CMOD_{min}=0.5$ mm, $CMOD_{amp}=1.0$ mm). The computed dynamic uplift forces in cracks and the computed uplift pressures in five different points along the cracks are shown in Fig. 5.26. The spatial pressure distributions along the cracks at an instant of opening time period are also plotted in Fig. 5.27. Comparing these graphs, the following points can be concluded.

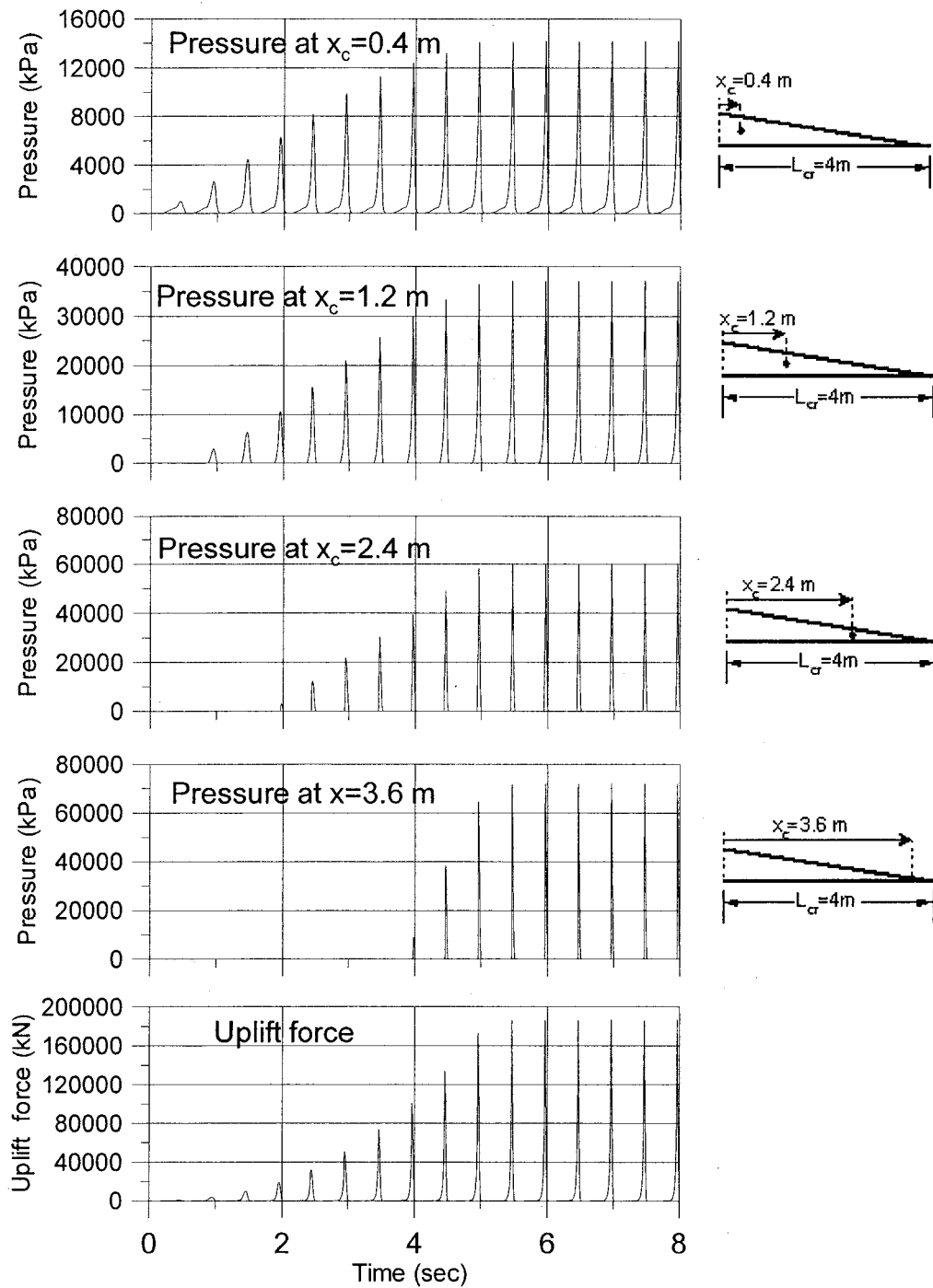
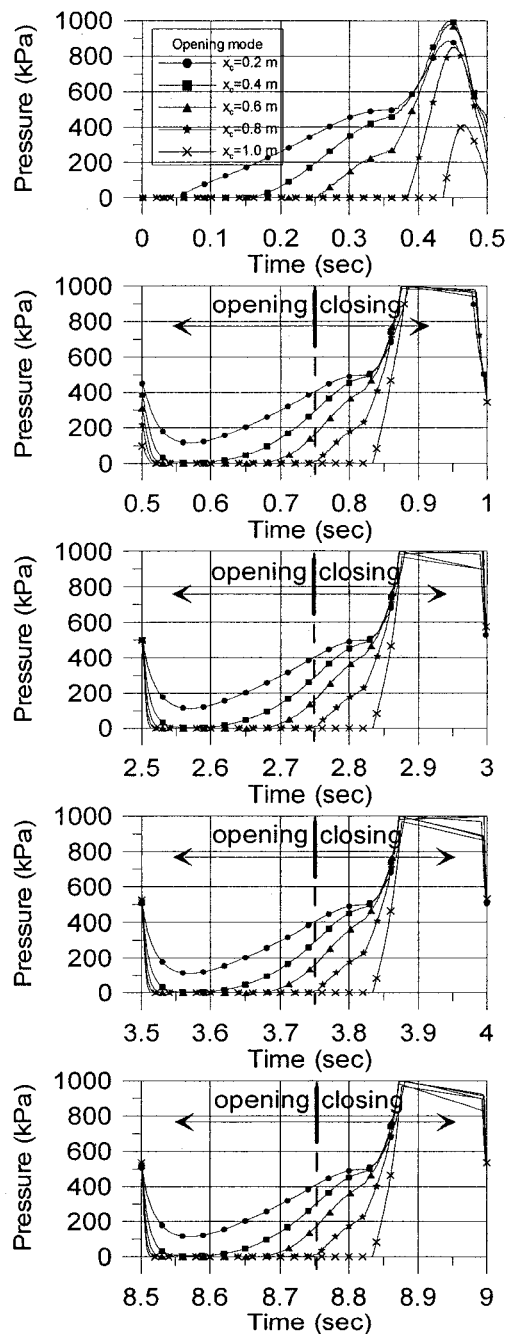


Figure 5.24 Pressure development along a new 4m crack due to harmonic motion

($P_{stat} = 500$ kPa, $CMOD_{amp} = 1.0$ mm, $CMOD_{min} = 0.5$ mm, $f = 2$ Hz).

a) Crack opening and closing mode



b) Crack closing mode

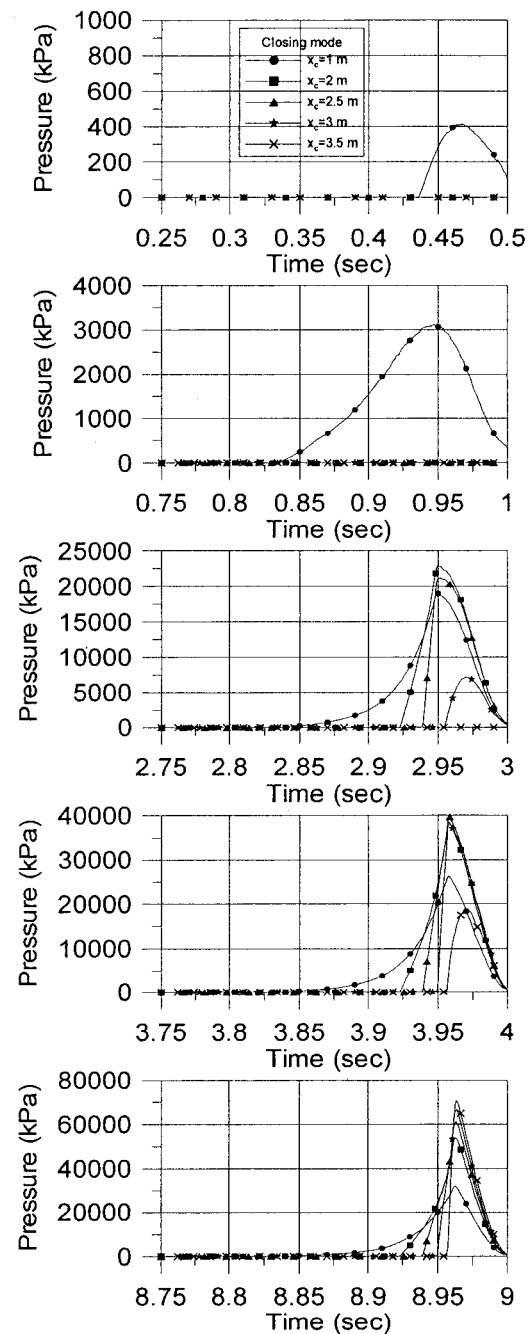


Figure 5.25 Pressure variations along a 4 m new crack in opening and closing modes at different cycles of harmonic oscillation of crack walls (to show the pressure variations in more details, pressure curves in part (a) has been cut at the magnitude of 1000 kPa).

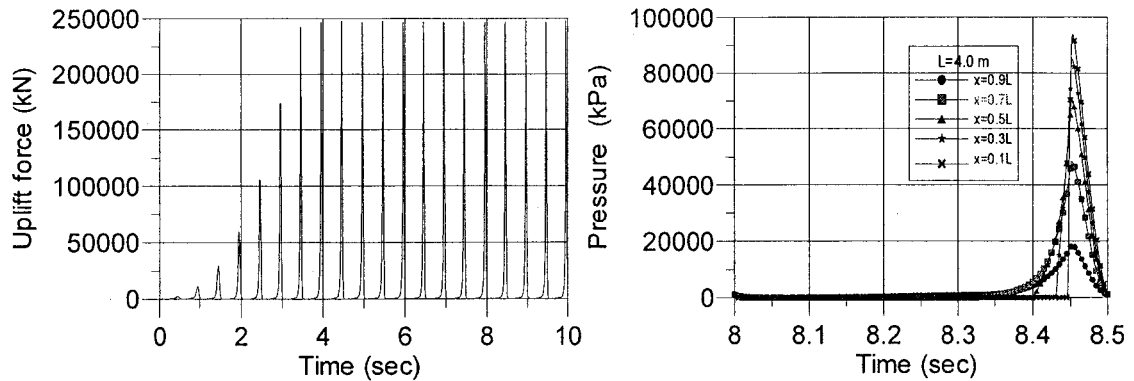
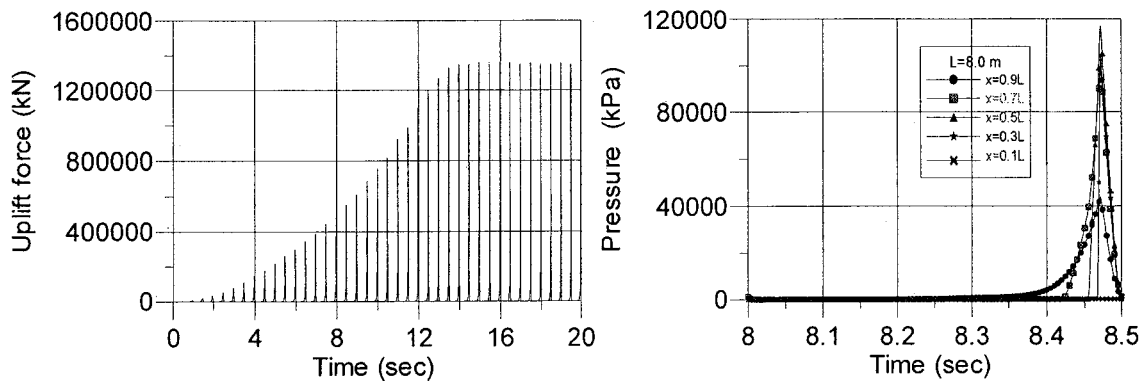
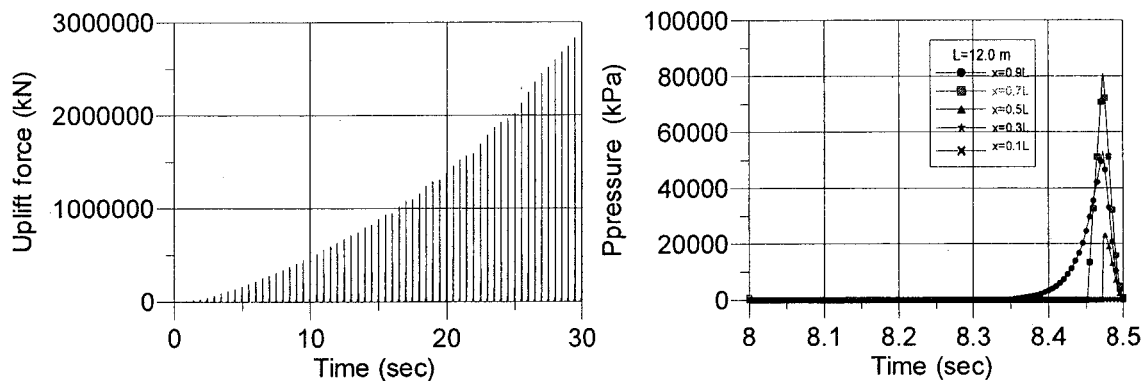
(a) Numerical simulation results for a crack $L=4.0$ m(b) Numerical simulation results for a crack $L=8.0$ m(c) Numerical simulation results for a crack $L=12.0$ m

Figure 5.26 Numerical simulation results for cracks with 3 different lengths ($L=4$ m, 8 m, and 12 m; $P_{stat}=1000$ kPa, $f=2$ Hz, $CMOD_{min}=0.5$ mm, $CMOD_{amp}=1.0$ mm).

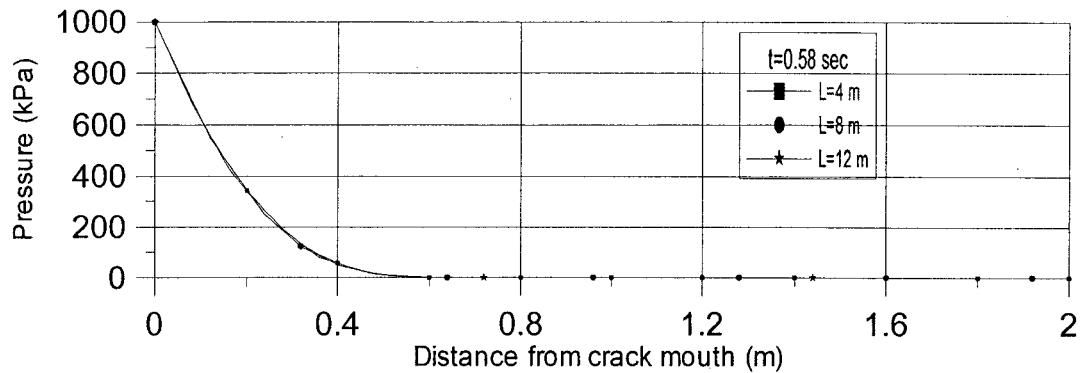


Figure 5.27 Pressure variations in opening mode for three different crack lengths.

- The pressure spatial distributions for the opening mode in Fig. 5.27 ($t=0.58$ sec) are the same for all cracks and the respective cavitation length (L_{cav} Fig. 5.13), for cracks of 4 m, 8 m, 12 m are $L_{cav}=3.6$ m, $L_{cav}=7.6$ m, and $L_{cav}=11.6$ m. In other words, the length of crack filled with water, the saturation length (L_{sat} Fig. 5.13), are almost equal in the three cases $L_{sat}=0.4$ m. This length is independent of the crack length and is a function of the crack opening displacement, the crack opening velocity and the quasi-static uplift pressure at the crack mouth. By increasing the quasi-static crack mouth uplift pressure, increasing the crack opening displacement, and decreasing crack mouth opening velocity, this length (L_{sat}) increases.
- The steady-state response of uplift forces in Fig. 5.26 show development of full saturation in cracks closing mode. It is concluded that full saturation of a 4 m new crack occurs after 3 sec while this time for a 8 m crack is 13 sec and for a 12 m crack it is more than 30 sec. Significant increase in water pressure is required to make the crack fully saturated in closing mode.
- In a real crack, such high pressure cannot be realistically developed due to actual boundary conditions limiting the development of high pressure. The crack walls cannot be considered completely impervious in a real dam, especially when water pressure is high. Due to high pressure gradient water, may penetrate into porous

crack walls that reduce water flow along the crack. In our tests, we have a nearly perfect lateral impervious confinement of the specimens' sides. In an actual dam a horizontal crack is likely to intercept vertical construction joint providing a 2D flow condition likely to reduce the peak pressure values. Finally if very high pressures develop, water density changes if compressibility is taken into account. In this case there will be a significant reduction in the magnitude of water flow relative to computed flow in the crack. As a result of reduced water flow in the crack the developed water pressure will be smaller than the estimated pressure.

It should be mentioned, that in the above analyses it is assumed that the developed dynamic water pressure does not affect the assumed crack wall motions (displacement control analysis). In a concrete gravity dam subjected to earthquake loads, the developed dynamic water pressures in the crack affects the dam response and the coupling effects of dynamic water pressures and the crack wall motions should be considered. It is expected that the magnitude of developed pressures in closing mode (computed in this section) may decrease significantly due crack closure history if we consider water-crack coupling phenomenon in a load control analysis. The developed pressure in cracks of concrete gravity dams considering the effect of transient uplift pressures on modifying the crack wall motion and its effects on dam stability will be studied in the next chapter.

5.9 Conclusions

Opening and closing of crack walls in a saturated concrete crack causes water pressure variations along the crack. The pressure gradient along the crack causes water flow inside the crack. The bulk modulus of water is considerably larger than the developed pressure in the crack, such that water density remains almost constant. Neglecting water density changes, the water flow in the crack can be computed using the continuity equation and the history of crack wall motions. Then the pressure gradient can be evaluated based on suitable flow laws in the crack. Dynamic pressure along the

crack can be computed by integration of pressure gradient along the crack. An analytical formulation is derived to evaluate water pressure in a crack with moving walls considering adequate simplifying assumptions for cavitation and pressure singularity at the crack tip. A computer program DUP-CRACK is developed based on the novel transient water-crack interaction model developed herein. The experimental pressure variations and the simulated pressure variations by the proposed model are generally in very good agreement.

Using DUP_CRACK an existing 4 m crack and a new 4 m crack responses are compared. The effects of the crack length on the developed dynamic pressures and the occurrence of cavitation is also investigated through analyses of three cracks with different lengths $L=4$ m, $L=8$ m, and $L=12$ m. The main conclusions are:

- If the cyclic wall motions of an existing crack and a new crack are similar, the developed water pressure in opening mode of these two cracks will be the same. During the opening crack mode (new or existing crack) a small section of the crack near to the crack mouth remains saturated and the cavitation phenomenon occurs in the rest of the crack. The length of this saturated region (L_{sat}) is basically independent of crack length, and is a function of the quasi-static pressure at crack mouth, crack aperture, and crack mouth opening velocity. For $P_{stat}=1000$ kPa, $CMOD_{min}=0.5$ mm, and $CMOD_{amp}=1$ mm, and $f=2$ Hz the average of L_{sat} in opening mode is almost 0.7 m.
- During crack closing (new or existing crack), the water pressure develops in the so called saturated region of the crack (L_{sat}). Water flows from the saturated region to the cavitation region eliminating cavitation gradually.
- In harmonic motion of new cracks (with an assumed residual opening), the saturation length increases gradually at the end of the closing mode at each cycle. The steady-state response, which is fully saturated at the end of closing mode, develops after some cyclic motions. The fully saturated response is developed after 4 sec and 13 sec in the 4 m and 8 m crack respectively.

- The length of the saturated region during the crack opening mode is relatively small with respect to crack length, however closing of a crack promotes the extension of this length and develops significant dynamic water pressures in this region. In a new developed crack during an earthquake cyclic opening and closing of crack will force water to penetrate into the crack. Therefore the assumption that rapidly oscillating nature of opening and closing the crack does not allow reservoir water to penetrate in the crack (USBR 1987) is highly questionable.
- Using the proposed method, the computed water pressures for the closing mode of a saturated long crack are very high. In a real crack, such high pressures cannot be realistically developed due to permeability of crack walls, lateral hydraulic and mechanical boundary conditions, compressibility of water, and the possible crack propagation due to wedge effect. All of these factors may reduce the developed pressure in the crack closing mode by reducing the existing water flow with respect to computed water flow in a real crack.
- The results discussed so far are valid for cracks in displacement control motion. In a real concrete dam, crack wall motion is affected by the developed dynamic pressure, so the coupling effects of the developed dynamic pressure and the structure response should be considered. It is expected that the magnitude of developed pressures in closing mode (computed in this section) could be decreased significantly due crack closure history if we consider water-crack coupled interaction phenomenon in a load control situation.

The significance of dynamic uplift pressure on seismic dam safety should be assessed by performing case study analyses. The response of cracked gravity dams subjected to earthquake, and the effects of developed dynamic water pressures on seismic dam responses are studied in the next chapter.

CHAPTER 6

NUMERICAL SIMULATIONS AND CASE STUDIES

6.1 Introduction

The developed pressure inside the concrete cracks with predefined time history of crack wall motions were investigated without considering the coupling effects of the developed pressure modifying the crack walls openings. In a concrete gravity dam subjected to earthquake the dam response and crack walls motions are affected by the applied external load as well as the developed hydrodynamic water pressures in the crack, and a hydro-mechanical coupled analysis is necessary for a realistic dynamic analysis. The main subroutines of DUP_CRACK are implemented in a finite element based computer program, INTRFACE, which is a computer program for dynamic analysis of concrete gravity dams with contact elements (Fronteddu 1997). The developed program called DUP_DAM is able to perform dynamic analysis of concrete gravity dams considering complete water-crack hydro-mechanical coupling effects. A brief description of INTRFACE and the implementation procedure of the proposed water-crack constitutive model is presented in section 6.2. Some case studies using DUP_DAM are presented in section 6.3. The recommendations for evaluating uplift pressure in crack opening mode to use in pseudo-static and pseudo-dynamic analysis of concrete gravity dams are presented in section 6.4. The conclusions based on the results of case studies ends this chapter.

6.2 Finite element analysis of dam considering dynamic uplift pressure

The dynamic analysis of a concrete dam subjected to earthquake, considering concrete cracking, is possible by most commercially available nonlinear structural analysis computer programs where contact elements are available. The computed time

history of CMOD can be used as known independent input data for DUP_CRACK computer program to evaluate the dynamic water pressure along the crack during the earthquake. However, the developed water pressure inside the crack modify wall motions, therefore independent analysis of these two phenomena is not realistic, at least in the closing mode, as it will be shown later. It is required to adjust the computed crack mouth opening displacement response (CMOD) and considering dynamic water pressure in the crack by an iteration procedure. The simplest way is to iterate manually by successive applications of finite element analysis to compute the complete CMOD time history assuming uplift pressure as dynamic external loads on the crack walls computed from previous iteration results, and then using DUP_CRACK to evaluate uplift pressure in the crack based on the computed CMOD. This procedure should be continued to get convergence of the results. This procedure works fine in crack opening modes and the results converge rapidly. However, the developed pressure in closing mode is very sensitive to CMOD changes and it is difficult to get good results for the crack closing mode.

The other way is to do the iteration at each dynamic computational time step in dynamic analysis to get a converged answer in each time step for the dam response and the developed uplift pressure. The finite element method based computer program called INTRFACE, developed by Fronteddu (1997) is a computer program for earthquake analysis of concrete gravity dams. INTRFACE is used to implement fully coupled hydro-mechanical dynamic water-crack interaction model. The nonlinear gap-friction elements are used to model the crack initiation and propagation (at the assumed lift joints levels).

6.2.1 Dynamic equilibrium equation

Dynamic equilibrium equations of a structure subjected to seismic excitations are expressed as:

$$[M]\{\ddot{u}\} + [C]\{\dot{u}\} + \{R\} = -[M]\{r\}\{\ddot{u}_g\} + \{f_{stat}\} = \{f\} \quad (6.1)$$

where $[M]$ is the mass matrix, $[C]$ is the damping matrix, $\{R\}$ is the restoring force vector, $\{f_{stat}\}$ is the vector of pre-seismic applied force, $\{u\}$, $\{\dot{u}\}$, $\{\ddot{u}\}$ are displacement, velocity and acceleration vectors respectively, $\{\ddot{u}_g\}$ is the vector of ground acceleration, and $\{r\}$ is the unit vector specifying the active dynamic degrees-of-freedom. Due to cracking in concrete dams, the restoring force vector, $\{R\}$, the damping matrix $[C]$, may vary with time. A time integration method is required for solving the dynamic equilibrium equations at discrete time steps, Δt . The α integration method has been adopted in INTRFACE for the analysis of cracking in concrete gravity dams using gap-friction elements. The restoring force is a function of gap element state, so it is not known a priori during integration and an iterative procedure is required to solve the equation. The modified Newton-Raphson method is used in INTRFACE for iteration in each mechanical time step.

6.2.2 Dynamic equilibrium equation for hydrodynamic coupling

The dynamic water pressure in the crack can be treated as an additional restoring force and the dynamic equilibrium equation 6.1 to consider transient water pressure in the crack can be written as:

$$[M]\{\ddot{u}\} + [C]\{\dot{u}\} + \{R + Wpr\} = -[M]\{r\}\{\ddot{u}_g\} + \{f_{stat}\} = \{f_{(t)}\} \quad (6.2)$$

where $\{Wpr\}$ is a force vector corresponds to the transient uplift pressure in the crack. The $\{Wpr\}$ vector, like the $\{R\}$ vector, is a function of displacement and velocity so nonlinear iterations should be used to adjust it at each integration time step. The nonlinear iteration scheme in INTRFACE was adjusted according to equation 6.2 and the main subroutines from DUP_CRACK were added to compute water pressure in each nonlinear iteration step. Due to rapid increase of uplift pressure in crack during the closing mode, the developed iteration procedure does not converge for all the cases (especially for initially saturated cracks). This problem needs more investigation to develop a suitable numerical procedure (similar to contact problem in structural

mechanics with rapidly increasing stiffness with closing displacements). However, the procedure is generally applicable for the new developed cracks where full saturation of the crack does not occur during relatively small period of earthquake events. The developed computer program, called DUP_DAM, can be used for nonlinear dynamic analysis of concrete gravity dams considering the water-crack interactions in newly developed cracks or existing cracks where the water pressure during crack closing does not occur instantaneously similar to impact phenomenon.

The inertia of the reservoir water induces an increased or decreased water pressure on the dam upstream face concurrently with dam inertia forces. In INTERFACE, the Westergaard added masses concept is used to represent this additional pressure. The parabolic approximation of Westergaard formula, equation 6.3, is used to compute the hydrodynamic pressure variations at the crack mouth during the earthquake.

$$P_{west} = -\frac{7}{8} \rho H \left(1 - \frac{y}{H}\right)^{1/2} \ddot{u}_g \quad (6.3)$$

where ρ is the mass density of water, H is the height of reservoir, y is the crack mouth height from the bottom of the reservoir, and \ddot{u}_g is the horizontal earthquake ground acceleration. The crack mouth pressure, P_{crm} , is then computed by the following formula:

$$P_{crm} = P_{stat} + P_{west} \quad (6.4)$$

The developed computer program, DUP_DAM, is used to investigate the fully coupled mechanical-hydraulic response of cracked concrete gravity dams subjected to earthquake ground motions.

6.3 Effect of coupling in developed crack water pressures

A typical 90 m gravity dam section subjected to two different base accelerations is analysed. The dam geometry and the assumed concrete properties are shown in Fig. 6.1.

The first base acceleration is a 10 Hz sinusoidal acceleration with 0.35g amplitude. It is also assumed that the application of the earthquake will develop a 4.5 m crack

(constant length) along the dam-foundation interface and a residual hydraulic aperture equal to 0.5 mm is also assumed. A fully coupled hydro-mechanical analysis of this dam is performed using the DUP_DAM program. To compare the results of coupled analysis with an uncoupled analysis, the INTRFACE program is first used to analyse the dam without any uplift pressure and a predefined 4.5 m crack. The computed CMOD time history from this analysis is used as input data for the DUP_CRACK, to compute independently the pressure along the crack (uncoupled analysis). The results of this uncoupled hydro-mechanical analysis are compared to those of a fully coupled hydro-mechanical analysis, where there are iterations between the computed crack wall pressures and the crack wall motions to maintain dynamic equilibrium within a time step (Fig 6.2). The CMOD time histories (Fig. 6.2) show that the steady-state response of dam in dry conditions starts after 2 sec, the required time for development of steady-state response in coupled analysis is almost the same. The responses of the dam in uncoupled or coupled hydro-mechanical analysis are basically similar except during the crack closing mode.

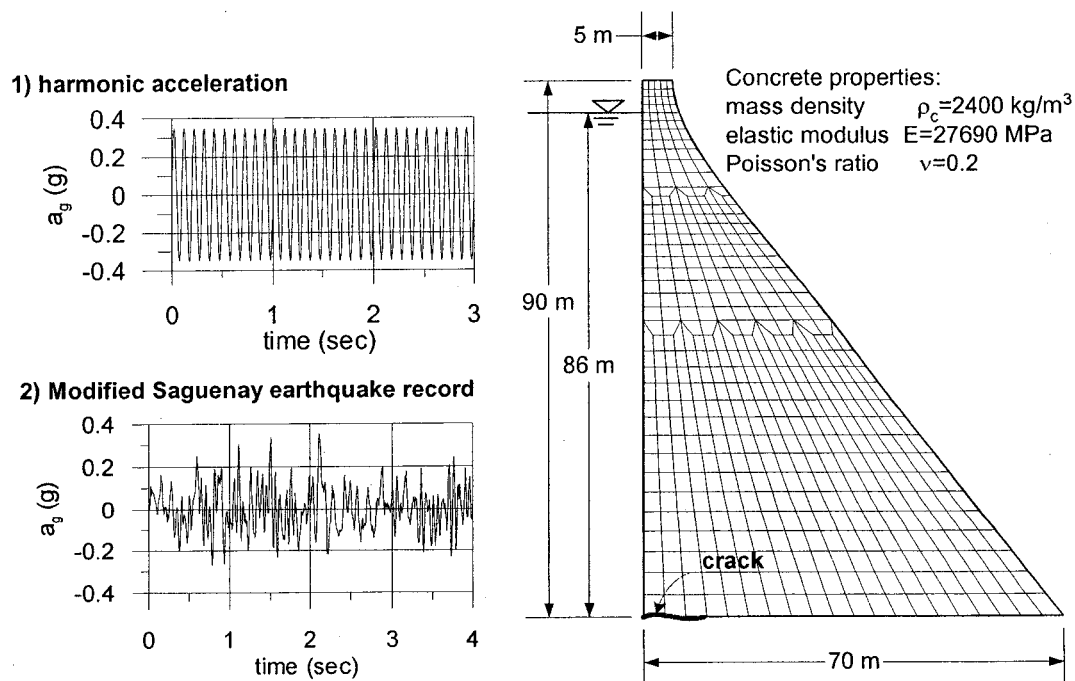
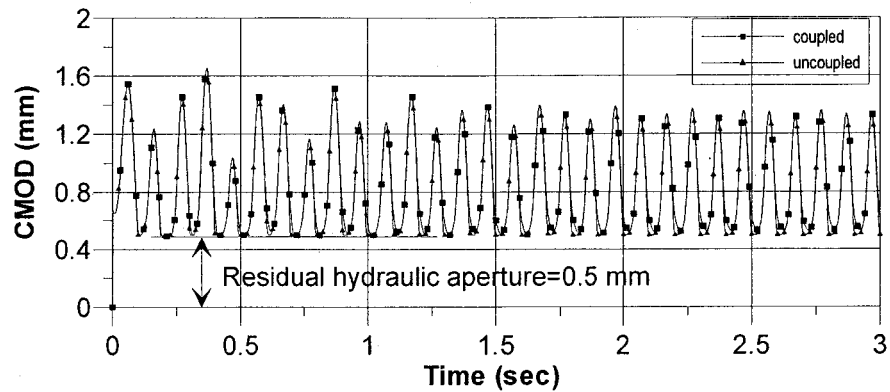


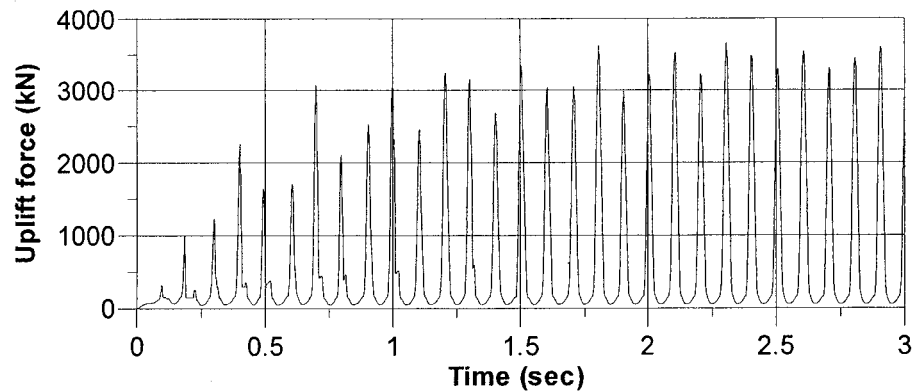
Figure 6.1 Dam model assuming a rigid foundation and applied base accelerations.

Comparing the developed uplift force for coupled and uncoupled types of analyses, there are significant differences between the magnitudes of maximum uplift forces. While the maximum uplift force in coupled analysis is 3700 kN, the corresponding value for the uncoupled analysis is 400000 kN. The structural response of the dam and the developed pressure for the coupled and uncoupled types of analyses are shown in more details in Figs. 6.3 and 6.4. Figure 6.3 shows the CMOD responses and the pressure variations in the crack from $t=0.55$ sec to $t=0.75$ sec while the steady-state response has not developed. Figure 6.4 shows similar graphs for the time period between $t=2.75$ sec to $t=2.95$ sec where steady-state response is developed. Comparing these figures, the following conclusions can be drawn:

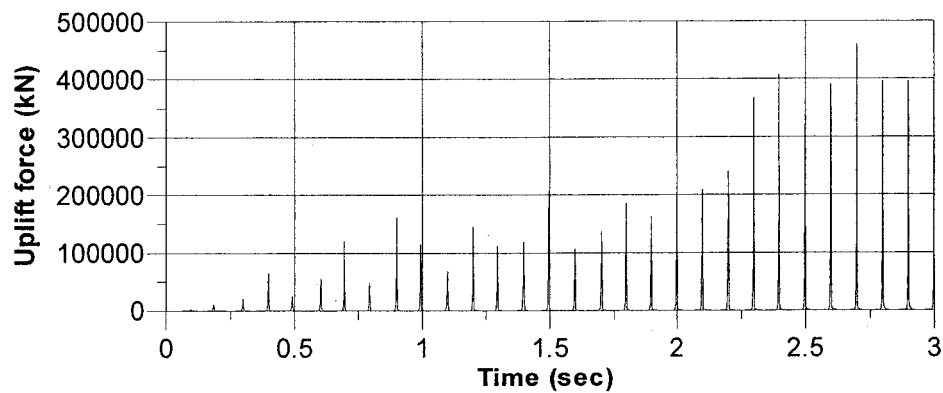
- Considering the coupling effect of water-crack in the dam subjected to earthquake does not change the opening response of the crack, however, the closing response changes due to hydro-mechanical coupling effect.
- The developed water pressure in the crack, during the crack closing mode, induces additional forces on crack walls and decreases the closing velocity of the crack. Because the crack closing velocity decreases, the developed pressure in the closing crack decreases significantly compared to an uncoupled analysis. If the pressure in the crack is high enough, it may prevent crack wall from complete closure.
- The length of the pressurized region in the closing mode (L_{sat}) is increasing in each cycle until it reaches a steady-state length. Full saturation of crack in crack closing mode of coupled analysis does not occur due to the small magnitude of pressure.



(a) Response of dam with and without hydro-mechanical coupling effect

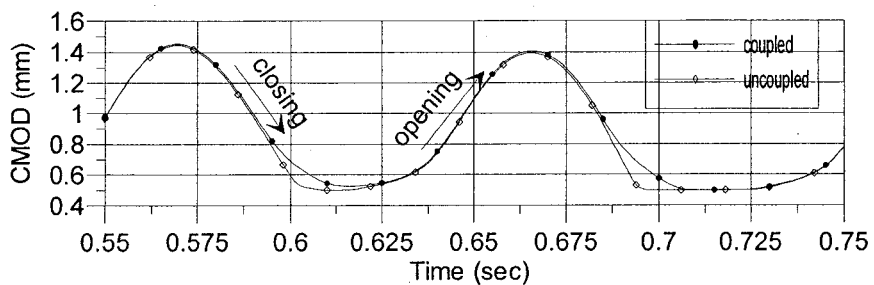


(b) Uplift force in crack considering hydro-mechanical coupling effect

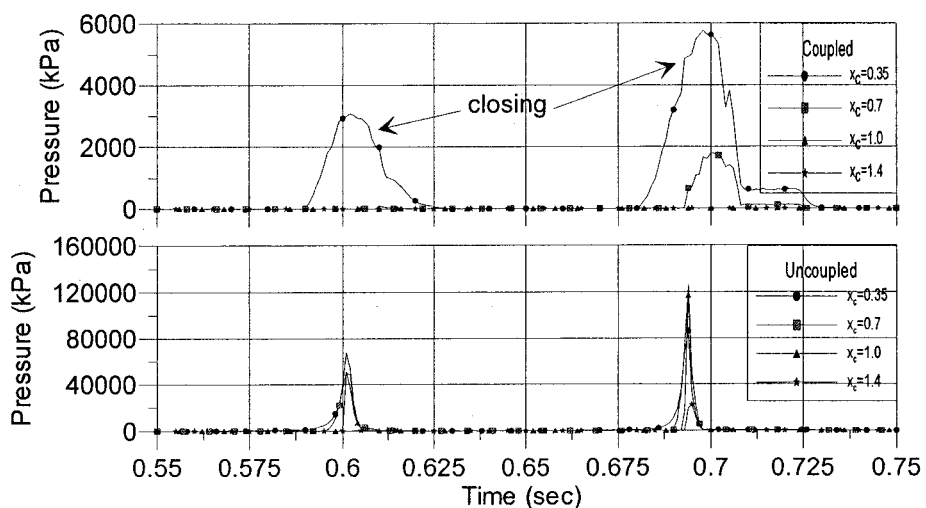
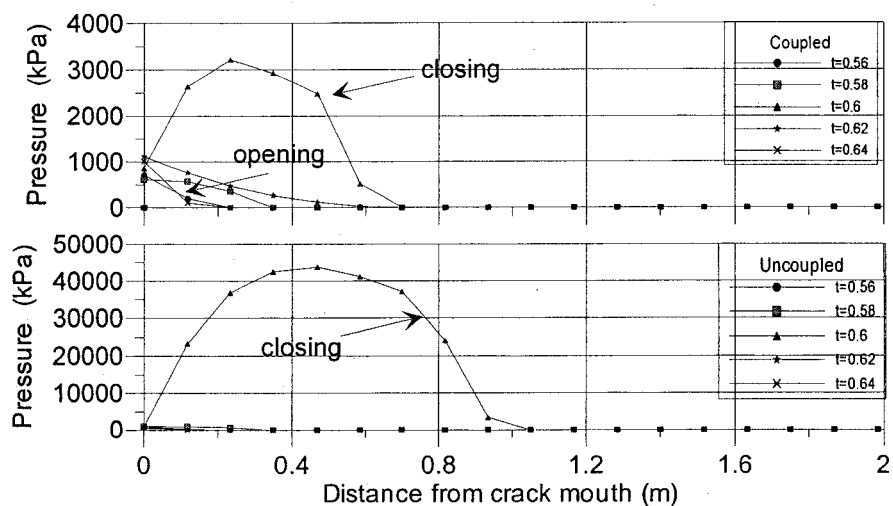


(c) Uplift force in crack based on the uncoupled analysis results

Figure 6.2 Coupled and uncoupled responses of a 90 m dam subjected to a sinusoidal earthquake record ($\ddot{u}_g(t) = 0.35g \sin 2\pi ft$; $f=10$ Hz).

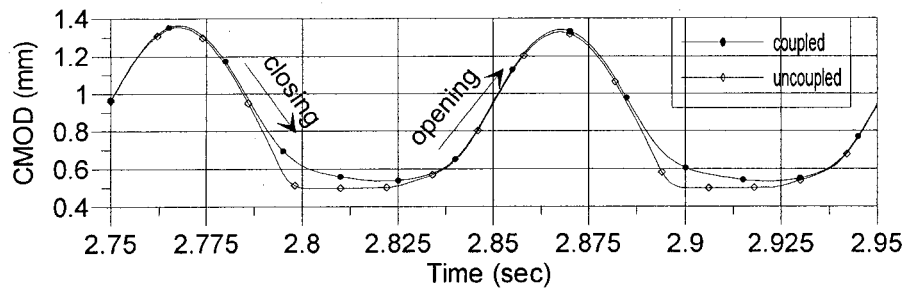


(a) Response of dam with and without coupling effect

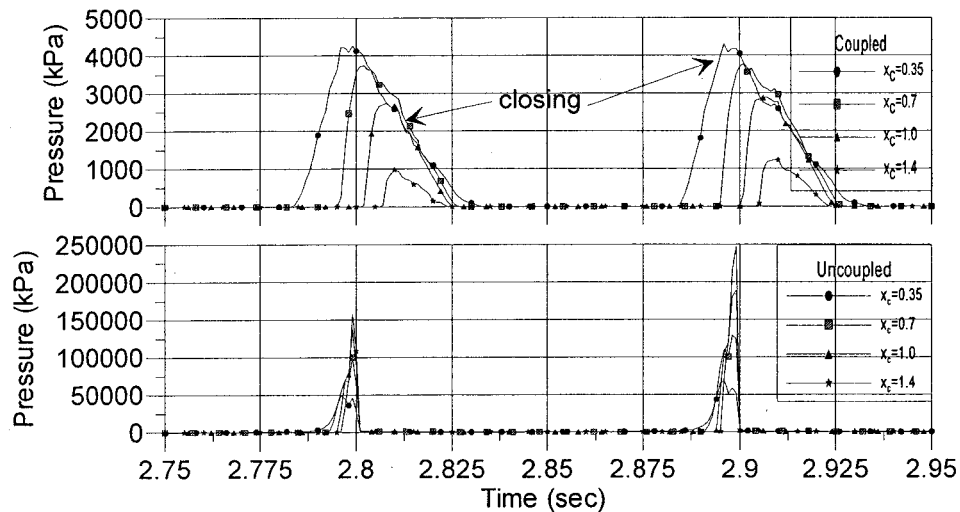
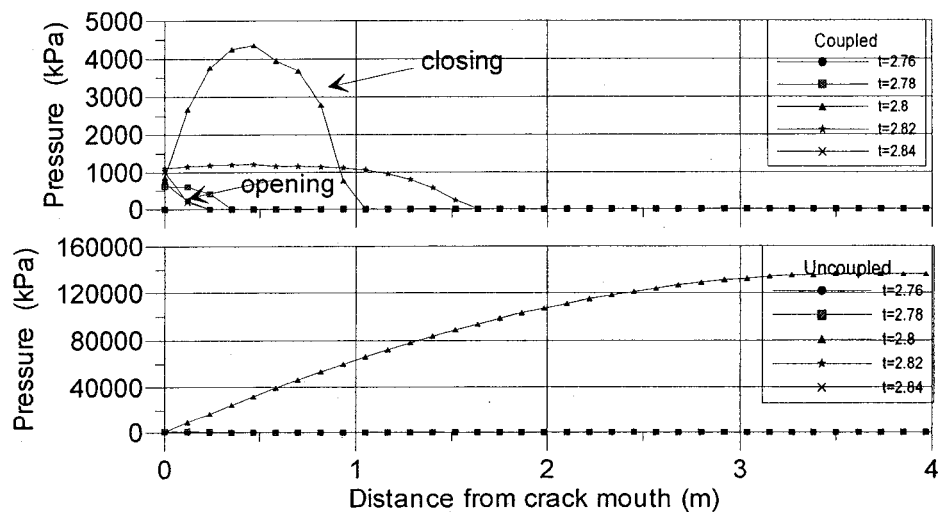
(b) Uplift pressure time variations (x_c =distance from crack mouth)

(c) Spatial distributions of pressure along the crack

Figure 6.3 Coupled and uncoupled transient responses of a 90 m dam subjected to a sinusoidal earthquake record ($\ddot{u}_g(t) = 0.35g \sin 2\pi ft$; $f=10$ Hz).



(a) Response of dam with and without coupling effect

(b) Uplift pressure time variations (x_c =distance from crack mouth)

(c) Spatial distributions of pressure along the crack

Figure 6.4 Coupled and uncoupled steady-state responses of a 90 m dam subjected to a sinusoidal earthquake record ($\ddot{u}_g(t) = 0.35g \sin 2\pi ft$; $f=10$ Hz).

- During the crack opening mode, the pressure magnitudes are similar for coupled and uncoupled analyses. The resultants of uplift pressures on crack walls are generally small and do not affect the dam response significantly. It is possible to evaluate approximately the water pressure for the opening mode of a crack by an uncoupled analysis using the history of crack opening based on transient CMOD results of dam analysis without considering uplift pressures.

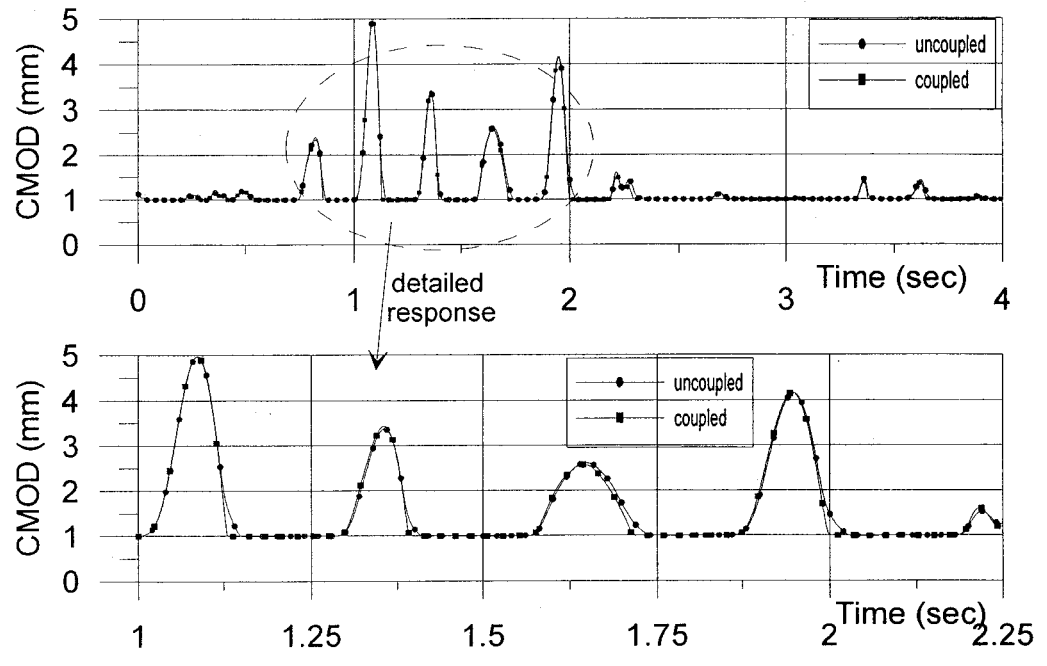
Since the possibility of crack propagation is not considered herein, this analysis is not completely representative with respect to the dam cracking response. However, this example is considered just to show the importance of hydro-mechanical coupling in a real dam. In the next analysis, the possibility of crack development along the dam-foundation interface will be considered.

The earthquake input motion for the second analysis is the modified Saguenay earthquake record with maximum peak ground acceleration $PGA=0.35g$. The gap elements are located all along the dam foundation interface to consider the possibility of crack development. Two analyses, an uncoupled analysis with no uplift pressure, and a coupled analysis with water pressure along the developed crack are performed. According to uncoupled analysis, the maximum cracked length is 35 m, for coupled analysis it is assumed that the crack length is 20 m, and a residual opening equal to 1.0 mm is considered. The results of the analyses are shown in Fig. 6.5. The maximum saturated length for closing mode is almost 2 m (see Fig. 6.5.c) and the rest of crack remains unsaturated, therefore the results are not sensitive to assumed crack length for pressure computations as long as the assumed length is longer than the saturated length. Using the crack length equal to 35 m (the maximum crack length in uncoupled analysis) does not change the results.

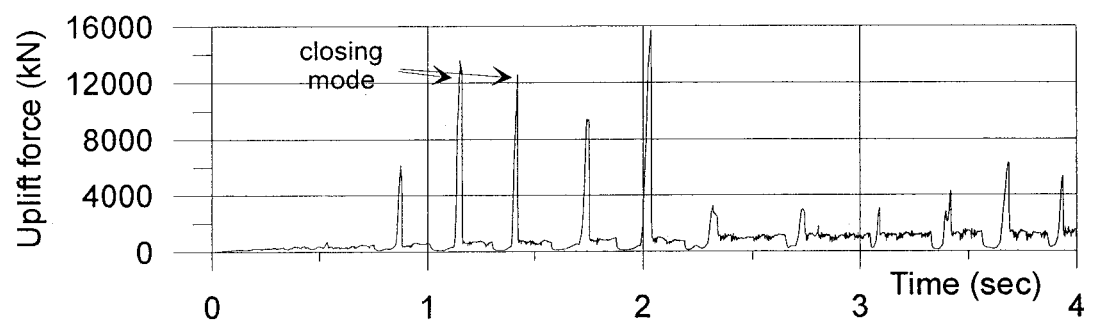
The maximum developed pressure during the closing crack mode, 16400 kPa, is significantly higher than the static uplift pressure at crack mouth, $P_{stat}=860$ kPa. However the saturation length, $L_{sat}=2$ m, is very small compared to the total length of crack, $L=35$ m. Comparisons of the crack length from hydro-mechanical coupled analysis with crack length from uncoupled analysis indicates that there are no

differences between these two cases. In other words, the wedge effect and propagation of crack, during crack closing mode of an initially unsaturated crack, may not occur in a concrete gravity dam cracking during the earthquake.

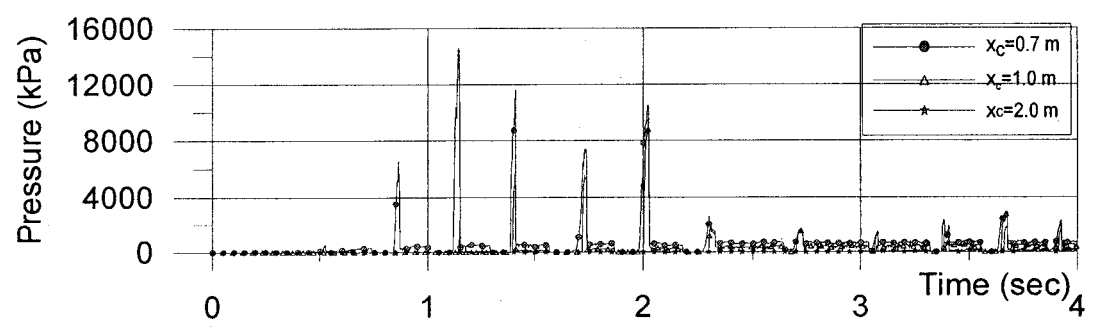
Comparing the hydro-mechanical coupled response of a 90 m dam with a 4.5 m base crack subjected to the sinusoidal earthquake record with the case of a crack $L=35$ m and modified Saguenay earthquake record, the general coupling process are similar in two cases. However, with $L=35$ m crack, the maximum uplift pressure during crack closing mode is around 14000 kPa while with $L=4.5$ it was only 4500 kPa (Fig. 6.4 and Fig. 6.5). Comparing crack opening and closing velocity in the $L=35$ m case is larger than the corresponding velocities with $L=4.5$ m, therefore the magnitude of developed pressure with $L=35$ m is larger. The dam momentum during the crack closing mode is so high, that the developed uplift force cannot reduce crack closing velocity significantly, and crack walls hit each other (mechanical aperture=0). Due to crack wall impact, the crack closing velocity diminishes and the developed pressure decreases instantaneously. Although with each cycle of opening and closing water penetrates progressively inside the crack (note to the Fig. 6.5.b,c) but it is not significant to prevent crack from impact and complete closing as in the case with $L=4.5$ m subjected to sinusoidal crack wall motions.



(a) CMOD response of dam with and without coupling effect



(b) Uplift force variations considering coupling effect



(c) Pressure variations along the crack considering coupling effect

Figure 6.5 Coupled and uncoupled responses of a 90 m dam subjected to modified Saguenay earthquake record (PGA=0.35g).

6.4 Recommendation for industrial application

6.4.1 Opening mode vs closing mode

The typical responses of a cracked concrete gravity dam, subjected to earthquake loads, for crack opening and closing modes are shown in Fig. 6.6. The opening mode corresponds to the instant of time when inertia forces are oriented toward the downstream direction, while the closing mode corresponds to the upstream direction of the effective inertia forces in the dam body. During the opening mode, the hydrostatic pressure, the hydrodynamic pressure and inertia forces are in the same direction and tend to open the crack. The resultant forces of the uplift pressure acting on the crack walls increase the crack opening magnitude. During the crack closing mode, the hydrostatic pressure is still acting toward the downstream direction, while hydrodynamic pressure and inertia forces are acting in the opposite direction. The total resultant force in this case is smaller than the resultant force during the opening mode, and oriented toward the upstream direction.

Considering the sliding and overturning stability of gravity dams, the opening mode is more critical than the closing mode. The good news is that the existing static uplift pressure before the earthquake will be reduced due to crack opening, and the reduction of dynamic pressure in the cracked part helps to improve the dam stability. During the closing mode, although the dynamic water pressure may be greater than the initial existing water pressure in the crack, but this increase may not be significant for sliding stability consideration. A simplified method to compute the water pressure in concrete gravity dam is developed only for the opening mode of the crack.

From the case studies, we have concluded that the developed water pressure during crack opening is relatively small, and that the dam CMOD response is not affected significantly by the developed water pressure during the crack opening mode. To derive a simplified formulation for dynamic uplift pressure computations during the crack opening mode, it is possible to use the DUP_CRACK program directly, to perform parametric analyses of cracks in opening phase.

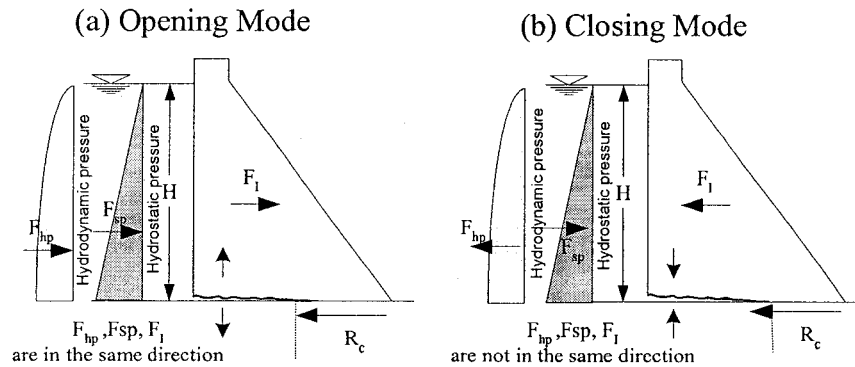


Figure 6.6 Horizontal forces for opening and closing cracks.

6.4.2 Opening crack mode

A series of analyses have been done with different parameters to develop a simplified relation to estimate water pressure inside an opening crack. The most important factors that may affect the developed total dynamic water pressures in the crack, and their magnitudes are considered as:

1. The existing water pressure at the crack mouth (P_{cm}). The static water pressure at crack mouth may be adjusted to consider water pressure variations during the earthquake estimated from the Westergaard formulation for example. The assumed values in the parametric analysis are $P_{cm}=100$ kPa, 500 kPa, 1000 kPa.

2. Minimum opening of crack ($CMOD_{min}$). This is the residual hydraulic aperture of the crack at the crack mouth. The assumed values are $CMOD_{min}=0.1, 0.25, 0.5, 0.75, 1.0, 2.0$ mm.

3. Dominant frequency of crack walls motions. The opening frequency depends on the dominant frequency of the earthquake, and the fundamental frequency of the cracked dam. The assumed values are $f=2, 5, 10$ Hz.

4. Maximum crack walls opening. This is the additional (in addition to the residual opening of crack) opening of crack due to the earthquake. It should be determined by a dynamic analysis of the cracked dam subjected to the applied loads without dynamic water pressure. The assumed values are $CMOD_{amp}=0.1, 0.25, 0.5, 0.75, 1.0, 3.0$ mm.

5. Crack length (L_{cr}). This is the estimated crack length for the dam subjected to the earthquake. The assumed values are $L_{cr}=1, 2, 5, 7, 10$ m.

The DUP_CRACK computer program is used to compute the uplift pressure variations in the crack for each case. Figure 6.7 shows typical results for two different cases when full saturated and partially saturated crack occurs during the crack opening. The time history of resultant uplift force and its mean average, during the opening period, is computed. The computed average can be interpreted as equivalent static uplift force for crack opening mode that can be used in pseudo-static or pseudo-dynamic analysis of dams.

Since the pressure variation along the crack is different for fully saturated and partially saturated crack in opening mode (Fig. 6.7), two different procedures should be used to compute water pressure for these two cases. For a partially saturated case, it is assumed that pressure variation is linear and its magnitude at the crack mouth is equal to the crack mouth pressure so by defining the saturation length for this case, one can compute the uplift force, assuming triangular pressure variation, using the following equation.

$$U = \frac{1}{2} P_{crm} L_{sat} \quad (6.5)$$

In a fully saturated case, a linear pressure variation is also assumed. In this case the developed uplift force is smaller than the uplift force assuming full static uplift pressure in the crack ($U_f = L_{cr} \cdot P_{crm}$). By defining the ratio of these two forces as an uplift reduction factor, R , one can compute total uplift force in the crack using equation 6.6.

$$U = R \cdot P_{crm} \cdot L_{cr} \quad (6.6)$$

The general procedure is that a saturation length is defined as a function of $CMOD_{amp}$ (mm), $CMOD_{min}$ (mm), opening frequency, and crack mouth pressure. For cracks longer than this saturation length, the magnitude of uplift force is independent of crack length and can be computed assuming triangular pressure variation along the crack using equation 6.5. For shorter crack, a reduction pressure factor is defined (a function

of key parameters) which gives the reduction of pressure with respect to full uplift pressure in the crack. These procedures are developed for 2, 5, and 10 Hz excitations and 100, 500, 1000 kPa crack mouth pressure (P_{crm}) cases. For other set of crack parameters interpolation should be used.

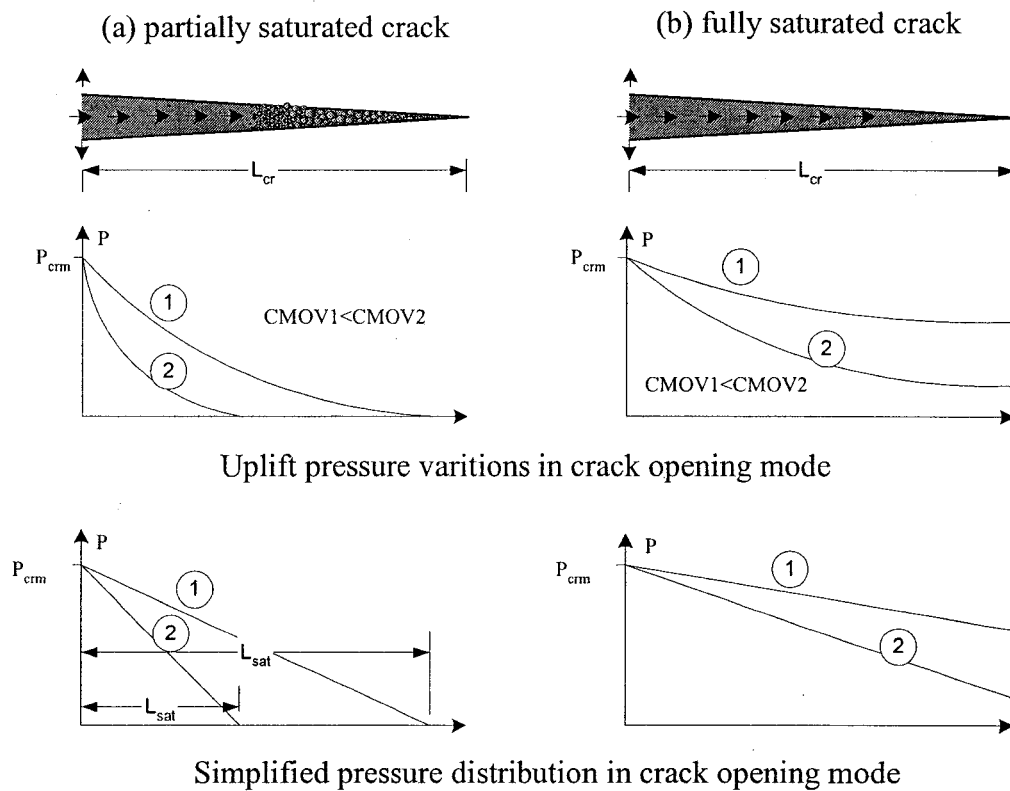


Figure 6.7 Exact vs simplified pressure spatial distributions in crack opening mode.

A base saturation length is first defined and the actual saturation length is computed from that. The base saturation length for a crack with known $CMOD_{amp}$, $CMOD_{min}$, f , and P_{crm} is the saturation length when $CMOD_{min}=2$ mm. Three base saturation length graphs are prepared based on the analyses results for 2, 5, and 10 Hz crack wall frequencies (Fig. 6.8). The saturation length for a particular $CMOD_{min}$ can be computed using the equation 6.7.

$$L_{sat} = L_{satb} - (L_{satb} - L_{satmin}) \left[\frac{2 - CMOD_{min}}{2} \right] \quad (6.7)$$

where L_{sat} is the saturation length (m), L_{satb} is the base saturation length, and L_{satmin} is a length that is defined in table 6.1. (L_{satmin} is the minimum saturation length which occurs in a new crack case when $CMOD_{min}=0.0$) ($CMOD_{min}$ is in mm).

Table 6.1 Values of L_{satmin} in equation 6.7

	L_{satmin} (m)		
	f=2 Hz	f=5 Hz	f=10 Hz
P=100 kPa	0.15	0.10	0.08
P=500 kPa	0.24	0.15	0.10
P=1000 kPa	0.34	0.19	0.15

When the crack length L_{cr} , is smaller than the saturation length L_{sat} , the crack will remain fully saturated during the opening, but depending on the velocity of opening, the pressure decrease and its magnitude is smaller than the full uplift pressure. For this case, the uplift force reduction factor, R, the ratio of resultant uplift dynamic force to the resultant force assuming full uplift pressure in the crack, is defined by equation 6.8. Linear pressure variation along the crack is also assumed for this case.

$$R = 1.0 - 1.1 \left(\frac{L_{cr}}{L_{sat}} \right) + 0.6 \left(\frac{L_{cr}}{L_{sat}} \right)^2 \leq 1 \quad (6.8)$$

For any frequency other than 2, 5, and 10 Hz and other pressures than 100, 500, 1000 kPa, linear interpolation should be used. Figure 6.9 shows the procedure to compute the uplift pressure for a crack in opening mode, that can be used in pseudo-static and pseudo-dynamic analysis of concrete gravity dams.

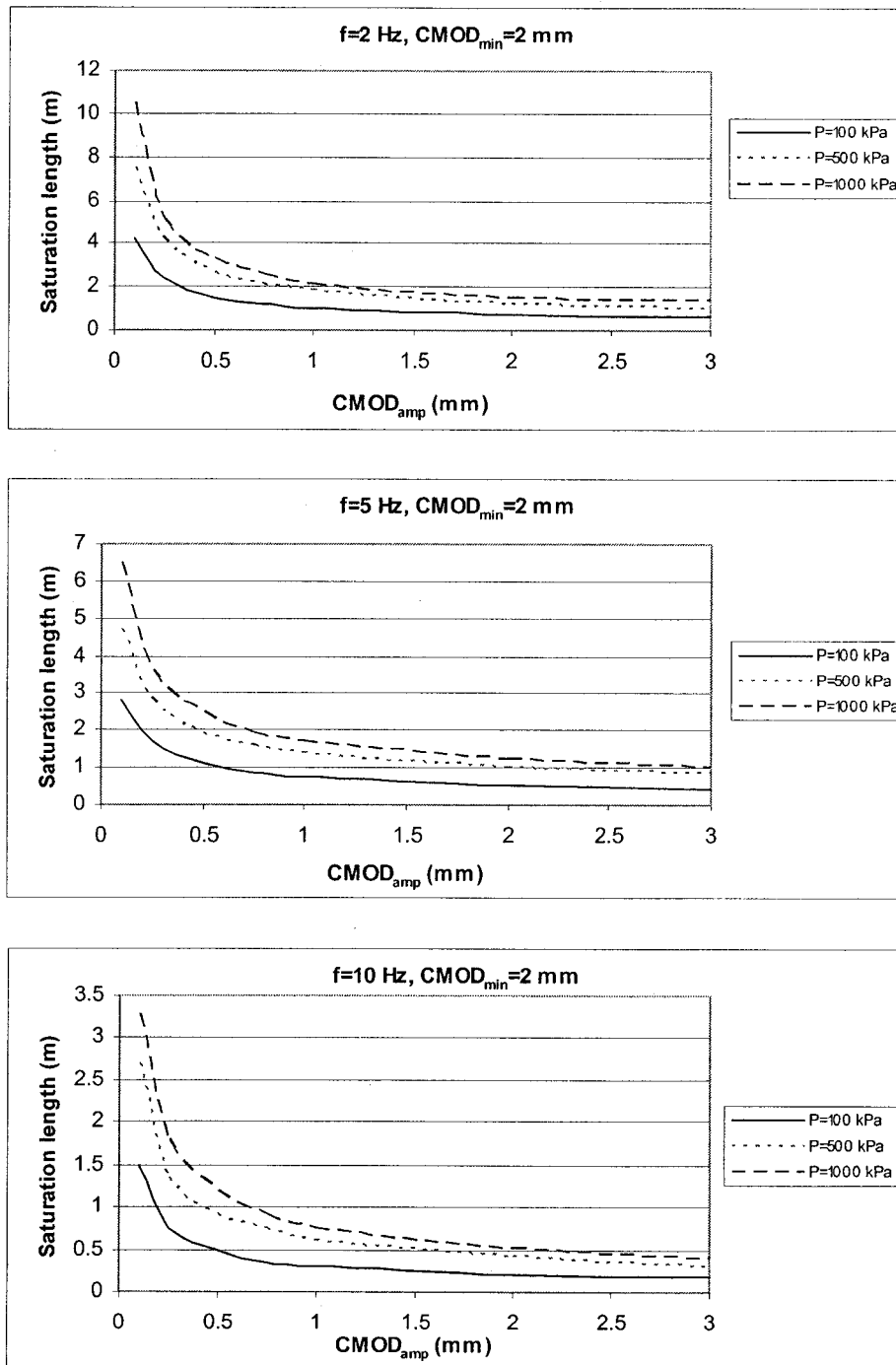


Figure 6.8 Base saturation length curves for $f=2, 5, 10$ Hz

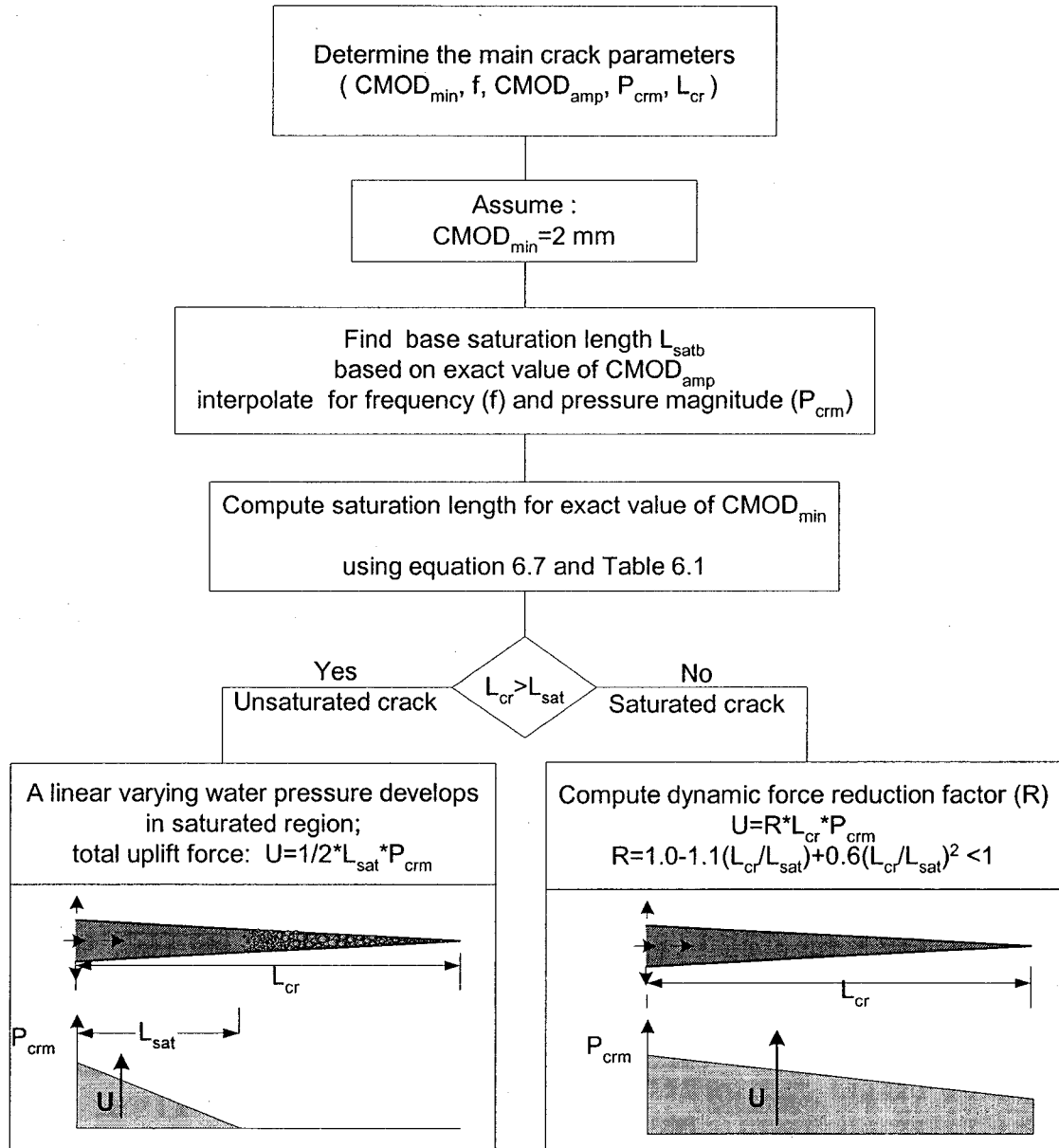


Figure 6.9 Procedure to compute dynamic pressure during seismic crack opening.

6.5 Sliding safety factor of 90 m dam

To investigate the transient dynamic pressure on the stability of concrete gravity dams, and comparing the result with the results of analyses performed in Chapter 1 (assuming three different uplift pressure assumptions from different guidelines), the 90 m dam of Fig. 1.7 is considered again. The proposed procedure in section 6.4 is used to evaluate the uplift pressure for crack opening mode only, since it represents the most critical situation. The magnitude of $CMOD_{amp}$ has been computed by a hydro-mechanical uncoupled finite element analysis, using the results of analysis from section 6.3 the average of $CMOD_{amp}$ is estimated equal to 3.0 mm. The dominant frequency of crack motion from Fig. 6.5.a can also be estimated as $f=4$ Hz.

The results of stability analysis are summarized in Fig. 6.10. As it is expected considering the dynamic pressure in the crack in this case is more close to the zero uplift pressure assumption in the crack. This is because of the small equivalent dynamic pressure in the crack. The developed pressure, as discussed before, is a function of the crack opening characteristics and crack mouth pressure. It is recommended that the dam stability is checked by this procedure but as a general consideration the uplift force effects is small when the crack opening displacement is larger than 0.5 mm.

6.6 Conclusions

The developed model of water pressure computation in cracks with moving walls was implemented in a nonlinear finite element computer program using gap-friction elements, for the analysis of a cracked gravity dam including complete water-crack coupling effect. The developed hydrodynamic water pressure is considered as external force acting on crack walls in dynamic equilibrium equations and the modified Newton-Raphson method is used for equilibrium iteration. The developed model is used to investigate the water pressure variations in cracks on concrete gravity dams subjected to earthquake.

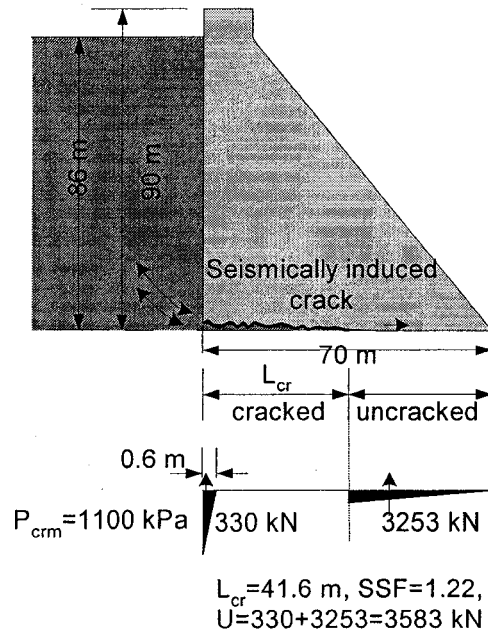


Figure 6.10 90 m dam stability considering transient uplift pressure in crack opening mode (see also Fig. 1.7 for additional information).

The water pressure variations in cracks of concrete gravity dams are different during the crack opening mode as compared to the crack closing mode. In the opening mode, water flow develops in a region close to the crack mouth, the saturated region (L_{sat}), and the rest of the crack is filled with water vapour due to cavitation phenomenon. The length of the saturated region changes during the opening mode and its magnitude is a function the crack mouth pressure, crack hydraulic and mechanical apertures, and crack opening velocity. The pressure develops in this region, and its magnitude at crack mouth is equal to pressure at this point and decreases toward the crack tip, almost linearly, to become zero at the end of the saturated area. The minimum saturation length can be as small as 0.1 m in a cracked dam subjected to strong earthquake motions, and can be increased up to 10 m in an existing crack that oscillates very slowly. A simplified method to estimate water pressure in opening mode of the concrete cracks is developed.

This method can be used for seismic stability analysis of concrete dams using pseudo-static and pseudo-dynamic method.

Although water pressure develops in a short region close to the crack mouth during the opening mode, the cyclic motion of crack walls fills, gradually, the residual opening of crack in each closing mode. The developed uplift force increases as water penetrates inside the crack. The increased uplift force inserts a resisting force against crack closing that reduce the closing velocity of the crack compared to a similar dry crack. If the resulting uplift force is high enough compared to the crack closing force, it may prevent the crack from complete mechanical closure, otherwise the mechanical impact of crack walls reduces the closing velocity and water pressure will be decreased significantly. The developed pressure along the crack is mainly controlled by the hydro-mechanical coupling effect. It is absolutely necessary to perform a coupled analysis to determine the pressure along the crack during the closing mode. The developed pressure in closing mode of a crack in a concrete gravity dam subjected to earthquake is significant but it is only along a small length of the crack. For a 90 m dam the maximum developed pressure is 14000 kPa along 2 m of crack near the crack mouth assuming that closing follows an initial opening condition.

The uplift pressure develops only in a region close to the crack mouth in closing mode and the rest of crack remains un-pressurised. The wedge effect that has been reported in fast closing of saturated cracks cannot occur during a new propagating crack in sound concrete in concrete gravity dams.

However for an initially saturated opened crack that tends to close during the first quake induced oscillatory motion, high water pressures can develop near the crack tip, especially if there exists some obstruction to the free water flow out of this region. In this case the potential for crack propagation can be estimated from the superposition of the total stresses (without uplift pressure) and water pressure to obtain effective stresses to be compared with the concrete tensile strength. Note that crack propagation is not necessarily critical to jeopardise the global stability of dam components as indicated by the Sefid-Rud dam, Konya dam, and Hsingfengkiang dam that all maintained structural

stability while suffering from complete cracking of their upper part separating the dam body into two distinct components.

CHAPTER 7 CONCLUSIONS

7.1 Summary of thesis

The effect of uplift pressure acting on concrete gravity dams during earthquake is very poorly understood. Review of dam safety guidelines indicates that the assumptions of uplift pressure in a crack during earthquake may vary from full reservoir pressure to zero pressure. The impact of these different assumptions on the seismic safety evaluation of dams is shown in Chapter 1 through pseudo-dynamic stability computation of a 90 m gravity dam. The lack of information about the dynamic uplift pressure in concrete gravity dams is mentioned by researchers in the dam engineering field. The dynamic water pressure developing in cracked concrete is investigated through an experimental program, and a theoretical model is developed for water pressure computation based on the crack wall motions. The procedure is implemented in a nonlinear finite element based computer program using gap-friction elements for complete hydro-mechanical coupled analysis of cracked concrete gravity dam subjected to earthquake considering the developed uplift pressure in the crack.

Review of the available literature indicates only few studies about the dynamic uplift pressure in concrete dams. There are two studies that addressed explicitly the dynamic uplift force in the cracked dams during the earthquake. The first one is a theoretical solution presented by Tinawi and Guizani (1994) to formulate dynamic water pressure in an existing notch, and the second one is a theoretical formulation supported by experimental data to evaluate dynamic pressure in new developing cracks by Slowick and Saouma (1994, 2000). Due to similar aspects of water flow in rock joints and concrete cracks, the results of research about water-joint interaction in the rock mechanic field can be used in this study. Numerous experimental studies show that the

well known cubic law for fluid flow between two parallel plates can be used with some modifications to presents flow of water in cracks and rock joints.

The main objective of the experimental program was defined to measure the water pressure variations inside concrete cracks with moving walls. Two procedures have been developed to measure water pressure in new developing cracks, and existing cracks using the same specimen. Five concrete specimens (1.5x0.55x0.15 m) are used to perform 5 new crack tests, and more than 250 existing crack tests are performed to study the effects of different parameter variations in the developed water pressure in the crack. The average crack length in the specimens was almost 0.40 m. Using a displacement control test set up harmonic displacements as well as seismic displacements are applied to induce the crack wall to dynamic motions. The main parameters were the frequency of excitation, static uplift pressure at crack mouth, the initial opening in existing crack tests, and the amplitude of opening in harmonic motion.

A dynamic water-crack interaction model is then formulated to reproduce the experimental results, and extrapolate the computed uplift pressure variations to cracks of arbitrary lengths likely to develop in actual dams. The transient pressure gradients in a crack of specified length is modelled as a function of the crack mouth opening displacement (CMOD(t)), the crack mouth opening velocity (CMOV(t)), and crack mouth pressure ($P_{cm}(t)$) time histories assuming: (i) 1D flow along the crack, (ii) continuity condition with an incompressible fluid of a constant viscosity, (iii) pressure-flow relations governed by the crack hydraulic conductivity using variations of the so-called "cubic law" accounting for the crack roughness, laminar or turbulent flow conditions according to Reynold's number, and cavitation, (iv) impervious crack walls, (v) constant crack length, (vi) and residual crack aperture during cyclic motions (zero or larger). Based on the proposed model, a computer program, DUP-CRACK, was developed to compute water pressure variations along the concrete cracks with known time history of crack wall motions. The experimental pressure variations and the simulated pressure variations by DUP_CARAK are generally in very good agreement.

The DUP_CRACK was used to investigate the developed pressure in cracks with different lengths, subjected to same harmonic motions of crack walls. The developed pressures for longer cracks are significantly large, and a coupled analysis to consider the effects of developed pressure on crack wall motions is necessary. The main subroutines of DUP_CRACK were then implemented in a nonlinear finite element program with gap-friction elements to represent the crack and compute the related dynamic water pressure. The interaction model is used to compute the dynamic pressure during typical crack opening and closing modes. It was found that for the opening mode, the key input parameters (CMOD(t), $P_{crm}(t)$ and crack length) could be estimated either (i) from FE analyses with gap-friction elements using commercial computer programs without modelling dynamic crack pressure variations, or (ii) from simplified formulation (Chopra's method (1988), rigid body dynamics, Westergaard added pressure). Analytical formulas are derived to estimate the maximum dynamic uplift force and resultant position to use in seismic dam stability evaluation using simplified pseudo-dynamic methods. An application example to study the dynamic stability of a 90 m dam model is then presented.

7.2 Conclusions

The following conclusions can be made based on the observations in the laboratory, investigation of test results, and subsequent development and application of the proposed water-crack interaction model to a typical 90 m dam.

Existing cracks (experimental observations):

- Frequency of excitation, amplitude of crack aperture, and minimum (residual) crack aperture are the most important factors that affect the magnitude of developed pressure in the crack with moving walls.
- The crack aperture amplitude and frequency of excitation can be interpreted as the velocity of crack walls in harmonic opening and closing motions. So the crack

opening and closing velocity appeared to have the most important effect on pressure development in crack with moving walls.

- The cavitation phenomenon occurs in the case of 6 Hz and 10 Hz exciting frequencies with small initial static pressures. The occurrence of cavitation causes transient short high frequency pressure response in the system (collapse of air bubbles).
- The initial static water pressure does not have any effect on the magnitude of developed dynamic pressure variations inside the crack if cavitation is not occurring.
- The developed pressure amplitude in closing mode of a saturated crack increases from the crack mouth toward its tip but decreases after reaching a maximum value close to the crack tip.

New cracks (experimental observations):

- During concrete cracking, negative pressure may be developed in the created void along the propagating crack front. Negative pressure, if low enough, may cause cavitation phenomenon in the crack.
- Water front velocity is a function of crack aperture, static pressure at crack mouth, and probably the roughness of crack. The estimated water front velocity for the experimental test conditions is around 1400-2000 mm/sec.
- As soon as water fills all the voids in a new crack in the first cycle of crack wall motion or subsequent cycles, the developed pressure history in new cracks and existing cracks will be similar if their crack wall motion characteristics are the same.

Effects of crack length:

The investigation of developed water pressure in cracks with different lengths using the developed computer program, DUP_CRC AK, subjected to harmonic wall motions shows that the developed pressures in opening mode and closing mode are basically different. The magnitudes of developed pressures are affected by the crack wall

motion characteristics ($CMOD_{amp}$, $CMOD_{min}$, and frequency) as well as crack mouth pressure. The following conclusions can be drawn from these analyses.

- The developed pressure in opening mode of an existing crack and a new crack is basically similar if their crack wall motions histories are similar (they may be different at the instant of cracking in new crack, but they become similar after first cycle of closing.)
- During the opening crack mode, water flow occurs in a region close to the crack mouth, the saturated region (L_{sat}), and the rest of the crack is filled with water vapour due to cavitation phenomenon. The length of the saturated region changes during the opening mode, and its magnitude is a function crack mouth pressure, crack aperture, crack opening velocity. The water pressure develops in this region, and its magnitude at crack mouth is equal to the existing pressure at this point and decreases toward the crack tip, almost linearly, to become zero at the end of the saturated area. The length of this saturated region (L_{sat}) is independent of crack length, and is a function of the static pressure at crack mouth, residual opening of crack ($CMOD_{min}$), amplitude of crack mouth opening ($CMOD_{amp}$), and the dominant frequency of crack wall motions (f).
- During crack closing, the existing water in the saturated region of crack flows in two different directions and a stagnation point, with no water flow, will exist in the saturated region. The water flows from the stagnation point toward crack mouth pushes some amount of water out of the crack. The water flow from the stagnation point toward the cavitation region fills the voids and eliminates cavitation gradually. In an existing crack, the residual opening is already filled with water and the water flow should fill the voids generated due to crack opening. However, in a new crack the water flow should fill the existing void due to residual opening plus the voids created during the crack opening mode. If the opening of an existing crack starts with an existing residual opening and comes back to the same position in the closing mode, the crack will become fully saturated. In a new crack, water flow fills a part of the residual opening in each closing cycle, and the saturated length during the

closing mode is increasing in successive opening closing cycles. When the residual opening of a new crack is filled completely (fully saturated) its response will be like that of an existing crack.

- The shape of pressure spatial distribution along an unsaturated crack during its closing mode is like a dome. Its magnitude at the boundaries is equal to pressure magnitude at these points (pseudo-static pressure at crack mouth and vapour pressure, assumed equal to zero, at the end of saturation region), and its maximum magnitude occurs at the location of the stagnation point. As soon as the crack becomes fully saturated in the closing mode, the spatial pressure variations along the crack changes. Its magnitude will be equal to crack mouth pressure at this point, and then increases to a maximum value at the crack tip.
- At the beginning of the closing mode when the crack closing velocity is small, the flow in the crack is in one direction just like the flow during the opening mode. In this case, the crack closing velocity is too small to generate significant pressure relative to the existing crack mouth pressure, and the existing pressure head pushes the water into the crack in one direction and the generated water pressure variation is more like during crack opening mode.

Hydro-mechanical coupled response of concrete gravity dams

A typical section of a 90 m concrete gravity dam subjected to two different earthquakes records were analysed assuming dry crack (no water pressure in cracks) and with water in cracks considering the hydro-mechanical coupling effects. The water pressure variations in the crack are also computed based on the response of a dry dam (uncoupled analysis) to compare the results of uncoupled and coupled analysis. The following conclusion can be made from these numerical analyses.

- The response of dam is generally similar for the coupled and uncoupled analysis. The major differences are related to the closing crack mode. In closing mode, the developed pressure in the crack reduces the closing velocity of crack and postpones the impact phenomenon of two crack walls. Due to impact of crack walls, crack

closing velocity and the magnitude of the developed pressure decreases significantly. In a new developed crack, increasing of saturation length and uplift force in successive closing modes, increases the hydro-mechanical coupling effects with time and if the developed force is high enough it may prevent the crack walls from complete closure and impact.

- The computed water pressures in crack opening mode are basically similar for both coupled and uncoupled analyses. It is possible to estimate the water pressure for the opening mode using an uncoupled analysis.
- The computed water pressures in coupled analysis are significantly lower than the computed water pressures from uncoupled analysis during the crack closing mode. Comparing a coupled analysis with an uncoupled one, the developed pressures in the closing mode put additional forces on crack walls that reduce the closing velocity. The rate of pressure development decreases due to smaller closing velocity compared to an uncoupled analysis. The complete saturation may not be developed for long cracks due to decreased water pressure in the crack.

Stability of concrete gravity dams

The dynamic response of the concrete gravity dam subjected to the earthquake is affected by the hydro-mechanical coupling effect of developed pressure in the cracked dam. The degree of coupling changes depending on the dam structural properties, the earthquake intensity, and the developed crack characteristics. It is recommended to do a hydro-mechanical coupled analysis for every concrete gravity dams if it is required to investigate the response of the dam accurately, otherwise, the developed simplified method in this study can be used for stability analysis of concrete gravity dams. The following conclusions can be drawn as guidelines based on the results of this research.

- Results of analyses show that the cyclic motions of crack walls in concrete dam during earthquake pushes the water into the crack in each closing period of motion (if a residual opening exists in the closing mode). Therefore the assumption that

rapidly oscillating nature of opening and closing the crack does not allow reservoir water to penetrate in the crack (USBR 1987) is highly questionable.

- The water pressure develops in a region close to the crack mouth. The water pressure magnitude is significant during the crack closing mode. For a 90 m dam subjected to modified Saguenay earthquake record with $PGA=0.35$ g, the maximum developed pressure along the 2.0 m of crack was 14000 kPa. This pressure is equivalent to 15000 kN uplift force and its point of application is close to the crack mouth (magnitude of the static uplift force is equal to 19800 kN).
- Due to the short saturated length during the crack opening mode the uplift force is relatively small but not equal to zero. A general qualitative description for water pressure during crack opening mode is somewhere between zero uplift pressure (USBR 1987, CDSA 1997 high seismic zones), and unchanged uplift pressure (USACE 1995, FERC 2002, CDSA 1997 low seismic zone). The magnitude of developed uplift force depends on the crack opening characteristics and crack mouth pressure as indicated by the novel water-crack interaction model developed in this thesis. The full uplift pressure assumption (ICOLD 1986) seems very conservative for stability calculation of cracked concrete dams during an earthquake.
- The uplift pressure develops only in a region close to the crack mouth in closing mode and the rest of crack remains un-pressurised. The wedge effect that has been reported for fast closing of saturated cracks cannot occur in new crack cases, or an existing crack when the crack motion starts with crack opening.

7.3 Future research and developments

7.3.1 Experimental research on transient uplift force

To extend the experimental part of this study the following can be considered in the future experimental programs.

- To perform more tests with increasing the testing parameters, the following new parameters are recommended.

Crack length, the crack length effect on dynamic pressure was not studied experimentally. It is recommended to perform some test with different crack lengths (longer than 0.4 m that has been used in this study) to verify the developed method for longer cracks.

Crack roughness, the effects of crack surface conditions were not investigated in this research, and it was assumed that the roughness of the crack surface is constant. More precise tests can be done with different crack surface conditions. It is possible to create cracks with variable surface roughness by using different concrete mix or by preparing crack surfaces artificially as has been done by Amadei and Illangasekare 1992.

- The water pressure applying and measuring systems may be modified to measure the pressure variations in the crack with more precision. Using shorter and smaller holes, it is recommended to minimize the holes effects on the measured pressure with respect to a real crack where no holes are present. Increasing the volume of steel tank may decrease the pressure variations at the crack mouth. It is also possible to use an expandable tank with deformable walls to eliminate or minimize the pressure variation in the crack mouth. Using the pressure transducers with capabilities for reading negative pressure will help to formulate negative pressure development in the crack.
- The testing procedure can also be extended by considering a modified procedure to investigate the effects of sliding and dilatation of concrete joints and cracks on the uplift pressure during the earthquake.
- A new testing procedure may be developed to study the cavitation phenomenon with more details in opening mode of crack.

7.3.2 Theoretical formulation and numerical analysis of transient water-crack pressure

The following considerations are recommended for extension of the theoretical and numerical formulations presented in this study:

- The developed water-crack interaction model may be modified to consider deformable crack walls and cracks with variable lengths. The permeability of crack walls may also be considered. Then the developed method may be then implemented in a finite element program to analyse the crack propagation in a concrete dam.
- To make the developed water-crack model more usable in the industrial application, it may be presented in a structural form. For example by introducing an equivalent system of spring and damper, instead of water inside the crack, with their related constitutive model. Using most commercially available finite element based structural analysis programs, it will be possible to perform transient nonlinear analysis of cracked dams using gap element with user defined constitutive models to represent water-crack interaction effects.
- In the developed water-crack interaction model, it was assumed that water pressure in unsaturated region remains equal to zero and no water flow is assumed in this area. More sophisticated formulation considering negative water pressure, and the water flow in the unsaturated part of crack using the two phase flow theories can be used to improve the water-crack model.
- The assumed one dimensional water flow in crack, may be extended to the two dimensional water flow (to consider the effects of lateral boundary conditions) and three dimensional flow (to consider the effects of crack wall permeability).

7.3.3 Seismic safety analysis of dam considering water-crack interactions

The following considerations are recommended for extension of the seismic safety analysis of dams considering water-crack interactions.

- More parametric investigations are needed to develop a procedure to evaluate water pressure to be used in pseudo-static or pseudo-dynamic analysis during the closing mode of cracks in concrete gravity dams.
- The variations of pressure are investigated for the cracked part of the dam. The water pressure in un-cracked part of dam-foundation interfaces is also affected by earthquake. More investigation to evaluate dynamic variation of pressure in the un-cracked part is recommended.

REFERENCES

AMADEI B., ILLANGASEKARE T., and CHINNASWAMY C., 1991. " Effect of crack uplift on concrete dam stability ", First Conference Research Needs in Dam Safety, 3-6 December 1991, New Dehli- India, pp. I 60-66.

AMADEI B., ILLANGASEKARE T., MORRIS D. I., and BOGGS H., 1989. " Estimation of uplift in older concrete gravity dams: analytical solution and parametric study ", ASCE, Journal of Energy Engineering, Vol. 115, No. 1, pp. 19-46.

AMADEI B., and ILLANGASEKARE T., 1992. " Uplift pressure cracks in concrete gravity dams-an experimental study ", Tech. Rep. TR-101672, Vol. 8, Electrical Power and Research Institute (EPRI), prepared by University of Colorado, Boulder, Colorado.

ARCANGELI E., and CIABARRI P., 1994, " Mengil dam rehabilitation by resin grouting and high capacity anchors ", Water Power and Dam Construction, Vol. 46, No. 2, February, pp. 19-25.

ASGIAN M., 1989. " A numerical model of fluid-flow in deformable naturally fractured rock masses ", Int. J. Rock Mech. Min. Sci. & Geomech. Abstr., Vol. 26, No. 34, pp. 317-328.

BARTON N., BANDIS S., and BAKHTAR K., 1985. " Strength, deformation and conductivity coupling of rock joints ", Int. J. Rock Mech. Min. Sci. & Geomech. Abstr., Vol. 22, No. 33, pp. 121-140.

BAZANT, Z.P., 1975. " Pore-pressure, uplift, and failure analysis of concrete dams ", Proc., Int. Symp. Criteria and Assumptions for Numerical Analysis of Dams, Naylor et al. Editors, pp. 782-808.

BHATTACHARJEE S.S., 1993, “ Smearred fracture analysis of concrete gravity dams for static and seismic loads ”, Ph.D. Thesis, Department of Civil Engineering and applied Mechanics, McGill University, Montreal, Canada.

BRUHWILER E., and SAOUMA V.E., 1991, “Water fracture interaction of cracked concrete gravity dams ”, Proceedings International Conference on Dam Fracture, Denver, Colorado, pp. 555-568.

BRUHWILER E., and SAOUMA V.E., 1995. “ Water fracture interaction in concrete; part I: fracture properties ”, ACI Material Journal, Vol. 92, No. 3, pp. 293-303.

BRUHWILER E., and SAOUMA V.E., 1995. “ Water fracture interaction in concrete; part II: hydrostatic pressure in cracks ”, ACI Material Journal, Vol. 92, No. 3, pp. 383-390.

CASAGRANDE A., 1961, “ Control of seepage through foundations and abutments of dams ”, Geotechnique, Vol. XI, pp. 161-182.

CHEN H.Q., HOU S.Z., QI J.H., 1982, “ Dynamic stability analysis of cracked top portion of the Xienfengjiang concrete diamond head buttress dam. ”, Proc. US-PRC Workshop on Earthquake Engineering, Harbin (PRC), Acad. Sinica B.2, pp. 1-20

CHOPRA A.K., 1988, Earthquake response analysis of concrete dams, Advanced Dam Engineering for Design, Construction, and Rehabilitation, Edited by R.B. Jansen, Van Nostrand Reinhold, pp. 416-465

CDSA (Canadian Dam Safety Association) 1997, “ Dam safety guidelines ”, Edmonton, Alberta.

DESCHAMPS R., YANKEY G., and BENTLER D. J., 1999. “ Modeling uplift pressure and drain flow at Bluestone dam ”, Proceeding Annual Association of Dam Safety Officials (ASDSO), StLouis, Missouri.

DVORKIN J., MAVKO, G., and NUR A., 1992. “ The dynamics of viscous compressible fluid in a fracture ”, Geophysics, Vol. 57, No. 5, pp. 720-726.

DVORKIN J., MAVKO G., and NUR A., 1990. “ The oscillation of a viscous compressible fluid in an arbitrarily-shaped pore ”, Mechanics of Materials, Vol. 9, pp. 165-179.

EL-AIDI B. M., 1988, “ Nonlinear earthquake response of concrete gravity dam system.”, Ph.D. Thesis, California Institute of Technology, Pasadena, California.

EPRI (Electrical Power and Research Institute) 1992. “ Uplift pressure, shear strengths and tensile strengths for stability analysis of concrete gravity dams ”, EPRI TR-100345, Vol. 1, Palo Alto, California, USA.

FENVES, G., and VARGAS-LOLI, L. M., 1988, “ Nonlinear dynamic analysis of fluid-structure systems ”, ASCE, Journal of Engineering Mechanics, Vol. 114, pp. 219-240.

FERC (Federal Energy Regulatory Commission) 2002, Engineering guidelines for the evaluation of hydropower projects. Washington, D.C.

FOX R.W., and MCDONALD A.T., 1992, “ Introduction to fluid mechanics ”, John Wiley and Sons, Inc. New York

FRENTEDDU L., 1997, “ Experimental and numerical evaluation of the effect of concrete lift joints on static and seismic response of gravity dams ”, Ph.D. Thesis, Département des génies civil, géologique et des mines, École Polytechnique de Montréal, Canada.

GOODMAN R. E., AMADEI B., and SITAR N., 1983, “ Uplift pressure in rock below dam ”, ASCE, Journal of Energy Engineering, Vol. 109, No. 4, pp. 207-221.

HAKAMI E., 1995, “ Aperture distribution of rock fractures ”, Ph.D. Thesis, Division of Engineering Geology, Royal Institute of Technology, Stockholm.

HALL J. F., 1998. “ Efficient non-linear seismic analysis of arch dams ”, Earthquake Engng. Struct. Dyn., Vol. 27, pp.1425-1444.

HALL J.F., 1988, “ The dynamic and earthquake behavior of concrete dams: review of experimental behavior and observational evidence ”, Soil Dynamics and Earthquake Engineering, Vol. 7, No 2, pp. 249-263.

HARDY M. P., and ASGIAN M. I., 1989, “ Fracture reopening during hydraulic fracturing stress determinations ”, Int. J. Rock Mech. Min. Sci. & Geomech. Abstr., Vol. 26, No. 6, pp. 489-497.

ICOLD (International Commission on Large Dams) 1986, “ Earthquake analysis for dams ”, Bulletin 52, Paris.

ICOLD (International Commission on Large Dams) 1998, “World register of dams”, Computerized version, Paris, France.

ILLANGASEKARE T., AMADEI B., and CHINNASWAMY C., 1992. “ CRFLOOD: A numerical model to estimate uplift pressure distribution in cracks in concrete gravity dams ”, Tech. Rep. TR-101671, Vol. 4, Electrical Power and Research Institute (EPRI), prepared by University of Colorado, Boulder, Colorado.

INDERMAUR W., BRENNER R.P., and ARASTEH T., 1992, “ The effects of Manjil earthquake on Sefid Rud buttress dam ”, Dam Engineering, Vol. II, No. 4, pp. 275-305.

INDRARATNA B., and RANJITH P., 2001, “ Hydromechanical aspects and unsaturated flow in jointed rock ”, A.A.Balkema Publishers, Lisse

JAVANMARDI F., LEGER P., and TINAWI R., 2002, “ Experimental measurements of water pressure in concrete cracks due to seismic loading ”, Proceedings CSCE 30th annual conference, Montreal, Quebec, June 5-8, paper ST-014, 10 pp.

JING L., MA Y., and FANG Z., 2001, “ Modeling of fluid flow and solid deformation for fractured rocks with discontinuous deformation analysis (DDA) method ”, Int. J. Rock Mech. Min. Sci., Vol. 38, pp. 343-355.

JING L., TSANG C. F., and STEPHANSSON O., 1995, “ DECOVALEX- An international co-operative research project on mathematical models of coupled THM processes for safety analysis of radioactive waste repositories ”, Int. J. Rock Mech. Min. Sci. & Geomech. Abstr., Vol. 32, No. 5, pp. 389-398.

LECLERC M., LÉGER P., and TINAWI R., 2002, “ Computer aided stability analysis of gravity dams – CADAM, Users Manual ”, Department of Civil Engineering, École Polytechnique, Montreal, Quebec, Canada (<http://www.struc.polymtl.ca/dams>).

LEE C-H., and FARMER, I., 1993, “ Fluid flow in discontinuous rocks ”, Chapman and Hall, London.

LOUIS C., 1969, “ A study of groundwater flow in jointed rock and its influence on the stability of rock masses ”, Rock Mechanic Progress Report 10, Imperial College, London, England.

MILLARD A., DURIN M., STIETEL A., THORAVAL A., VUILLOD E., BAROUNDI H., PLAS F., BOUGNOUX A., VOUILLE G., KOBAYASHI A., HARA K., FUJITA T., and OHNISHI Y., 1995, , “ Discrete and continuum approaches to simulate the thermo-hydro-mechanical coupling in a large, fractured rock mass ”, Int. J. Rock Mech. Min. Sci. & Geomech. Abstr., Vol. 32, No. 5, pp. 409-434.

NCR (National Research Council) 1990, “ Earthquake engineering for concrete dams: design, performance, and research needs “, National Academy Press, Washington, D.C., USA.

NOORISHAD J., AYATOLLAHI M. S., and WITHERSPOON P. A., 1982, “A finite-element method for coupled stress and fluid flow analysis in fractured rock masses “, Int. J. Rock Mech. Min. Sci. & Geomech. Abstr., Vol. 19, pp. 185-193.

NOORISHAD J., TSANG C. F., and WITHERSPOON P. A., 1992, “ Theoretical and field studies of coupled hydromechanical behavior of fractured rocks-1. Development and verification of a numerical simulator ”, Int. J. Rock Mech. Min. Sci. & Geomech. Abstr., Vol. 29, No. 4, pp. 401-409.

OHMACHI T., ZHANG H., YABUKI N., and TSUKADA N., 1998, “ Experimental study of hydrodynamic pressure inside narrow cavities ”, Dam Eng., JSDE, Vol. 8, pp. 35-40.

OLSSON R., and BARTON N., 2001, “ An improved model for hydro-mechanical coupling during shearing of rock joints ”, Int. J. Rock Mech. Min. Sci., Vol. 38, pp. 317-329.

REINHART H. W., SOSORO M., and ZHU X., 1998, “ Cracked and repaired concrete subject to fluid penetration ”, Materials and Structures, Paris, Vol. 31, pp. 74-93.

SAOUMA V. E., and MORRIS D. I., 1997, “ Improving concrete dam safety evaluation: a look at research contributions ”, Hydro Review, pp. 65-72.

SCADA (Smearred Crack Arch Dam Analysis), 1996, User's manual, Report No. EERL 96-01, Earthquake Engineering Research Laboratory, California Institute of Technology, Pasadena, California

SLOWIK V., and SAOUMA V. E., 2000, “ Water pressure in propagating concrete cracks.”, ASCE, Journal of Structural Engineering, Vol. 126, No. 2, pp. 235-242.

SLOWIK V., and SAOUMA, V.E., 1994, “ Investigation on cracking of concrete with application to the seismic safety of dams,” Proc. EURO-C, Innsbruck, Austria, March 22-25, pp. 679-688.

TINAWI R., and GUIZANI L., 1994, “ Formulation of hydrodynamic pressure in cracks due to earthquake in concrete dams.”, Earthquake Engineering and Structural Dynamics, vol. 23, pp. 699-715.

TINAWI R., LÉGER P., GHRIB F., BHATTACHARJEE S., and LECLERC M., 1998, “ Structural safety of existing concrete dams: influence of construction joints”, Report for the Canadian Electricity Association, Vol. A Review of literature and background material.

UDEC (Universal Distinct Element Method) Version 3.1 Users Manuals, 2000, Itasca Consulting Group, Inc., Minneapolis, Minnesota, USA.

USACE (US Army Corp of Engineers) 1995. Engineering and design, gravity dams. EM 1110-2-2200, Washington, D.C. USA.

USBR 1987, Design of small dams. 3rd Edition, Denver, Colorado, USA.

WITHERSPOON P. A., WANG J. S. Y., IWAI, K., and GALE J. E. (1980). "Validity of cubic law for fluid flow in a deformable rock fracture.", Water resources Research., Vol. 16, No. 6, pp 1016-1024.

YEH C-H., 1999, " Criteria for overturning stability of gravity dams in the United States.", International conference on dam safety and monitoring, 19-22 Oct.,1999 TGP Site, Yinchang, Hubei, China.

ZHANG H., and OHMACHI T., 1998, " 2 Dimensional analysis of seismic cracking in Concrete gravity dams.", Dam Eng., JSDE, 8, pp. 93-101.

ZIENKIEWICZ O. C., 1963, " Stress analysis of hydraulic structures including pore pressure effects ", Water Power, March, pp.104-108.

ZIENKIEWICZ O. C., and PARK J., 1958, " Effect of pore pressure on stress distribution in some porous elastic solids ", Water Power, January, pp.12-19.

ZIENKIEWICZ O. C., PAUL D.K., and HINTON E., 1983, "Cavitation in fluid-structure response (with particular reference to dams under earthquake loading) ", Earthquake Engineering and Structural Dynamics, Vol. 11, pp.463-481.